

1997/22  
C.3

AGSO

# Stream Sediment Geochemistry of the Hann River Region, Cape York Peninsula, North Queensland

by

*B. I. Cruikshank & P. C. Brugman*



Record 1997/22

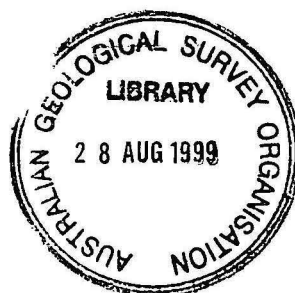
AGSO



AUSTRALIAN  
GEOLOGICAL SURVEY  
ORGANISATION

BMR COMP  
1997/22  
C.3

**Stream sediment geochemistry of the  
Hann River Region,  
Cape York Peninsula,  
north Queensland**  
*Record 1997/22*



**B I Cruikshank and P C Brugman**



## DEPARTMENT OF PRIMARY INDUSTRIES AND ENERGY

Minister for Primary Industries and Energy: Hon. J. Anderson, M.P.  
Minister for Resources and Energy: Senator the Hon. W.R. Parer  
Secretary: Paul Barrett

## AUSTRALIAN GEOLOGICAL SURVEY ORGANISATION

Executive Director: Neil Williams

© Commonwealth of Australia 1997

ISSN: 1039-0073

ISBN: 0 642 25030 8

This work is copyright. Apart from any fair dealings for the purposes of study, research, criticism or review, as permitted under the Copyright Act, no part may be reproduced by any process without written permission. Copyright is the responsibility of the Executive Director, Australian Geological Survey Organisation. Inquiries should be directed to the **Principal Information Officer, Australian Geological Survey Organisation, GPO Box 378, Canberra, ACT, 2601.**

AGSO has endeavoured to use techniques and equipment to achieve results and information as accurately as possible. However, such equipment and techniques are not perfect. AGSO has not and does not make any warranty, statement or representation about the accuracy or completeness of any information contained in this document. **USERS SHOULD NOT RELY SOLELY ON THIS INFORMATION WHEN CONSIDERING ISSUES WHICH MAY HAVE COMMERCIAL IMPLICATIONS.**

# Contents

<b>SUMMARY.....</b>	<b>v</b>
<b>1. INTRODUCTION.....</b>	<b>1</b>
1.1 Survey Area.....	1
1.2 Climate.....	1
1.3 Physiography.....	2
1.3.1 Central Uplands.....	2
1.3.2 Carpentaria Plain.....	4
1.3.3 Kalpowar Plain.....	4
<b>2. GEOLOGY and MINERALISATION.....</b>	<b>4</b>
2.1 Geology.....	4
2.1.1 Dixie Area.....	7
2.1.2 Yambo Area.....	7
2.1.3 Sedimentary Rocks.....	8
2.2 Mineralisation.....	8
2.2.1 Silver.....	8
2.2.2 Gold.....	8
2.2.3 Copper.....	10
2.2.4 Lead and Zinc.....	10
2.2.5 Antimony.....	10
2.3 Recent Exploration History.....	10
2.3.1 Precious Metals.....	10
2.3.2 Base Metals.....	11
2.3.3 Tin.....	11
2.3.4 Heavy Minerals.....	11
2.3.5 Uranium.....	11
<b>3. SAMPLING, CHEMICAL ANALYSIS and DATA PROCESSING.....</b>	<b>12</b>
3.1 Sampling.....	12
3.2 Chemical Analysis.....	12
3.2.1 AGSO Analyses.....	14
3.2.2 ICP-MS Analyses.....	15
3.2.3 Bulk Cyanide Leach Analyses.....	15
3.3 Data Analysis.....	16
<b>4. STATISTICAL ANALYSIS.....</b>	<b>18</b>
4.1 Duplicate Samples.....	18
4.2 Summary Univariate Statistics.....	18
4.3 Summary Multivariate Statistics.....	19
4.3.1 Correlations.....	19
4.3.2 Factor Analysis.....	19
<b>5 INTERPRETATION.....</b>	<b>24</b>
5.1 Factor 1 (U, Ce, Th, Y, Nd, La, Nb, P, W, Zr and Hf).....	24
5.2 Factor 2 (Fe, V, Cu, Ni, Sc, Zn, Cr, Ti, Mn, As and Cd).....	34
5.3 Factor 3 (Rb, Ba, Sr, Be, Ga, Pb and Tl).....	43



5.4 Factor 4 (Sb, W, Sn, Mo and Ag).....	53
5.5 Factor 5 (Bi).....	56
5.6 Factor 6 (Pt, Pd and Au).....	56
5.7 Mineral Potential.....	60
5.7.1 Element Residuals.....	62
5.7.2 Additive Indices.....	62
5.7.2.1 Gold Index.....	62
5.7.2.2 Base Metal Index.....	64
5.7.2.3 Heavy Mineral Index.....	64
5.7.3.4 Porphyry Copper Index.....	64
5.7.3.5 Platinum Index.....	67
5.7.2.6 Uranium Index.....	67
<b>6. CONCLUSIONS.....</b>	<b>67</b>
<b>7 ACKNOWLEDGEMENTS.....</b>	<b>69</b>
<b>8 REFERENCES.....</b>	<b>70</b>
<b>APPENDICES A, B and C.</b>	

## SUMMARY

A regional stream sediment sampling program over parts of the Coen and Yambo Inliers and adjacent sedimentary rocks was carried out in association with geological and regolith mapping by the Australian Geological Survey Organisation and the Geological Survey of Queensland, under the National Geoscience Mapping Accord. The survey area covered parts of the HANN RIVER, COOKTOWN, WALSH and MOSSMAN 1:250 000 map sheet areas. The samples were analysed for 39 elements, including Au by the bulk cyanide leach method, and image maps showing the spatial distribution of each element and a number of statistically derived parameters, including factor scores, element residuals and additive indices, have been prepared. The full dataset is available separately, and colour versions of all image maps are available in a separate atlas.

Variability in the data can be accounted for by 6 factors with the most important being the accumulation of resistant minerals such as monazite and xenotime in the stream sediment (Factor 1), Fe geochemistry, either as Fe-rich minerals in the bedrock or as Fe scavenging in the secondary environment (Factor 2), and the weathering of K-rich minerals (Factor 3). Residual values for Cu, Pb, U and Zn, for which bedrock lithochemical contributions have been removed, showed areas which may be prospective for these elements.

The greatest potential appears to be for gold, base metals and tin, with some possibility for uranium and Rare Earth-rich heavy minerals.



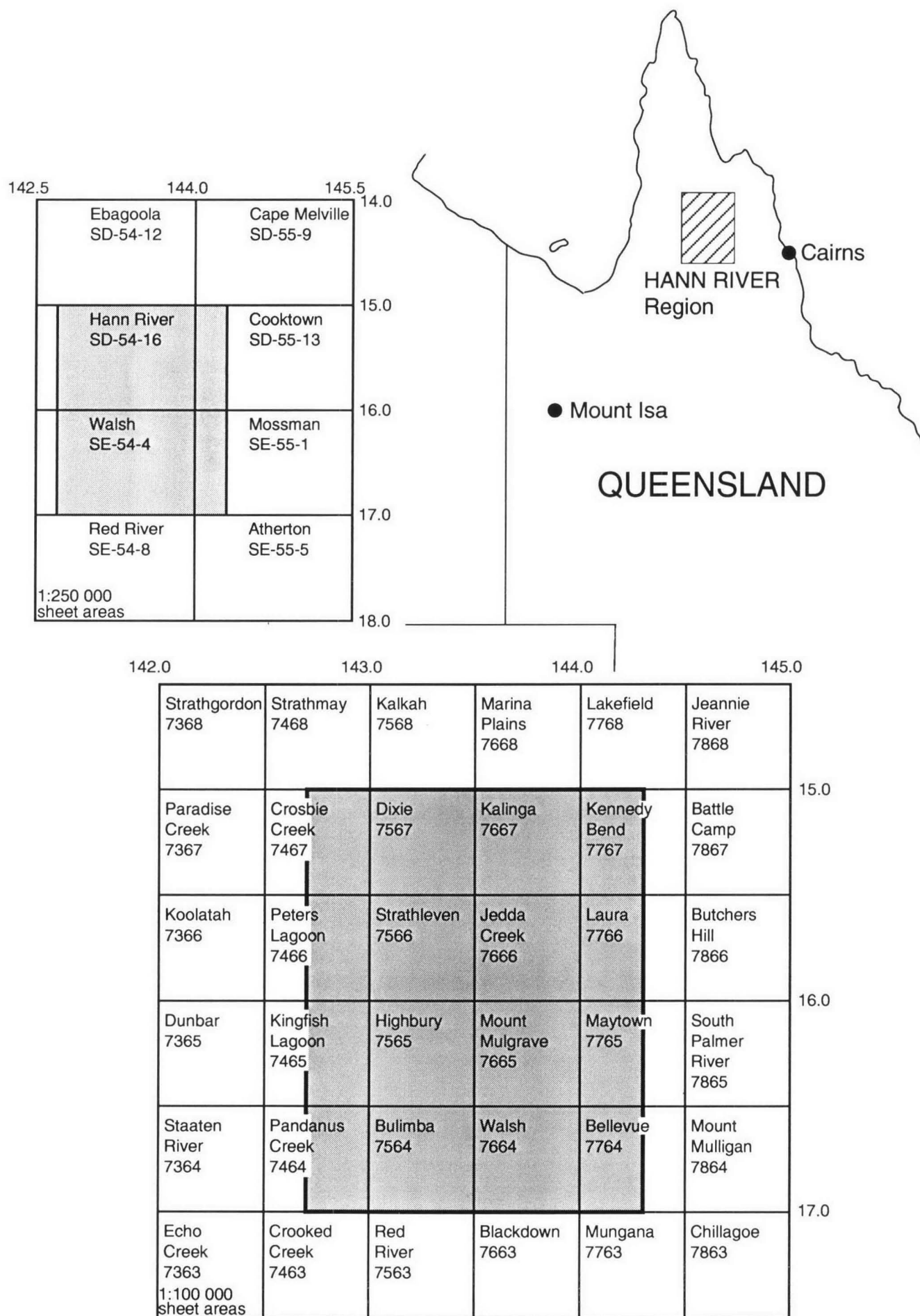


Figure 1. Location of the HANN RIVER REGION survey area.

# INTRODUCTION

This survey forms part of the North Queensland, National Geoscience Mapping Accord (NGMA) project undertaken by the Australian Geological Survey Organisation (AGSO) and the Geological Survey of Queensland (GSQ). The NGMA, endorsed by the Australian (now Australian and New Zealand) Minerals and Energy Council in August 1990, is a joint Commonwealth/State/Territory initiative to produce, using modern technology, a new generation of geoscientific maps, data sets, and other information on strategically important regions of Australia.

The project area covers Cape York Peninsula and extends from Charters Towers in the south to Normanton in the west and Cape York in the north, and includes the islands in the Torres Strait. The area has important mineral resources, for example the bauxite deposits at Weipa, but is also an area of world heritage value. The project was undertaken to provide the sound, current geoscientific data necessary for resolution of potentially conflicting land-use demands.

The 1993 field season centred on the HANN RIVER Region, essentially on those parts of the HANN RIVER and WALSH 1:250 000 map sheet areas and the western parts of the neighbouring COOKTOWN and MOSSMAN sheet areas (Figure 1), which cover the pre-Mesozoic granitic and metamorphic rocks of the geological Coen Region (formerly known as the Coen and Yambo Inliers).

## 1.1 Survey Area

Stream sediment sampling was carried out over most of DIXIE, JEDDA CREEK and MOUNT MULGRAVE, and parts of the CROSBIE CREEK, KALINGA, STRATHLEVEN, LAURA, Highbury, MAYTOWN, WALSH and BELLEVUE, 1:100 000 map sheet areas, which are components of the four 1:250 000 sheet areas listed above. The area is bounded by 15.0° and 17.0°S latitude, and 142.7° and 144.3°E longitude.

Land tenure in the area is almost exclusively pastoral holdings, including Bellevue, Fairlight, Gamboola, Imooya, Kalinga, Killarney, Kimba, King Junction, King River, Koolburra, Mount Mulgrave, New Dixie, Oroners, Palmerville, Pinnacles, Strathleven, Wrotham Park and Yambo stations. The area also includes several small gold mining leases.

The area is reasonably remote with the main regional access, the Peninsula Development Road, off to the east. This and the secondary access and station roads are usually impassable during the wet season due to the many river and creek crossings. Off-road vehicle and foot access is generally good in the pastoral leases because of tracks and fence lines pushed into remote areas by the pastoralists, and because of the cattle-paths along stream banks.

The township of Laura lies to the east of the survey area on the Peninsula Development Road, and is serviced by scheduled commuter flights.

## 1.2 Climate

The area has a semi-arid, monsoonal climate with heavy rains largely restricted (about 95%) to the period November-April. Average annual rainfall at Laura township is 903 mm. River and stream flow patterns closely follow rainfall (Bureau of Meteorology, 1971).

The mean maximum temperature at Laura for January is 34.5°C, and the mean July minimum is 16.3°C.



### 1.3 Physiography

The physiography of the survey area has been described in the explanatory notes accompanying each of the 1:250 000 geological maps listed above. Land-resource surveys by the CSIRO (Twidale, 1966; Galloway and others, 1970) includes descriptions of relief, soils, land-systems and vegetation. Trail and others (1968) and Wilmott and others (1973) describe the general physiography of the inlier areas, and Douth and others (1972) the physiography of the Carpentaria Basin to the west. The generalised physiography of the area is shown in Figure 2 (after Grimes and Whitaker, 1977), with the area sampled outlined. The regolith and landforms of the HANN RIVER sheet area have been mapped as part of the North Queensland Project's current program (Wilford and others, 1995).

There are three main physiographic regions in the survey area: the Central Uplands trending northwest to southeast across the area, the Carpentaria Plain to the west and southwest, and the Kalpowar Plain to the northeast. The area is drained by the Morehead, Hann and Kennedy Rivers in the northeast. These rivers rise in the uplands, flow through the Kalpowar Plain and discharge into Princess Charlotte Bay on the east coast. The remainder of the survey area is drained by the west flowing Mitchell River and its major tributaries, the Palmer, Lynd, Walsh, King and Alice Rivers. All except the King and Alice Rivers rise to the east or southeast of the survey area. The Mitchell River system has the highest mean annual discharge of any river in Queensland, and is one of the largest river systems in Australia. The Statten River drains the southwest corner of the area but its catchment was not sampled.

#### 1.3.1 Central Uplands

The Central Uplands have the highest elevations in the survey area, at 577 m in the Bald Hills in the MAYTOWN 1:100 000 sheet area. The Central Uplands comprise the Coleman Plateau, the Kimba Plateau, the Mulgrave Plain and the Palmer-Hodgkinson Uplands. Parts of the Deighton Tableland lie between the uplands and the plain to the northeast.

The **Coleman Plateau** (Wilmott and others, 1973) is at the northern end of the uplands in the survey area. It comprises gently undulating hills formed over pre-Mesozoic granitic and metamorphic rocks (rocks of the Dixie area, formerly known as the Coen Inlier). Elevation varies from about 100 m in the west, where the plateau merges with the Carpentaria Basin, to about 230 m in the east where a scarp drops into the Morehead Foothills and then the Kalpowar Plain. Drainage is broadly dendritic with smaller streams generally in flat, swampy valleys, and larger streams in more incised, V-shaped valleys. Access is good with many well maintained tracks.

The **Kimba Plateau** (Trail and others, 1968) lies to the southeast of the Coleman Plateau and has formed on deep, sandy soils at elevations of 200 m to 300 m. Local relief is very low with little or no obvious surface drainage and rainfall appears to permeate rapidly into the thick beds of loose sand. The area is named 'The Desert' on the KALINGA, STRATHLEVEN and JEDDA CREEK 1:100 000 topographic maps due to the lack of obvious drainage, but it has a thick coverage of tall trees. The area was not sampled.

The **Mulgrave Plain** also has formed over pre-Mesozoic granitic and metamorphic rocks (formerly the Yambo Inlier). It consists of undulating hills with ridges of resistant quartzite. It is similar to the Coleman Plateau in elevation and form, and also had generally good access. However, unlike most of the survey area the central and northern parts of the MOUNT MULGRAVE 1:100 000 sheet area were not used to run cattle commercially and therefore had few viable access tracks. Much of this area was sampled using a helicopter.

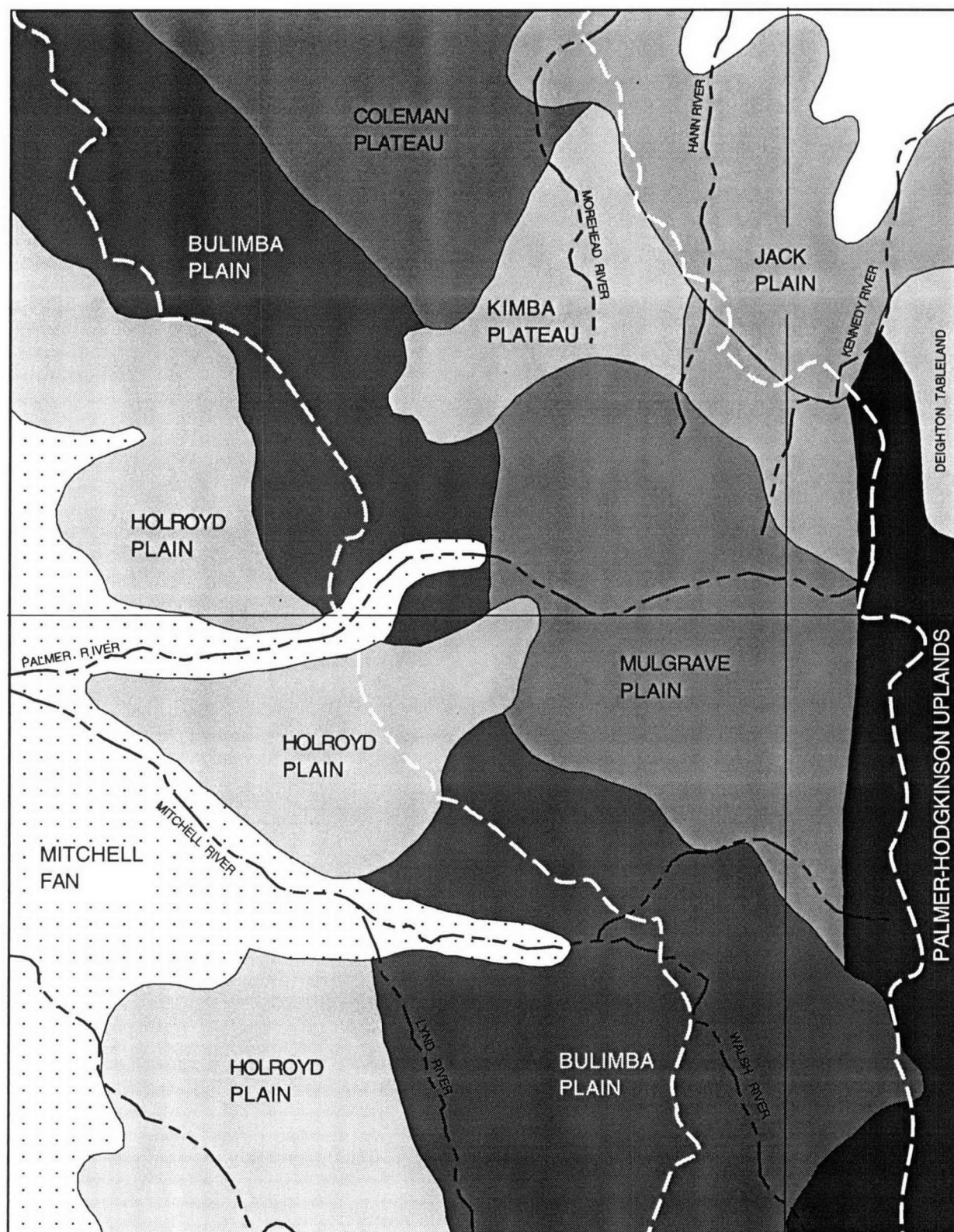


Figure 2. Physiography of the Hann River Region survey area. (after Grimes and Whitaker, 1977). White dotted line shows approximate boundary of area sampled.



The **Palmer-Hodgkinson Uplands** (Amos and Keyser, 1964) abuts the eastern end of the Mulgrave Plain and, in the survey area, have formed over the sediments and volcanics of the Chillagoe Formation, and over the sediments of the western margin of the Hodgkinson Formation. In this area the stony hills and ridges of the uplands are interspersed with prominent, dark-grey ridges and pinnacles formed from limestone bands common in the area resulting in a north-south, valley-ridge type, topography. Access into most areas was possible, but was controlled by the north-south topography.

The Coleman Plateau, Mulgrave Plain and Palmer-Hodgkinson Uplands are erosional surfaces, and so regolith probably formed in-situ. The Kimba Plateau is an 'old' land surface, possibly preserved because of the lack of surface drainage.

### 1.3.2 The Carpentaria Plain

The Carpentaria Plain slopes gently from the survey area to sea level on the Gulf of Carpentaria, about 140 km to the west. The plain comprises the Bulimba Plain, the Holroyd Plain and the Mitchell Fan. The Bulimba Plain is an erosional surface, the Holroyd Plain is an 'old' land surface and the Mitchell Fan is a depositional environment.

The **Bulimba Plain** lies over sandstone, siltstone, etc, of the Bulimba Formation and consists of a dissected plateau in the south of the survey area and gently rolling hills elsewhere. Access was good although in the northwest sampling was carried out over areas of the plain immediately adjacent to the pre-Mesozoic rocks only as stream development was poor.

The **Holroyd Plain** is to the west of the Bulimba Plain with elevation falling from 200 m in the east to about 100 m in the west. Local relief is low and the stream environment appears to be one of low energy with many streams inactive and choked with detritus (Doutch and others, 1972). Stream development was generally very poor and large areas were infested with rubber vine. The plain was not extensively sampled.

The **Mitchell Fan** is more developed to the west and with local relief of generally less than 2 m stream development was almost non-existent. This area was not sampled.

### 1.3.3 The Kalpowar Plain

The Central Uplands are generally bounded in the east by a steep scarp which drops from the Coleman Plateau into the Morehead Foothills, and passes into the rolling hills of the Jack (erosional) and Normanby (depositional) Plains.

The **Morehead Foothills** are a narrow belt of hills which rise from the Jack Plain east of the Coleman Plateau and have been formed by the retreat of the scarp (Whitaker and Grimes, 1977).

The **Jack Plain** is similar to the Holroyd Plain though relief can be greater. Access was adequate although the area was not extensively sampled.

The **Normanby Plain** comprises merging alluvial flood plains and was of little interest.

---

## GEOLOGY and MINERALISATION

### 2.1 Geology

The following is a brief account of the principal features of the surficial geology of the survey area, which covers parts of four (4) 1:250 000 geological map sheet areas, namely HANN RIVER, WALSH, COOKTOWN and MOSSMAN.

In 1993 the NGMA's North Queensland Party remapped the metamorphic and igneous rocks, and regolith, of the HANN RIVER (Blewett and Wilford, 1995 and 1996) and WALSH (Bultitude and Rees, 1996) 1:250 000 sheet areas. GSQ has remapped the MOSSMAN (Bultitude and others, 1996) and the COOKTOWN (Domagala, in prep) sheet areas. AGSO and GSQ are in the process of compiling a synthesis volume and accompanying colour atlas covering the Cape York Peninsula.

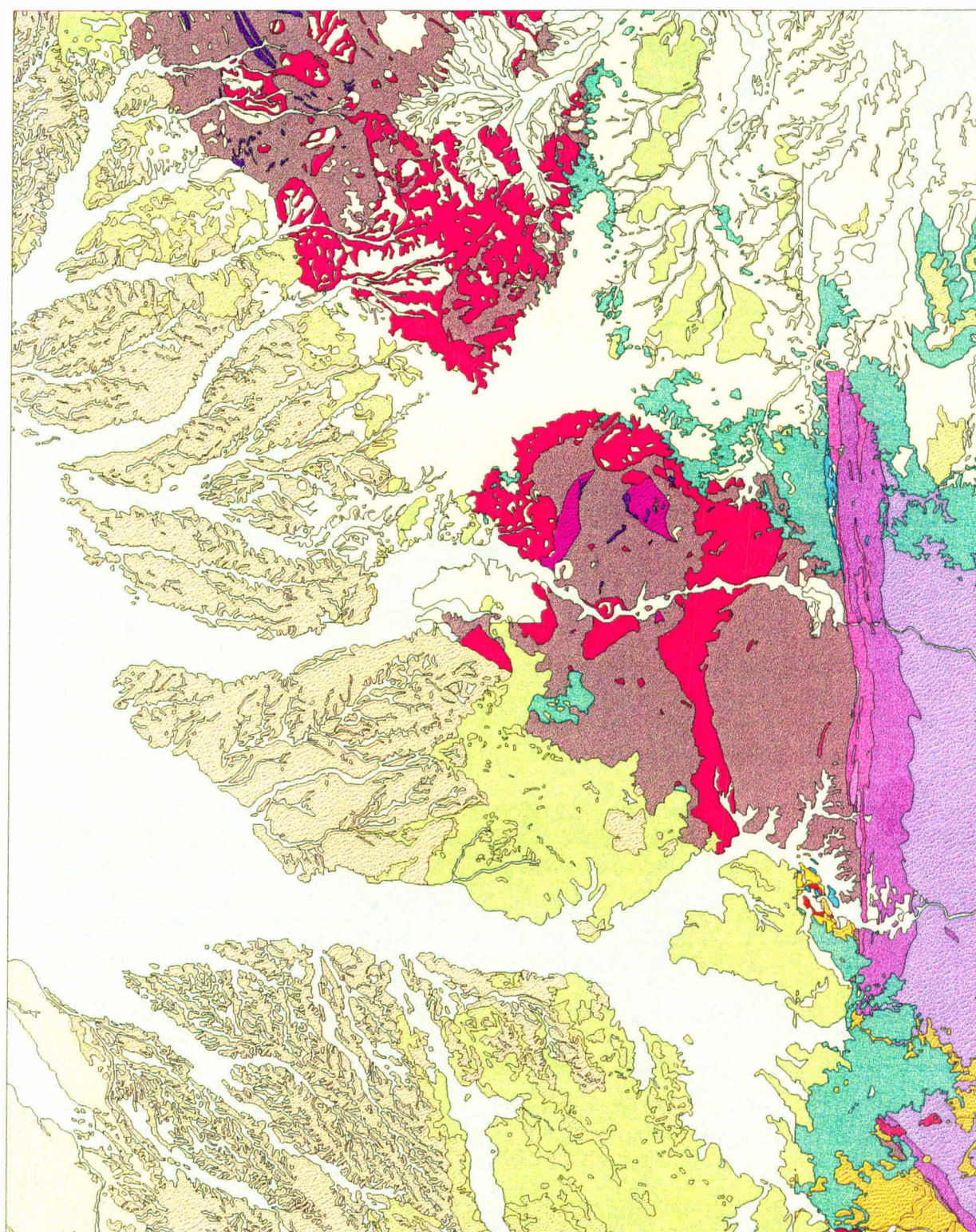
For a more detailed account of the geology and mineralisation of the survey area refer to the following AGSO and GSQ maps, bulletins and records:

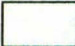
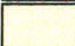


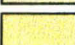
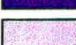
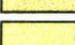

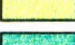
- Amos and Keyser, 1964 - geology of the MOSSMAN 1:250 000 sheet area
- Lucas and Keyser, 1965 - geology of the COOKTOWN 1:250 000 sheet area
- Keyser and Lucas, 1968 - geology of Hodgkinson and Laura Basins
- Trail and others, 1968 - igneous and metamorphic rocks
- Douth and others, 1972 - geology of the Carpentaria Basin
- Willmott and others, 1973 - igneous and metamorphic rocks of the area
- Oversby and others, 1975 - regional geology
- Whitaker and Grimes, 1977 - geology of the HANN RIVER 1:250 000 sheet area
- Grimes and Whitaker, 1977 - geology of the WALSH 1:250 000 sheet area
- Lam and others, 1991 - mineral occurrences, MAYTOWN 1:100 000 sheet area
- Culpeper and Burrows, 1992 - mineral occurrences, HANN RIVER 1:250 000 sheet area
- Culpeper and others, 1992 - recent exploration history
- Blewett and others, 1994 - pre-Mesozoic geology of the HANN RIVER 1:250 000 sheet area
- Denaro and others, 1994 - mineral occurrences, Laura 1:100 000 sheet area
- Blewett and Wilford, 1995 - geology of the HANN RIVER 1:250 000 sheet area, map
- Wilford and others, 1995 - regolith of the HANN RIVER 1:250 000 sheet area, map
- Blewett and Wilford, 1996 - geology of the HANN RIVER 1:250 000 sheet area, commentary
- Bultitude and Rees, 1996 - geology of the WALSH 1:250 000 sheet area
- Bultitude and others, 1996 - geology of the MOSSMAN 1:250 000 sheet area
- Bultitude and others, 1997 - geology of the Hodgkinson Basin, map
- Domagala, in prep - geology of the COOKTOWN 1:250 000 sheet area
- Bain and Draper (Editors), in prep - North Queensland Geology

The geology described below is condensed from the most recent maps and the draft of the synthesis volume (Bain and Draper, in prep).

Geochemically the most interesting rocks cropping out in the survey area are the Silurian-Devonian granites and Proterozoic metamorphics of the Coen Region (formerly the Coen Inlier), which occupy the northern-central part of the HANN RIVER sheet area, and south-eastern part of the HANN RIVER, and northeastern part of the WALSH sheet areas (formerly the Yambo Inlier). As there is little geological or geochemical difference between the rocks of the two 'inliers', these have been combined as the Coen Region. They are flanked in the east by the sediments and mafic volcanics of the Chillagoe Formation in the MOSSMAN and COOKTOWN sheet areas. The generalised geology of the area is shown in Figure 3. The granitic and metamorphic rocks north of the 'Desert' (the southern Coen Inlier) will be referred to as the rocks of the Dixie area, while those south of the 'Desert' (Yambo Inlier) will be referred to as the rocks of the Yambo area.





	Alluvial quartzose sand, silt and clay		Silurian/Devonian Granites of the Kintore and Flyspeck Supersuites
	Residual quartzose and ferruginous quartz sand		Proterozoic metamorphic rocks
	Wyaaba Beds		Greenstones
	Bulimba Formation		Hodgkinson Formation
	Rolling Downs Group		Chillagoe Formation
	Gilbert River Formation		

**Figure 3.** General geology of the Hann River Region.



### 2.1.1 Dixie Area

The granites are extensions of the Kintore (S-type) and Flyspeck (I-type) Supersuites in the EBAGoola 1:250 000 sheet area to the north (Mackenzie and Knutson, 1992; Mackenzie and others, 1992; Cruikshank, 1994).

The **Kintore Supersuite** is further divided into the equigranular to sparsely porphyritic muscovite-biotite granites of the Ebagoola Suite, which, by area, is the more important, and the less felsic, abundantly porphyritic, muscovite-biotite granites of the Lankelly Suite. The Ebagoola Suite consists of the Mena (felsic and mafic phases), Bunira, Culpin, Ingleby, Dixie, Goanna, Pelican Creek, Ukin, Imooya, Kintore, Burton Lagoon and Morehead Granites, whereas the Lankelly Suite consists only of the Turtle Swamp Granite. A number of unassigned granites (Pine Tree, King Junction, Artella, Strathleven, Terrible Creek, Fish Creek and Warner Granites) also occur in the area. Accessory minerals include zircon, monazite, iron oxide(s) and apatite.

The **Flyspeck Supersuite**, consisting of the Gumhole, Alberts Creek, Watch Branch and Wulpan Monzogranites, and the Yellowwood, Artemis and Permana Granodiorites, vary from strongly porphyritic to even grained. Accessory minerals include allanite, titanite, zircon apatite and rare monazite.

To the west the metamorphics are schists, gneisses, quartzites, metasediments and metabasics of the **Holroyd Group**. In the east are gneisses and quartzites of the **Newberry Metamorphic Group**. As with the granites, both groups are extensions of rocks in the EBAGoola sheet area (Blewett and others, 1992). The Holroyd Group consists of the Strathburn Formation, Gorge Quartzite, Newirie Formation, Carew Greenstone, Carysfort Quartzite, Astrea Formation, Sugarbag Creek Quartzite and the Dinah Formation, while the Newberry Metamorphic Group consists of Penny, Kitja and Kimba Gneisses.

### 2.1.2 Yambo Area (including Chillagoe and Hodgkinson Formations)

The Yambo area granites also belong to the Kintore Supersuite and are divided into the medium-grained, abundantly porphyritic, muscovite-biotite granites of the Aralba Suite, the medium-grained, slightly porphyritic, biotite-muscovite granites of the Fish Creek Suite, and the medium-grained, variably porphyritic, biotite-muscovite granites and granodiorites of the Lukinville Suite. The **Aralba Suite** consists of Top Pinnacle, Lilyponds, Kingvale, Kopu, Chevy Creek, Wongu, Kokomini, Laia and Aralba Granites. The **Fish Creek Suite** consists of the Fish Creek and Terrible Creek Granites, and the **Lukinville Suite** of Rocky King and Fernhill Granites, and the Lukinville Granodiorite.

The metamorphics are schists and gneisses of the **Yambo Metamorphic Group**, including the Daintree, Chelmsford, Arkara and Pombete Gneisses, the Twelve Mile, Kokojelandji, Jeddah, Saraga, Rosser, Annie Creek and Oswald Schists, and the Chuko Quartzite.

The **Chillagoe Formation** consists of sediments varying from mudstone to conglomerate, plus chert, fossiliferous limestone, basaltic tuff and metabasalt. The sediments trend north-south just east of the western margin of the COOKTOWN and MOSSMAN sheet areas, and contain some Cu mineralisation (Amos and Keyser, 1964).

The **Hodgkinson Formation** lies to the east and south of the Chillagoe Formation. The beds comprise greywacke, siltstone, chert, conglomerate, limestone and some mafic volcanics. In the west the formation also hosts minor Cu mineralisation.

### 2.1.3 Sedimentary rocks

Areas in the west of the survey area, and between and around the two inliers, are covered by the ubiquitous sediments of the Wyaaba Beds, the Rolling Downs Group and



the Gilbert River Formation. Other areas are covered by sediments consisting of residual, colluvial and alluvial sands.

As the scales of the images used in this record (approximately 1:1 500 000) and in the associated atlas (1:750 000) preclude showing the boundaries of most rock units, the areas underlain by each of the rock units can be seen in the respective 1:250 000 geology maps. These can be purchased from the AGSO and GSQ sales centres. Analyses of rock units of interest were extracted from AGSO's ROCKCHEM database, copies of which can be purchased from the AGSO sales centre.

## **2.2 Mineralisation**

A general overview of mineralisation in the region is given in Bain and others (1990), and in the commentaries for the 1:250 000 geological map sheets. The MINLOC Database (Bureau of Resource Science/AGSO) lists 84 mines, abandoned mines, prospects and mineral occurrences in, or immediately adjacent to, the survey area (Figure 4). Overall these occurrences contain, as major constituents, Ag (12 occurrences), Au (47), Bi (1), Cu (20), Ni (1), Pb(7), Sb (20) and Zn (7), plus a number of non-metallic mineral occurrences such as ilmenite, mica, monazite, rutile, xenotime and zircon. The distribution of Ag, Au, Cu, Pb-Zn and Sb occurrences are shown in Appendix A.

Most occurrences are of historical interest only, or are small and therefore sub-economic to uneconomic. The only active mining seen in the area during the period of the survey were a small gold mine at the junction of the Alice River and Dickies Creek, near Imooya homestead in the DIXIE 1:100 000 sheet area (reported to have ceased operation during the period of the field work), and a small (3-4 man) gold dredging operation in the bed of the Palmer River west of the Palmerville Road crossing in the JEDDA CREEK 1:100 000 sheet area.

### **2.2.1 Silver**

Silver occurrences in or near the survey area are shown in Figure A1 in Appendix A. No active mining for Ag alone appears to have occurred, although about 257 kg of Ag were recovered from the King Vol Pb-Zn mine (Amos and Keyser, 1964).

### **2.2.2 Gold**

Gold occurrences are shown in Figure A2 (Appendix A). These do not include alluvial workings in the Palmer River.

The main gold mining area was the Palmer Gold and Mineral Field (Amos and Keyser, 1964; Lucas and Keyser, 1965), the most productive part of which lies in the MOSSMAN and COOKTOWN sheet areas east of the Palmer River-Fish Creek junction, to the east of the survey area. The field was discovered in 1872 with mining peaking in 1875, and thereafter declining rapidly to all but cease by the turn of the century. Since then a number of dredging operations have been carried out as far west as Strathleven. About 40,000 kg of gold were reported to have been recovered, with about 90 percent of this from alluvial mining, although many gold-bearing quartz reefs were found and mined mostly near Maytown township.

The Alice River Mining Field (Cameron, 1906) was discovered in 1903 and worked from 1904 to 1909. Total recorded production to 1917 is about 93 kg. The lode comprised two main reefs hosted by Kintore Granite. The small operating mine mentioned above would be in this field.

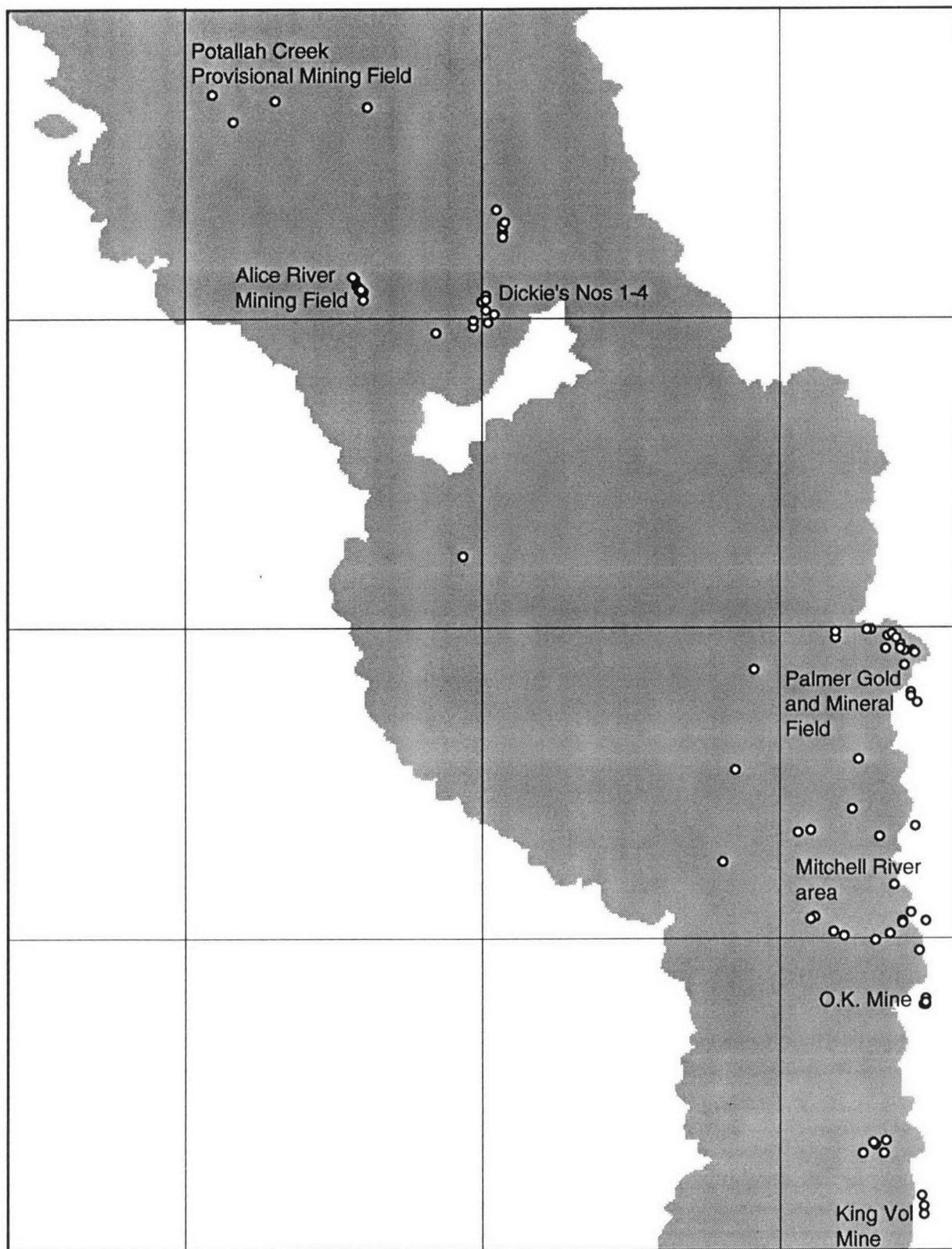


Figure 4. All mineral occurrences (N = 84) in, or immediately adjacent to, the HANN RIVER Region survey area (after MINLOC, December, 1994).

Perseverance, a single reef in Holroyd Metamorphics, has been worked at the Potallah Creek Provisional Mining Field (Cameron, 1906) yielding about 18 kg of gold in 1903-4. An attempt to reopen the mine in 1946 appears to have been unsuccessful (Whitaker and Grimes, 1977).

Minor alluvial gold was found in St George River, a tributary of the Mitchell River just east of the survey area. In 1981 5000m<sup>3</sup> of alluvium from the Mitchell River near Mount Mulgrave homestead were processed for 1 kg of gold as part of a testing program (Culpeper and others, 1992).

### **2.2.3 Copper**

Copper occurrences are shown in Figure A3 of Appendix A. Few are of any economic significance.

Several minor occurrences of copper oxides and carbonates, usually associated with metabasalts, have been reported in the Chillagoe Formation north of Palmerville in the COOKTOWN sheet area (Lucas and Keyser, 1965).

The O.K. Mine(s), 10 km southeast of the Bellevue homestead in the MOSSMAN sheet area, were discovered in 1901 and worked during several periods until 1942 (Amos and Keyser, 1964). About 7,600 tonnes of Cu were recovered. The deposit occurs in sediments of the Hodgkinson Formation immediately east of the survey area.

### **2.2.4 Lead and Zinc**

Figure A4 in Appendix A shows Pb-Zn occurrences. Most are mineral occurrences only and the only mine in or near the survey area, the King Vol about 20 km southwest of the Nychum homestead in the MOSSMAN sheet area, was discovered in 1899 (Amos and Keyser, 1964). Little is known of its operations immediately after its discovery, but the mine produced about 360 tonnes of Pb and 257 kg of Ag between 1922 and 1925.

Sites in the north are mineral occurrences and sub-economic prospects in the Potallah Provisional Mining Field.

### **2.2.5 Antimony**

Antimony occurrences are shown in Figure A5 in Appendix A. As with most other commodities in the survey area these are mostly mineral occurrences only.

## **2.3 Recent Exploration History**

The recent exploration history (1969-90) of the survey area is detailed in Culpeper and others (1992).

### **2.3.1 Precious Metals**

Most activity has centred on the search for alluvial gold in the Palmer River between Palmerville and west of Strathleven homestead. This included the delineation of paleochannels and of terraces and bars by airborne reconnaissance and air photo interpretation. Gravel terraces up to 2 km from the present river channel were found but proved to be uneconomic. Techniques used included stream sediment sampling, pan concentrate sampling, auger, churn and rotary drilling, and pitting and costeaning by backhoe. Results varied from disappointing to encouraging, although some of the latter results were downgraded during follow-up testing by poor recovery rates due to the fineness of the gold.

Work has also been carried out in the Mitchell River, the King River, in the headwaters of the Kennedy and Morehead Rivers, in the former Alice River Mining Field and at Potallah Creek. Most areas gave shows of gold, but several promising areas were relinquished

because parts of the target areas were under existing (unworked?) mining leases. One exploration program at Potallah Creek targeted gold and platinum, the latter from possible Proterozoic greenstones. However, the results were disappointing and the greenstones were interpreted as submarine basalts.

Interest in exploration for gold continued through the 1980's.

### **2.3.2 Base Metals**

Exploration for base metals near Mount Mulgrave homestead and to the north-west between the Mitchell and Palmer Rivers, and in the area between the Palmer and King Rivers has been unrewarding with several areas of apparent Zn anomalies ultimately being attributed to normal background levels for different rock units. Cu and Pb values were low. High W values were found in the headwaters of the King River, but no mineralisation was found.

In the Dixie area exploration for base metals centred largely on the Crosbie and Potallah Creeks area. The Gossan Prospect, containing about 50 000 tonnes of Cu-Pb-Zn ore has been evaluated several times but remains uneconomic. Several occurrences of Cu-Ni mineralisation have been found, usually related to ultramafics, but are also uneconomic. The Copper Prospect (Cu-Ni) and Dickies No.1 and 2 (Sb-Au-Ag) were converted to mining leases in 1972 but did not progress beyond this.

Interest in exploration appears to have waned after the mid 1980's.

### **2.3.3 Tin**

Alluvium containing cassiterite was found east of the Alice River Mining Field in the early 1970's. However the volume of alluvium was too small to be economic. Later exploration for alluvial gold in part of the same area showed no gold but minor cassiterite.

Interest was never strong, and all but ceased after the mid 1970's.

### **2.3.4 Heavy Minerals**

Early exploration in tributaries of the Mitchell River confirmed the presence of monazite, xenotime, zircon and rutile but grades were not high and the volume of prospective alluvium was too low to have economic potential. Similarly, work in the Palmer River between Strathleven and Drumduff and west of Palmerville, and in the Alice and Morehead River systems, indicated little or no economic potential for these areas.

Areas near the King River, between King Junction and Pinnacles homesteads, showed some potential with concentrates containing up to 2.45% Ce, 1.16% La and 0.77% Y, but the authority was relinquished in 1989.

Despite the lack of success, interest in heavy minerals remained relatively strong throughout the 1980's.

### **2.3.5 Uranium**

Exploration for U has been unrewarding, and interest fell away during the latter part of the 1980's. Several companies followed-up high U/Th ratios recorded by a BMR airborne survey in 1971, but these, and other ground radiometric anomalies, appear to be due to concentrations of Th and U-bearing resistant minerals such as monazite. Areas explored include south of, and near, Mount Mulgrave homestead, between the Mitchell and Palmer River east of the homestead, near the King River and in the headwaters of the Morehead River.



---

## **SAMPLING, CHEMICAL ANALYSIS and DATA PROCESSING**

### **3.1 Sampling**

The sampling program was regional in concept and was based on an average sample density of one sample per 10 to 15 km<sup>2</sup>. The aim was to cover as much of the survey area as possible, including some areas overlying sedimentary rocks. Major drainage basins were outlined on 1:100 000 topographic maps and sample sites positioned to give basins of the required average size while ensuring good coverage of important rock units, specifically the granitic and metamorphic rocks in the Dixie and Yambo areas.

For the first 9 weeks of the sampling program sample sites were accessed by 4-wheel drive vehicle with occasional walks into sample sites in more rugged, or otherwise isolated, terrain. Each sampling team was equipped with a Magellan Nav 1000 Pro Global Positioning System (GPS) for navigation and site location. During the sampling program twenty-four hour GPS coverage was available in 2-D mode.

This was followed by a helicopter sampling program of one week duration. The Bell Jet Ranger II helicopter was equipped with a Pronav GPS100 for navigation. Three or four samplers were dropped in sequence at sample sites and then leap-frogged to new sites as available. The helicopter was used to access the more rugged and/or remote areas in the BLACKDOWN and MUNGANA (samples included in the RED RIVER Region Survey - Cruikshank, 1997), and WALSH and MOUNT MULGRAVE sheet areas.

At each sample site two size fraction samples were collected. The first was 50 to 70 g of -180  $\mu$ m (-#80 mesh) fine sediment stored in a plastic vial and is considered to be the 'standard' sieved stream sediment for the region (Rossiter, 1975). The second was 5-6 kg of -1 mm coarse sediment doubled bagged in large plastic sample bags and was collected specifically for bulk cyanide leach determination of Au (+Pd and Pt), and for possible heavy mineral analysis. Where possible sieving was carried out at the sample site using aluminium bodied sieves fitted with nylon bolting cloth to minimise contamination. Wet samples were placed in plastic trays on return to base camp, dried in the sun and sieved. The fine sediment was pulverised further using motor driven mortar grinders fitted with agate vessels.

Duplicate samples (labelled as splits A and B) were collected at a number of sites to test the reproducibility of the sampling. These were analysed separately, but for many of the statistical tests and mapping exercises the average value of the two splits was used.

A total of 1191 sites were sampled (Table 1), including 25 in duplicate. The sample sites and a map of the area sampled are shown in Figure 5. The area covered is approximately 16,000 km<sup>2</sup>.

Residual portions of all samples are archived at AGSO.

### **3.2 Chemical Analysis**

The fine sediment was analysed for 31 elements in AGSO's Geochemical Laboratory using X-ray Fluorescence Spectrometry (XRFS). An aliquot of the fine sediment was split off and sent to Analabs in Perth for analysis of 9 elements by Inductively-Coupled Plasma/Mass Spectrometry (ICP-MS).

A 2 kg aliquot of each coarse sample was split off and sent to Australian Laboratory Services (ALS) in Brisbane for Bulk Cyanide Leach (BCL) analysis of Au. Pt and Pd were included for screening purposes although the BCL method is generally considered as not completely suitable for Pt (only about 20% extraction?).

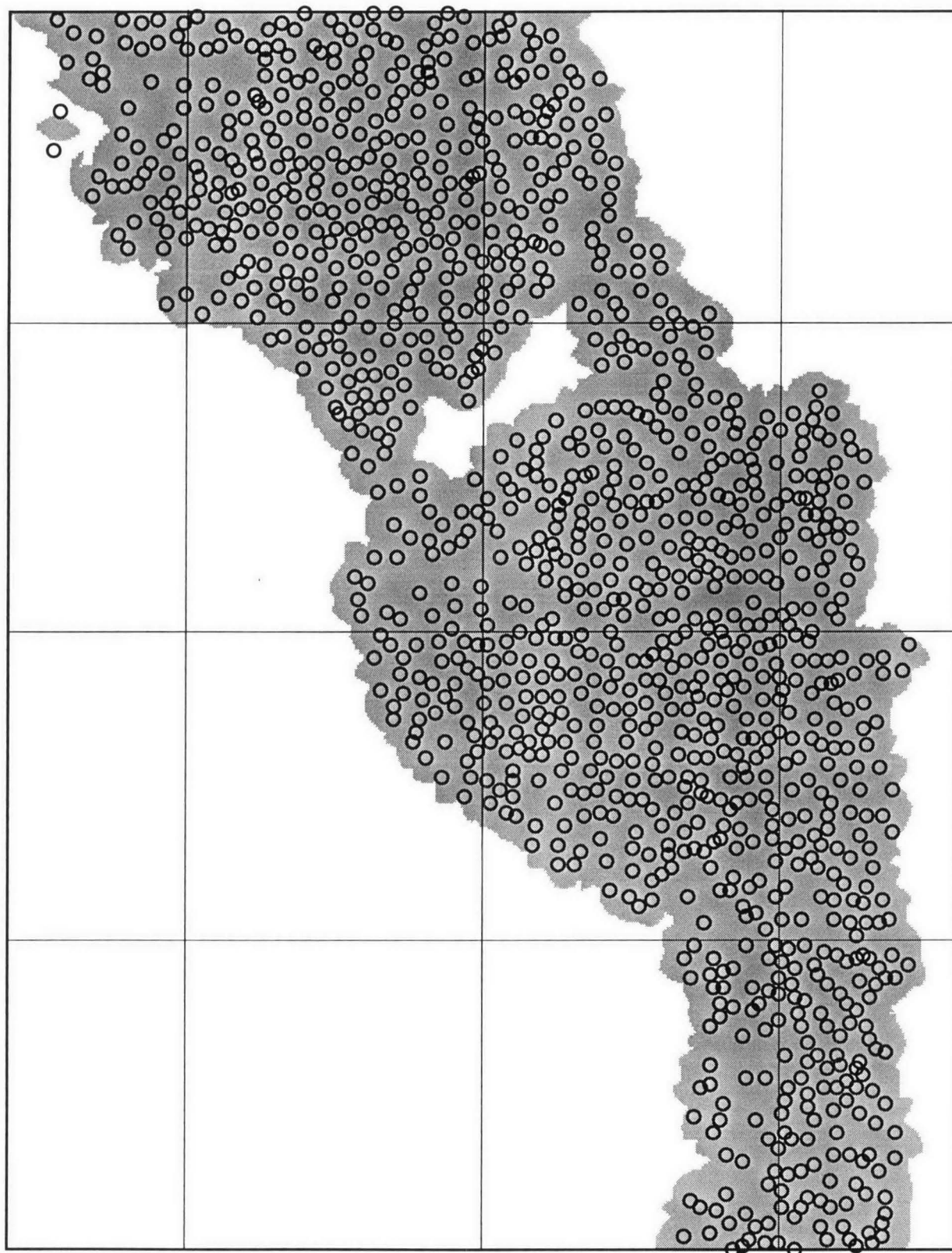


Figure 5. Sample sites (N=1183) for the Hann River Region survey.

**Table 1.** Map sheet areas sampled. All maps are in Series R631, Edition 1-AAS, Australian Geodetic Datum 1966 (Royal Australian Survey Corps).

Sheet name(Number)	Number of samples	Sample numbers
Crosbie Creek (7467)	53	6301-6374
Dixie (7567)	226	6001-6244
Kalinga (7667)	99	6601-6705
Strathleven (7566)	90	5301-5419
Jedda Creek (7666)	197	5001-5205
Laura (7766)	49	5601-5700
Highbury (7565)	40	4301-4400
Mount Mulgrave (7665)	198	4001-4222
Maytown (7765)	83	4601-4720
Walsh (7664)	65	3001-3087
Bellevue (7764)	91	3601-3724

Samples are prefixed by 9302

### 3.2.1 AGSO analyses

Thirty-one elements (As, Ba, Bi, Ce, Cr, Cu, Fe, Ga, Ge, Hf, La, Mn, Mo, Nb, Nd, Ni, Pb, Rb, Sc, Se, Sn, Sr, Ta, Th, Ti, U, V, W, Y, Zn and Zr) were analysed for by XRFS.

Sample powder was mixed with a binder and pressed into a 40 mm diameter pellet. After air-drying, the pellet was analysed using Philips PW1404 and PW1450 X-ray spectrometers with 72 and 60 position sample changers, respectively. Raw count-rates were corrected for inter-element and mass-absorption effects and converted into element concentrations using the methodology of Norrish and Chappell (1977). Analysis was in 3 separate runs determined by the X-ray tube used, the inter-element corrections necessary and the excitation conditions used. The instrument runs are listed in Table 2.

**Table 2.** Analytical runs for XRFS listing tube target, and tube voltage and current. Values in parenthesis are detection limits in ppm.

	1	2	3
Tube target	Mo	Au	Au
Voltage (kV)	190	90*/60	60
Current (mA)	30	30*/40	40
	Th (2)	Sn (2)*	Fe (1000)
	Rb (1)	Nb (2)*	Ti (5)
	Pb (2)	Zr (1)*	Mn (2)
	Y (1)	Mo (2)*	V (2)
	Sr (1)	Ni (1)	Cr (1)
	U (0.5)	Cu (1)	Ba (4)
	Se (1)	Zn (1)	La (2)
	Ga (1)	Hf (2)	Ce (5)
	As (0.5)	Ta (2)	Nd (2)
	Bi (2)		Sc (1)
	W (3)		
	Ge (0.5)		

Two samples from those collected in the 1990 program (and subsequently labelled CY-1 and CY-2) had been used as temporary XRFS secondary standards and were analysed with each batch of the HANN RIVER samples. Estimated from these replicate analyses, the analytical precision (1s level) for most elements was better than +/-8% for concentrations about 10 ppm, better than +/-4% between 20 and 100 ppm, and less than +/-2% at concentrations greater than 100 ppm. Precision for XRFS Runs 1 and 2 was consistently better by a factor of about 2 than that for Run 3, which involved measurements at long wavelengths (>1.74A) and used an Fe corrected mass absorption coefficient.

Full descriptions of the methodology used are given in Cruikshank and Pyke (1993).

### **3.2.2 ICP-MS Analyses**

Several of the 31 elements listed above, for example Bi, Mo and W, gave few detectable values by XRFS. Analabs offer an ICP-MS method (Code GI201) involving a HClO<sub>4</sub>/HCl/HF total digestion and detection limits an order of magnitude or more better than XRFS and AAS. Aliquots of the fine sediment samples were split off and sent for analysis by this scheme. Several elements not in the original list were added. The elements analysed, with detection limits (ppm) in parenthesis, were Ag (0.1), Be (0.1), Bi (0.1), Cd (0.1), Mo (0.1), P (20), Sb (0.05), Ti (0.5) and W (0.1). The initial Ag results were called into question and were repeated.

The sensitivity and ability to analyse for most naturally occurring elements makes the ICP-MS technique highly suitable for environmental geochemical studies.

### **3.2.3 Bulk Cyanide Leach Analyses**

The Bulk Cyanide Leach (BCL) method has become a de facto standard for the detection of Au mineralisation. Its advantages include the ability to detect the ultra fine grain size of Au common to epithermal deposits, and the large sample weight (1-10 kg) used gives very low detection limits at the ppt level (Elliot and Towsey, 1989). Unfortunately methodology for both sampling and analysis varies greatly starting with the coarseness of the material collected, through the use of static or dynamic leaching, and ending with the analytical method used to determine Au in the cyanide solution. It was intended that all coarse samples collected during the life of the North Queensland Project will be of the same size fraction, that is -1 mm, and that the same laboratory also would be used, if possible. Fortunately, this was the case.

After examining technical details of commercially available methodology Australian Laboratory Services (ALS) in Brisbane were chosen and the 2 kg aliquots were analysed by their method PM216. Although the extraction of Pt is reputed to be as low as 20% by BCL, both Pt and Pd were included in the analyses for screening purposes.

The analytical data, along with location data, were collated into a flat ASCII data files in MS-DOS format for data analysis. For distribution the dataset was divided into two files representing the northern (HANN RIVER and COOKTOWN sheet areas) and southern (WALSH and MOSSMAN sheet areas) parts of the survey area, and copies of the data file (CY93ASGD and CY93BSGD respectively) are available from:

AGSO Sales Centre  
GPO Box 378  
CANBERRA ACT 2601  
AUSTRALIA  
Phone: (06) 2499519  
Fax: (06) 2576466  
Email: sales@agso.gov.au



### 3.3 Data Analysis

The large quantity of data resulting from a regional geochemical survey can be reduced to more manageable proportions by the application of univariate and multivariate statistical methods to describe the behaviour of the elements and their inter-element relationships. Similarly, the spatial distribution of the elements can be shown by either using a digitised representation of each sample's drainage basin coloured (or greyscaled, patterned, etc) according to the concentration of the element in the sample (Bonham-Carter and others, 1987; Cruikshank, 1990), or as images prepared from data systematically grided from the essentially random data (sample) points of the survey (Eggo and others, 1990, 1995; Cruikshank, 1994; Cruikshank and Butrovski, 1994). The former honours the spatial integrity of the data but is time consuming to implement, while the later is quick and, with care, sufficiently spatially honest to adequately show regional geochemical distribution patterns.

Basic univariate and multivariate statistics for the dataset were estimated using proprietary software on an IBM-compatible micro-computer.

More detailed univariate and multivariate analyses of the data, including multiple and stepwise regression and principal component factor analysis, were made using STATVIEW II (Abacus Concepts, Berkeley, California) and DATA DESK IV (Odesta Corporation, Northbrook, Illinois) running on an Apple Macintosh II computer. DATA DESK IV also allowed a more visual/intuitive approach to data analysis. These programs also produced tables and graphs (histograms, scattergrams, etc) which were cut and pasted into CANVAS 3.5 (Deneba Software, Miami, Florida) for sizing, annotation and printing. Line maps and diagrams were also produced on CANVAS.

Locations on the Australian Map Grid (AMG) were converted to Latitude/ Longitude using a proprietary program so that plots could cross zone boundaries. XYZ data for each element (X=Longitude, Y=Latitude, Z=Element value) were grided using GRID from SURFER V4 (Golden Software, Golden, Colorado) on an IBM-compatible computer. Eight equal area panels bounded by longitudes 142.70°, 143.50° and 144.30°, and latitudes 15.00°, 15.50°, 16.00°, 16.50° and 17.00° (each 321 columns by 201 rows, or 64,521 grid points) were grided since GRID could produce only 65,536 grid points per grid file. The grid files for the 8 panels were seamlessly combined to give a working grid file with the parameters shown in Table 3.

Table 3. Parameters for HANN RIVER Region grid files.

Longitude	minimum	142.70°
	maximum	144.30°
Latitude	minimum	15.00°
	maximum	17.00°
Grid spacing		0.0025°
No. of columns		641
No. of rows		801
Interpolation method		Kriging
Search radius		0.050°
Nearest neighbours		10

A location approximating to the geometric centre (centroid) of each sample basin was used in preference to the sample site as this more accurately represents the spatial relationship between drainage basins, and reduces the possibility of averaging effects on

data points which may be close together although actually representing widely spaced drainage basins. This later effect is a significant problem when gridding data from low density sampling programs (Eggo and others, 1990, 1995). A buffer zone, equivalent to 0.05° of latitude, along the southern margins of the STRATHMAY, KALKAH and MARINA PLAINS 1:100 000 sheet areas, which lie immediately to the north of the HANN RIVER Region (EBAGoola Survey - Cruikshank, 1994), and along the northern margins of the BLACKDOWN and MUNGANA 1:100 000 sheet areas (RED RIVER Region - Cruikshank, 1997), which lie immediately to the south of the HANN RIVER Region, were included in the raw element data to be grided to enhance continuity with images from the previous surveys. No buffer was added for images of statistically derived parameters since these were estimated from data for the HANN RIVER Region only. Grid files were converted to 8-bit (0-255) 'image' files by 'slicing' (classification) into 9 ranges based on preset proportions of the number of non-zero values (Table 4). All grid points more than the distance equivalent to 0.050° (about 5.5 km) from any sample point have been assigned a value of zero and a colour of white. The conversion programs also added border and location marks, usually decimals of degrees of latitude and longitude.

**Table 4.** Percentage ranges for 'sliced' images and corresponding pseudo colours and greyscales.

	Percentage of values	Range	Approximate pseudo colour	Greyscale
1	100.0-99.9	0.1	Black	Black
2	99.9-99.0	0.9	Red	Darkest grey
3	99.0-98.0	1.0	Orange	
4	98.0-95.0	3.0	Yellow	
5	95.0-90.0	5.0	Yellow-green	8 steps
6	90.0-80.0	10.0	Green	of grey
7	80.0-60.0	20.0	Green-blue	
8	60.0-30.0	30.0	Light blue	
9	30.0- 0.0	30.0	Dark blue	Lightest grey

Image files were translated into Macintosh format and loaded into IMAGE (National Institute of Health, USA) using the pseudo colour or greyscale palettes listed in Table 4.

Additional image processing, including production of RGB composite images, was carried out using PHOTOSHOP V2.0 (Adobe Systems Inc.). The pseudo colour or greyscale images were stored as PICT files and imported into CANVAS for annotation and addition of the concentration key. Colour and greyscale images were reproduced on a Canon Postscript colour photocopier/printer.

Although colour images are more visually appealing and permit rapid identification of areas belonging to each concentration range (Cruikshank, 1994), low volume colour printing is relatively expensive and in this record greyscale images have been used for reasons of economy. Colour images for most elements (raw data) and for many statistically derived parameters are included in a separate colour atlas covering the HANN RIVER Region (Cruikshank and Brugman, 1995).

---

## STATISTICAL ANALYSIS

Element values below the detection limit of the analytical method used (Not Detected or ND values) appear in the datafile as the negative of the detection limit value. For the following statistical calculations the generally accepted value of half the detection limit has been substituted. For example, Sn by XRFS has a theoretical detection limit of 2 ppm under the analytical conditions used, and ND values appear as -2 in the datafile and are treated as 1 (ppm) in the calculations.

An element symbol suffixed with an asterisk (\*) indicates that analysis was by ICP-MS at Analabs, Perth. Similarly, a cross-hatch (#) indicates BCL/GFAAS by ALS, Brisbane. No suffix indicates analysis in AGSO's laboratory.

### 4.1 Duplicate Samples

Duplicate samples were collected at a number of sample sites to test the overall reproducibility of the sampling and analytical procedures. Data for 25 pairs of duplicate samples were compared using the 'paired t-test' (Koch and Link, 1970) which computes a confidence interval for the population mean of the differences between paired observations, in this case the duplicate samples. A confidence interval is used because experimental error (sampling + analytical) would normally preclude obtaining the same results for the duplicate samples. If the confidence interval includes zero, or the calculated t-statistic is inside the range  $\pm T$ , then the conclusion is that the duplicate samples are not statistically different. No significant difference was found at the 2% confidence level and only Ni differed at the 10% confidence level. The sampling, and analysis, was held to be statistically reproducible at the confidence levels tested. An average value for each element in each 'duplicate' sample has been used for all following data analysis and imagery.

### 4.2 Summary Univariate Statistics

Summary univariate statistics are shown in Table 5. These include the minimum, maximum, median, arithmetic mean, standard deviation, skewness (raw data), coefficient of variation, geometric mean, geometric deviation, skewness (log-transformed data), and arithmetic mean, standard deviation and skewness of a trimmed sample population in which the top and bottom 15% of values for the total dataset were deleted (Ellis and Steel, 1982). The trimmed data and geometric statistics are considered (Ellis and Steele, 1982; Eggo and others, 1990) to be more robust, that is less subject to the effects of outliers, than the raw data statistics, and therefore better define the background character of the data. Data for four elements (Bi, Mo, Se and Ta) contained a large number (>80%) of ND values and no statistical parameters other than minimum, maximum and median were recorded.

The number of sample populations and their distribution types for each element were assessed from histograms, and raw data and log-transformed data probability plots (Sinclair, 1972, 1991) generated by DATA DESK IV and STATVIEW II. Most populations had one or more outliers which did not fit the assessed distributions, but which were of insufficient numbers to constitute a separate population. Where two or more populations were identified, the element concentration corresponding to the break in slope of the probability plots was estimated. The plots are shown in Appendix B and in the following section as appropriate.

### 4.3 Summary Multivariate Statistics

#### 4.3.1 Correlations

The statistical correlation between pairs of elements often highlights significant geochemical associations but must be treated with some caution. A high correlation 'does not prove cause and effect' (Eggo and others, 1990 and 1995.) but, if an underlying geochemical rationale can be elucidated, may quantify the relationship. The size of the HANN RIVER dataset (N=1191) reduces the possibility of chance correlations sometimes found in small datasets. The Pearson product-moment correlation method assumes normally distributed sample populations and as many elements appear to follow the log-normal distribution, matrices of coefficients calculated from both raw data and log-transformed data are shown in Table C1 in Appendix C. Spearman Rank Correlation is a non-parametric method which makes no assumptions about the distributions the data follow. A matrix of correlation coefficients from this method is shown in Table C2 in Appendix C. All data were included in the calculations but coefficients for Bi, Mo, and Se may be considered as suspect but informative.

For a population of 1191 samples any Pearson coefficient greater than 0.13 or less than -0.13 is statistically significant. However, to separate highly correlated associations from the less correlated and potentially chance associations, only coefficients of 0.50 and higher, or -0.50 or less (for which variation in element X cause 25% or more of the variation in element Y) have been considered and several highly correlated groupings are discernible from all three sets of coefficients. These are:-

- Ce - La - Nd - P\* - Th - U - W - Y
- Cr - Cu - Fe - Mn - Ni - Sc - Ti - V - Zn
- Be\* - Ga - Rb - Tl\*
- Hf - Zr
- Ba - Sr

#### 4.3.2 Factor Analysis

The data were subjected to Principal Component Factor Analysis in order to quantify the obvious interdependence of many of the variables. Factor analysis determines whether multi-variate data occupy the same number of dimensions as the number of variables, or are contained in a smaller number of dimensions implying a lesser number of independent variables (Koch and Link, 1971: Dillon and Goldstein, 1984).

The procedure operates from a matrix of Pearson product-moment correlation coefficients and therefore is bound by the same assumptions and limitations of that technique, principally the assumption that data are normally distributed, and the limitation of the adverse effects of outliers. For these reasons log-transformed data were used and scattergrams of apparently highly correlated element pairs were viewed to reduce the incidence of outlier effects. The procedure was carried out, using STATVIEW II, on log-transformed data for the 38 elements for which full parameters are listed in Table 5. The analysis produced 8 factors each with Eigenvalues greater than 1 and which between them 'explained' at least 75% of the variability in the data (STATVIEW II manual: Feldman and others, 1990).

The factor loadings indicate the correlation between the variables and the factors. In this exercise the pattern matrix contains 304 values from 38 variables and 8 factors and many loadings, although statistically significant, are below an arbitrary level of 'practical significance'. This is the minimum amount of a variable's variance which reasonably is to be accounted for by the factor, a general level being  $\pm 0.30$  (Dillon and Goldstein, 1984). Alternatively, only the loading with the largest absolute value for each variable is



**Table 5.** Basic statistical parameters for HANN RIVER Region data (N=1191). Values are in parts per million (ppm), except for Au#, Pd# and Pt# which are in parts per billion (ppb). Trimmed statistics have top and bottom 15% of values deleted (N=834).

Element	Min.	Max.	Med.	Raw data			
				Mean	S.D.	Skew	C.o.V.%
Ag*	-0.1	0.5	-0.1				
As	-0.5	29.5	1.5	2.45	2.91	3.04	118
Au#	-0.05	5.0	0.10	0.18	0.31	7.18	173
Ba	26	1298	319	351.4	224.0	0.90	63.8
Be*	0.1	13.3	1.0	1.17	0.84	3.92	72.0
Bi	-2	9	-2				
Bi*	-0.10	2.30	0.20	0.21	0.17	3.87	80.0
Cd*	-0.10	3.10	0.05	0.11	0.15	8.56	135
Ce	10	4951	78	211.5	430.7	5.60	204
Cr	-1	787	47	61.9	63.8	3.93	103
Cu	-1	159	5	9.10	13.4	4.45	147
Fe	1000	99000	13000	17020	14180	1.60	83.4
Ga	-1	29	5	5.45	3.37	1.13	61.8
Ge	-0.5	96.5	1.5	1.63	3.82	24.14	234
Hf	-2	480	14	24.9	40.8	6.13	164
La	2	2560	37	106.2	225.7	5.65	213
Mn	6	2863	237	335.9	338.0	2.27	101
Mo	-2	5	-2				
Mo*	-0.10	10.5	0.30	0.35	0.41	13.96	116
Nb	-2	167	13	19.9	20.8	3.05	104
Nd	5	2173	33	92.4	188.7	5.57	204
Ni	-1	60	5	8.34	8.83	2.25	106
P*	-20	4770	212	366.5	532.9	4.20	158
Pb	2	103	16	18.6	11.4	1.49	61.6
Pd#	-0.05	1.44	0.12	0.15	0.11	4.77	74.0
Pt#	-0.1	0.30	0.05	0.06	0.02	5.48	40.0
Rb	1	246	40	46.9	37.2	1.44	79.4
Sb*	-0.05	6.89	0.28	0.45	0.55	4.53	123
Sc	-1	46	6	7.61	6.14	1.99	80.7
Se	-1	1	-1				
Sn	-2	3299	2	16.4	117.5	21.87	712
Sr	3	209	41	46.4	33.3	1.00	72.0
Ta	-2	132	-2				
Th	-2	1381	18	52.9	111.0	5.51	210
Ti	208	99999	3704	6354	9399	5.48	148
Tl*	-0.5	17.8	0.25	0.35	0.54	27.87	155
U	-0.5	187.5	4	7.41	11.4	6.59	154
V	-2	403	42	58.6	51.6	2.10	88.0
W	-2	44	4	4.72	3.93	3.32	83.3
W*	-0.10	13.9	0.90	1.15	0.94	4.75	82.1
Y	6	1148	42	69.0	85.8	4.79	124
Zn	2	392	17	24.5	25.2	4.56	103
Zr	44	14280	622	1098	1488	4.12	135

Element	Log-transformed data			Trimmed data		
	Mean	G.D.	Skew	Mean	S.D.	Skew
Ag*						
As	1.28	3.39	-0.08	1.79	1.27	0.53
Au#	0.10	2.89	0.41	0.11	0.07	0.70
Ba	278.8	2.07	-0.50	322.0	128.3	0.19
Be*	0.94	2.00	-0.48	1.06	0.36	0.15
Bi						
Bi*	0.17	1.94	0.17	0.18	0.07	0.38
Cd*	0.08	1.98	1.75	0.06	0.02	0.98
Ce	97.0	3.00	0.85	102.5	67.9	1.29
Cr	41.2	2.64	-0.60	50.2	23.8	0.35
Cu	4.49	3.47	-0.14	5.99	4.03	0.90
Fe	12110	2.37	-0.20	14170	7136	0.56
Ga	4.29	2.19	-1.03	5.12	1.91	0.30
Ge	1.45	1.34	3.92	1.47	0.11	-4.00
Hf	15.1	2.46	0.57	15.8	7.40	0.81
La	45.4	3.19	0.76	49.4	34.6	1.34
Mn	203.8	3.01	-0.53	263.9	144.9	0.64
Mo						
Mo*	0.26	2.12	-0.01	0.29	0.12	0.26
Nb	14.3	2.16	0.47	14.5	6.06	0.97
Nd	41.9	3.03	0.83	44.5	29.9	1.31
Ni	5.00	2.93	-0.25	6.28	3.74	0.70
P*	207.5	2.85	0.00	234.4	123.1	0.80
Pb	15.5	1.84	-0.15	16.7	5.95	0.50
Pd#	0.13	1.61	0.96	0.13	0.03	0.66
Pt#	0.05	1.27	4.43			
Rb	32.2	2.67	-0.77	41.1	19.1	0.31
Sb*	0.28	2.74	-0.26	0.33	0.17	0.88
Sc	5.73	2.17	-0.26	6.32	2.68	0.66
Se						
Sn	3.09	3.89	1.36	3.20	2.85	1.52
Sr	33.4	2.48	-0.67	42.3	19.8	0.22
Ta						
Th	20.5	3.62	0.49	24.2	18.6	1.32
Ti	4030	2.41	0.40	4178	1753	0.92
Ti*	0.31	1.53	2.32	0.27	0.07	2.87
U	4.31	2.71	0.19	4.78	2.61	0.94
V	40.5	2.55	-0.68	48.5	24.2	0.63
W	3.66	2.03	0.17	3.95	1.68	-0.09
W*	0.92	1.95	-0.16	0.99	0.34	0.46
Y	45.7	2.34	0.54	48.1	24.4	0.85
Zn	16.4	2.52	-0.07	19.6	10.8	0.61
Zr	672.2	2.53	0.54	719.3	392.4	0.80

Table 6(a). Rotated factor loadings, eigenvalues and communalities for HANN RIVER Region log-transformed data (N=1191).

	Communalities	F1	F2	F3	F4	F5	F6
Ag*	0.212				0.383		
As	0.718		0.643		0.461		
Au#	0.547		0.490				0.487
Ba	0.844			0.863			
Be*	0.786		0.312	0.756			
Bi*	0.863					0.912	
Cd*	0.212		0.399				
Ce	0.969	0.926					
Cr	0.717		0.800				
Cu	0.874		0.921				
Fe	0.939		0.951				
Ga	0.788		0.471	0.732			
Ge	0.319						-0.463
Hf	0.818	0.655	0.341	-0.408			
La	0.962	0.915					
Mn	0.827		0.677	0.516			
Mo*	0.517		0.348		0.471		
Nb	0.832	0.719	0.461				
Nd	0.967	0.921					
Ni	0.884		0.912				
P*	0.822	0.711		0.438			
Pb	0.838	0.586		0.655			
Pd#	0.512		0.400				0.551
Pt#	0.555						0.682
Rb	0.908			0.923			
Sb*	0.700	-0.335			0.758		
Sc	0.865		0.902				
Sn	0.540			-0.449	0.519		
Sr	0.871			0.861			
Th	0.951	0.925					
Ti	0.929	0.508	0.713				
Tl*	0.636		-0.389	0.568	0.329		
U	0.911	0.936					
V	0.927		0.939				
W	0.604	0.706					
W*	0.490				0.650		
Y	0.914	0.923					
Zn	0.894		0.809	0.355			
Zr	0.858	0.696		-0.442			
Eigenvalues		12.26	6.64	5.22	2.28	1.61	1.31
Proportion of original variance (%)		31.4	17.0	13.4	5.9	4.1	3.3
Cumulative (%)		30.8	48.4	61.8	67.7	71.8	75.1

considered. In this exercise a composite approach has been used with the largest absolute value for each element labelled as a major contribution to a factor (the element being a major contributor), while other 'practically' significant loadings for an element will be labelled as minor contributions to other factors. Table 6(a) lists the more significant factor loadings and the proportion of variation in the dataset due to each factor, and Table 6(b) the primary intercorrelations between factors. The communalities represent the proportion of the variance of the variable that can be predicted by the factors extracted, that is high communalities (i.e. >0.6) are desirable since low communalities are generally given by elements which have significant numbers of 'not detected' values, or which are not strongly correlated with any other element (Eggo and others, 1990).

**Table 6(b).** Primary intercorrelations for Factors above.

	F1	F2	F3	F4	F5	F6
F1						
F2	0.278					
F3	0.282	0.174				
F4	-0.022	0.070	0.039			
F5	0.004	0.038	0.054	0.185		
F6	-0.019	0.287	0.204	-0.215	-0.219	

**Factor 1** comprises a strong association between U, Ce, Th, Y, Nd, La, Nb, P\*, W, Zr and Hf, with minor contributions from Pb and Ti, and accounts for 31.4% of the total variability in the data analysed. The communalities of the prime elements are all high (>0.8) indicating that most of the variance due to these elements is accounted for by the factor extracted. There is strong statistical ( $r > 0.8$ ) and spatial (see next section) correlation between the Light Rare Earth Elements (LREE) Ce, La and Nd, and P\*, Th, U, W and Y, and between these and Hf and Zr.

**Factor 2** comprises Fe, V, Cu, Ni, Sc, Zn, Cr, Ti, Mn, As and Cd\*, with minor contributions from Ga, Nb, Pd#, Mo\*, Be\* and Au#, and a negative contribution from Ti\*. This factor accounts for 17.0% of the total variability and all prime elements have high communalities.

**Factor 3** comprises Rb, Ba, Sr, Be\*, Ga, Pb and Ti\*, with minor contributions from Mn, Pb and Zn, and a negative contributions from Sn, Zr and Hf. This factor accounts for 13.4% of the total variability. All prime elements have high communality values (>0.65).

**Factor 4** comprises Sb\*, W\*, Sn, Mo\* and Ag\*, with minor contributions from As and Ti\*. This factor accounts for 5.9% of the total variability.

**Factor 5** comprises Bi\*. This factor accounts for 4.1% of the total variability.

**Factor 6** comprises Pt#, Pd# and Au#, and a negative contribution from Ge. It accounts for 3.3% of the total variability.



---

## INTERPRETATION

As with the EBAGoola and RED RIVER stream sediment surveys (Cruikshank, 1994, 1997), the surficial geochemistry is interpreted in terms of the factor groupings discussed in the previous section. An element 'high' refers to a group of grid points in the top 5 percentile of grid values (sometimes 10%), as shown in the sliced image map (see Table 4).

### 5.1 Factor 1 (Resistant heavy minerals)

Factor 1 comprises U, Ce, Th, Y, Nd, La, Nb, P\*, W, Zr and Hf, with minor contributions from Pb and Ti, and a negative contribution from Sb\*. It is considered to be due to the concentration of resistant accessory minerals, such as the phosphate minerals monazite and xenotime, and zircon, from the weathering of granitic and metamorphic rocks. The relative abundances of the prime elements are shown in box plots in Figure 6, and the spatial distributions of U, Ce, Y, Nb, Zr and F1 in the HANN RIVER Region are shown in image maps contained in Figure 7. Ce, La, Nd and Th show strong correlation (Figure 8; and coefficients >0.98 for raw and log-transformed data, and for Spearman's ranked, correlations as listed in Appendix C), and virtually identical spatial distribution patterns (see image maps in Cruikshank and Brugman, 1995). Scattergrams showing the relationships between other selected element pairs are also shown in Figure 8.

Factor 1 scores are concentrated in one general area (Area 1A in Figure 7), although two smaller areas (areas 1B and 1C) are of interest.

Area 1A is roughly bounded by the Pinnacles homestead in the north-west, the Fairlight homestead in the east, and the Mount Mulgrave homestead in the south. The area is drained by tributaries of the King, Palmer and Mitchell Rivers, including Fox (twice), Twelve Mile, Terrible (twice), Sandy, Mountain, Big, Stewart and King Creeks. Regolith in the area is in-situ and moderately to very highly weathered saprolite. The highs are generally over schists and gneisses of the Yambo Metamorphic Group rather than over granites of the Aralpa and Lukinville Suites, in the Yambo area. This is consistent with the generally higher values for REE (eg Ce), Th and Y in the metamorphic rocks than in granites (Table 7). The image maps show a sharp cut-off in the east where the granites and metamorphics abut the Chillagoe Formation. All prime Factor 1 elements have highs concentrated in the area with most conforming to the patterns shown by Factor 1 scores. However, Nb, Zr and Hf are patchier than the others with Nb highs concentrating in, and extending beyond, the south-western part of the area, and Zr and Hf highs concentrating in the eastern part of the area, mostly over Chelmsford Gneiss. The area overlaps area 2A (see Section 5.2) in the south and east and shows patchy highs for Fe, Sc, V, Sr and Mn. Some elements, in particular Sn, are generally very low.

Area 1B lies between Kimba and Kilarney homesteads in the Dixie area. The area is drained by Dickies and Jerry Dodds Creeks, and overlies granites of the Lukinville and Kintore Suites, and the Kimba Schist. Regolith is highly to very highly weathered saprolite. Y, W and U show the strongest highs of the prime Factor 1 elements.

Area 1C lies south-west of Area 1A, west of Mount Mulgrave homestead over sediments, but in streams draining the Saraga and Rosser Schists. The area shows only moderate enrichment in REE, Th and Y, but contains a W high, and is part of a larger Nb and Ti high which encloses the area (see Figure 7).

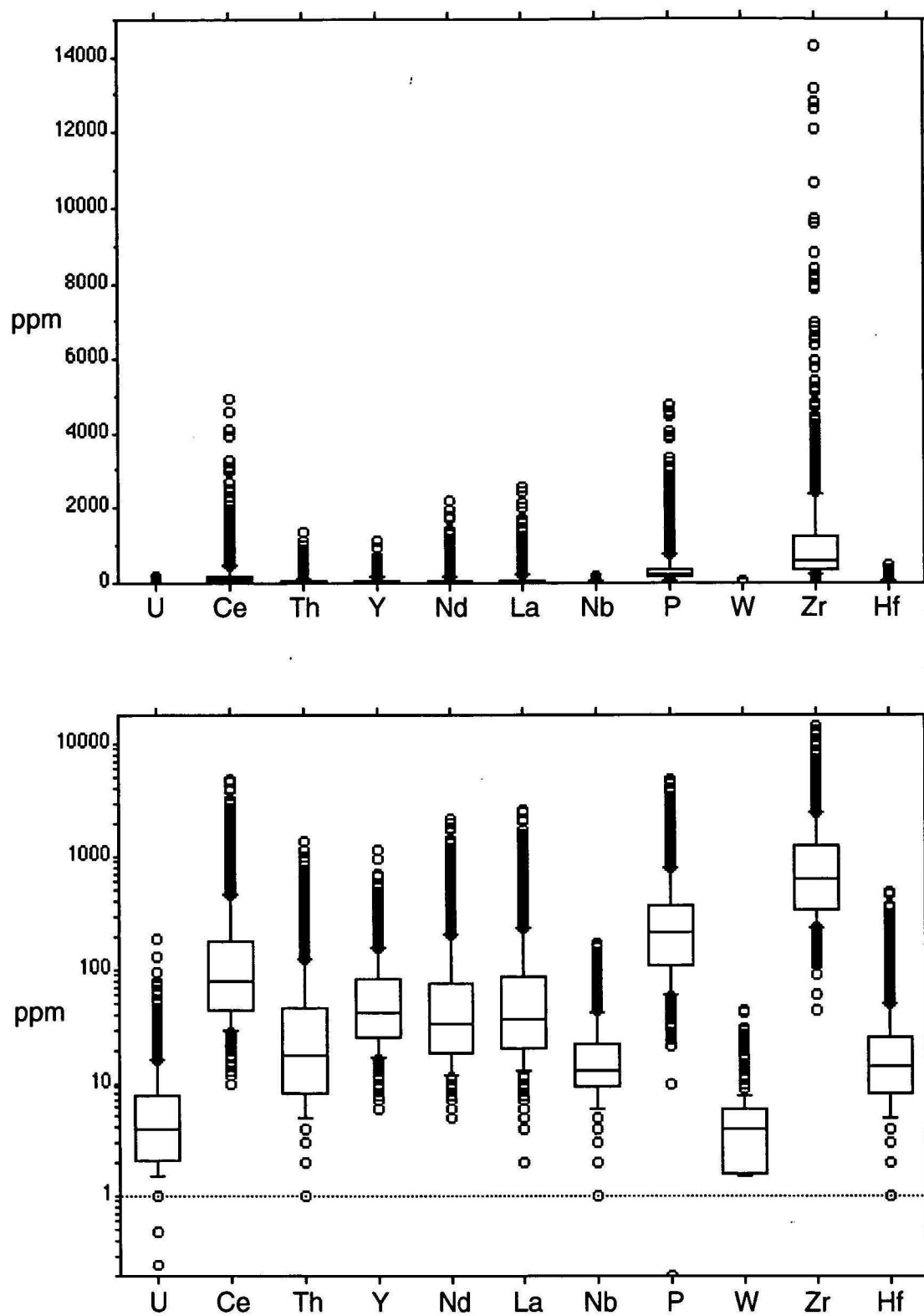


Figure 6. Relative abundances of Factor 1 elements.

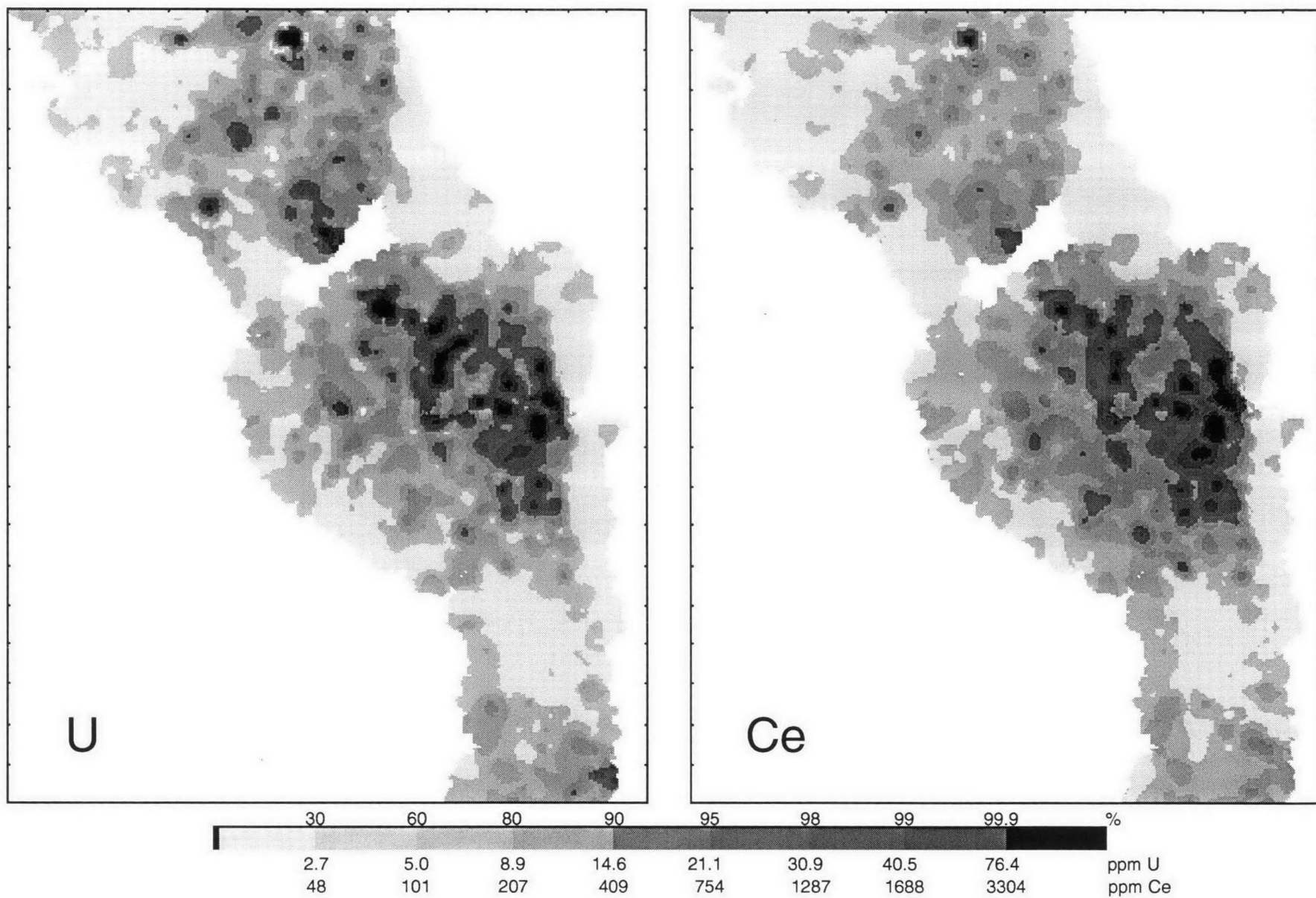
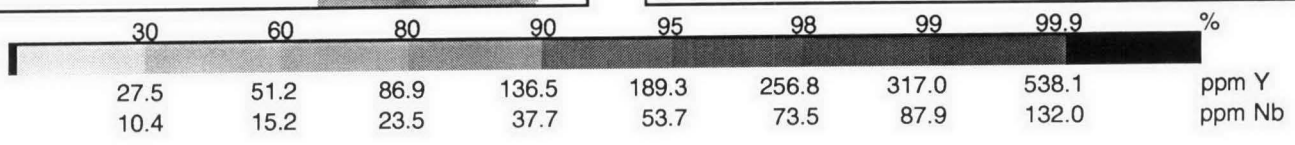
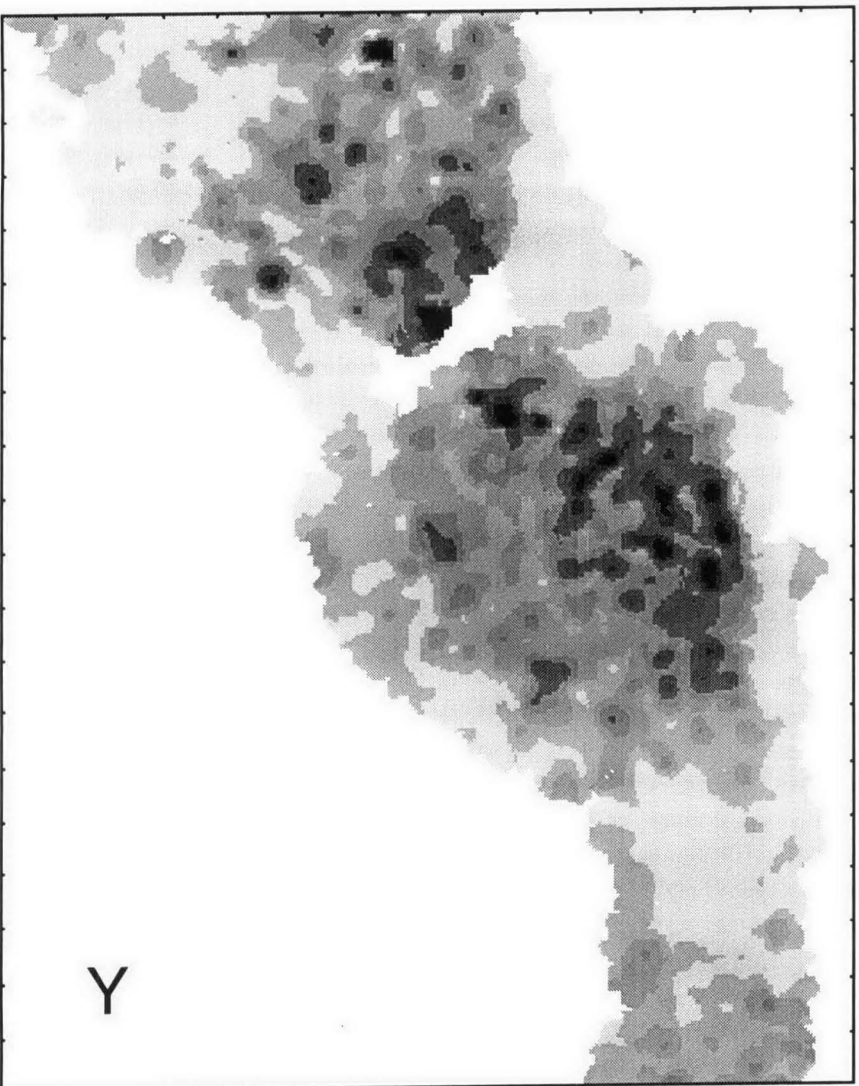
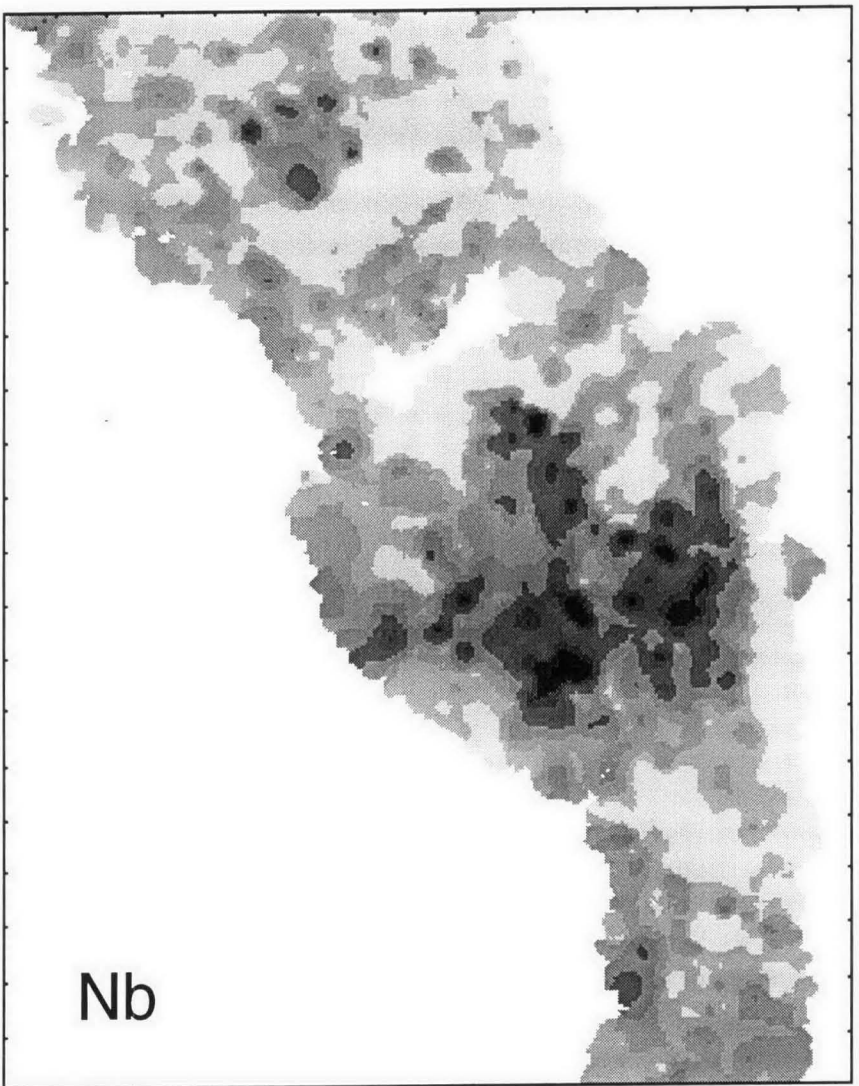
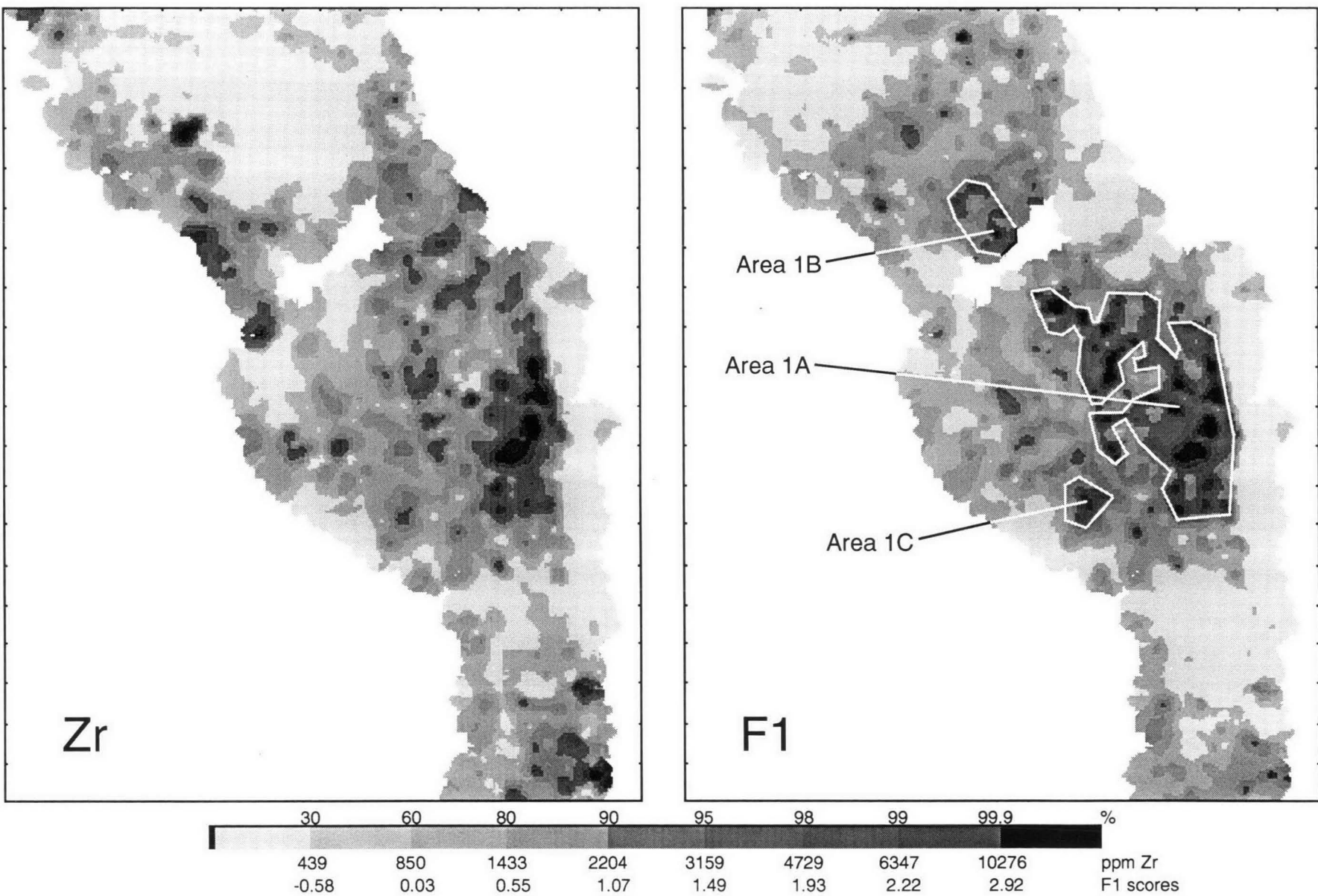


Figure 7. Image maps showing the distribution of U, Ce, Y, Nb, Zr and Factor 1 scores in the Hann River Region.







**Table 7.** Average Ce, Th, Y and Zr values for metamorphic and granitic rocks in the Yambo area (in ppm).

	Ce	Th	Y	Zr	(N)
Annie Creek Schist	48	10	30	109	3
Arkara Schist	106	26	24	240	8
Chelmsford Gneiss	80	16	24	223	5
Daintree Gneiss	45	9	31	153	2
Jeddah Schist	69	16	33	158	3
Oswald Schist	-5	-2	13	8	1
Pombete Schist	40	11	24	115	2
Saraga Schist	71	18	14	229	8
Average	73	17	23	194	
Aralba Granite Suite	42	9	18	82	6
Kingvale Granite	58	10	16	96	3
Lilyponds Granite	26	4	16	46	2
Rocky King Granite	58	14	13	103	1
Average	45	9	17	81	

The extremely strong statistical and spatial correlation between the LREE's, Ce, La and Nd, and Th is believed to be due to their presence in the resistant phosphate mineral monazite ( $[\text{Ce,La,Y,Th}]\text{PO}_4$ ; Price and Ferguson, 1980; Cruikshank, 1994). P\* shows strong correlation with Ce, La, Nd and Th ( $r$ 's in range 0.91-0.93), adding further weight to the proposition. Although Y is also included in the generalised composition of monazite, the reduced statistical correlation and the slight but discernible differences in spatial distribution between this element, and the LREE's and Th, are probably due to the co-existence, albeit in slightly differing relative proportions, of another resistant phosphate mineral, xenotime ( $\text{YPO}_4$ ). The inclusion of Zr and Hf in the factor suggests the presence of a third resistant mineral, zircon ( $\text{ZrSiO}_4$ ). All three minerals occur as accessory minerals in granites, although, on the analyses available (Table 7), the metamorphics appear to contain higher concentrations of the minerals. They also concentrate in the bed lodes of streams because of their high chemical and physical resistance to weathering, and relatively high specific gravities (quartz - 2.7, monazite - 5.2, xenotime - 4.3, zircon - 4.3). These heavy, resistant minerals may have economic significance of their own as sources of REE, etc, and on the basis of the REE, Y and Th concentrations measured, albeit in the fine fraction, there may be up to 2% heavy minerals present in some streams in area 1A. Parts of Area 1A have been explored for heavy minerals (AP's 597M, 2679M and 2580M - Culpeper and others, 1992) but were considered as uneconomic because of low grades or a general lack of alluvial material.

In sharp contrast with common rock forming silicate minerals, which rarely contain more than 10 ppm U, the three resistant minerals, monazite, xenotime and zircon, can contain relatively high concentrations of U (Price and Ferguson, 1980) ranging from up to 10,000 ppm for zircon, to 35,000 ppm for xenotime. These minerals accumulate in the bed lodes of streams, most likely without significant loss of U. Unfortunately it is not U in this form which is of economic interest, but the more mobile species which may have originated in mineralisation and which may be adsorbed onto clays and hydrated Fe and Mn oxides. The problem is to define the later in the presence of the former. The most satisfactory method to estimate mobile U is to leach the samples with a leachate designed to extract only mobile U, and determine U in the leachates (Hall and others, 1996). Complex methodology such



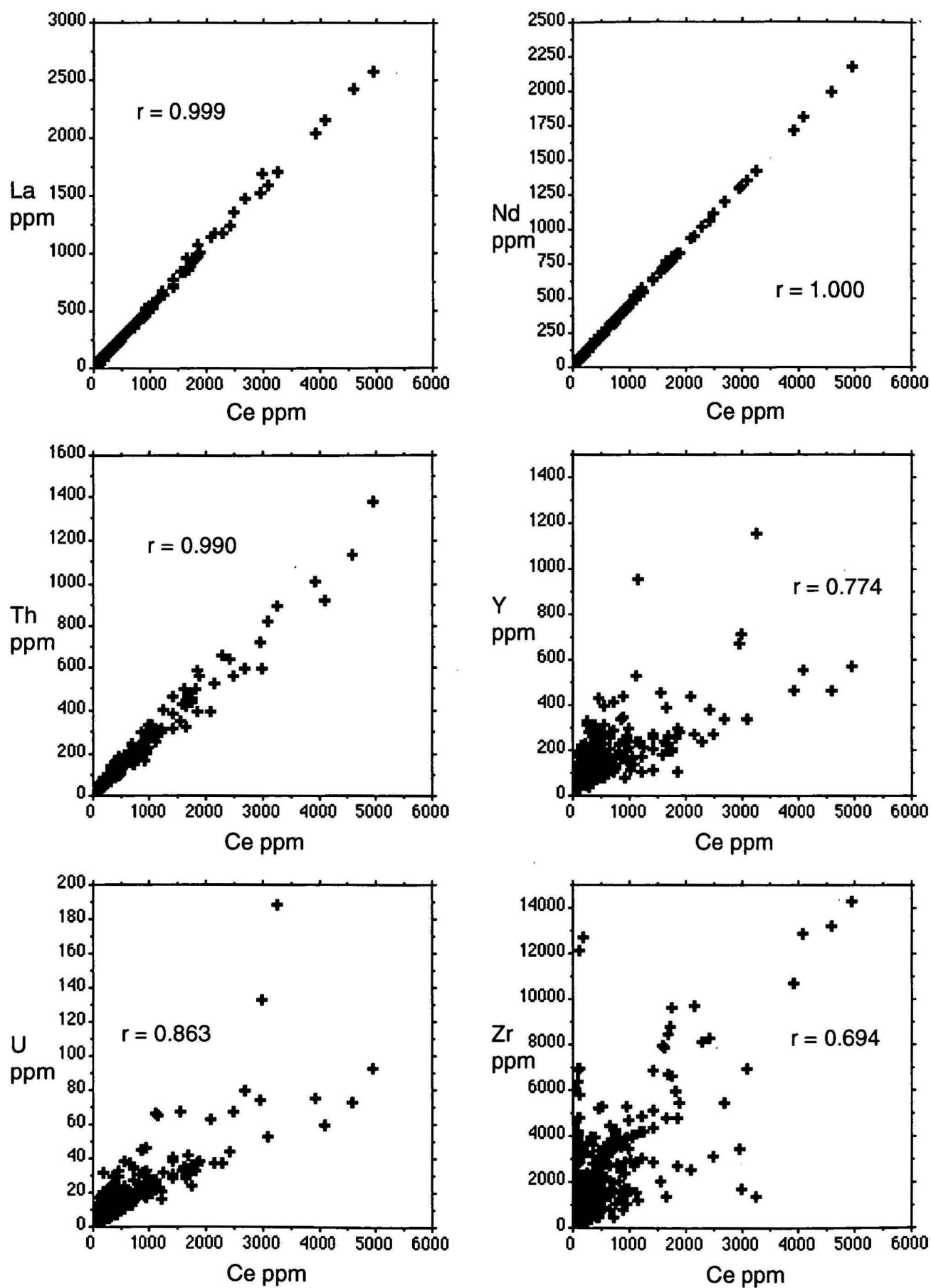
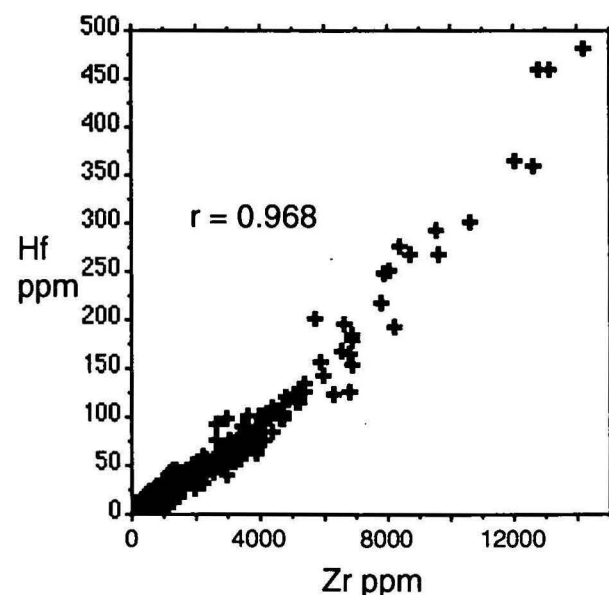
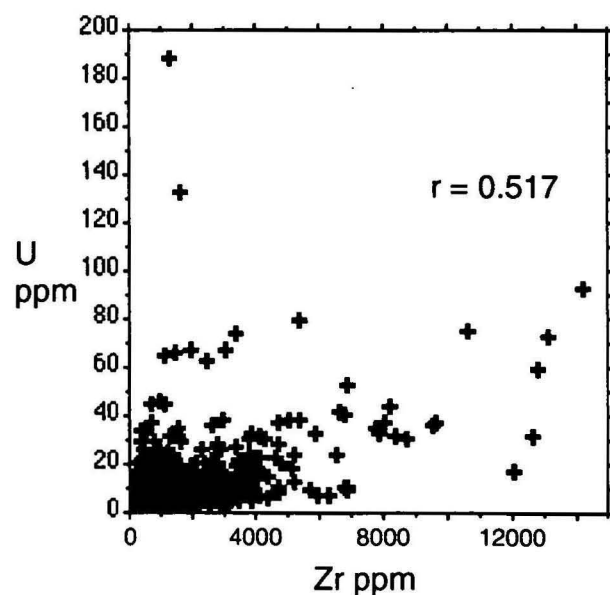
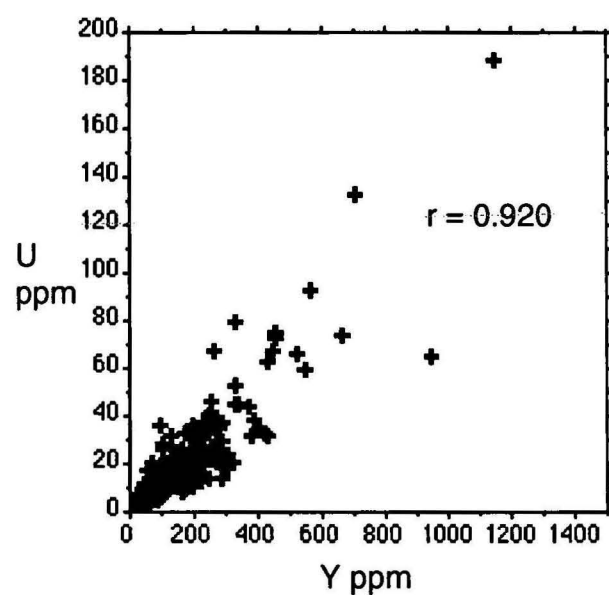
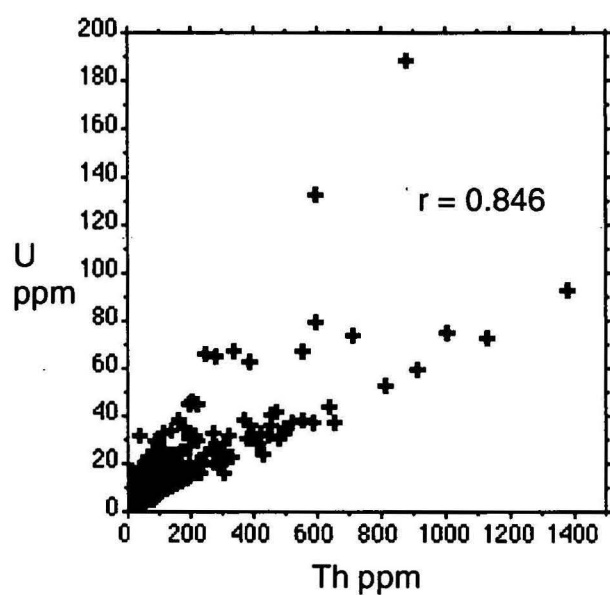
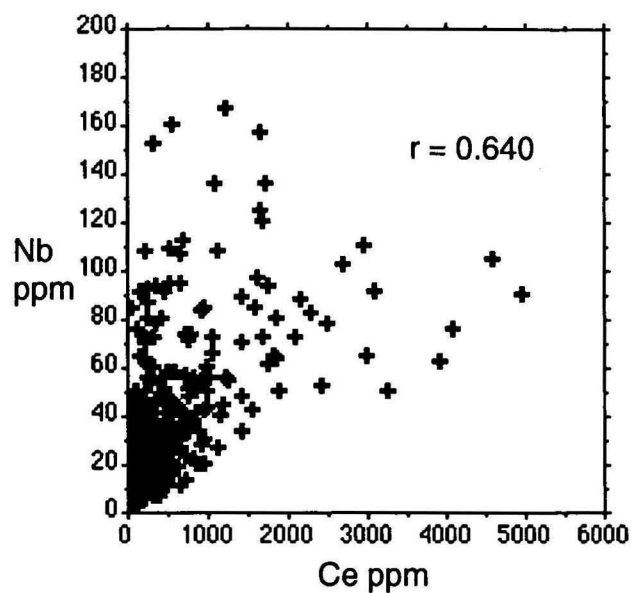
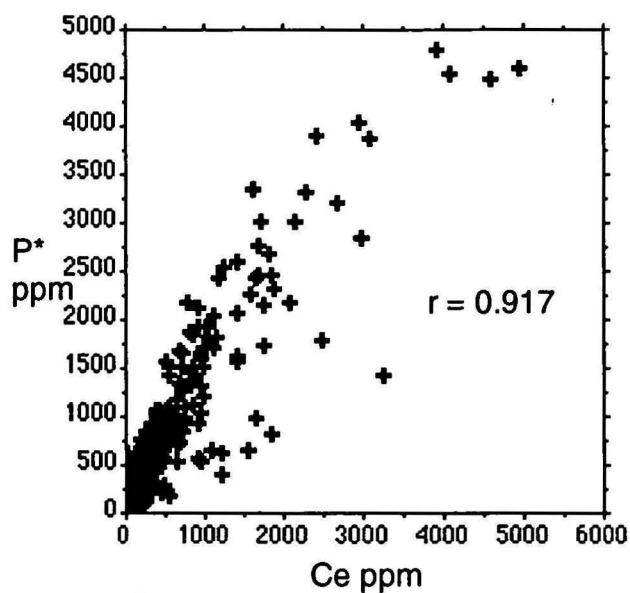


Figure 8. Scatterplots of selected pairs of Factor 1 elements.



as this is not always practical, especially on a regional scale where large numbers of samples may be involved. In the absence of these data Price and Ferguson (1980) substituted a form of lithochemical compensation by examining the ratios of U to elements which were characteristic of each of the resistant minerals, for example Hf for zircon, Ce and Th for monazite and Dy for xenotime. The author used a similar approach in the EBAGoola survey (Cruikshank, 1994) using instead (Ce+La+Nd+Th) for monazite, Y for xenotime and Zr for zircon. Price and Ferguson (1980) also used estimates of 'residual' U contents derived from total U concentrations corrected for estimates of U contained in common rock forming minerals, the resistant minerals mentioned above, and in other entities such as organic phases. Lithochemical correction from predicted values from linear regressions of U against the values of associated elements, and against principal component factor scores were also considered. Unfortunately, U has a relatively short dispersion train (<1 km) in the secondary environment downstream from mineralisation in northern Australia (Foy and Gingrich, 1977; Cruikshank and others, 1993). For a sampling density of 1 sample per 10-15 km<sup>2</sup> most basins have stream runs of 3 km or more, so that U from mineralisation could be easily lost in a background due to the resistant minerals.

The most promising, and convenient, of the approaches outlined above is that of step wise regression of U (actually log(U)) against factor scores (Cruikshank, 1997), with deletion of highly anomalous residuals to produce a regression equation more accurately representing the background population (Eggo and others, 1990 and 1995; Cruikshank, 1994). All factors were included in the regression as none appeared to be directly related to U mineralisation. The stepwise regression of log(U) against the 6 factor scores resulted in the elimination of Factor 5 scores from the regression. The regression was recalculated after deletion of 18 samples with residual values greater than 7.55 ppm, giving the following regression equation:

$$\log(U_p) = 0.400 \cdot F1 - 0.031 \cdot F2 + 0.071 \cdot F3 + 0.017 \cdot F4 - 0.012 \cdot F6 + 0.631$$

where  $U_p$  is the predicted value for U from the lithochemical information held in the factor scores, for example the likely concentration of resistant minerals indicated by factor scores. The residual value ( $U_{res}$ ) was calculated by subtracting the predicted value ( $U_p$ ) from the measured U value. Figure 9 compares image maps of the distributions of U (as measured) and  $U_{res}$ .

Highs for  $U_{res}$  are patchy and much of area 1A shows up as a low indicating that U in this area is notionally bound up in the resistant minerals. However, the north western part of area 1A shows two very strong  $U_{res}$  highs, over Oswald and Annie Creek Schists, and over Pombete Gneiss and Saraga Schist. Analyses for these units show no evidence of unusual/high U values (maximum of 6 ppm U). The highs are thought to occur in areas covered by several Authorities to Prospect (AP's) (Culpeper and others, 1992) between the Palmer and King Rivers. The AP holders found high U/Th ratios in one small area and several other low-order anomalies. Follow-up stream sediment sampling gave only low values for U and high Th values which were ascribed to the possible presence of monazite. The authorities were subsequently relinquished.

Some areas in the Dixie area, near the New Dixie homestead, are also more prominent in the  $U_{res}$  image. The highest of these is over Astrea and Dinah Formation metamorphics. A number of AP's have been taken out in the area usually targeting graphitic schists in the metamorphics. However, no significant anomalies were found and all AP's were subsequently relinquished.



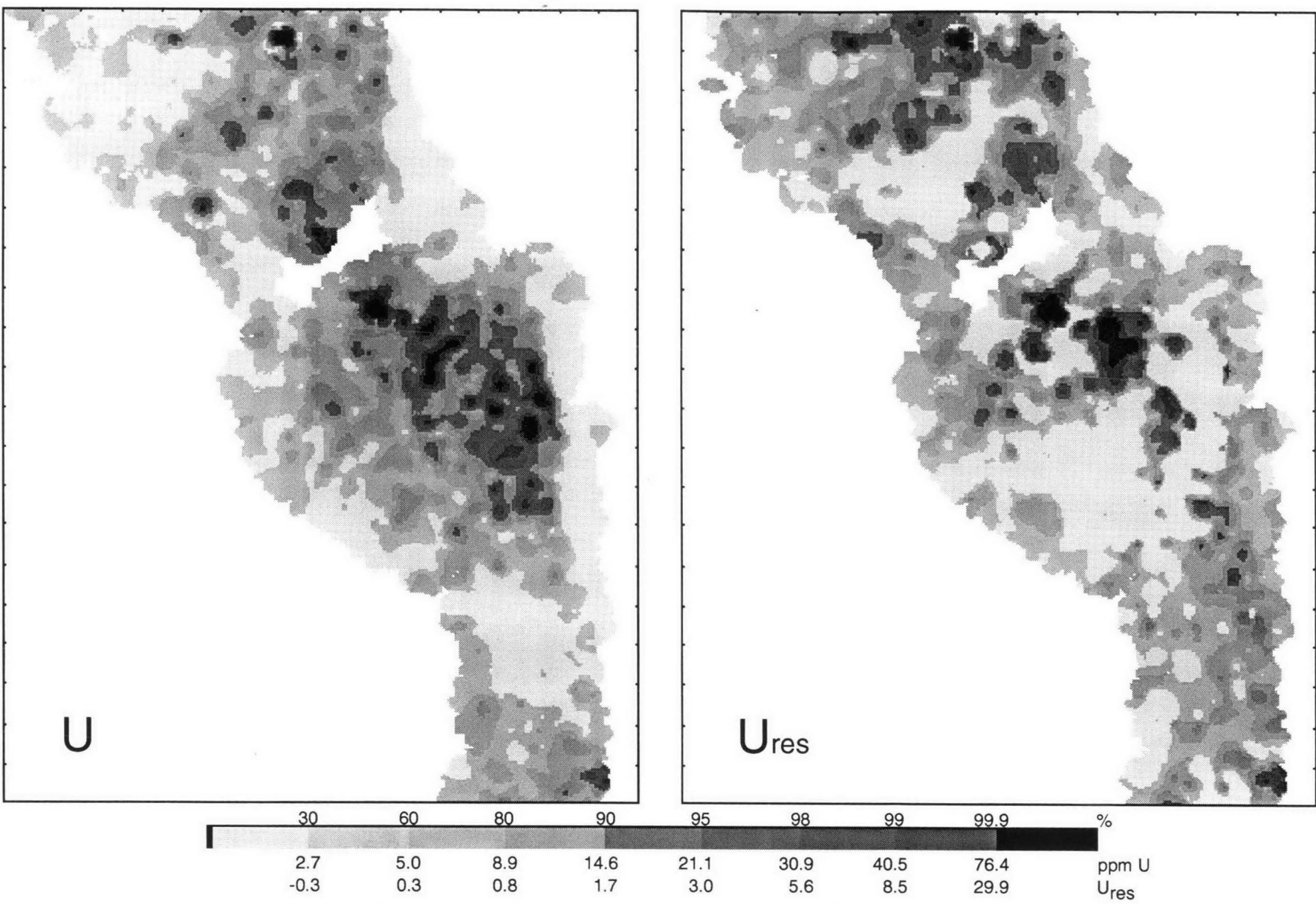


Figure 9. Image maps of distribution of U and U<sub>res</sub> in the Hann River Region.

## 5.2 Factor 2 (Fe-Mn geochemistry)

Factor 2 comprises Fe, V, Cu, Ni, Sc, Zn, Cr, Ti, Mn, As, Au# and Cd\*, with minor contributions from Ga, Nb, Pd#, Mo\*, Be\* and Au#, and a negative contribution from Ti\*. Although the transformation factor for Au# is marginally higher for Factor 2 (i.e. 0.490), it has an almost identical factor (0.487) in Factor 6 which includes Pd# and Pt#. Therefore Au# will be discussed with Factor 6 although the relationship with As (and Cu and Zn) in this factor is noted. The relative abundances of the prime elements are shown in Figure 10, and image maps for Fe, Cu, Ni, Ti, Mn and F2 in Figure 11 (Zn in Figure 15).

The factor relates to the geochemistry of Fe, including the entry of Cr, Cu, Ni, Sc, V, etc, into Fe-rich mafic minerals such as pyroxene, amphibole and biotite in basalt, diorite and their metamorphic products, and to the co-precipitation with, or adsorption onto, hydrated Fe-oxides in the secondary environment of these and other elements such as Zn (Wedepohl, 1972). Scatterplots showing the relationship between Fe and elements of Factor 2 are shown in Figure 12. Fe, V and Sc show great similarity in their spatial distributions, and to that of the Factor 2 scores, with the other elements showing minor (Cu, Mn, Ni, Ti and Zn) to significant (Cr, As and Cd) differences. Indeed Cr, As and Cd show little similarity to Factor 2 scores. As is concentrated in the southern part of the survey area and is an extension of an As high in the Cardross area observed in the Red River Region survey (Cruikshank, 1997). Cd\* shows an unusual banding effect in the image map covering the HIGHBURY, MOUNT MULGRAVE and MAYTOWN 1:100 000 sheet areas. The significance of this is not obvious except, possibly, as an artefact from the analyses. Factor scores, and generally the values of most Factor 2 prime elements, are low to very low in the Dixie area.

Factor 2 scores show two coherent highs over rocks of the Chillagoe Formation along the eastern margin of the survey area, and over rocks of the Yambo Metamorphic Group immediately to the west.

Area 2A (see Figure 11) is along the eastern margin of the survey area, overlaying the Chillagoe Formation and some of the Yambo Metamorphic Group, mostly over Chelmsford Gneiss, to the west. The area over the sediments, limestone and basalts of the Chillagoe Formation is characterised by stony hills and ridges, which form a north-trending valley-ridge topography (Amos and de Keyser, 1964). The metamorphics to the west tend to form generally flat plains. The area is drained by tributaries of the Palmer and Mitchell Rivers, including the headwaters of the Little Mitchell, St Georges and Little Kennedy Rivers, and Terrible, Twelve Mile, Sandy, Mountain, Fox, Limestone, Glenroy and Flood Creeks. Fe, V and Sc, as stated above, show similar spatial distributions to the Factor 2 scores and are concentrated over both the Chillagoe Formation, and the Yambo Metamorphics to the west. Cu and Ni are concentrated mostly over the Chillagoe Formation with a lower presence over the metamorphics. Mn is concentrated mainly over the metamorphics with only moderate values over the Chillagoe Formation. This trend is also shown by Zn except in that its highest concentrations are over areas of metamorphics in the northwest and southwest of the Yambo area rather than those in area 2A. Ti is similar to Zn but with only moderate to low values over the Chillagoe Formation.

Area 2B lies to the west of area 2A and the Mount Mulgrave homestead, and is over Saraga Schist and intruding dolerite. The topography is relatively flat but the area is drained by the Reid, Rosser and Arkara Creek systems. The area shows strong highs for Zn, Ti and Mn, and moderate to low values for Fe, V, Cu and Sc.

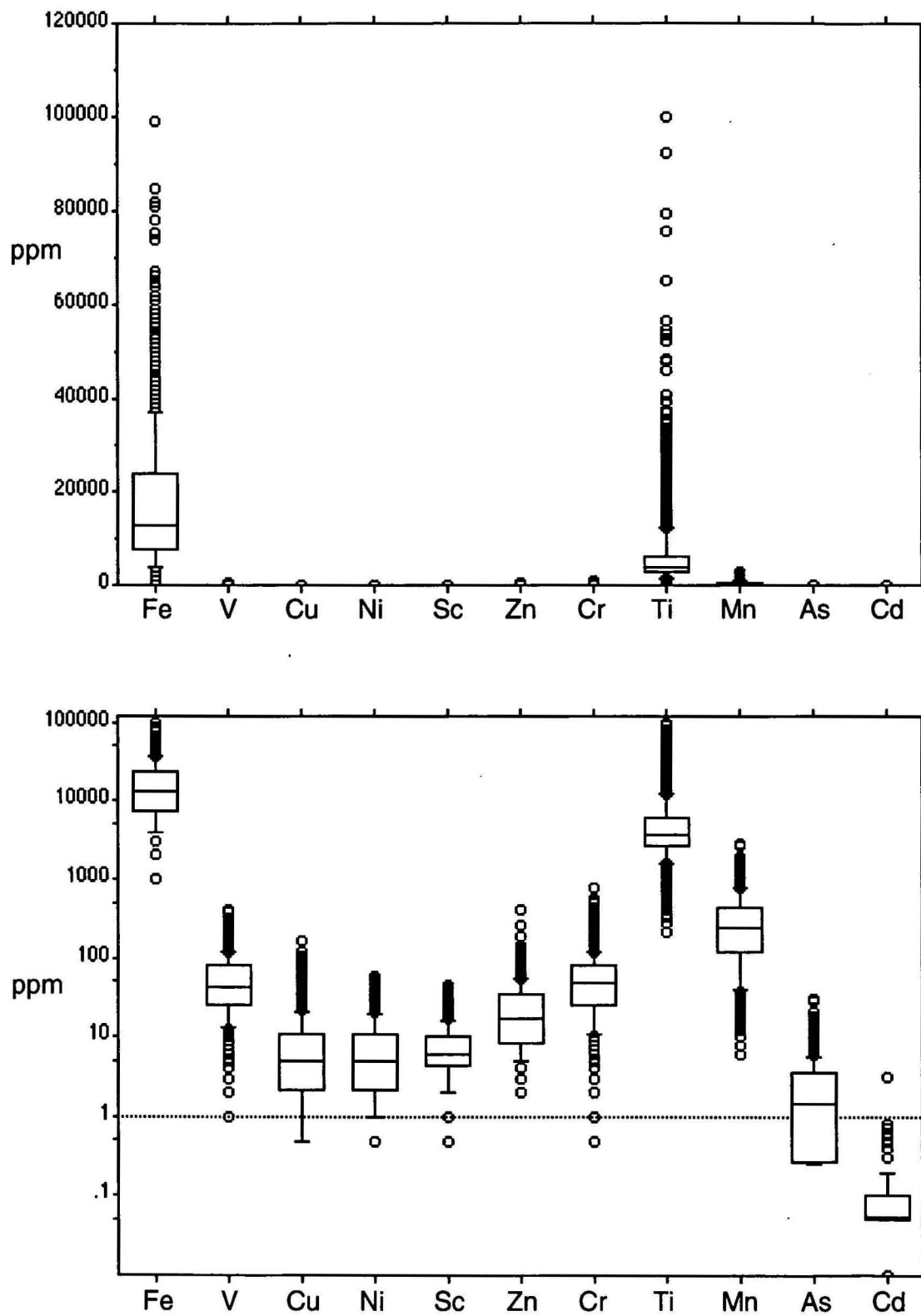


Figure 10. Relative abundances of Factor 2 elements.

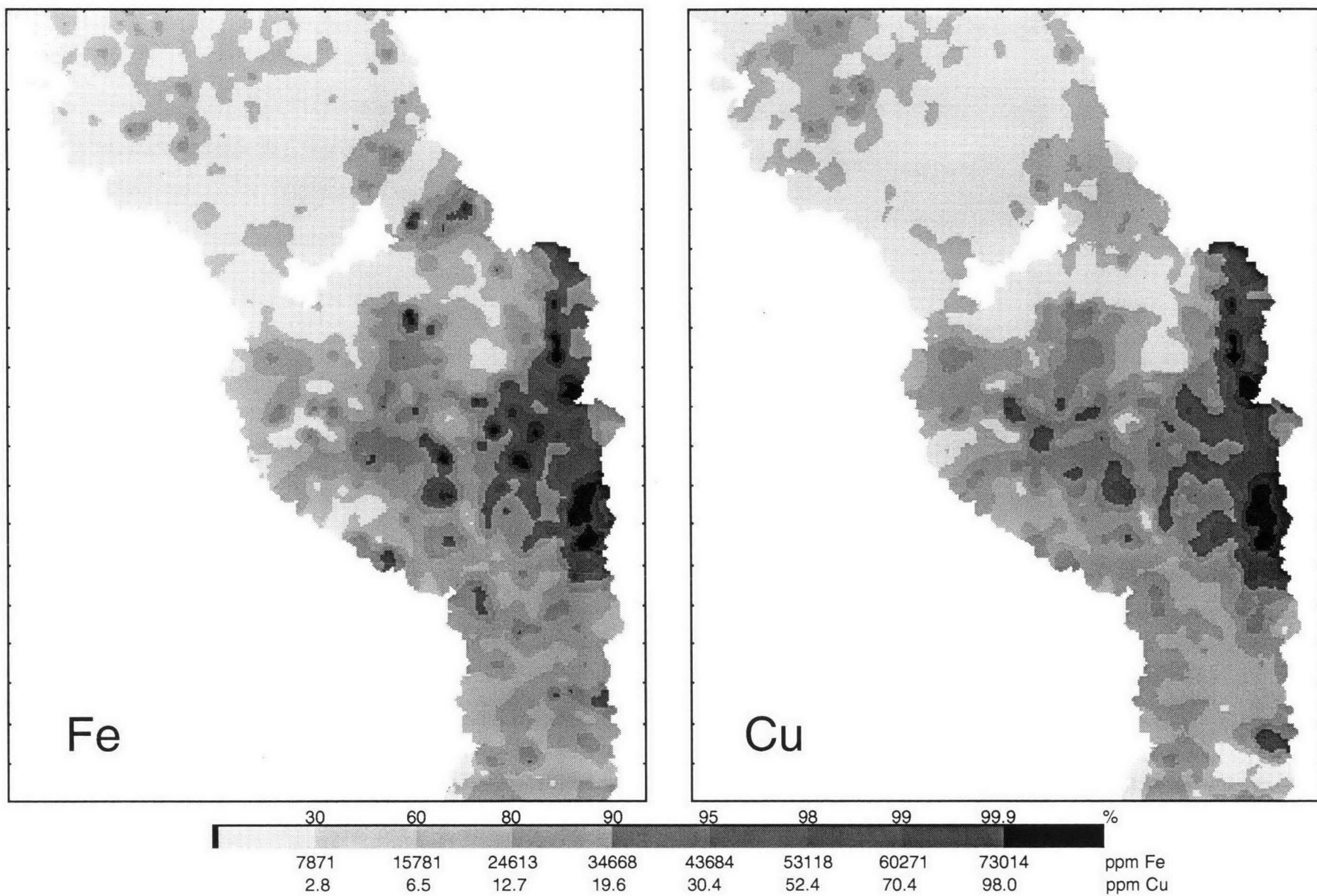
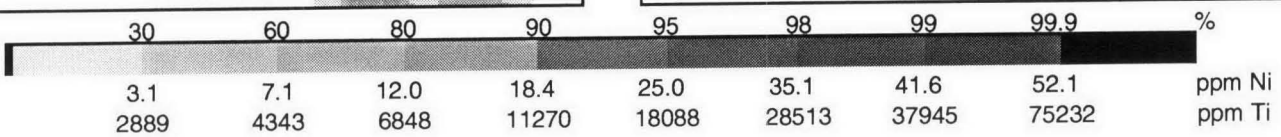
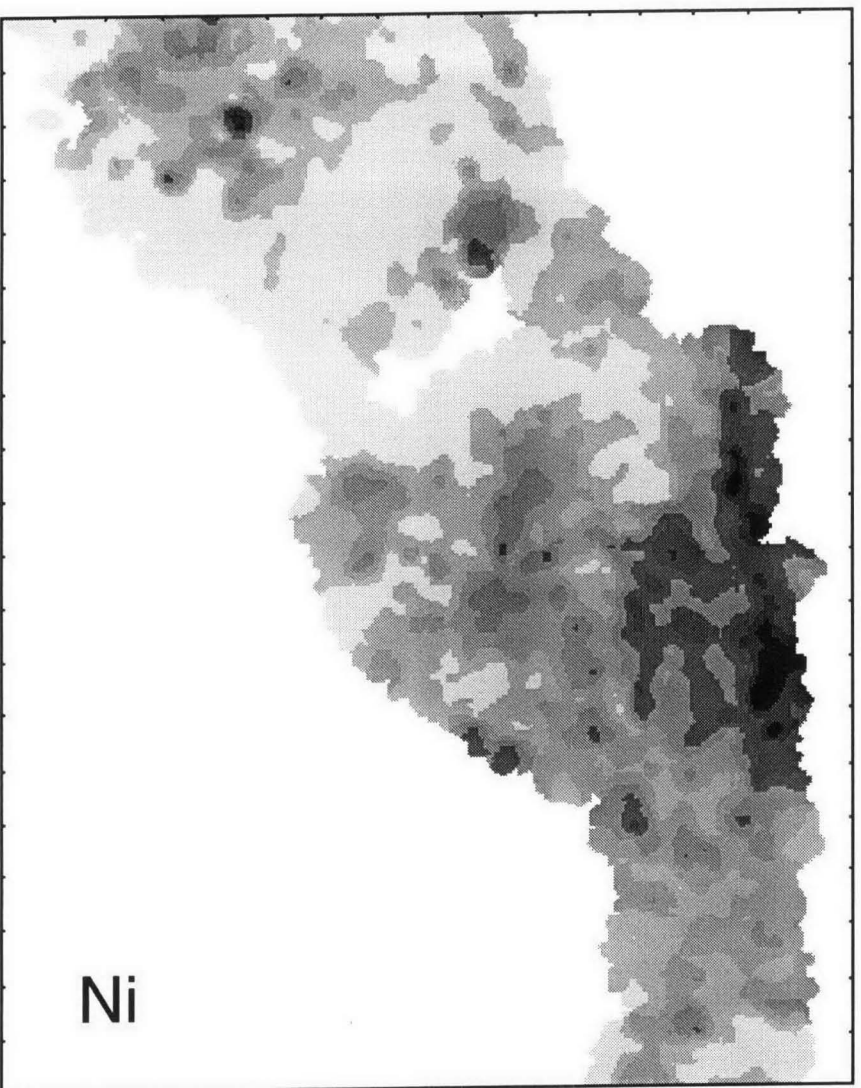
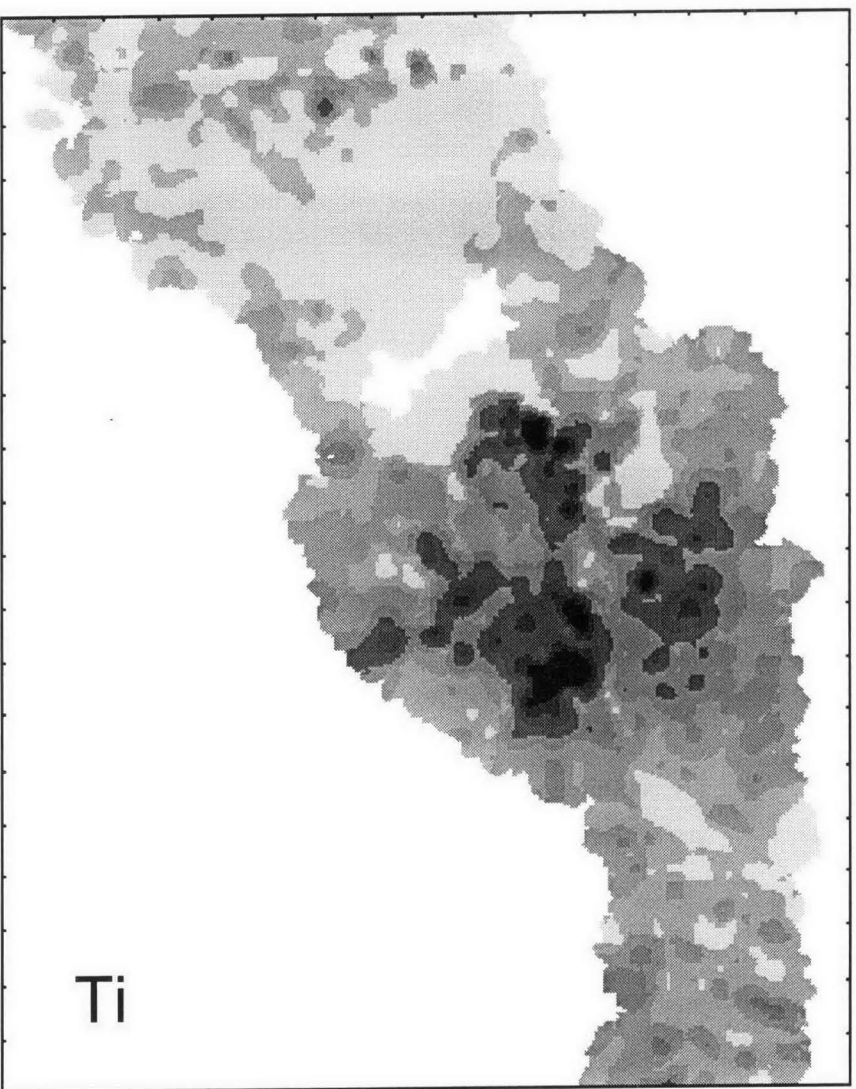
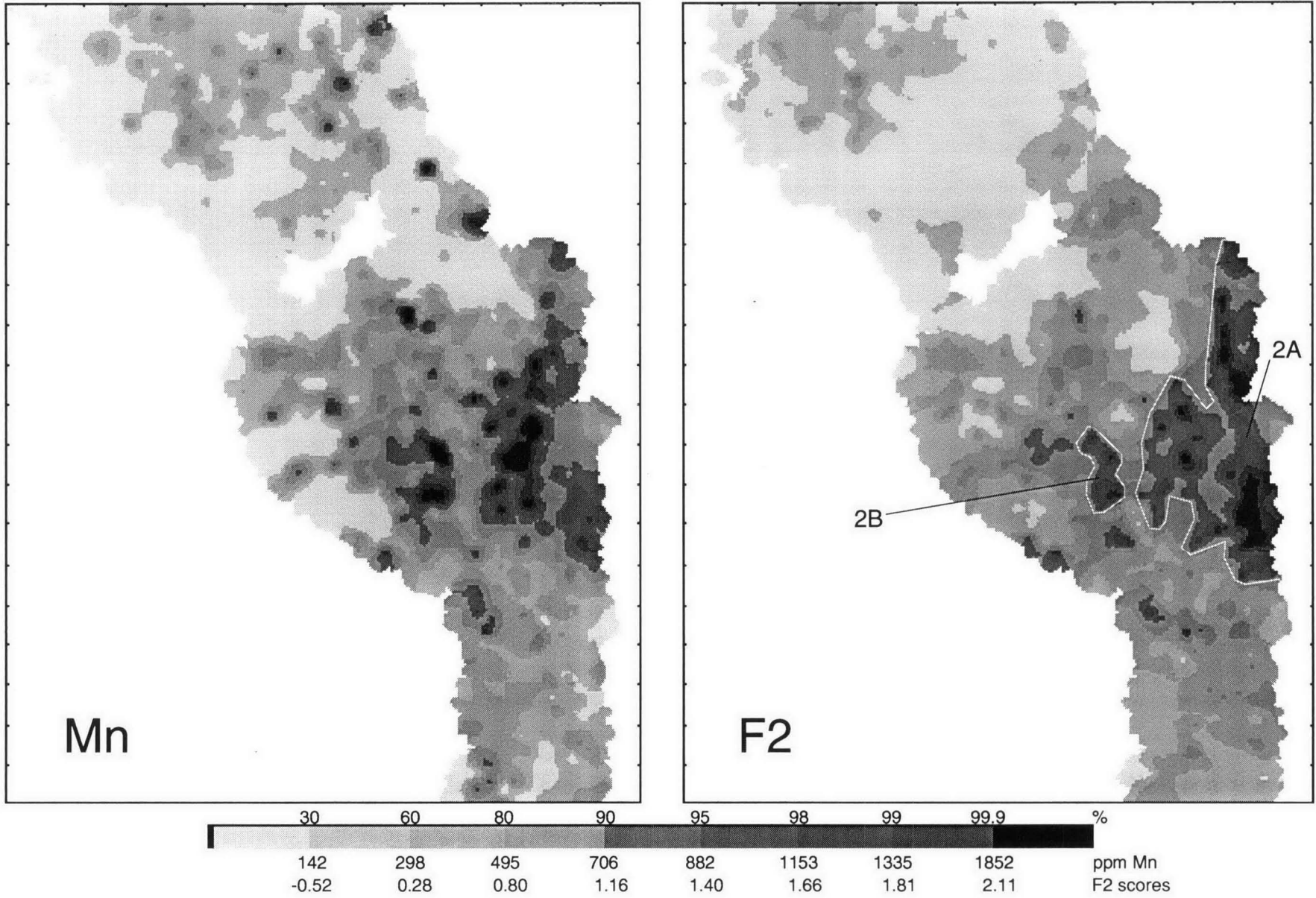


Figure 11. Image maps of the distribution of Fe, Cu, Ni, Ti, Mn abd Factor 2 scores in the Hann River region.







The most obvious difference between the spatial distributions of Fe and Mn is the greater presence of Fe over the Chillagoe Formation. Mn highs over the metamorphics correspond to Fe highs but, because of the percentage slice used in the image maps, appear more intense and extensive than the Fe patterns. No whole rock analyses for the Chillagoe Formation in the survey area are available.

Ti is also concentrated over the metamorphics rather than the Chillagoe Formation. Ti highs show marked spatial similarity to those of Nb which was extracted in Factor 1, but the separation may be due to moderate Ti values versus very low Nb values over the Chillagoe Formation, and to a patch of moderate Nb values in the Dixie area not reflected by Ti.

As stated above, As shows little concurrence with the plot of Factor 2 scores, or of Fe. The major As high is in the south of the survey area over Pratt Volcanics and adjacent sediments. It is an extension of a large As-Bi-Sb high at the Cu-mining Cardross area in the Red River Region (Cruikshank, 1997), and will be discussed later with regard to its' relationships with Sb\* and Au#.

Although Ni and Cr are often closely associated, especially when derived from mafic rocks, the only close correspondence appears to be several minor highs over outcrops of the Carew Greenstone in the Dixie area. Elsewhere the two elements show markedly differing distributions with Ni showing coherent highs over the Chillagoe Formation, and some lesser highs over adjacent metamorphics (mostly Chelmsford Gneiss). The Chillagoe Formation has many units containing metabasalt and 'mafic volcanics'. The Ni values do not appear high enough (i.e. up to 60 ppm) to indicate mineralisation as opposed to a lithochemical signature associated with mafic rocks. In contrast Cr highs consistently occur over the sedimentary rocks (>500 ppm Cr and <10 ppm Ni) to the north and south of the granites and metamorphics in the Yambo area: to the north over Dalrymple Sandstone and Gilbert River Formation, and to the south over Walumbilla and Gilbert River Formations. The reason for this is not obvious but similar Cr patterns were occur in the north of the Red River Region to the south of the survey area (Cruikshank, 1997).

The Chillagoe and Hodgkinson Formations both contain Cu mineralisation (Amos and Keyser, 1964), and copious quantities of metabasalt and mafic volcanics. One would therefore expect high Cu backgrounds over, or adjacent to, the rocks of these formations and Cu highs in the survey area are largely restricted to the Chillagoe Formation north of the Mitchell River, with some carry over into the metamorphics to its west. To remove lithochemical contributions a stepwise multiple regression of log(Cu) against factor scores (41 samples with greater than 9.90 ppm residual on the first pass were eliminated) gave the equation:

$$\log(\text{Cu}_p) = 0.486 \cdot \text{F2} + 0.048 \cdot \text{F5} + 0.069 \cdot \text{F6} + 0.643$$

where  $\text{Cu}_p$  is the background Cu value predicted from the lithochemical information expressed in the factors. All factors were included as none appeared to be related exclusively to Cu mineralisation. Distribution of the residual,  $\text{Cu}_{\text{res}}$  (or  $\text{Cu} - \text{Cu}_p$ ), is shown in Figure 13. Although patchier, most highs still occur over Chillagoe Formation, including highs near the sites of the Hannahbelle, Red Hill and Mitchell Surprise Cu deposits (Amos and Keyser, 1964) in the south of the area. Greater emphasis is placed on the area north of Palmerville where secondary Cu minerals have been found disseminated in altered mafic volcanics, and in a small lode about 5 km from Palmerville (Lucas and Keyser, 1965). Two areas to the west and south show up. Area 2Z to the west is a small high on the border of

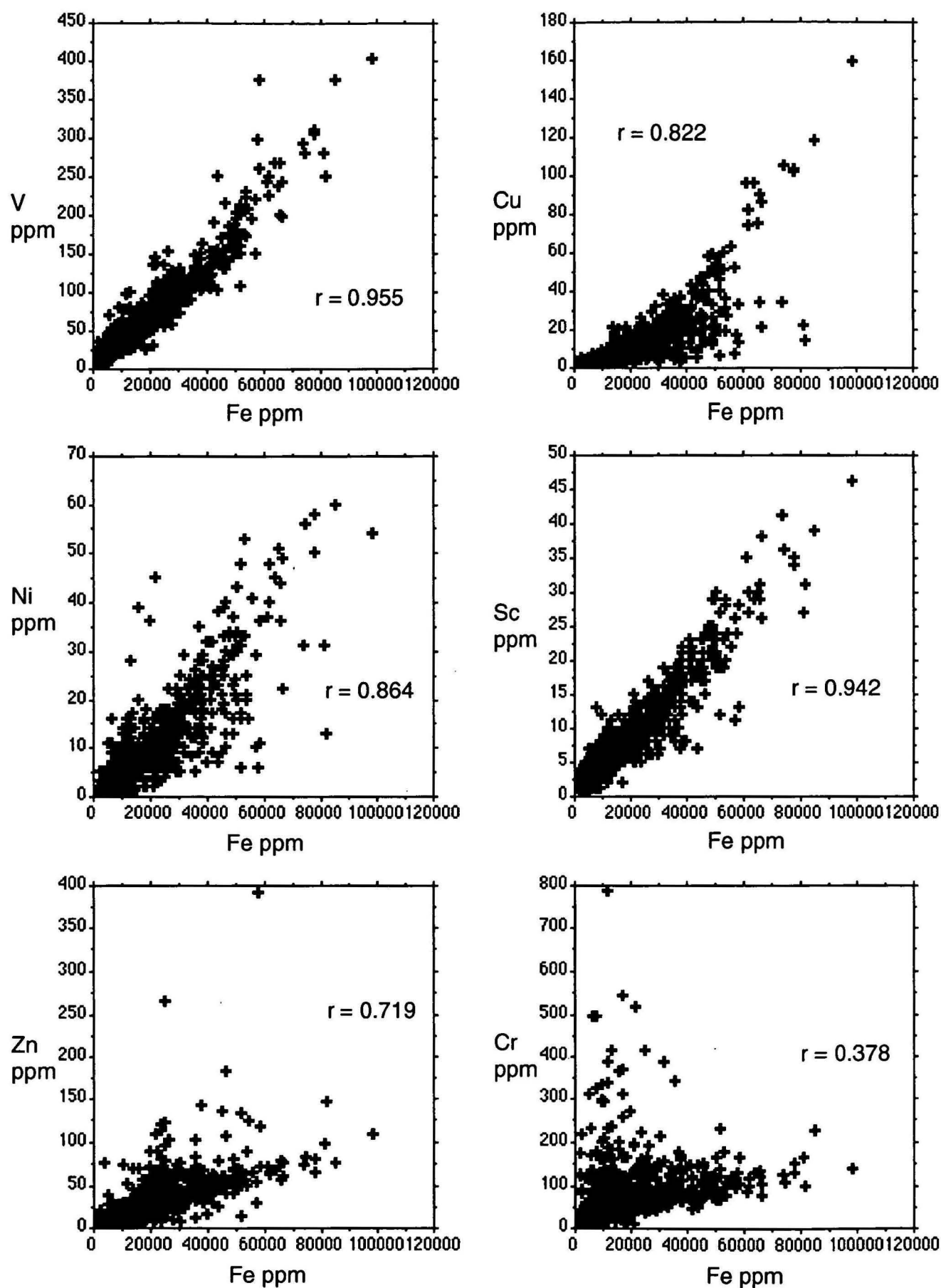
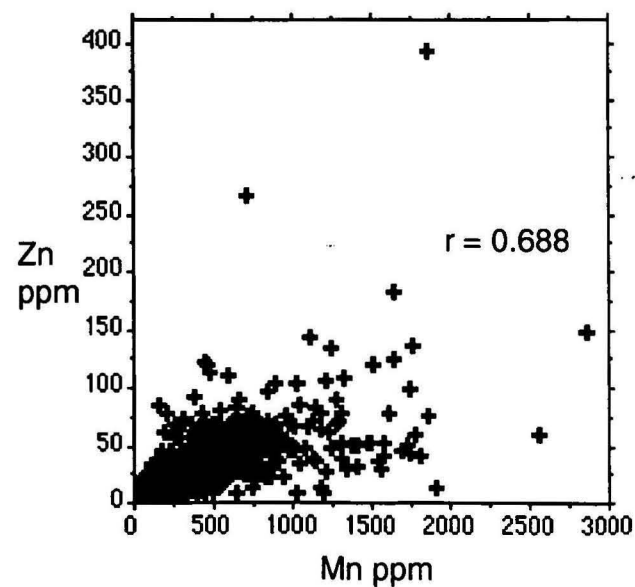
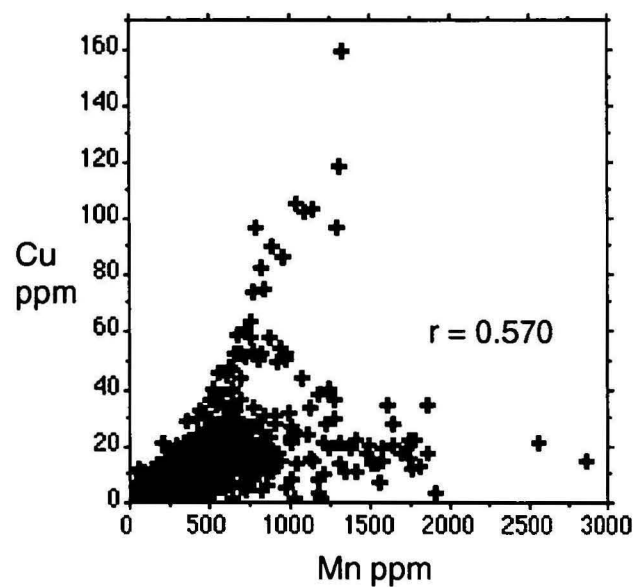
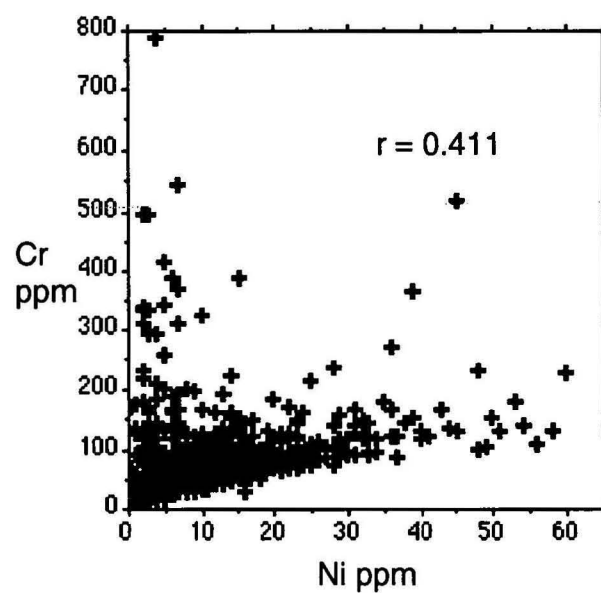
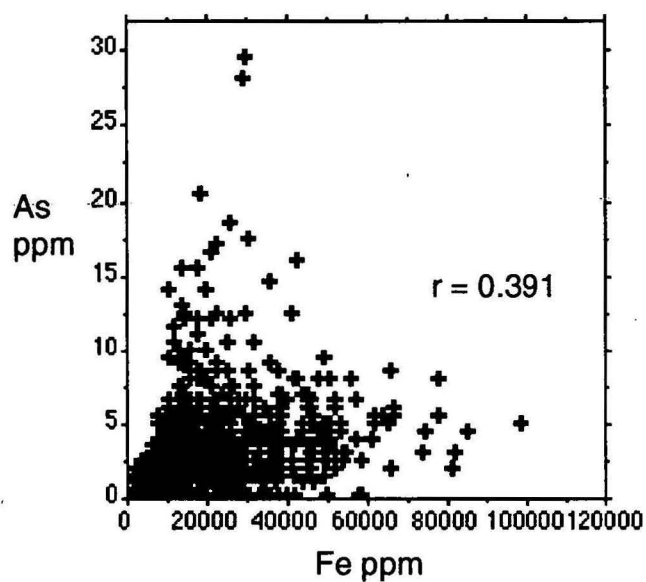
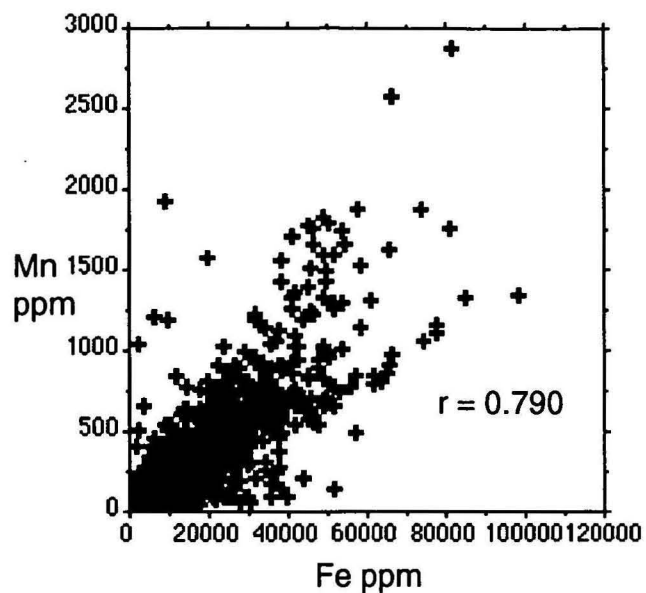
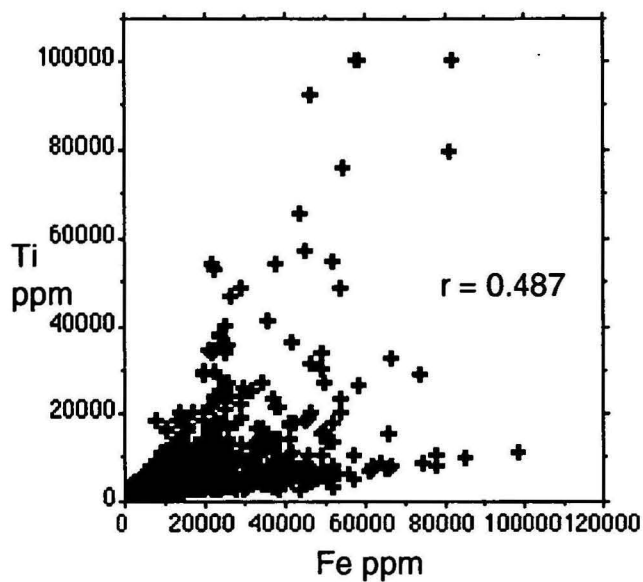


Figure 12. Scatterplots of selected pairs of Factor 2 elements.





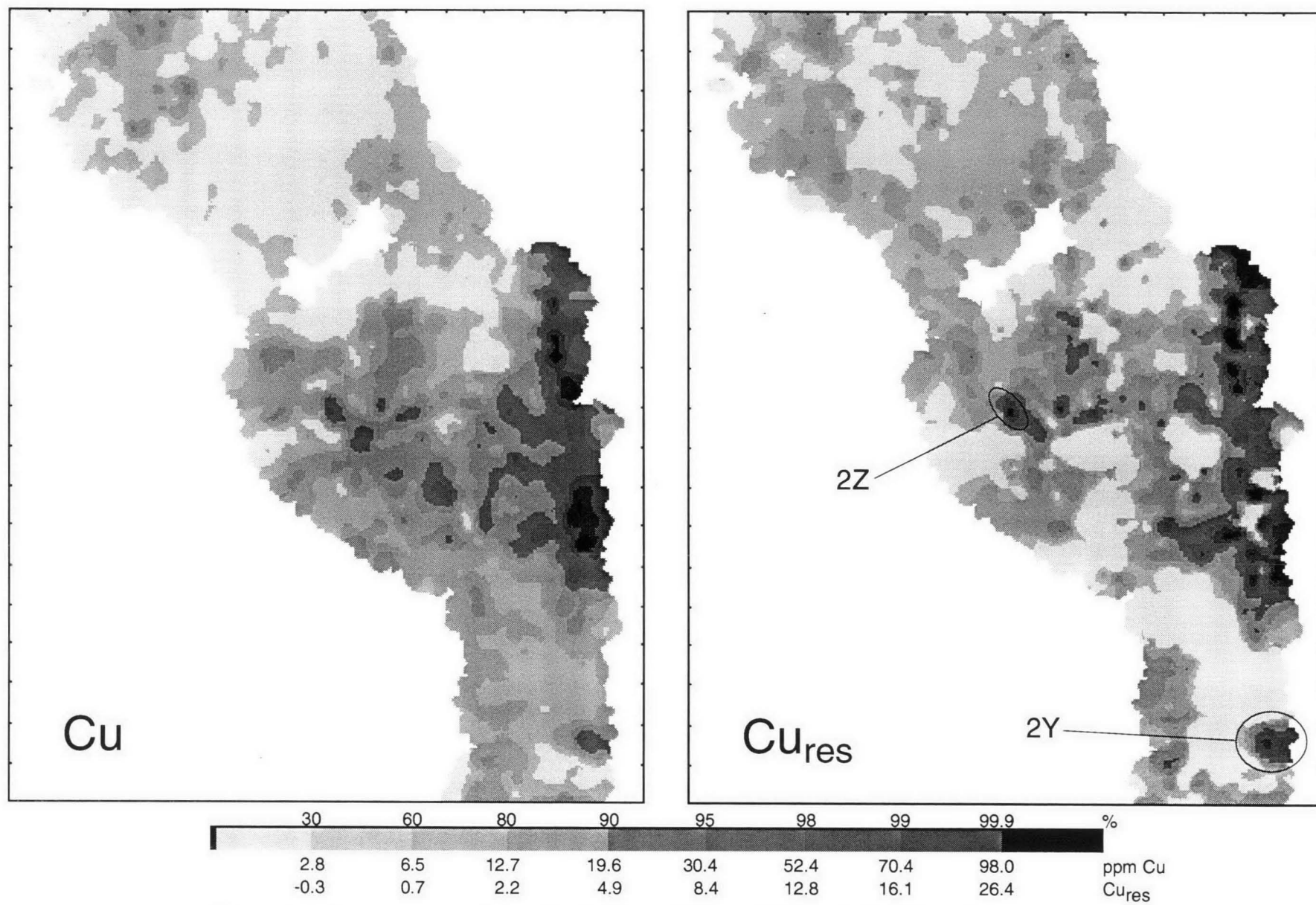


Figure 13. Image maps of the distribution of Cu and Cu<sub>res</sub> in the Hann River Region.

the MOUNT MULGRAVE and WALSH 1:100 000 sheet areas overlying metamorphics, mostly Oswald Schist, and undifferentiated granite. Area 2Y to the south is over another outcrop of Chillagoe Formation which contain several Cu mines (Montevideo, King Vol and Tartana - Amos and Keyser, 1964).

Zinc, while relatively mobile in the secondary environment under normal conditions, is particularly prone to concentration by coprecipitation with, or adsorption onto, hydrated Fe and Mn oxide precipitates (Nichol and others, 1967; Jenne, 1968). Consequently, false anomalies due to scavenging often appear in geochemical surveys, anomalies which have little or no direct relationship to either Zn bedrock geochemistry or to Zn mineralisation. Therefore moderate to high Zn values in samples relatively low in Fe and/or Mn might be of greater interest than higher Zn values in samples with high Fe and/or Mn contents. Interactive scatterplots (from DATA DESK) depicting Zn/Fe, Zn/Mn and location are shown in Figure 14; interactive in that points highlighted in one plot (ie Zn/Fe) are automatically highlighted in all other active plots. Two areas (Areas 2X and 2W) of interest are defined by high, or by clusters of high and moderate, Zn/low Fe-Mn values.

Factor 2, Zn's prime factor, appears to represent the Zn/Fe/Mn relationship. Multiple stepwise regression of log(Zn) against factor scores (25 samples with Zn residuals greater than 27.5 ppm eliminated after first pass) gave the equation:

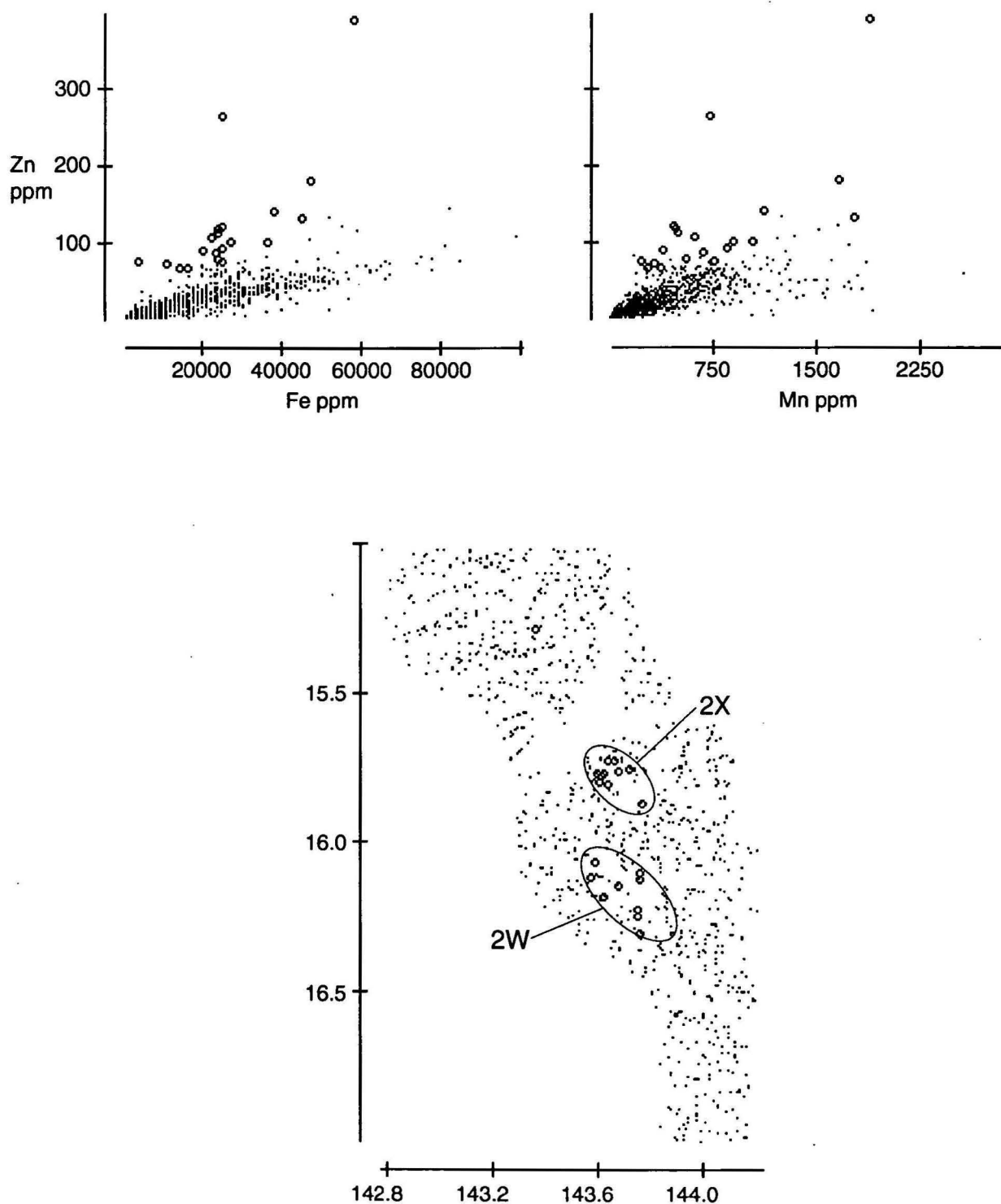
$$\log(\text{Zn}_p) = 0.086 \cdot \text{F1} + 0.320 \cdot \text{F2} + 0.144 \cdot \text{F3} - 0.020 \cdot \text{F4} + 0.076 \cdot \text{F5} + 0.021 \cdot \text{F6} + 1.207$$

The distribution of  $\text{Zn}_{\text{res}}$  is shown in Figure 15. The moderate Zn highs over Chillagoe Formation have been greatly reduced and apart from a few patchy  $\text{Zn}_{\text{res}}$  highs in the south of the survey area, Areas 2X and 2W from Figure 14 stand out clearly. Area 2X is over Oswald, Annie Creek and Saraga Schists and is drained by tributaries of the King River. Area 2W is over Rosser and Saraga Schists and is drained by the Rosser and Reid Creek systems. Both areas have been intruded by andesite-dolerite dykes. Both areas have been explored for base metals on several occasions. Possible anomalous Zn values were found in the AP's covering Area 2W but after no evidence of base metal mineralisation was found, these anomalies were ascribed to 'an extensive pre-Mesozoic regolith' (Culpeper and others, 1992). Base metals (presumably including Zn) were reported as low in AP's over Area 2X.

### 5.3 Factor 3 (Felsic rocks and minerals)

Factor 3 comprises Rb, Ba, Sr, Be\*, Ga, Pb and Ti\*, with minor contributions from Mn, P\* and Zn, and negative contributions from Sn, Zr and Hf. Box plots of the relative abundances of the prime elements are shown in Figure 16, and image maps for Rb, Ba, Sr and F3 are shown in Figure 17 (Pb in Figure 20). Scatterplots of selected element pairs are shown in Figure 18.

The factor is thought to relate to the weathering of K-rich minerals, probably from granites, since all prime elements are known to concentrate in the common K-Al minerals such as K-feldspar, biotite, muscovite, etc (Cruikshank, 1994). In the survey area highs for Factor 3 scores occur over granites, mostly over Kintore Supersuite granites in the Dixie area, and are generally low over the adjacent sedimentary rocks. The factor appears to be more of a composite of its component parts than the previous two factors (which essentially followed REE/Th and Y, and Fe respectively) in that no one element showed a distribution pattern which was essentially identical to that of the factor scores (Ba would be the closest).



**Figure 14.** Plots of Zn against Fe and Mn. Samples selected in Fe/Zn plot are also high-lighted in Mn/Zn and location plots.



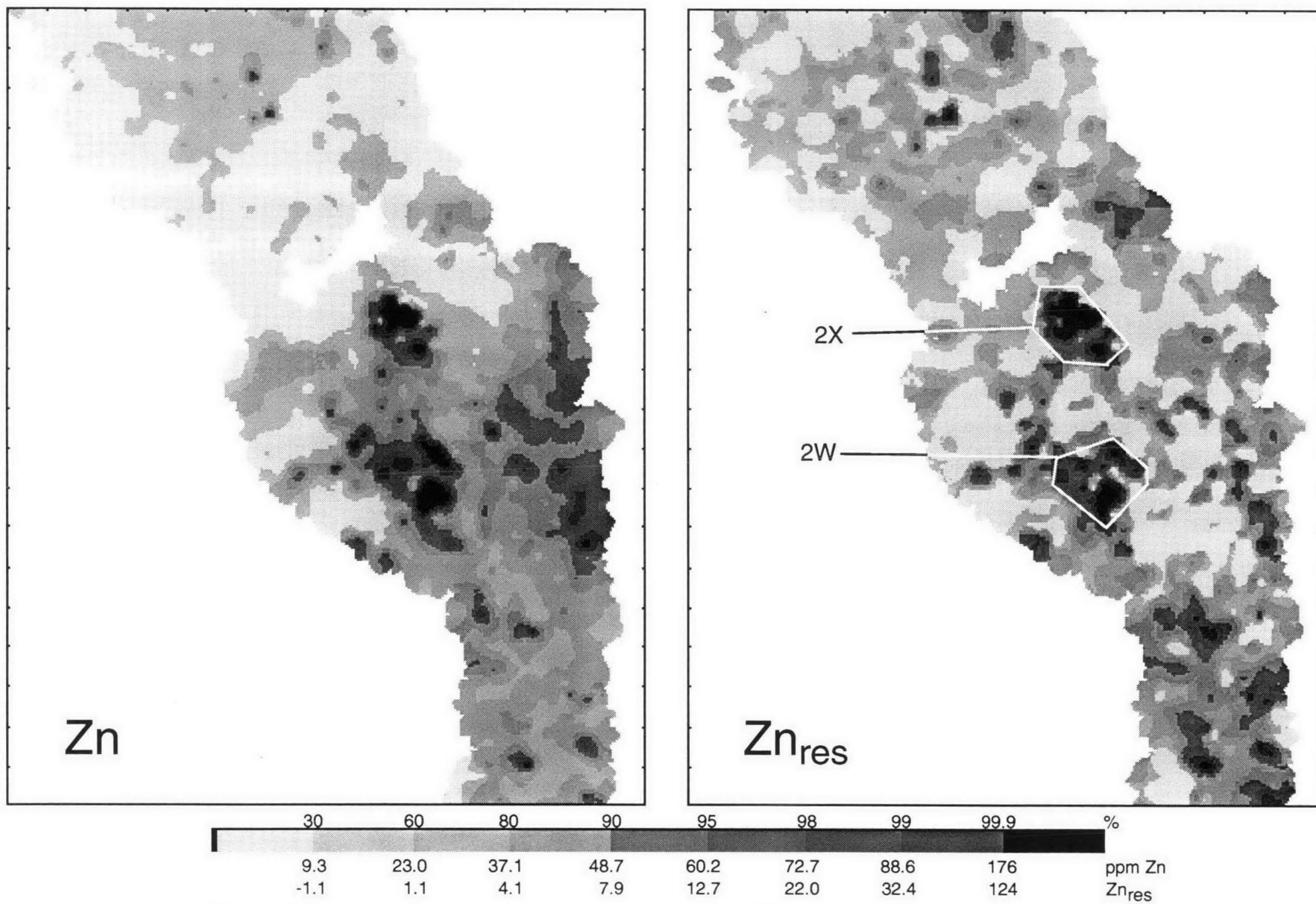


Figure 15. Image maps of the distribution of Zn and Zn<sub>res</sub> in the Hann River Region.

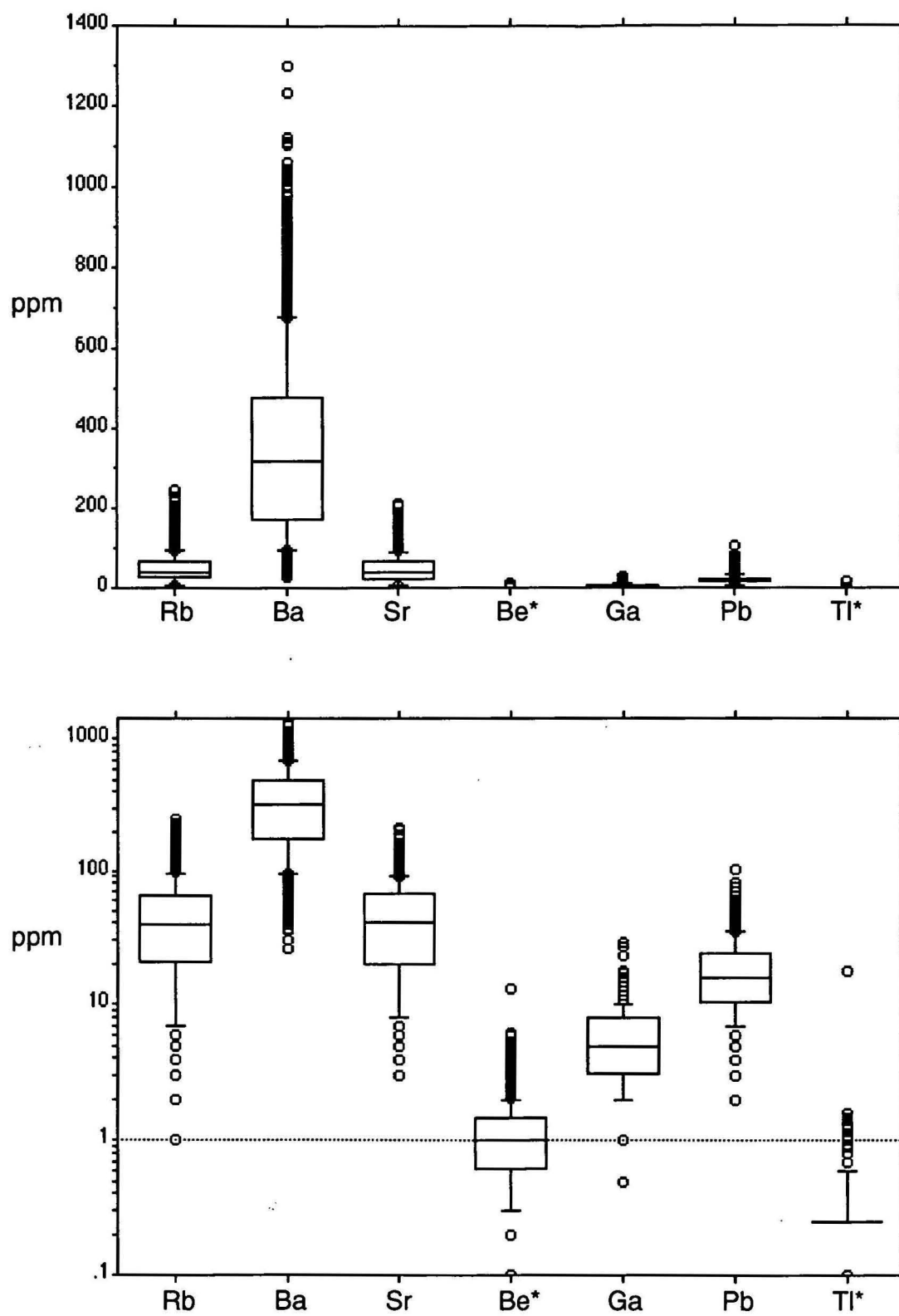


Figure 16. Relative abundances of Factor 3 elements.

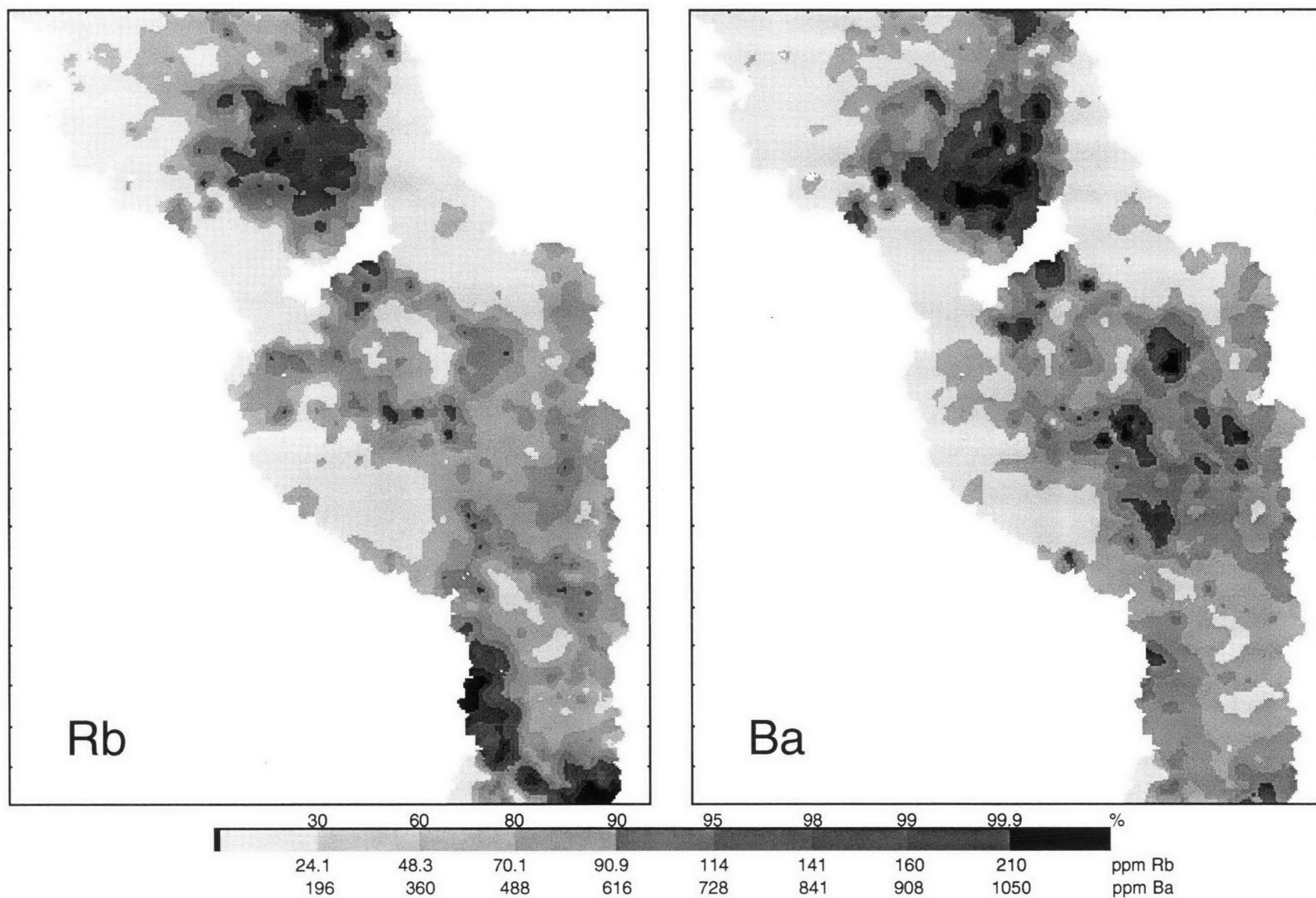
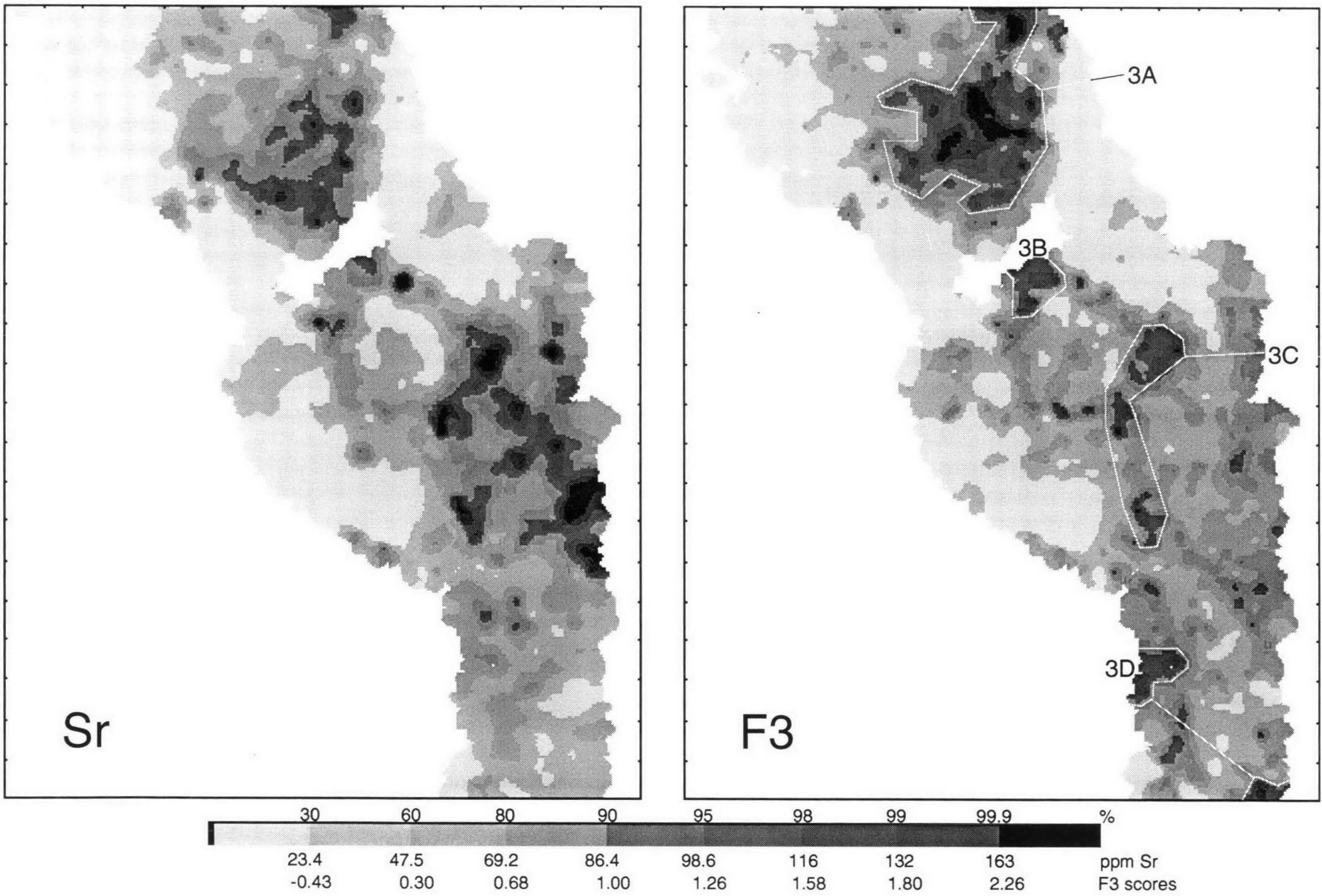


Figure 17. Image maps of the distribution of Rb, Ba, Sr and Factor 3 scores in the Hann River Region.





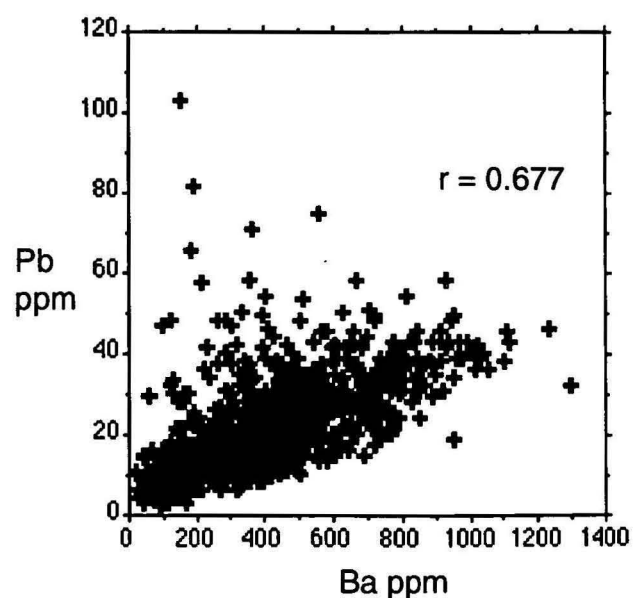
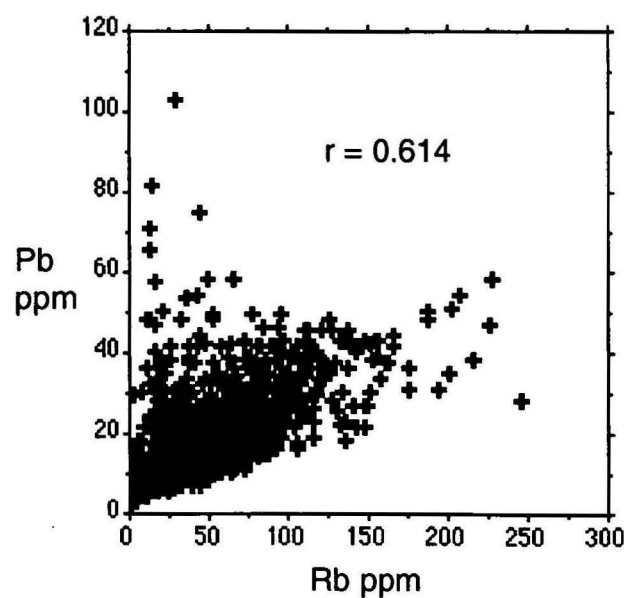
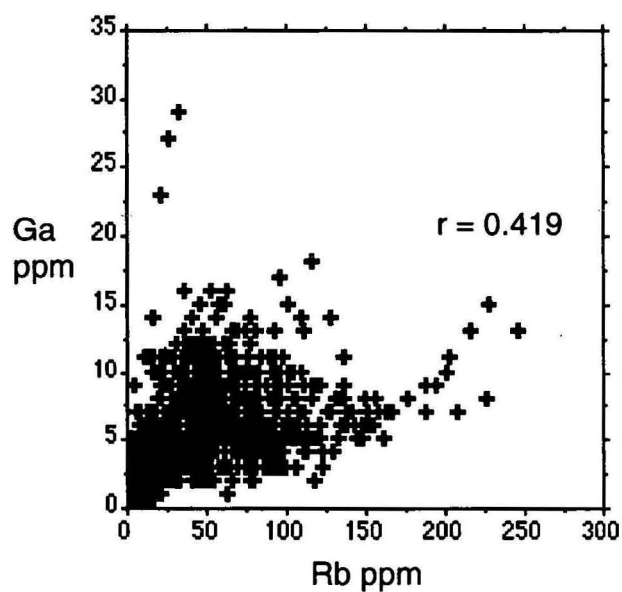
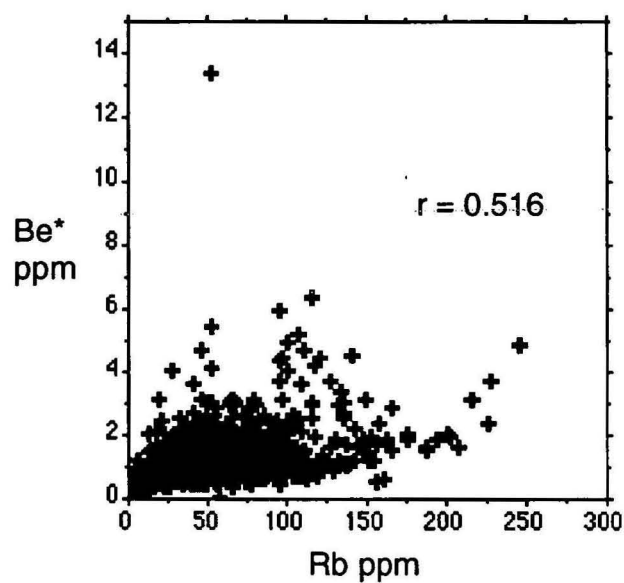
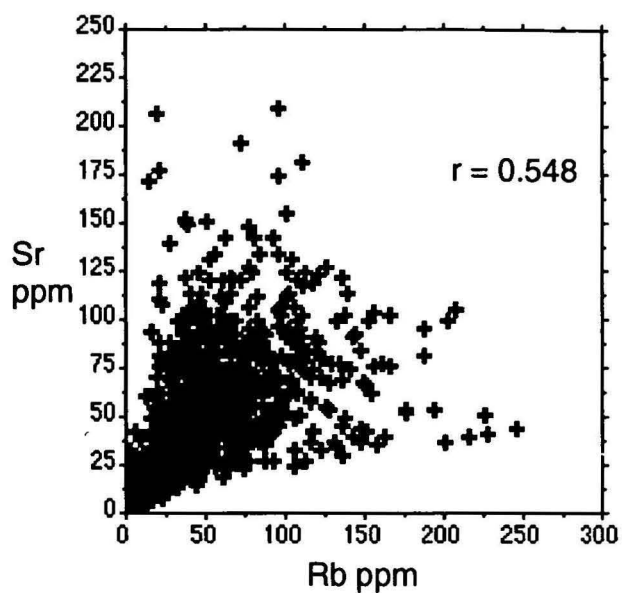
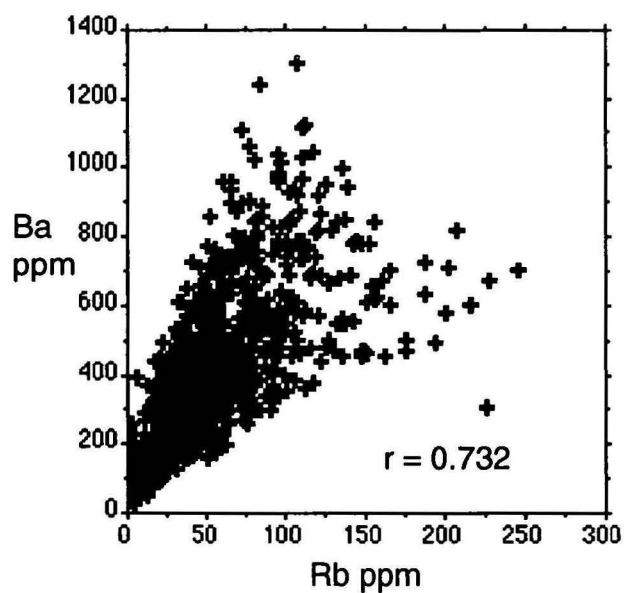


Figure 18. Scatterplots for selected pairs of Factor 3 elements.

Indeed, Ga, which tends to associate with Al rather than K, shows more differences than similarities. Factor 3 highs are:

Area 3A is on the Coleman Plateau east to southeast of New Dixie homestead. The plateau is an erosional surface so that the regolith, over granites of the Kintore Supersuite (Morehead, Imooya, Kintore and Mena Granites), is likely to have developed in-situ. The area is drained by tributaries of the northeast flowing Morehead River, and of the southwest to west flowing Alice River and Eight Mile Creek. The area shows strong Rb, Ba and Pb, and strong but more localised highs for Be\* and Ti\*.

Area 3B is on the Mulgrave Plain east of Pinnacles homestead. The area is over the Top Pinnacles Granite of the Aralpa Supersuite and is drained by the headwaters of the King River. The 'Desert' lies to the northwest. The area shows only moderate highs for Ba, Be\* and Pb.

Area 3C also is in the Mulgrave Plain and encompasses a number of factor score highs over the Lukinville Granodiorite. The northern most high is drained by tributaries of the Palmer River, and the headwaters of the north flowing Kennedy River. The other highs are northwest of the Mount Mulgrave homestead, drained by the Fox Creek system, and west of the homestead, drained by tributaries of the Mitchell River. The area shows strong highs for Ba, Sr, Pb and Be\*. Sr also shows highs to the east over metamorphics and Chillagoe Formation. Ga also shows highs in the immediate area but the most intense of these do not correspond to the factor score highs.

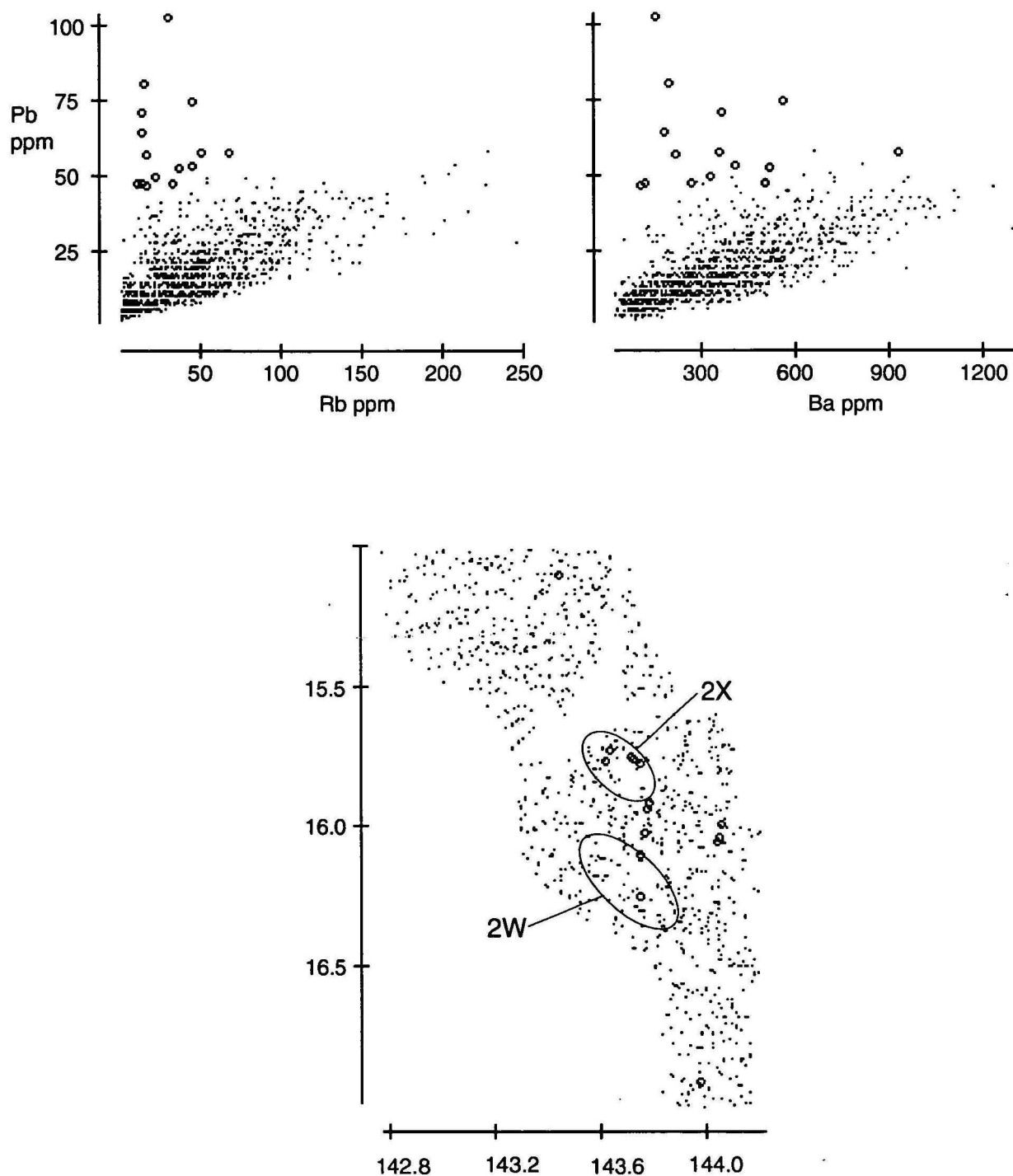
Area 3D is two highs in the Bulimba Plain southwest and south of Wrotham Park homestead. The first area lies between the Walsh River and Brown Creek in Quaternary sediments. The area shows highs for Rb, Ti\* and Be\*. To the south-east, over Pratt Volcanics and drained by tributaries of the Walsh River, the second Rb-Ti\*-Be\* high lies on the southern edge of the survey area and may be the source of materials responsible for the first high.

The only element in Factor 3 with any direct economic significance is Pb. In the EBAGoola sheet area to the north, Pb appeared to be due mainly to the weathering of K-rich minerals (Cruikshank, 1994: maximum Pb - 75 ppm), whereas in the Red River Region to the south there appears to be a greater possibility of Pb (+Zn) mineralisation (Cruikshank, 1997: maximum Pb - 179 ppm). Rb and Ba are probably the best indicators of K in the bedrock so that samples with moderate to high Pb values and low Rb and Ba values may be of more interest than samples which are high in all three. Figure 19 shows interactive scatterplots of Pb/Rb, Pb/Ba and localities. One cluster of high Pb, low Rb/Ba values occurs in Area 2X where interesting Zn values also occurred (see Figures 14 and 15).

Stepwise multiple regression of log(Pb) against all factor scores (after elimination of 39 samples with first pass residuals greater than 11.58 ppm) gave the equation:

$$Pb_p = 0.151 \cdot F1 - 0.027 \cdot F2 + 0.169 \cdot F3 + 0.012 \cdot F4 + 0.058 \cdot F5 + 1.183$$

The spatial distributions of Pb and Pb<sub>res</sub> are shown in Figure 20. There are few noteworthy differences between the two images although Area 2X is slightly emphasised at the expense of Pb other highs in the immediate area. This could indicate that although



**Figure 19.** Plots of Pb against Rb and Ba. Samples selected in Pb/Rb plot are also high-lighted in Pb/Ba and location plots.

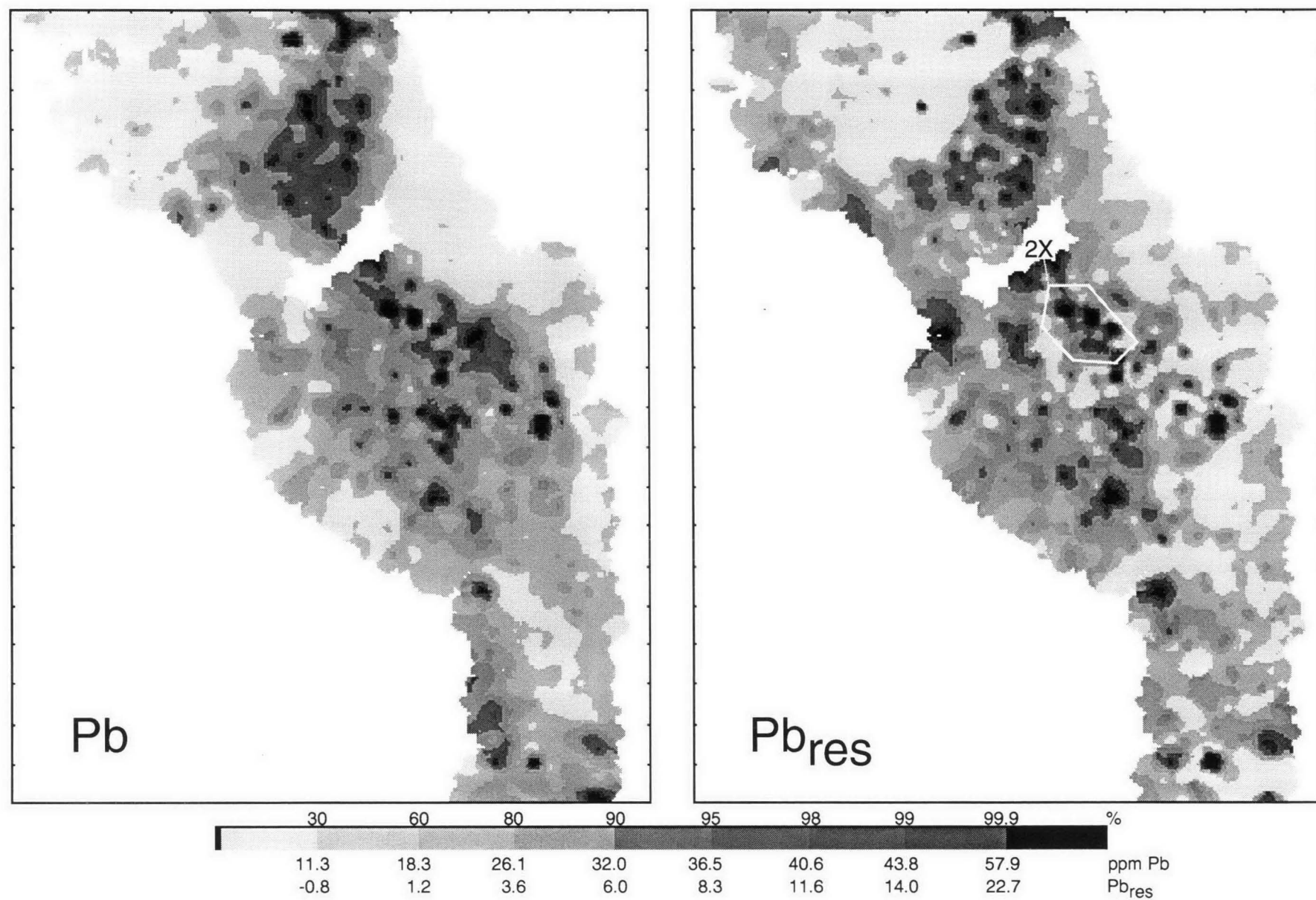


Figure 20. Image maps of the distribution of Pb and Pb<sub>res</sub> in the Hann River Region.



potential for Pb mineralisation is not high, the best chance is in Area 2X (also site of  $Zn_{res}$  high, and unsuccessful base metal exploration - see Section 5.2). The relatively coherent Pb high over granites in the Dixie area becomes patchier in the  $Pb_{res}$  image but retains the same general pattern.

#### 5.4 Factor 4 (Sn-W heavy minerals)

Factor 4 comprises  $Sb^*$ ,  $W^*$ ,  $Sn$ ,  $Mo^*$  and  $Ag^*$ , with minor contributions from  $As$  and  $Tl^*$ . The communalities of all but  $Sb^*$  are on the moderate ( $W^*$ ,  $Sn$  and  $Mo^*$ ) to low side ( $Ag^*$ ) (see Table 6(a)) indicating that much of each elements total variance is not accounted for by the factors (Dillon and Goldstein, 1984). Figure 21 shows image maps of  $Sb^*$ ,  $Sn$ ,  $Mo^*$  and F4.

The elements in the factor do not show the similarity of distribution patterns characteristic of Factors 1 and 2, and, to a lesser extent, Factor 3. However, all show highs in the southern most part of the survey area, north of Cardross in the Red River Region (Cruikshank, 1997). The differences are mainly in the distribution of moderate and low values.  $Sn$  with  $W^*$  and  $Mo^*$  may suggest tin-tungsten mineralisation, as is common near granites of the O'Briens Creek Supersuite in the Red River Region to the south, but in the Hann River Region Factor 4 highs occur only rarely over, or near, granites.

Factor 4 highs occur in:

Area 4A is in the southern most part of the survey area. The most intense of the highs is in the south-east is over the Palmer-Hodgkinson Uplands, mostly over Pratt Volcanics. Other highs to the west and northwest are over the Bulimba Plain over sedimentary rocks of the Gilbert River and Wallumbilla Formations, and Quarternary sediments. The area is drained by tributaries of the Walsh River. The area shows highs for  $Sb^*$ ,  $W^*$ ,  $Sn$ ,  $Mo^*$  and  $Ag^*$  (and  $As$  and  $Bi^*$ ), and is an extension of the regional As-Bi-Sb high in the north of the Red River Region (Cruikshank, 1997).

Area 4B is over the Chillagoe Formation and adjacent metamorphics to the north of Area 4A. The high is due to  $Sb^*$ . The area also shows highs for  $As$  and  $Au^{\#}$ , consistent with known lode gold mineralisation in the Palmer River Gold Field.

Area 4C is over Wyaaba beds in the Bulimba Plain. The area shows moderate highs for  $W^*$ ,  $Mo^*$  and  $Sn$ .

Area 4D contains a number of small highs over Wyaaba beds and some Quarternary sediments in the Bulimba Plain. The highs is due to a number  $Sn$  highs over sediments west of the granites in the Yambo area, and south of those in the Dixie area.

The area shows elevated levels of  $Sn$ , although not to the same extent as the Red River Region to the south. The  $Sn$  average for samples collected in the Hann River Region is 16.5 ppm (geometric mean 3.1 ppm), compared with 33.6 ppm (9.8 ppm) for the Red River Region (Cruikshank, 1997), and 5.0 ppm (2.1 ppm) for the EBAGoola sheet area to the north (Cruikshank, 1994). As in the EBAGoola sheet area, and some of the Red River Region, most  $Sn$  highs occur over sedimentary rocks adjacent to the granitic and metamorphic rocks in the Dixie and Yambo areas, notably residual unconsolidated sediments, Wyaaba Beds and Bulimba Formation at Dixie, and unconsolidated

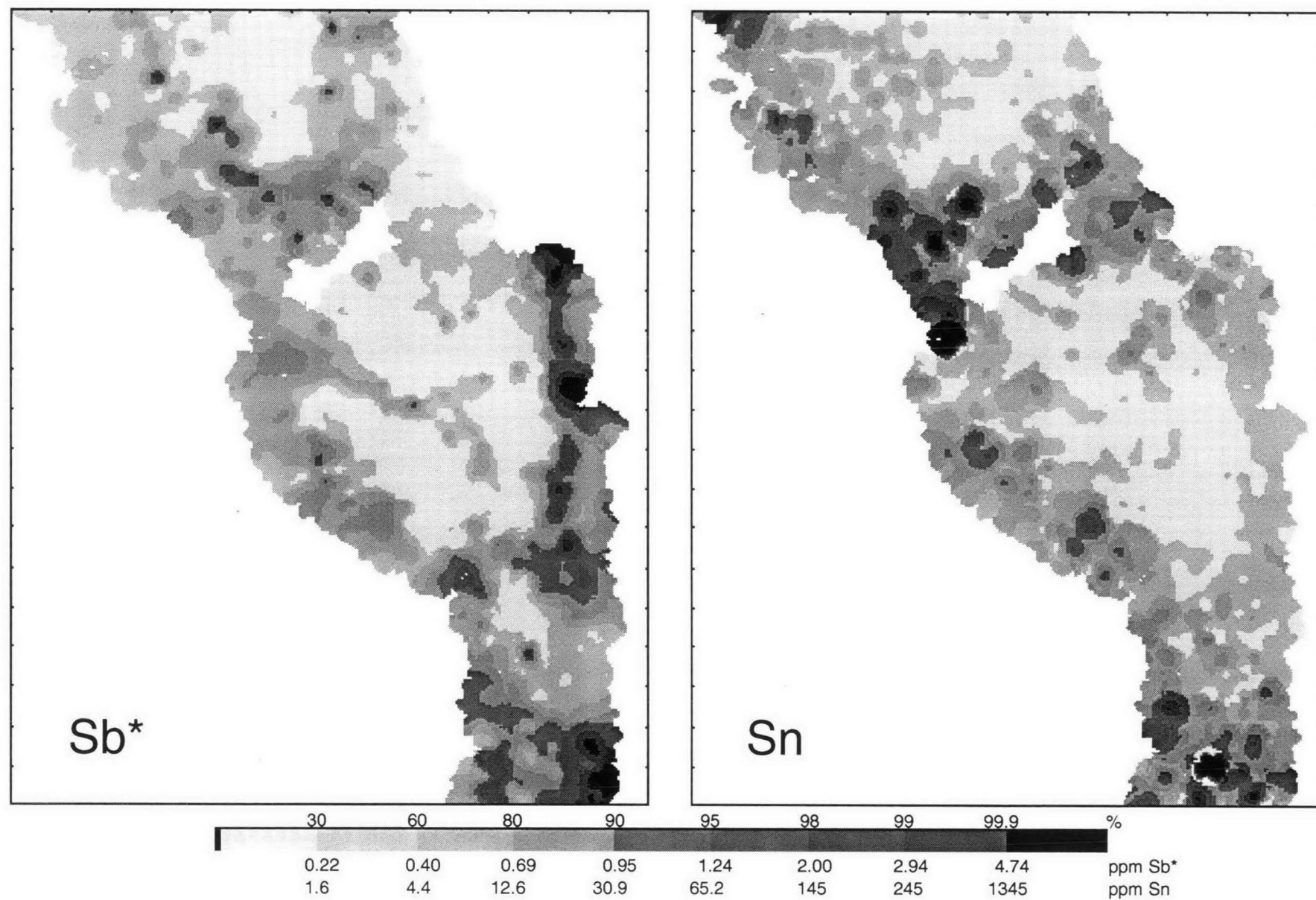
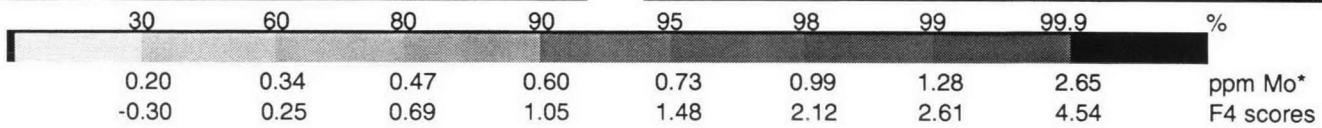
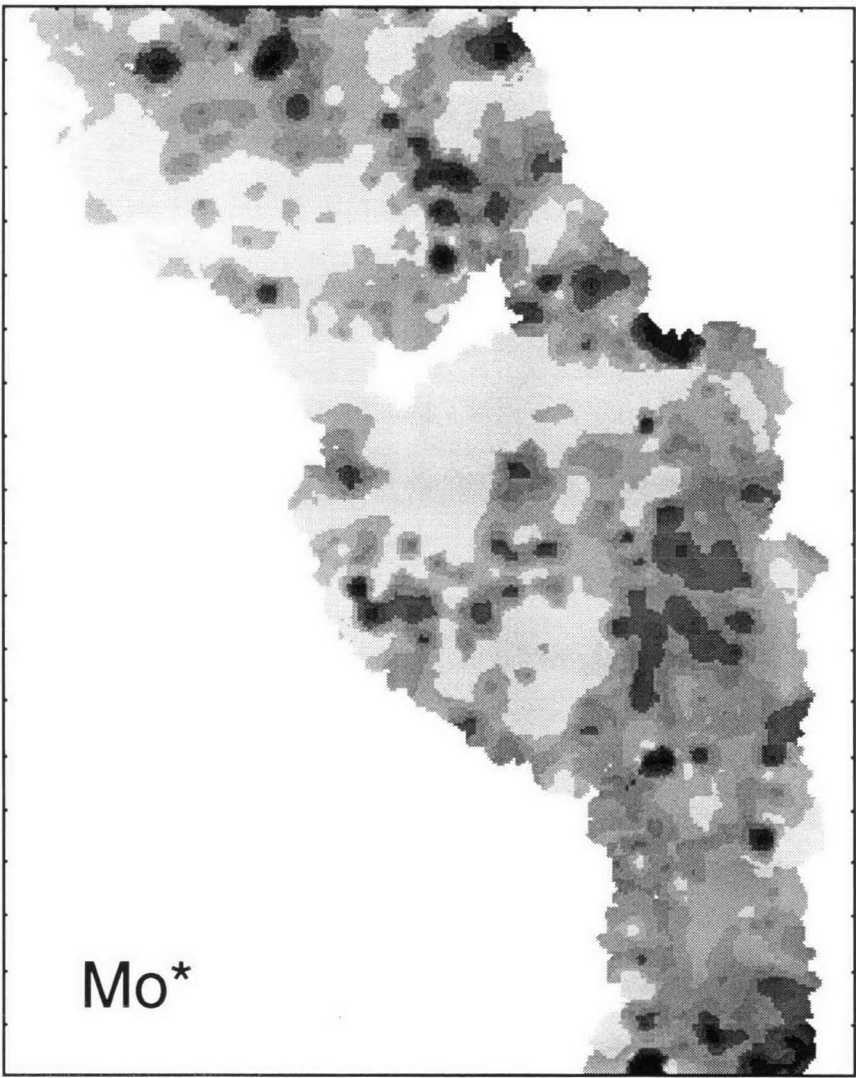
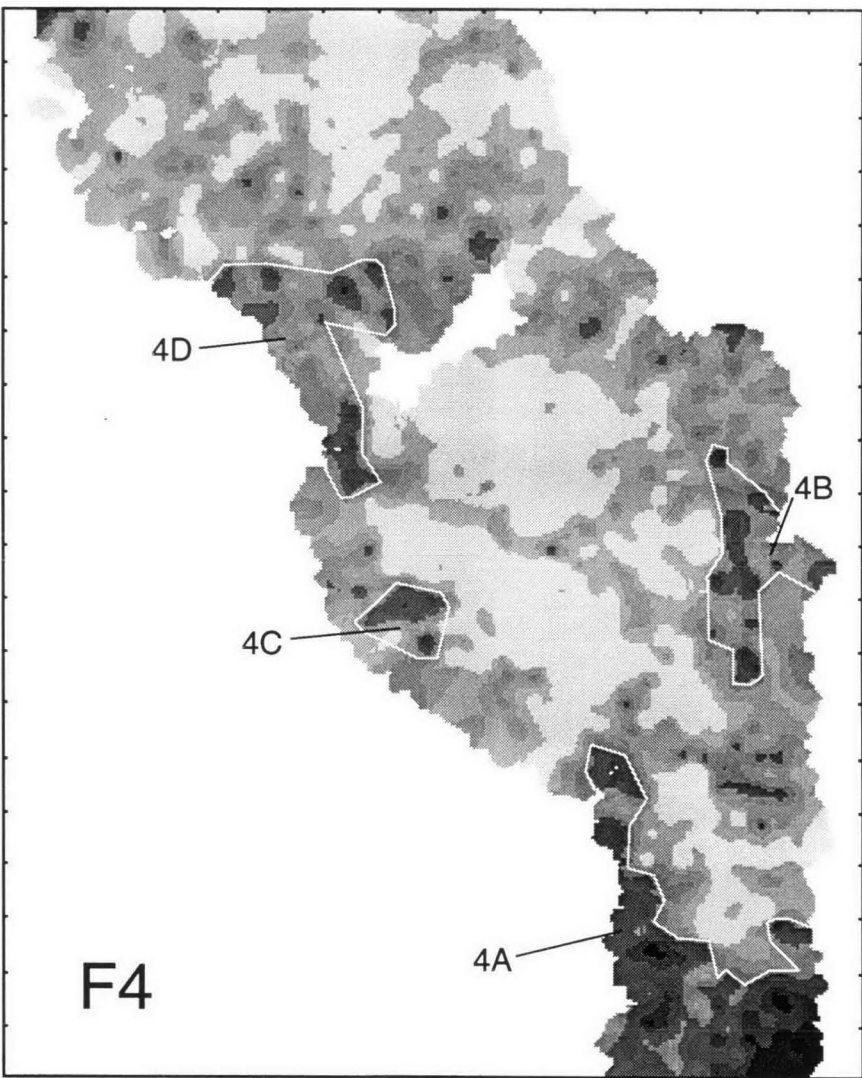


Figure 21. Image maps of the distribution of Sb\*, Sn, Mo\* and Factor 4 scores in the Hann River Region.



alluvial sediments, Wallumbilla and Gilbert River Formations in the south of the survey area. Indeed, Sn values over the granitic and metamorphic rocks (and the Chillagoe Formation) are almost uniformly low (<5 ppm). There is also little correspondence between the distributions of Sn and W, such that primary Sn-W mineralisation would appear unlikely. The reason for the Sn distribution is not obvious, but may be related to reworked (secondary) cassiterite from palaeo-drainage systems (Cruikshank, 1994), or from sedimentary rocks derived from higher level granites long eroded away. Parts of Area 4D have been covered by several AP's and, although concentrations of about 200 ppm (0.6 kg/m<sup>3</sup>) Sn were found (Culpeper and others, 1992), the amount of alluvial material was insufficient to be economic.

Lode gold mineralisation in the Palmer River Gold Field is usually quartz veins containing 'native gold, some pyrite and arsenopyrite, and a little stibnite' (Amos and Keyser, 1964). The northern part of the goldfield shows intense highs for Au# (see Figure 23) and Sb\*, but only a moderate high for As. However, Sb\* appears to be more prominent in the area because its values are generally much lower across the survey area (Sb\* at 95% is 1.24 ppm, As is 7.9 ppm) than coincident As values.

As stated above, Area 4A is an extension of a regional As-Bi-Sb high in the mineralised (Cu-Au-Ag) Cardross area of the Red River Region, although at a somewhat lower level and largely over Wallumbilla Formation and Quarternary sediments. The more intense of the factor and primary element highs occur over Pratt Volcanics and may be of interest. About 90 kg of Au, 2700 kg of Ag and 2000 tonnes of Cu were taken from the Cardross area in the early part of the century (Keyser and Wolff, 1964), and 360 tonnes of Pb, 260 kg of Ag and 0.3 tonnes of Cu were taken from the King Vol mine in the southern part of the survey area, so the area is mineralised. The Ag\* high in the south-east is in the general area of the King Vol mine.

### 5.5 Factor 5 (Bismuth?)

Factor 5 has Bi\* as its sole prime element. Therefore, it is not surprising that the image maps for Factor 4 scores and Bi\* are almost identical (Figure 22) with only minor modifications, usually of intensity only, due to the small contributions of the other elements in the dataset.

Bi\* shows highs in Area 4A as detailed above in the extension of the regional As-Bi-Sb high over the Cardross area in the Red River Region. The reason why Bi\* was not extracted in Factor 4 is probably a series of scattered highs over metamorphic rocks in the Yambo area, which are not shared with the prime elements of Factor 4. With one exception, a high over Rosser Schist and adjacent sediments, these are scattered and of low tenor.

### 5.6 Factor 6 (Au-Pd-Pt mineralisation)

Factor 6 is a precious metal of Pt#, Pd# and Au# with a negative contribution from Ge. Image maps for Au#, Pd#, Pt# and F6 are shown in Figure 23. The distribution of F6 scores is controlled more by Pd# and Pt# than by Au# (which has an almost identical factor loading in Factor 2) as these have higher transformation factors, but from the analytical values Au# is the more economically important and interesting. The relationship between Au# and As in Factor 2 is of interest.



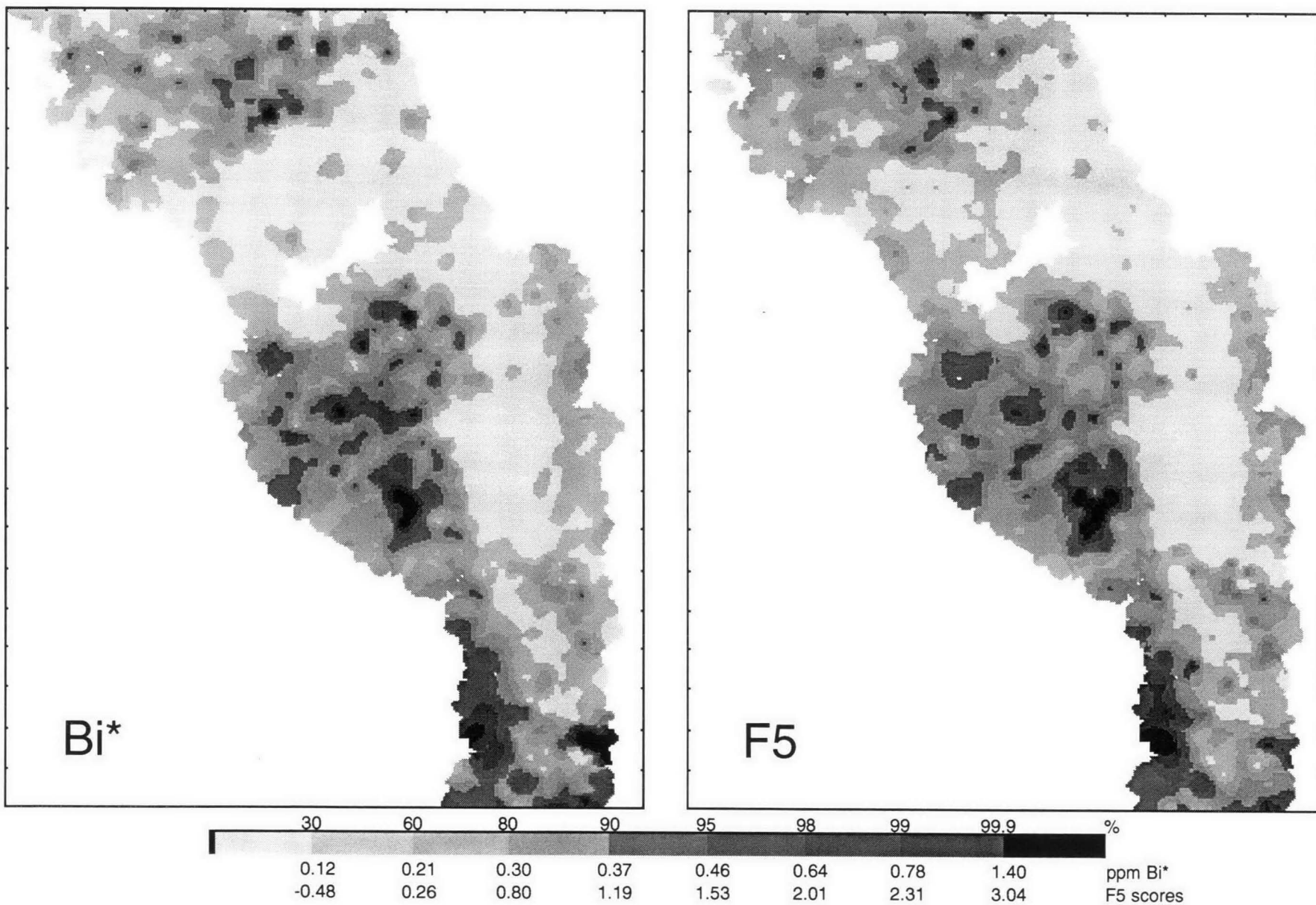


Figure 22. Image maps of the distribution of  $\text{Bi}^*$  and Factor 5 scores in the Hann River Region.

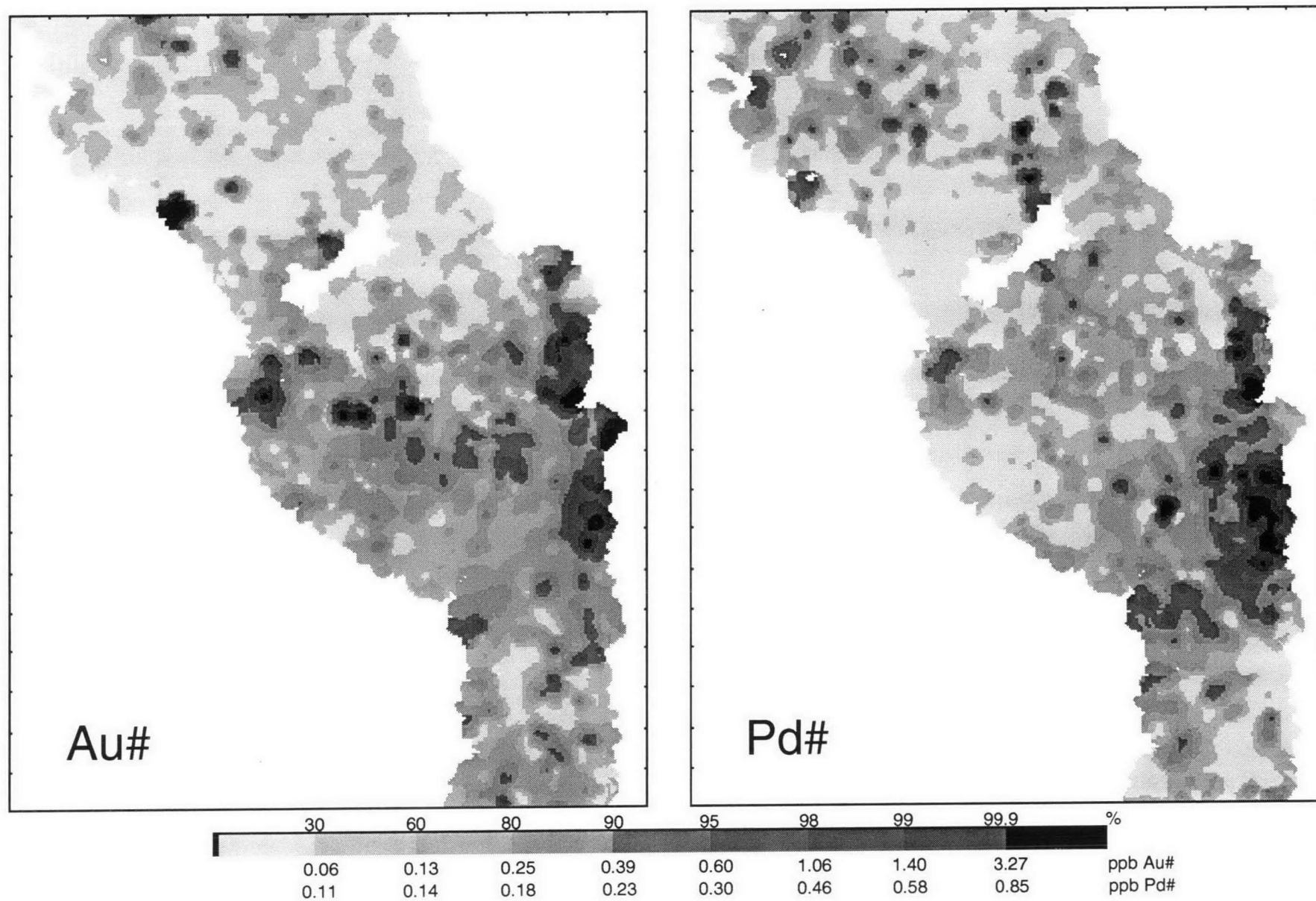
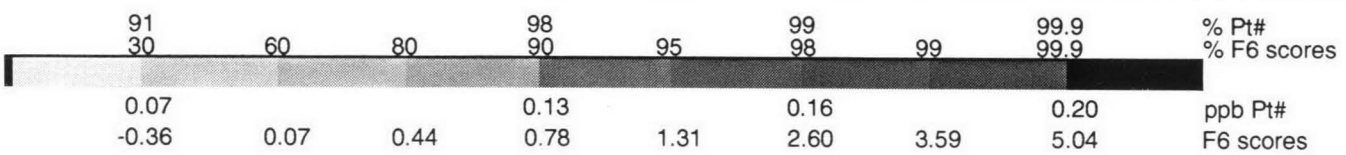
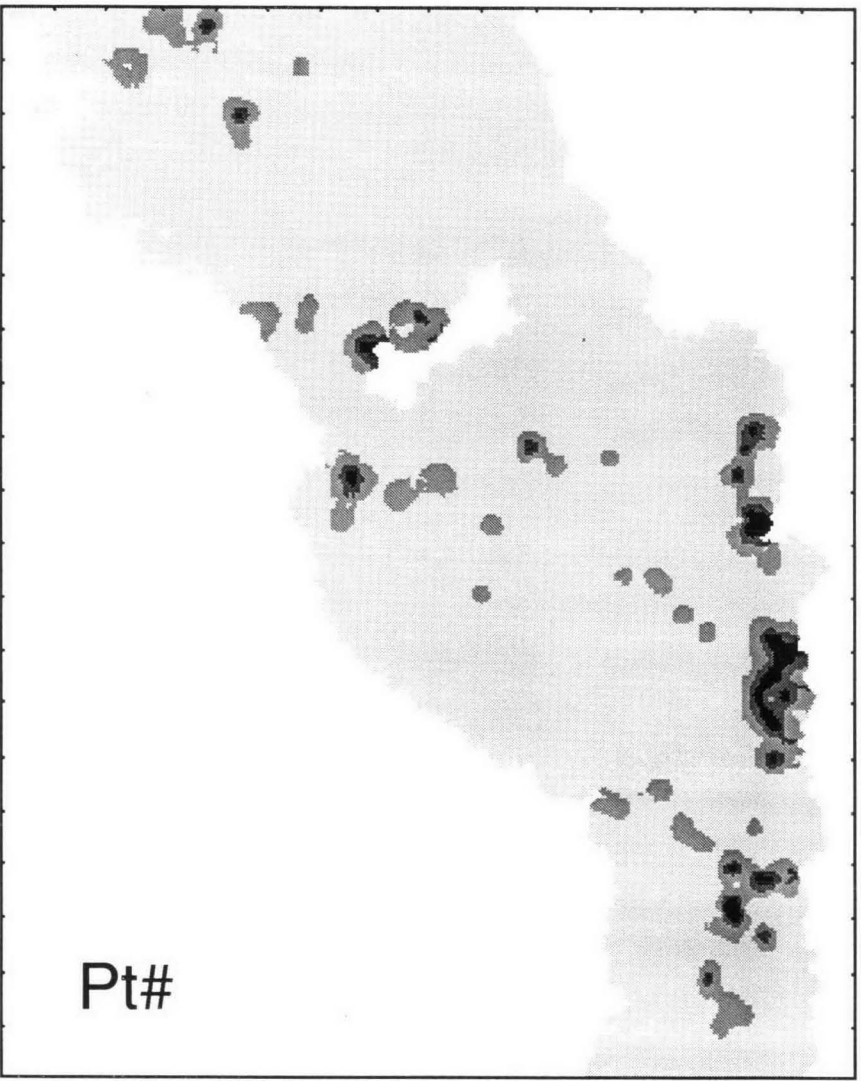


Figure 23. Image maps of the distribution of Au#, Pd#, Pt# and Factor 6 scores in the Hann River Region.



The survey area contains part of the Palmer River Gold Field and the Alice River Gold Field (Figure 24).

More than 90% of production from the Palmer River Gold Field was alluvial gold from tributaries of the Palmer River and from the Palmer River itself. Some lode gold was recovered near Maytown and in the limestone district to the south (Amos and Keyser, 1964). There, lode mineralisation was native gold with some pyrite, arsenopyrite and stibnite in quartz veins in greywackes of the Hodgkinson Formation. The most intense Au# high is west the site of Maytown township over Hodgkinson Formation in tributaries north and south of the Palmer River. Other highs, also north and south of the Palmer River, are mostly over Chillagoe Formation. Those north of the river and near Maytown are coincident with strong Sb\*, and moderate As highs. These Au# highs are north-south trending groups of anomalous (>0.6 ppb - Figure 24) samples in an area drained by Flood Creek north of Fairlight homestead on the Palmerville road, in an area stretching from immediately east of Fairlight south to the Palmer River, in the limestone district east to south-east of Palmerville and drained by Limestone Creek, and in the headwaters of the Little Mitchell River to the south.

Near Strathleven homestead tributaries of the Palmer River show a large Au# high (see Section 2.3.1). Although some sample sites are well removed from the current river bed, the area drained by these streams is mapped as Quarternary alluvial sediments (Qa) consisting largely of unconsolidated quartzose sand, silt and clay, and is part of the Mitchell Fan (see Figure 2). Alluvial gold may have originated much further upstream in the Palmer River Gold Field and been deposited in alluvial terraces. Several highs between Strathleven and Palmerville near the Palmer River, may be associated with granites of the Aralpa and Fish Creek Suites.

The Au# high on the Alice River also occurs over largely unconsolidated sediments, in this case Quarternary alluvial sediments, Tertiary residual sediments and rocks of the Bulimba Formation, and all occur in the Bulimba Plain. Several small Au# highs occur in the Dixie area in areas drained by Crosbie, Seventy Mile and Potallah Creeks, and over Holroyd Metamorphics. The area was known as the Potallah Creek Provisional Mining Field (Whitaker and Grimes, 1977).

Pt# and Pd# also show highs over the Chillagoe Formation, not surprising given that Fe, V, Cu and Ni also show highs in the area. The range of Pd# values (Pt# is only partially extracted by BCL) is not high (top 5% >0.30 ppb) but is the same order of magnitude as Au# values and may be of interest. An association based largely on the elements mentioned above (i.e. Cr+Ni+Pd#+Pt#+V) is used in the Platinum Index (Ptl - see Section 5.7.2.5), which highlights the Chillagoe Formation.

## 5.7 Mineral Potential

The assessment of the economic potential of an area can be facilitated by plotting the spatial distributions of elements of economic interest and of pathfinder elements, both of which may have been derived directly or indirectly from mineralisation. It is therefore advantageous to minimise the effects due to lithochemical and/or secondary processes by estimating 'residuals' for elements of direct economic interest with suffer significant lithochemical overprinting (eg Cu, Pb, U and Zn), and to high-light coincident concentrations of groups of elements associated with various styles of mineralisation.



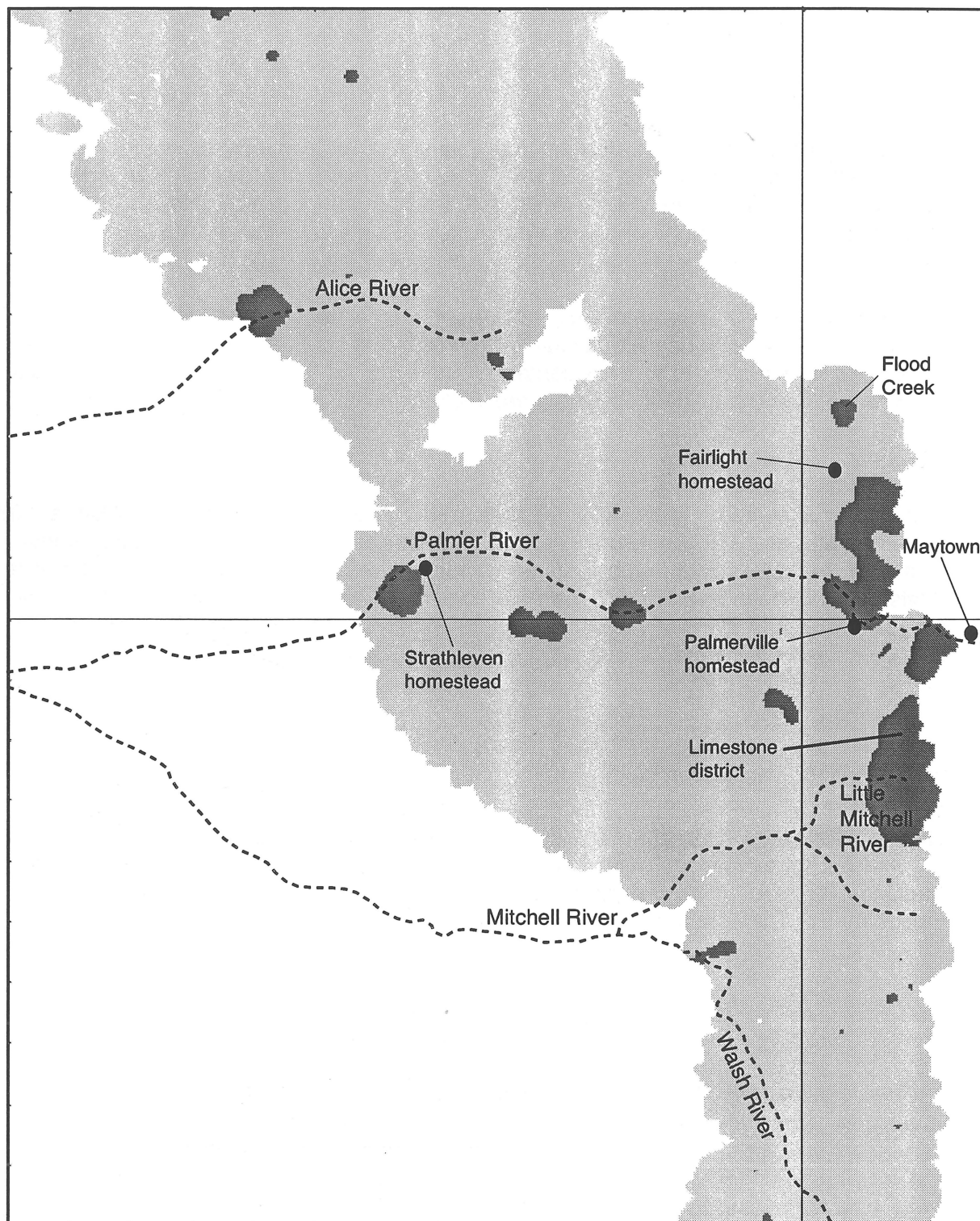


Figure 24. Top 5% of grid values (>0.60 ppb - see Figure 23) for the Hann River Region.

### 5.7.1 Element Residuals

Residuals were estimated for Cu (Figure 13), Pb (Figure 20), U (Figure 9) and Zn (Figure 15) by regression of the element against factor scores in which the elements have significant lithochemical contributions (or conversely against factors in which the element has no obvious mineralisation association). The spatial distributions (discussed in Sections 5.2 and 5.3), and coincidences, of the upper 5% of grid values for each of  $Cu_{res}$  (Red),  $Pb_{res}$  (Green) and  $Zn_{res}$  (Blue) are shown in Figure 25, where the patterns for the elements were combined as an RGB image and superimposed on a greyscale representation of the area sampled.

Two large areas of coincident  $Pb_{res}$  and  $Zn_{res}$  highs (Areas 2X and 2W from Section 5.2) are again highlighted, along with a Cu-Pb-Zn area in the southeastern corner of the survey area. This corresponds to an area containing the King Vol (Pb-Ag-Cu), Tartana (Cu) and Montevideo (Cu) mines, near Bowler Creek (Amos and Keyser, 1964).

### 5.7.2 Additive Indices

A powerful method of defining potential targets is that of additive indices (Chaffee, 1983; Eggo and others, 1995; Cruikshank, 1994) in which values for economic and pathfinder elements characteristic of particular types of mineralisation are summed with the highest totals defining the most likely target areas. To compensate for the large variations in the ranges of absolute element values that the components of a particular characteristic group may contain, a standardised value (SV) is estimated as follows:

$$SV_i = (X_i - X)/SD$$

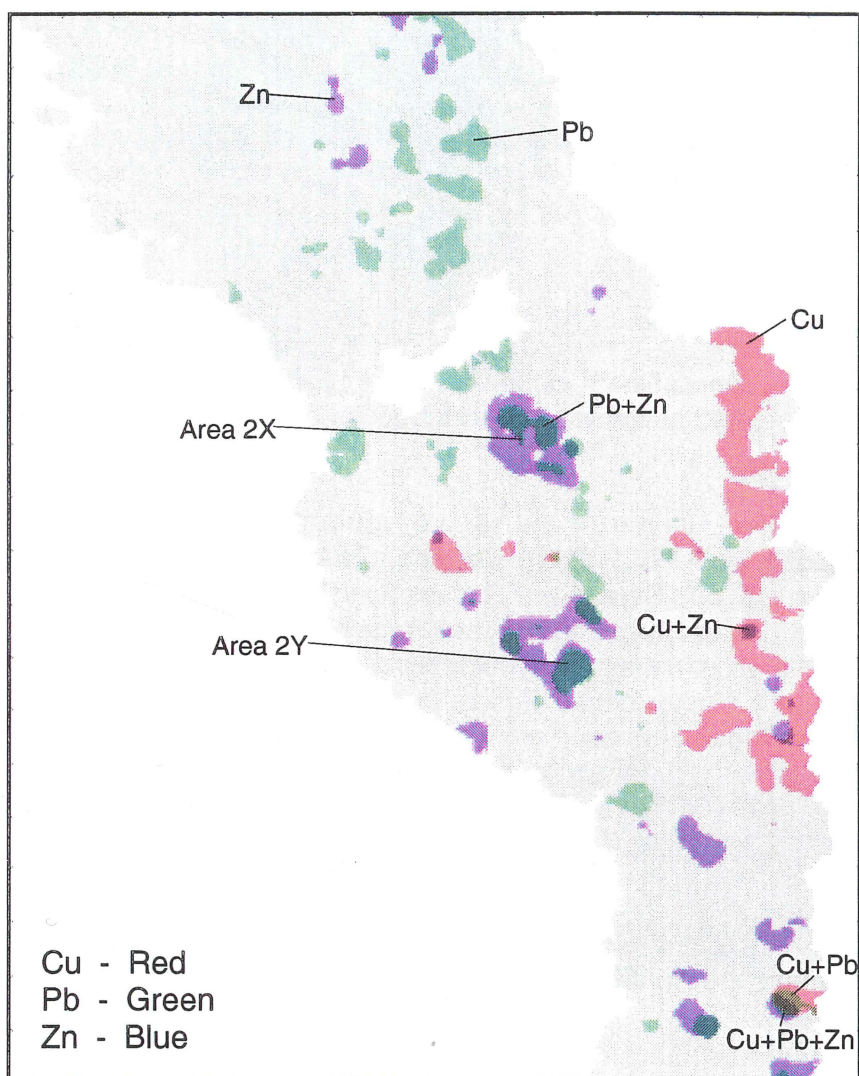
where  $X_i$  is the value of an element in sample  $i$ , and  $X$  and  $SD$  are the mean and standard deviation respectively for that element estimated from the total population. The standardised value is therefore in 'SD' or standard deviation units with a mean of zero, and high values, for example greater than 2, may be considered to be 'highly' anomalous in traditional terms as these are greater than 'mean plus two standard deviations'. Index values for each sample were calculated as follows:

$$Index_i = \sum_{e=1}^{e=n} SV_{e,i}$$

Residual values for U, Cu, Zn and Pb have been used in place of the total or as measured values since these are assumed to be a better representation of the concentration which may be due to mineralisation rather than lithochemical sources. Index values for a number of mineralisation types were calculated for each sample, grided and are presented as image maps. The choice of elements to be included in an index is essentially arbitrary but should be based on common element/mineralisation associations and any available knowledge of mineralisation in the general area. The mineralisation types and the elements used to calculate the indexes were:

#### 5.7.2.1 Gold Index (Aul) - $Ag^* + As + Au\# + Sb^*$

Lode gold mineralisation in the Maytown area often contains arsenopyrite and stibnite,



**Figure 25.** RGB image map of top 5% of grid points for Cu (Red), Pb (Green) and Zn (Blue) showing overlaps.

and Ag is frequently associated with gold mineralisation as a small amount of Ag was recovered from the Palmer River Gold Field (Amos and Keyser, 1964).

Figure 26(a) is an image map of Aul and shows highs over the Chillagoe and Hodgkinson Formations, and over the southern part of the survey area. The latter is due mainly to the As, Sb\* and Ag\* highs discussed above (Sections 5.2 and 5.4), as Au# values in the area are low to moderate (0.13-0.6 ppb) only. The Au# highs at Strathleven and in the Alice River area are also evident. Highs are annotated with the elements or combination of elements which appear to be responsible. All four elements, and the additive index, are generally low to moderate (weakly so) over the granites and metamorphics in both the Dixie and Yambo areas. Major drainage such as the Palmer and Mitchell Rivers were not sampled.

#### 5.7.2.2 Base Metal Index (BMI) - $Ba + Cu_{res} + Pb_{res} + Zn_{res}$

The BMI represents simple Pb-Zn or Cu-Pb-Zn sulphide mineralisation (Levinson, 1974) in which Ba may be present as barite. The distributions of BMI values is shown in Figure 26(b).

Areas 2X and 2W (see Figures 14 and 15) are high-lighted and are due mainly to  $Zn_{res}$  with lesser contribution from  $Pb_{res}$ . The underlying rocks are Saraga, Oswald and Annie Creek Schists (Area 2X), and Saraga and Rosser Schists (Area 2W), of the Yambo Metamorphic Group. Metamorphics in both areas have been intruded by andesite and dolerite dykes. Exploration in the areas (Culpeper and others, 1992) showed some anomalous Zn values but no evidence of base metal mineralisation.

Highs over the Chillagoe Formation are due to  $Cu_{res}$ , possibly due to pockets of Cu mineralisation related to the metamafics in the sequence. Highs in the Dixie area are due to Ba and, to a lesser degree,  $Pb_{res}$ , and are probably related to K-bearing minerals in the granites rather than mineralisation. One high in the area is due to  $Zn_{res}$ .

#### 5.7.2.3 Heavy Mineral Index (HMI) - $Ce + La + Nd + P^* + Th + Y$

The HMI represents the Rare Earth-bearing minerals monazite and xenotime, and is shown in Figure 27(a).

The image maps for Ce, La, Nd, P\* and Th are almost identical, and that of Y is very similar in form with differences in one or two small areas only. Therefore, it is not surprising that the image map of HMI is essentially that of Ce (or any of the others) with most highs over metamorphic rocks of the Yambo Metamorphic Group (see Section 5.1). Calculations based on the fine fraction concentrations of the elements above suggest that some streams may contain up to 2% of monazite and xenotime, but no estimates of the amount of alluvial material in the streams are available. Some of the area covered by the highs has been explored for heavy minerals but were considered uneconomic due to low grades or insufficient alluvial material.

#### 5.7.2.4 Porphyry Copper Index (PCI) - $Cu_{res} + Mo^* + Rb$

Porphyry copper deposits at Moonmera in central coastal Queensland (Dummett, 1978), and at Coalstoun in southeast Queensland (Ashley and others, 1978) also contain Mo. Rb



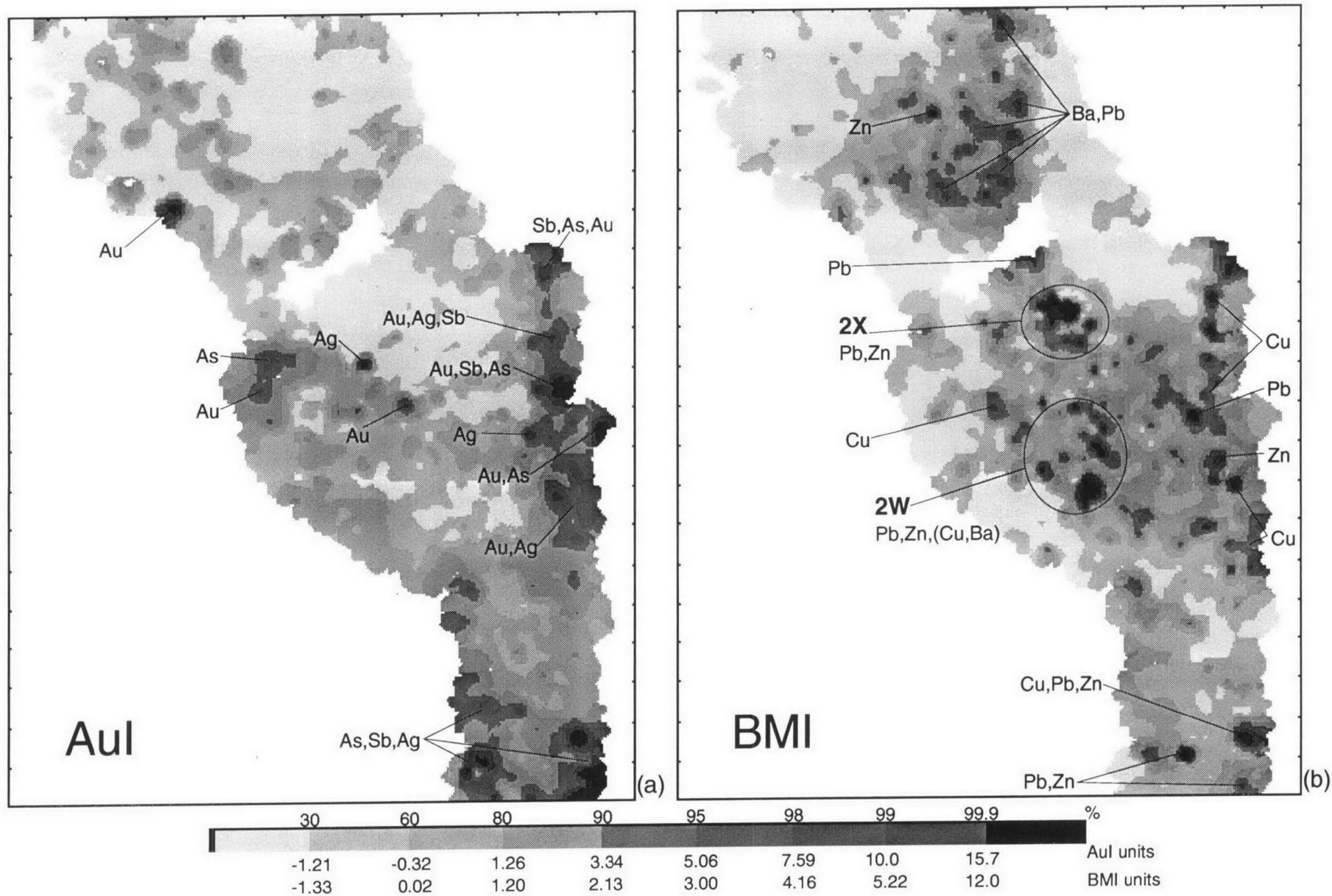


Figure 26. Image maps of the distribution of Gold Index (Aul) and Base Metal Index (BMI) values in the Hann River Region.

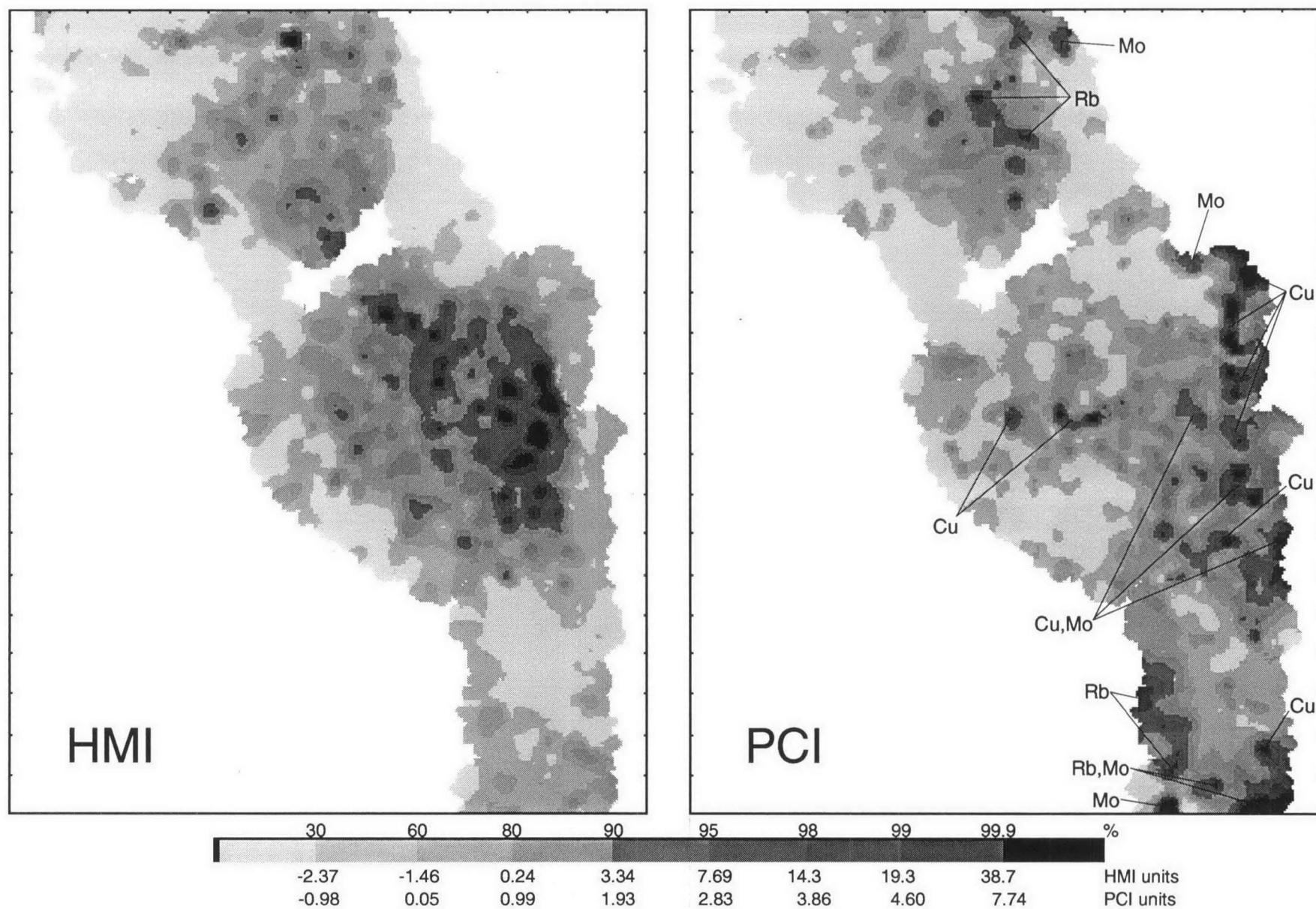


Figure 27. Image maps of the distribution of Heavy Mineral Index (HMI) and Porphyry Copper Index (PCI) values in the Hann River Region.

enrichment in the mineralised zone was also noted at Moonmera, and Rb was included in PCI which is shown in Figure 27(b).

There appears to be few if any, significant coincidences of  $Cu_{res}$  and Rb and/or  $Mo^*$ . Rb is concentrated over the granites in the Dixie area, and in the south of the survey area north of Cardross. While  $Mo^*$  shows several highs near Cardross, its patterns are more diffuse. On the other hand  $Cu_{res}$  is concentrated over the Chillagoe Formation. On this basis there appears to be little likelihood of significant porphyry copper mineralisation.

#### 5.7.2.5 Platinum Index (PTI) - $Cr + Ni + Pd\# + Pt\# + V$

PTI defines areas likely to contain mafic/ultramafic rocks which may have potential for platinum group elements. The PTI is shown in Figure 28(a) and highlights the Chillagoe Formation and, to a lesser extent, the adjacent Yambo Metamorphics. The Chillagoe Formation contains many metamafic units, and the metamorphics are intruded by andesite and dolerite dykes.

The only exploration directly targeting Pt carried out recently in the survey area (AP 4723M) occurred in the Dixie area near Potallah Creek. Proterozoic greenstones were targeted and one PTI high in the area is due to Cr, Ni and Pt (plus Pd). The greenstones were interpreted as submarine basalts and the authority was dropped.

#### 5.7.2.6 Uranium Index (UI) - $As + Bi^* + Mo^* + U_{res}$

Uranium deposits in the Georgetown Region to the south generally contain As, Bi and Mo (Rossiter and Scott, 1978). Figure 28(b) shows the UI image map

$U_{res}$  appears to have been swamped by As,  $Bi^*$  and  $Mo^*$ , especially in the south of the survey area. Therefore  $U_{res}$  alone may be a better indicator of potential U mineralisation (see Section 5.1).

## CONCLUSIONS

Colour (and greyscale) image maps of the survey area effectively represent the spatial distributions of the elements, and of a number of derived statistical parameters, and were invaluable in the interpretation of the regional stream sediment geochemistry of the survey area. Colour image maps (as in the associated atlas) have greater impact than the greyscale versions but are more costly to reproduce.

Variations in the data are accounted for by the extraction of 6 factors, the first 3 of which account for most of the variation. These are:

- Factor 1 (U, Ce, Th, Y, Nd, La, Nb,  $P^*$ , W, Zr and Hf) is believed to be due to the presence in the stream sediment of the resistant phosphate minerals monazite (LREE and Th) and xenotime (Y). These minerals can contain significant concentrations of U.
- Factor 2 (Fe, V, Cu, Ni, Sc, Zn, Cr, Ti, Mn, As and  $Cd^*$ ) is thought to reflect the geochemistry of Fe-rich minerals in bedrock, and scavenging by hydrated Fe (and Mn) oxides in the secondary environment.

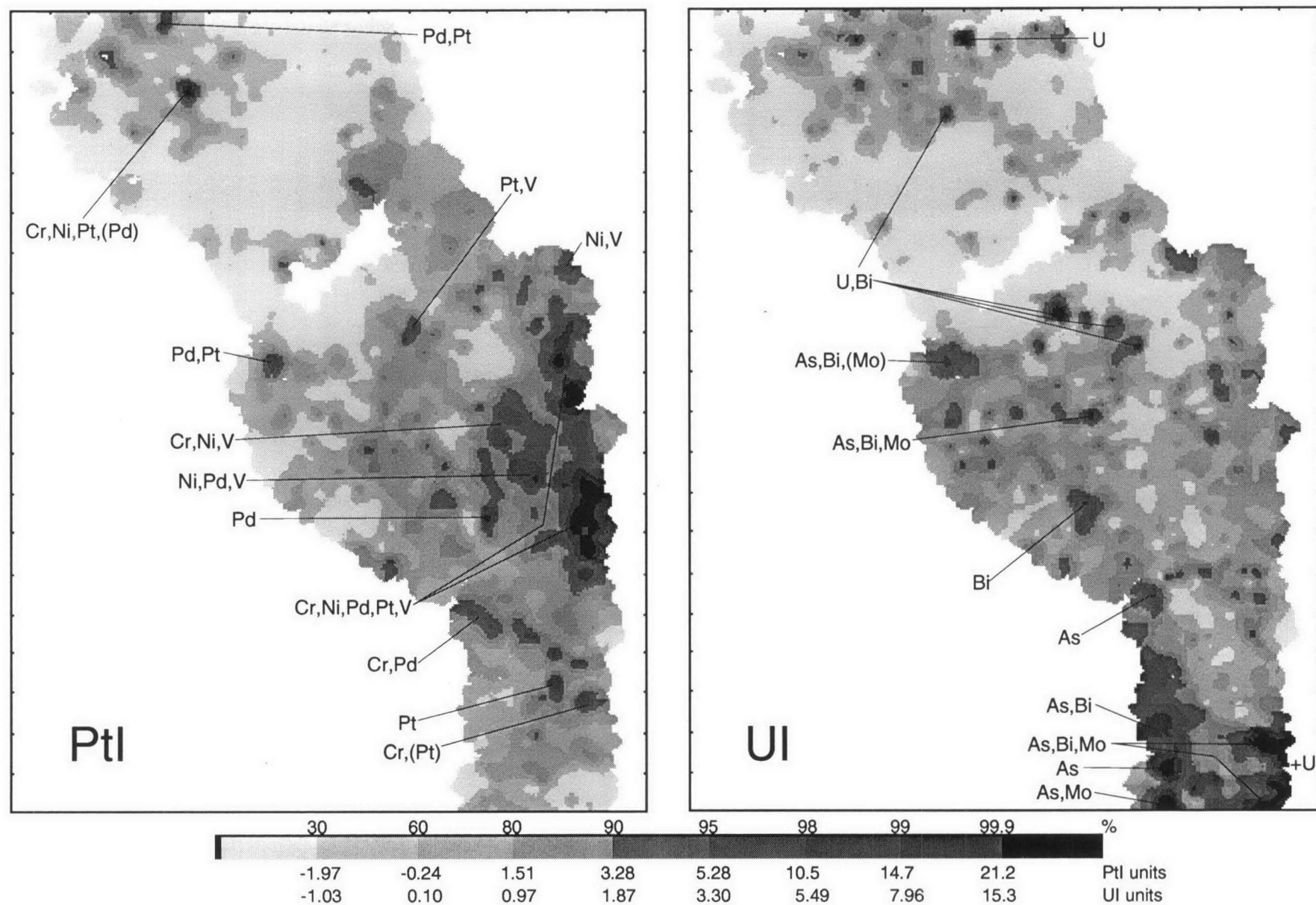


Figure 28. Image maps of the distribution of Platinum Index (Ptl) and Uranium Index (UI) values in the Hann River Region.



- Factor 3 (Rb, Ba, Sr, Be\*, Ga, Pb and Tl\*) is believed to be due to the weathering of K-rich minerals.

There appears to be some potential for gold and tin mineralisation in the region, although no new gold areas were defined by the survey, and tin anomalies were mostly over Mesozoic sediments rather than associated with tin-bearing granites.

Several zinc and, to a lesser extent, lead anomalies were defined but were in areas already explored for base metals and in which no mineralisation was found.

---

## ACKNOWLEDGMENTS

The authors wish to thank J.G. Pyke, J. Pye, L. Roberts, M. Crawford, G. Doblinger, J. Groves, J-P. Kanis, S. Neil, B. Smith, L-A. Smith, D. Warren-Smith and M. Webster for their invaluable assistance in carrying out the sampling program, J.G. Pyke, W. Pappas and L. Webber for analysing the samples in AGSO's Geochemical Laboratory, J.H.C. Bain and D.M. Hoatson for their critical reviews of the manuscript.

## REFERENCES

- AMOS, B.J., and KEYSER, F. de, 1964. Mossman 1:250 000 geological series - explanatory notes. Bureau of Mineral Resources, Canberra.
- ASHLEY, P.M., BILLINGTON, W.G., GRAHAM, R.L., and NEALE, R.C., 1978. Geology of the Coalstoun porphyry copper prospect, southeast Queensland, Australia. *Economic Geology*, v73, p945-965.
- BAIN, J.H.C., WITHNALL, I.W., OVERSBY, B.S., and MACKENZIE, D.E., 1990. North Queensland Proterozoic inliers and Palaeozoic provinces - regional geology and mineral deposits. In Hughes, F.E., (Editor), *Geology of the Mineral Deposits of Australia and Papua New Guinea*. The Australasian Institute of Mining and Metallurgy, Melbourne, p963-978.
- BLEWETT, R.S., MACKENZIE, D.E., WELLMAN, P., BULTITUDE, R.J., TRAIL, D.S., von GNIELINSKI, F.E., REES, I.D., and BAIN, J.H.C., 1994. Hann River - Pre-Mesozoic geology (1:250 000 scale map). Australian Geological Survey Organisation, Canberra.
- BLEWETT, R.S., TRAIL, D.S., and von GNIELINSKI, F.E., 1992. The stratigraphy of metamorphic rocks of the Ebagoola 1:250 000 sheet area in Cape York Peninsula, north Queensland. Australian Geological Survey Organisation, Canberra, Record 1992/71 (unpublished).
- BLEWETT, R.S., and WILFORD, 1995. 1:250 000 Geological map series - Australia: Hann River, Queensland (SD54/16), Australian Geological Survey Organisation, Canberra.
- BLEWETT, R.S., and WILFORD, J., 1996. 1:250 000 geological series - Commentary, Hann River, Queensland, Sheet SD54/16 International Index. Australian Geological Survey Organisation, Canberra.
- BONHAM-CARTER, G.F., ROGERS, P.J., and ELLWOOD, D.J., 1987. Catchment basin analysis applied to surficial geochemical data, Cobequid Highlands, Nova Scotia. *Journal of Geochemical Exploration*, v29, p259-278.
- BOYLE, R.W., and JONASSON, I.R., 1973. The geochemistry of arsenic and its use as an indicator element in geochemical prospecting. *Journal of Geochemical Exploration*, v2, p251-296.
- BULTITUDE, R.J., GARRAD, P.D., and ROBERTS, C.W., 1997. Hodgkinson Basin Geology, 1:500 000 Scale Map, Second Edition. Department of Minerals and Energy, Queensland.
- BULTITUDE, R.J., and REES, I.D., 1996. Walsh, 2nd Edition, Queensland, 1:250 000 geological series - explanatory notes. Geological Survey of Queensland, Department of Mines and Energy, Queensland.
- BULTITUDE, R.J., REES, I.D., GARRAD, P.D., CHAMPION, D.C., and FANNING, C.M., 1996. Mossman, 2nd Edition, Queensland, 1:250 000 geological series - explanatory notes. Geological Survey of Queensland, Department of Mines and Energy, Queensland.
- BUREAU of METEOROLOGY, 1971. Bureau of Meteorology (1971) climatic survey - region 16. Bureau of Meteorology, Australia.

- CAMERON, W.E., 1906. Some goldfields of Cape York Peninsula. II. The Alice River (Philp) goldfield. III. The Hamilton goldfield. IV. The Coen goldfield. Queensland Government Mining Journal, v7, p643-647.
- CHAFFEE, M.A., 1983. SCORESUM - a technique for displaying and evaluating multi-element geochemical information, with examples of its use in regional mineral assessment programs. In: PARSLOW, G.R., (Editor), Geochemical Exploration, 1982. Journal of Geochemical Exploration, v19, p361-381.
- CRUIKSHANK, B., 1990. Stream-sediment geochemistry of the original Kakadu Conservation Zone, BMR Research Newsletter, No. 12 (April, 1990), Bureau of Mineral Resources, Canberra.
- CRUIKSHANK, B.I., 1994. Stream sediment geochemistry of the Ebagoola 1:250 000 sheet area, Cape York Peninsula, north Queensland. Australian Geological Survey Organisation, Canberra. Record 1994/8 (unpublished).
- CRUIKSHANK, B.I., 1995. Stream Sediment Geochemical Atlas Series #2, Red River Region, north Queensland. Australian Geological Survey Organisation, Canberra.
- CRUIKSHANK, B.I., 1997. Stream sediment geochemistry of the Red River Region, Cape York Peninsula, north Queensland. Australian Geological Survey Organisation, Canberra, Record 1996/21. (unpublished).
- CRUIKSHANK, B.I., and BRUGMAN, P.C., 1995. Stream Sediment Geochemical Atlas Series #3, Hann River Region, north Queensland. Australian Geological Survey Organisation, Canberra.
- CRUIKSHANK, B.I., and BUTROVSKI, D., 1994. Stream Sediment Geochemical Atlas, Ebagoola sheet area, north Queensland. Australian Geological Survey Organisation, Canberra.
- CRUIKSHANK, B.I., HOATSON, D.M., and PYKE, J.G., 1993. A stream-sediment geochemical orientation survey of the Davenport Province, Northern Territory. AGSO Journal of Australian Geology and Geophysics, 14, 77-95.
- CRUIKSHANK, B.I., and PYKE, J.G., 1993. Analytical methods used in Minerals and Land Use Program's geochemical laboratory. Australian Geological Survey Organisation, Canberra, Record 1993/26 (unpublished).
- CULPEPER, L.G., and BURROWS, P.E., 1992. Mineral occurrences - Hann River 1:250 000 sheet area, Cape York Peninsula, Queensland. Department of Resource Industries, Queensland, Record 1992/18 (unpublished).
- CULPEPER, L.G., DENARO, T.J., WILLMOTT, W.F., WHITAKER, W.G., BRUVEL, F.J., MORWOOD, D.A., and SHIELD, C.J., 1992. A review of mineral exploration, Cape York Peninsula, 1969 to 1990. Department of Resource Industries, Queensland, Record 1992/10 (unpublished).

- DENARO, T.J., CULPEPER, L.G., MORWOOD, D.A., and BURROWS, P.E., 1994. Mineral occurrences - Laura 1:100 000 sheet area, Cape York Peninsula, Queensland. Department of Resource Industries, Queensland, Record 1994/14 (unpublished).
- DILLON, W.R., and GOLDSTEIN, M., 1984. Multivariate analysis, methods and applications. John Wiley and sons, New York.
- DOUTCH, H.F., SMART, J., GRIMES, K.G., NEEDHAM, R.S., and SIMPSON, C.J., 1972. Progress report on the geology of the central Carpentaria Basin. Bureau of Mineral Resources, Canberra, Record 1972/64 (unpublished).
- DUMMETT, H.T., 1978. Geology of the Moonmura porphyry deposit, Queensland, Australia. *Economic Geology* v73, p922-944.
- EGGO, Alfred J., HARDING, Tony, and BAIN, John, 1990. Advanced interpretation techniques applied to regional stream sediment geochemical data from the Georgetown region, SE54-12, Northeast Queensland. CRAE Report No. 16614 (unpublished).
- EGGO, Alfred J., HARDING, Tony, and BAIN, John, 1995. Removal of background processes controlling trace element variability in -80# stream sediment geochemical data, Georgetown Region, Northeast Queensland, Australia. In *Extended Abstracts, 17th IGES, Exploring the Tropics*, 15-19 May, 1995, Townsville, Australia.
- ELLIOTT, S.M., and TOWSEY, C.A., 1989. Regional drainage geochemical gold exploration techniques used in Queensland, Australia. NQ Gold '89 Conference, Townsville.
- ELLIS, P.J., and STEELE, T.W., 1982. Five robust indicators of central value. *Geostandards Newsletter*, v6(2), p207-216.
- FELDMAN, D.S., GAGNON, J., HOFMANN, R., and SIMPSON, J., 1990. Statview II, the solutions for data analysis and presentation graphics (manual for computer program). Abacus Concepts, Berkeley.
- FLETCHER, W.K., 1990. Dispersion and behaviour of gold in stream sediments. Ministry of Energy, Mines and Petroleum Resources, Province of British Columbia, Geological Survey Branch, Open File 1990-28 (unpublished).
- FOY, M.F., and GINGRICH, J.E., 1977. A stream-sediment orientation programme for uranium in the Alligator River Province, Northern Territory, Australia. *Journal of Geochemical Exploration*, v8, p357-364.
- GALLOWAY, R.W., GUNN, R.H., and STORY, R., 1970. Lands of the Mitchell-Normanby area, Queensland. Commonwealth Scientific and Industrial Research Organisation, Australia, Land Research Series, No 26.
- GRIMES, K.G., and WHITAKER, W.G., 1977. Walsh 1:250 000 geological series - explanatory notes. Bureau of Mineral Resources, Canberra.
- HALL, G.E.M., VAIVE, J.E., BEER, R., and HOASHI, M., 1996. Selective leaches revisited, with emphasis on the amorphous Fe oxyhydroxide phase extraction. *Journal of Geochemical Exploration*, v56, 59-78.



- JENNE, E.A., 1968. Controls on Mn, Fe, Co, Ni, Cu and Zn concentrations in soils and water: the significant role of hydrous Mn and Fe oxides. *Advances in Chemistry series, No. 73, Trace Inorganics in Water.* The American Chemical Society.
- KEYSER, F. de, and LUCAS, K.G., 1968. Geology of the Hodgkinson and Laura Basins, north Queensland. Bureau of Mineral Resources, Canberra, Bulletin No 84.
- KEYSER, F. de, and WOLFF, K.W., 1964. The geology and mineral resources of the Chillagoe area. Geological Survey of Queensland, Brisbane, Publication No. 317.
- KOCH, G.S., and LINK, R., 1970. Statistical analysis of geological data. John Wiley and sons, New York.
- KOCH, G.S., and LINK, R., 1971. Statistical analysis of geological data, volume II. John Wiley and sons, New York.
- KRAUSKOPF, K.B., 1967. Introduction to geochemistry. McGraw-Hill Book Company, New York, p639.
- LAM, J.S., DENARO, T.J., BURROWS, P.E., and GARRAD, P.D., 1991. A summary of the mineral occurrences of the Maytown 1:100 000 sheet area (7765), north Queensland. Department of Resource Industries, Queensland, Record 1991/10 (unpublished).
- LEVINSON, A.A., 1974. Introduction to exploration geochemistry. Applied Publishing Ltd., Calgary.
- LUCAS, K.G., and KEYSER, F. de, 1965. Cooktown 1:250 000 geological series - explanatory notes. Bureau of Mineral Resources, Canberra.
- MACKENZIE, D.E., and KNUTSON, J., 1992. Igneous rocks of the Ebagoola 1:250 000 sheet area, Cape York Peninsula: field, petrographic, and geochemical data. Australian Geological Survey Organisation, Canberra, Record 1992/75 (unpublished).
- MACKENZIE, D.E., and KNUTSON, J., BLACK, L.P., and SUN, S-S., 1992. Paleozoic. In EWERS, G.R., and BAIN, J.H.C., (Editors), Preliminary map commentary - Australia 1:250 000 basement geology and regolith landforms: Ebagoola (SD54-12), Queensland. Australian Geological Survey Organisation, Canberra, Record 1992/71 (unpublished).
- NICHOL, Ian, HORSNAIL, R.F., and WEBB, J.S., 1967. Geochemical patterns in stream sediment related to precipitation of manganese oxides. *Transactions of the Institute of Mining and Metallurgy, Section B, v76, pB113-B115.*
- NORRISH, K., and CHAPPELL, B.W., 1977. X-ray fluorescence spectrometry. In ZUSSMAN, J., (Editor), *Physical methods in determinative Mineralogy*, 2nd Edition. Academic Press, London. p201-272.
- OVERSBY, B.S., PALFREYMAN, W.D., BLACK, L.P., COOPER, J.A., and BAIN, J.H.C., 1975. Georgetown, Yambo, and Coen Inliers - regional geology. In KNIGHT, C.L. (Editor), *Economic Geology of Australia and Papua New Guinea.* Australasian Institute of Mining and Metallurgy, Monograph No. 5, v1, 511-516.

- PRICE, V., and FERGUSON, R.B., 1980. Stream sediment surveys for uranium. *Journal of Geochemical Exploration*, v13, p285-304.
- ROSSITER, A.G., 1975. An orientation geochemical survey in the Georgetown area, north Queensland, Bureau of Mineral Resources, Canberra, Record 1975/164 (unpublished).
- SINCLAIR, A.J., 1974. Selection of threshold values in geochemical data using probability graphs. *Journal of Geochemical Exploration*, v3, p129-149.
- SINCLAIR, A.J., 1991. A fundamental approach to threshold estimation in exploration geochemistry; probability plots revisited. *Journal of Geochemical Exploration*, v41, p1-22.
- TRAIL, D.S., PONTIFEX, I.R., PALFREYMAN, W.D., WILLMOTT, W.F., and WHITAKER, W.G., 1968. The igneous and metamorphic rocks of the southern part of Cape York Peninsula, Queensland. Bureau of Mineral Resources, Canberra, Record 1968/26 (unpublished).
- TWIDALE, C.R., 1966. Geomorphology of the Leichhardt-Gilbert area, north-west Queensland. Commonwealth Scientific and Industrial Research Organisation, Australia. Land Research Series, No. 16.
- WEDEPOHL, K.H., 1972. Zinc. In K.H. Wedepohl (Editor), *Handbook of Geochemistry*, vII-3, Springer-Verlag, Berlin.
- WHITAKER, W.G., and GRIMES, K.G., 1977. Hann River 1:250 000 geological series - explanatory notes. Bureau of Mineral Resources, Canberra.
- WILFORD, J.W., DOHRENWEND, J.C., and PAIN, C.F., 1995. HANN RIVER Regolith-Landforms, Australian 1:250 000 Regolith Landform. Sheet SD54-12, Australian Geological Survey Organisation, Canberra.
- WILLMOTT, W.F., WHITAKER, W.G., PALFREYMAN, W.D., and TRAIL, D.S., 1973. Igneous and metamorphic rocks of Cape York Peninsula and Torres Strait, Bureau of Mineral Resources, Canberra, Bulletin 135.

# Appendix A

Figures A1-A5. Mineral occurrences in, or immediately adjacent to, the HANN RIVER Region survey area (after MINLOC, December, 1994).

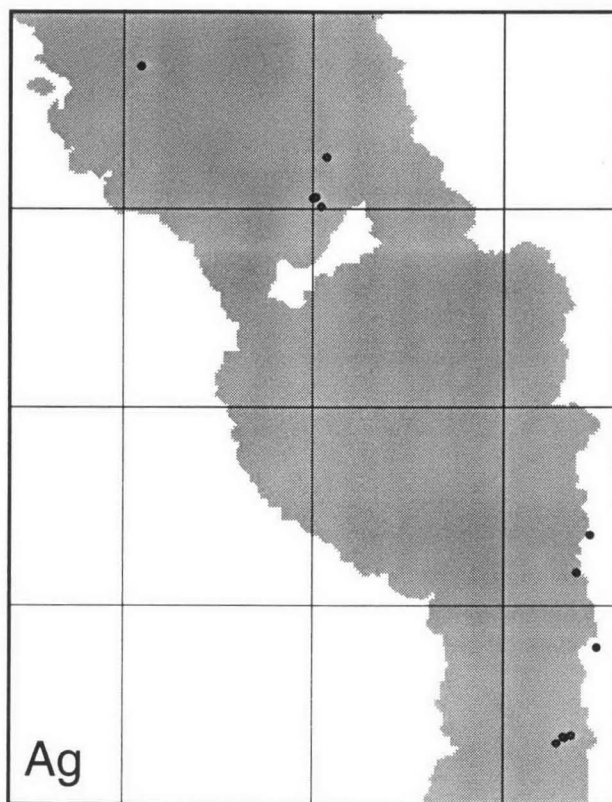


Figure A1 Silver (N=12)

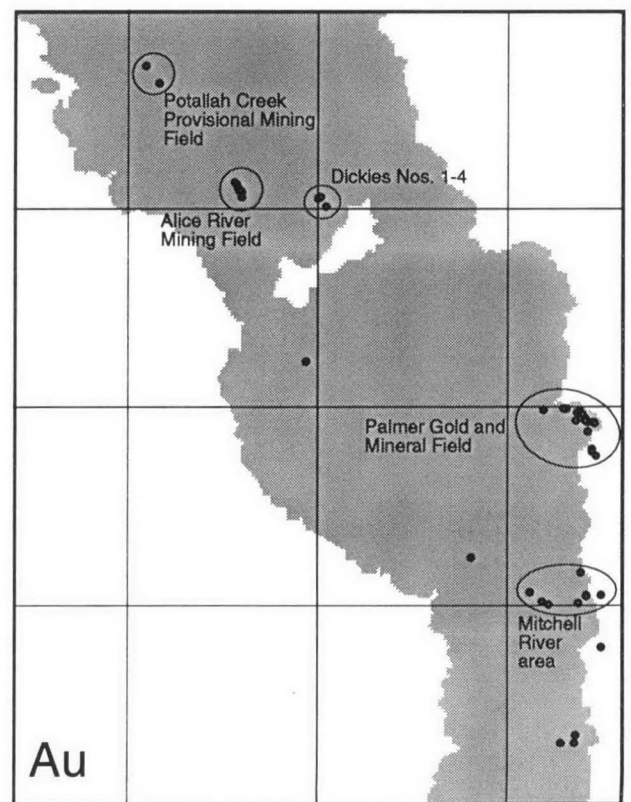


Figure A2 Gold (N=47)

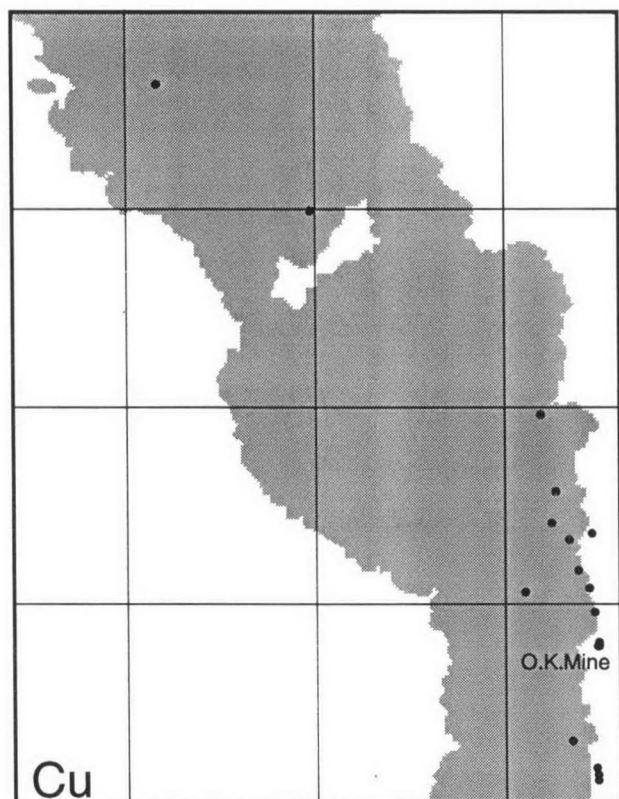


Figure A3 Copper (N=20)

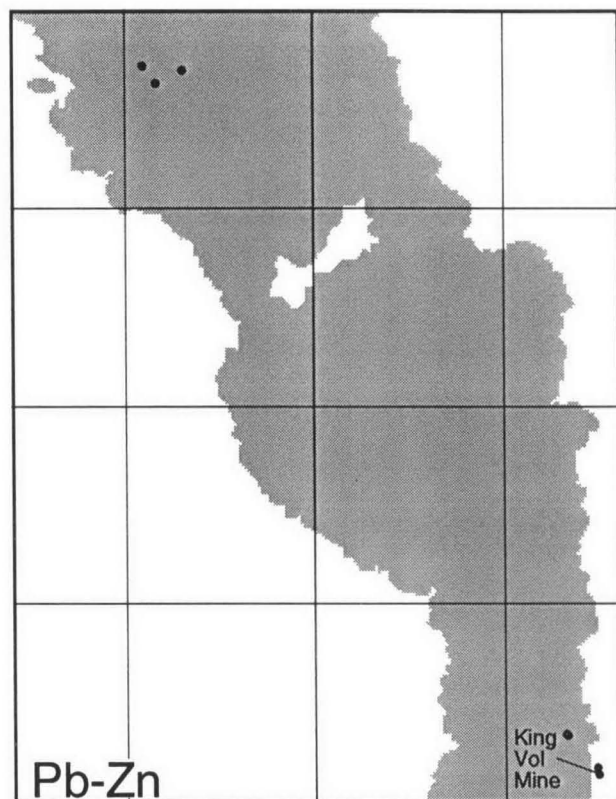


Figure A4 Lead-zinc (N=7)

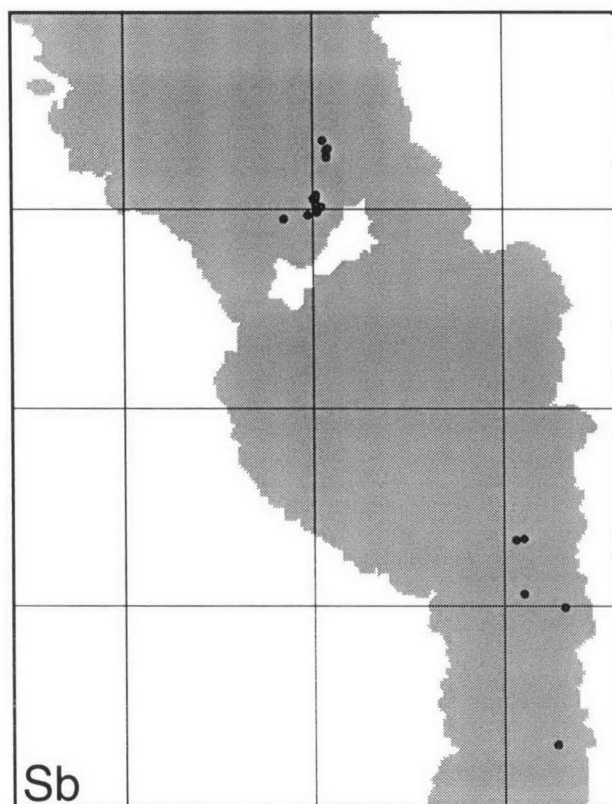


Figure A5 Antimony (N=20)

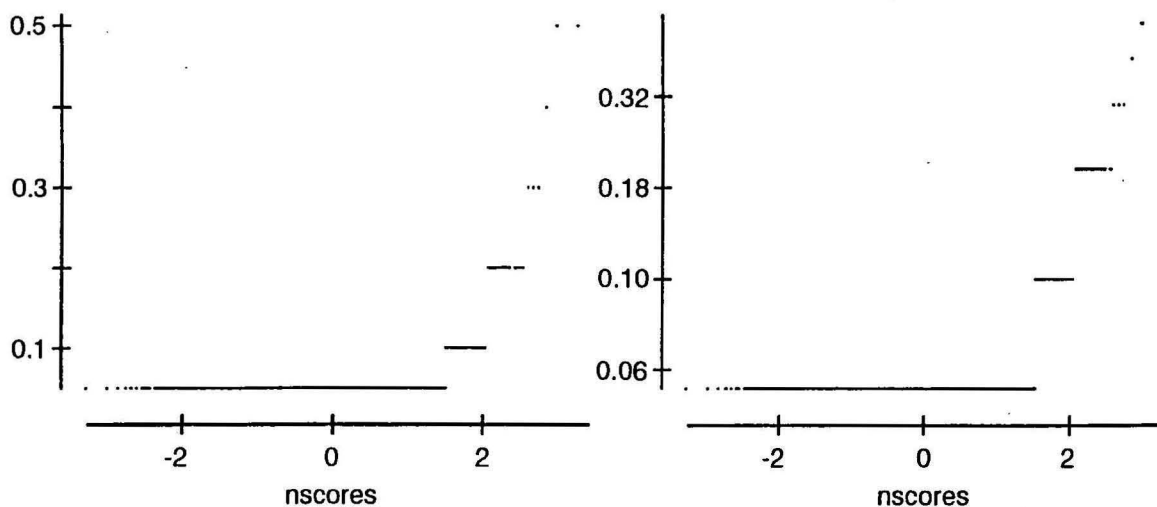
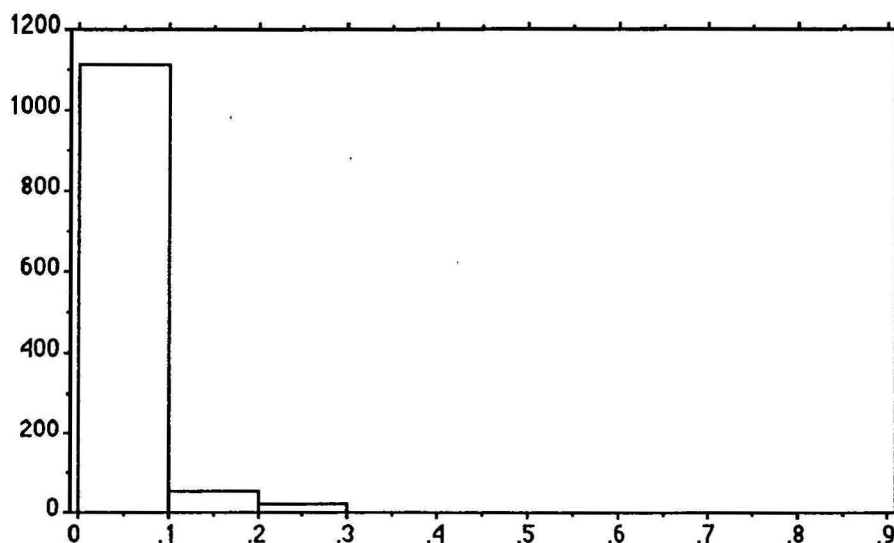


# Appendix B

# **X<sub>1</sub> : Ag@ ppm**

Mean:	Std. Dev.:	Std. Error:	Variance:	Coef. Var.:	Count:
.056	.032	.001	.001	56.699	1191
Minimum:	Maximum:	Range:	Sum:	Sum of Sqr.:	# Missing:
.05	.5	.45	66.85	4.958	0
† 95%:	95% Lower:	95% Upper:	# < 10th %:	10th %:	25th %:
.002	.054	.058	0	.05	.05
50th %:	75th %:	90th %:	# > 90th %:	Mode:	Geo. Mean:
.05	.05	.05	76	.05	.053
Har. Mean:	Kurtosis:	Skewness:			
.052	87.297	8.263			

Detection limit is 0.10ppm - a value of 0.05ppm has been used in calculations and table

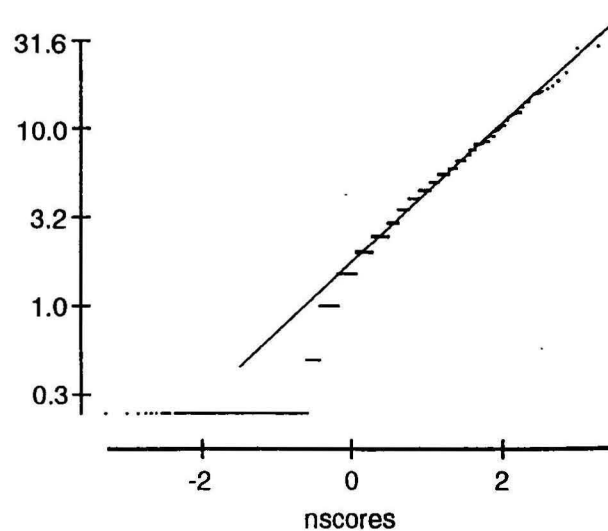
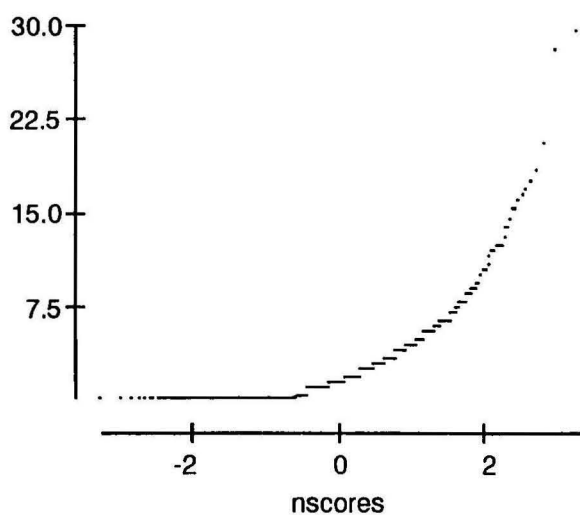
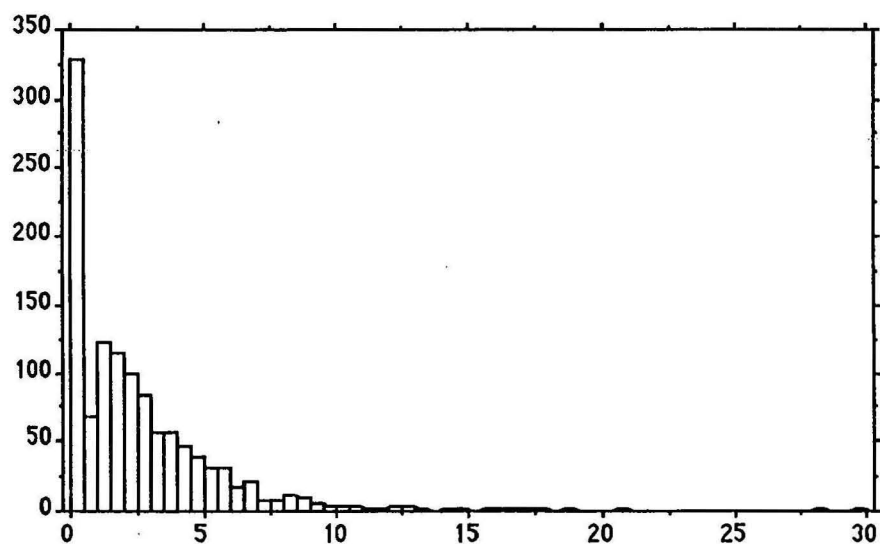


Ag\*

# X<sub>1</sub> : As ppm

Mean:	Std. Dev.:	Std. Error:	Variance:	Coef. Var.:	Count:
2.448	2.909	.084	8.465	118.875	1191
Minimum:	Maximum:	Range:	Sum:	Sum of Sqr.:	# Missing:
.25	29.5	29.25	2915	17208	0
1 95%:	95% Lower:	95% Upper:	# < 10th %:	10th %:	25th %:
.165	2.282	2.613	0	.25	.25
50th %:	75th %:	90th %:	# > 90th %:	Mode:	Geo. Mean:
1.5	3.5	5.5	114	.25	1.279
Har. Mean:	Kurtosis:	Skewness:			
.657	15.959	3.039			

Detection limit is 0.50ppm - a value of 0.25ppm has been used in calculations and table

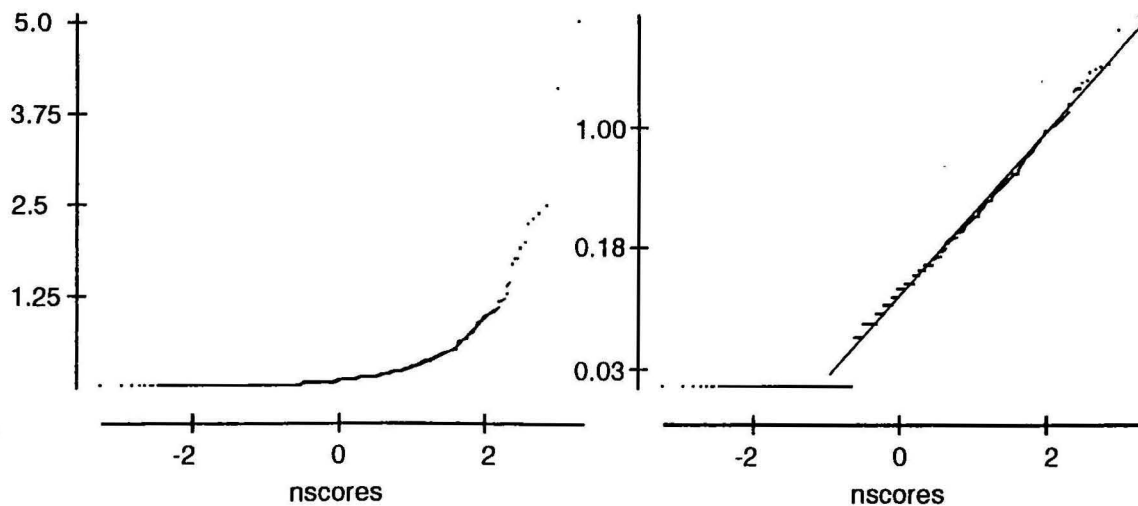
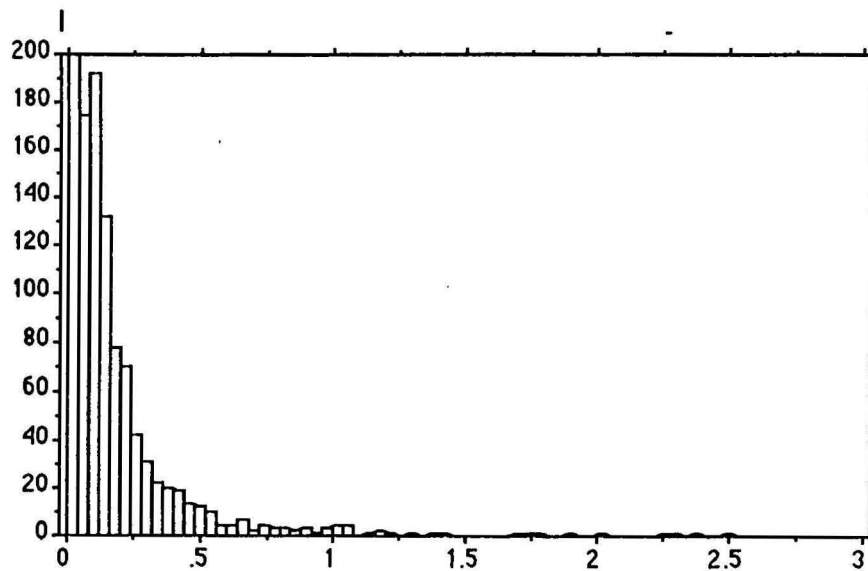


As

# X<sub>1</sub>: Au\* ppb

Mean:	Std. Dev.:	Std. Error:	Variance:	Coef. Var.:	Count:
.18	.312	.009	.097	173.201	1191
Minimum:	Maximum:	Range:	Sum:	Sum of Sqr.:	# Missing:
.025	5.02	4.995	214.63	154.61	0
† 95%:	95% Lower:	95% Upper:	# < 10th %:	10th %:	25th %:
.018	.162	.198	0	.025	.025
50th %:	75th %:	90th %:	# > 90th %:	Mode:	Geo. Mean:
.1	.2	.39	118	.025	.096
Har. Mean:	Kurtosis:	Skewness:			
.06	79.881	7.175			

Detection limit is 0.050ppb - a value of 0.025ppb has been used in calculations and table

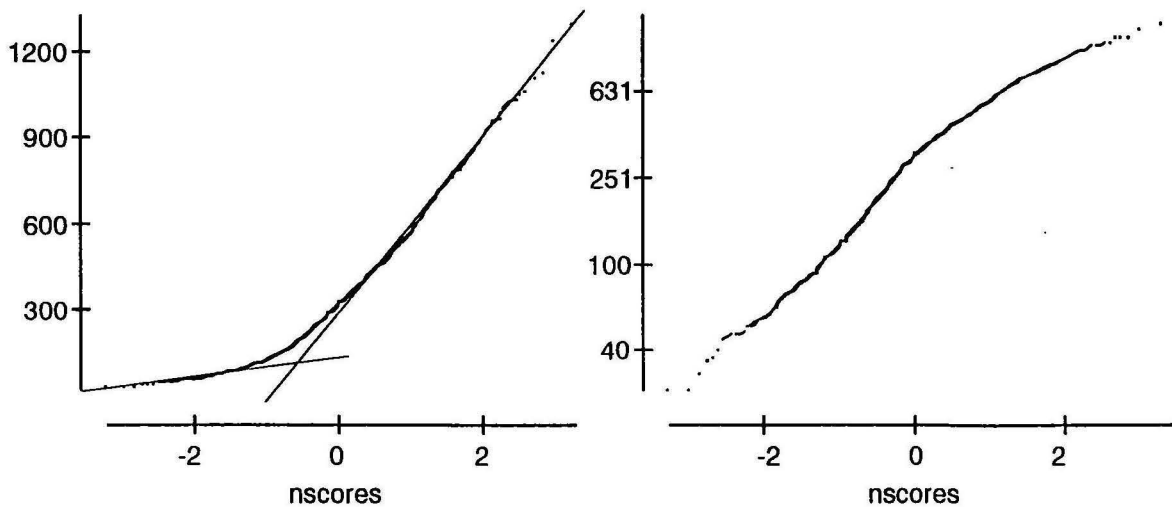
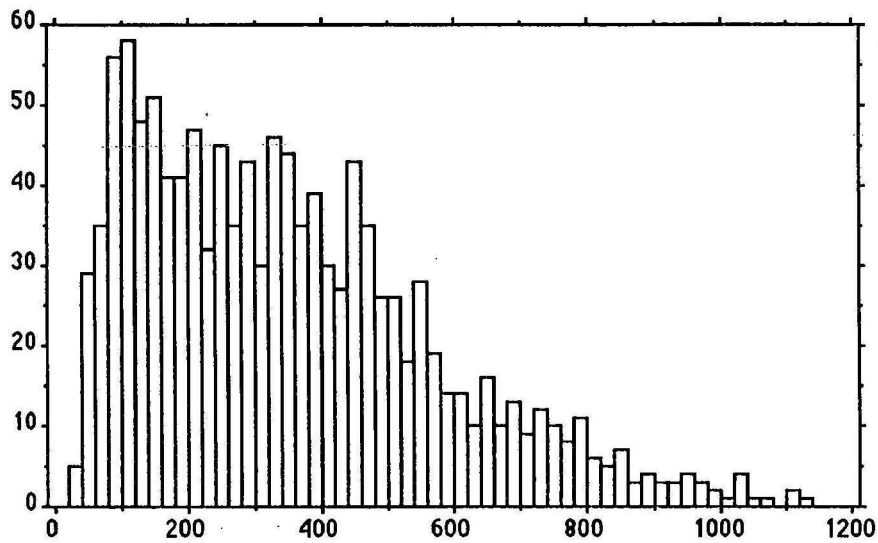


Au#



# **X1 : Ba ppm**

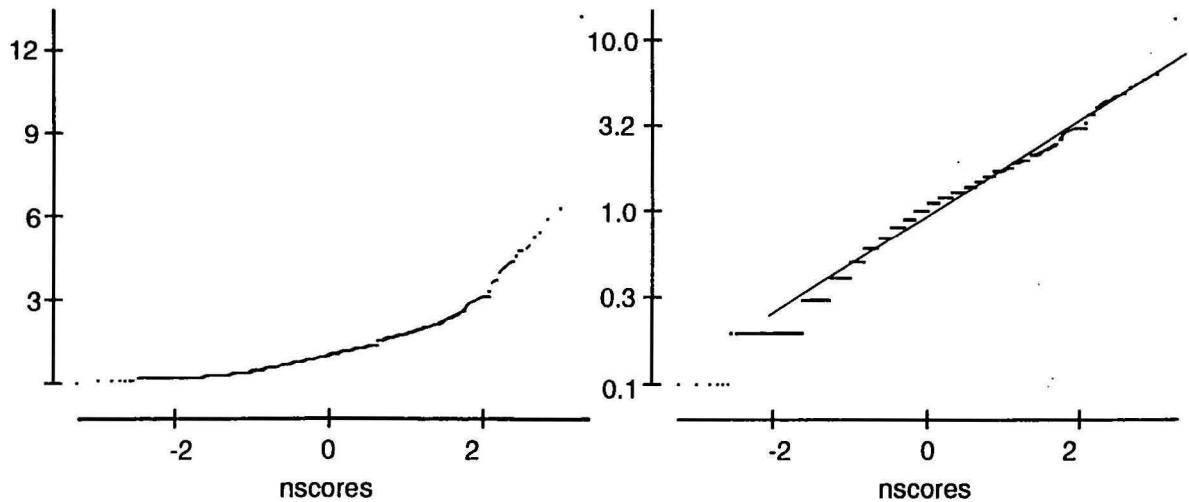
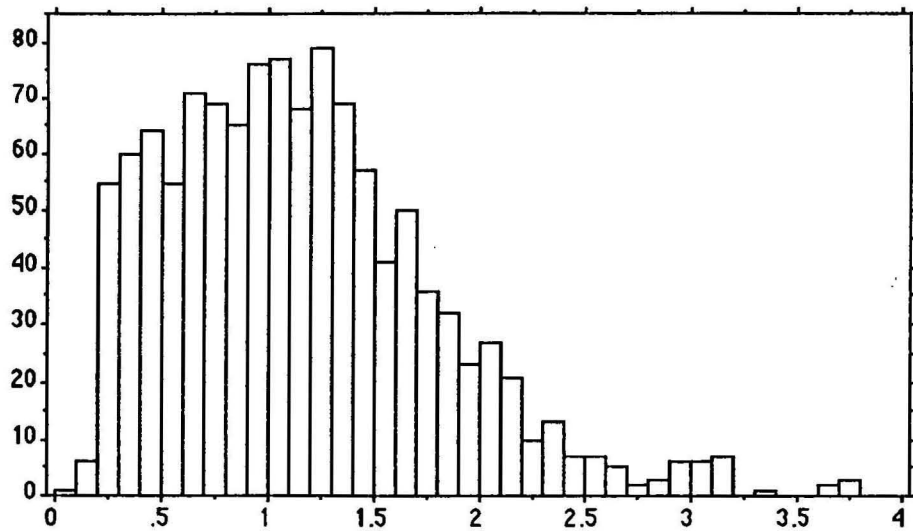
Mean:	Std. Dev.:	Std. Error:	Variance:	Coef. Var.:	Count:
351.429	224.08	6.493	50211.815	63.762	1191
Minimum:	Maximum:	Range:	Sum:	Sum of Sqr.:	# Missing:
26	1298	1272	418552	206843392	0
† 95%:	95% Lower:	95% Upper:	# < 10th %:	10th %:	25th %:
12.74	338.689	364.169	119	96.6	166
50th %:	75th %:	90th %:	# > 90th %:	Mode:	Geo. Mean:
319	477.75	677	117	111	278.834
Har. Mean:	Kurtosis:	Skewness:			
208.661	.544	.896			



Ba

# X1 : Be<sup>±</sup> ppm

Mean:	Std. Dev.:	Std. Error:	Variance:	Coef. Var.:	Count:
1.171	.842	.024	.708	71.889	1190
Minimum:	Maximum:	Range:	Sum:	Sum of Sqr.:	# Missing:
.1	13.3	13.2	1393	2472.64	0
t 95%:	95% Lower:	95% Upper:	# < 10th %:	10th %:	25th %:
.048	1.123	1.218	61	.3	.6
50th %:	75th %:	90th %:	# > 90th %:	Mode:	Geo. Mean:
1	1.5	2	110	1.2	.941
Har. Mean:	Kurtosis:	Skewness:			
.721	39.898	3.922			

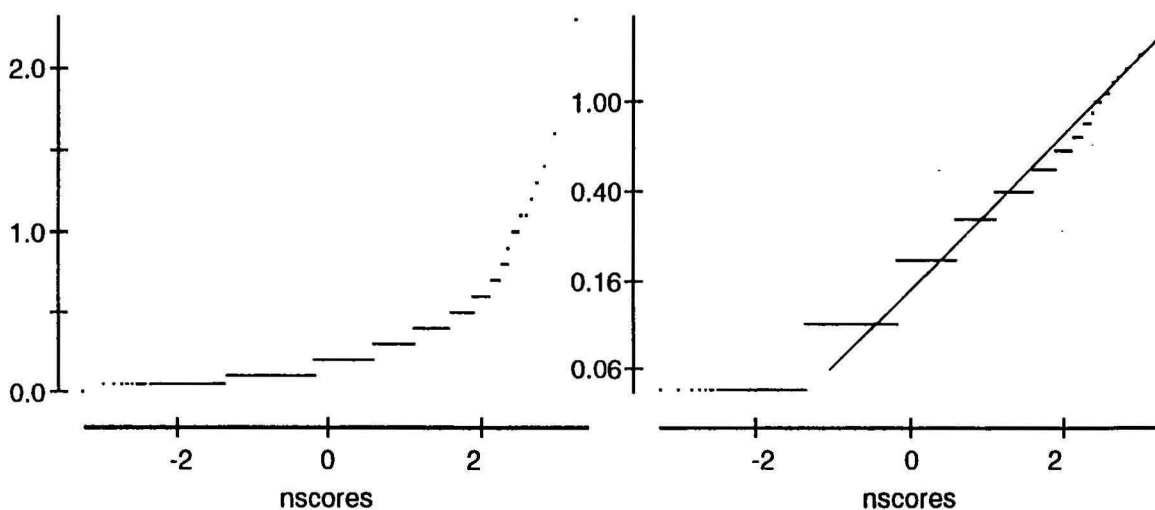
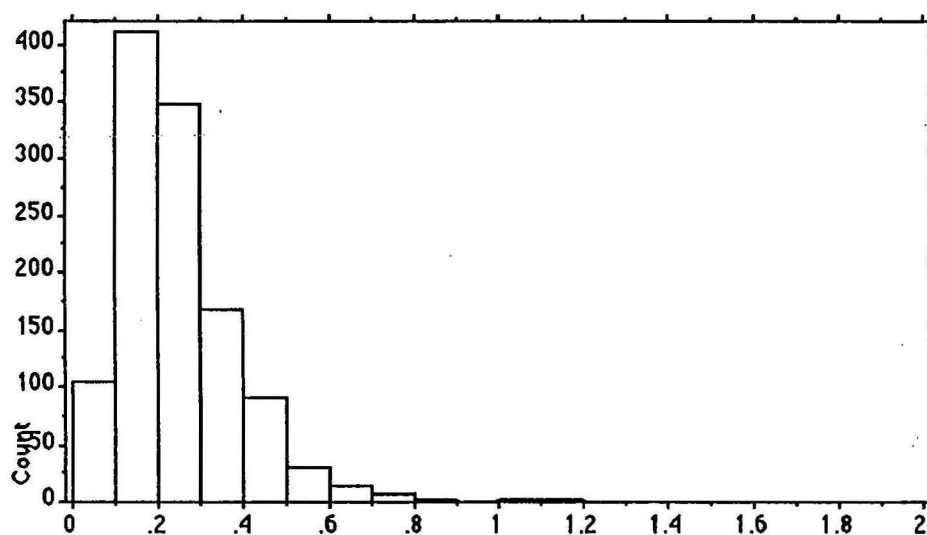


Be<sup>\*</sup>

# **X1 : Bi\* ppm**

Mean:	Std. Dev.:	Std. Error:	Variance:	Coef. Var.:	Count:
.209	.168	.005	.028	80.472	1190
Minimum:	Maximum:	Range:	Sum:	Sum of Sqr.:	# Missing:
.05	2.3	2.25	248.4	85.4	0
1 95%:	95% Lower:	95% Upper:	# < 10th %:	10th %:	25th %:
.01	.199	.218	104	.1	.1
50th %:	75th %:	90th %:	# > 90th %:	Mode:	Geo. Mean:
.2	.3	.4	66	.1	.166
Har. Mean:	Kurtosis:	Skewness:			
.135	30.289	3.88			

Detection limit is 0.10ppm - a value of 0.05ppm has been used in calculations and table

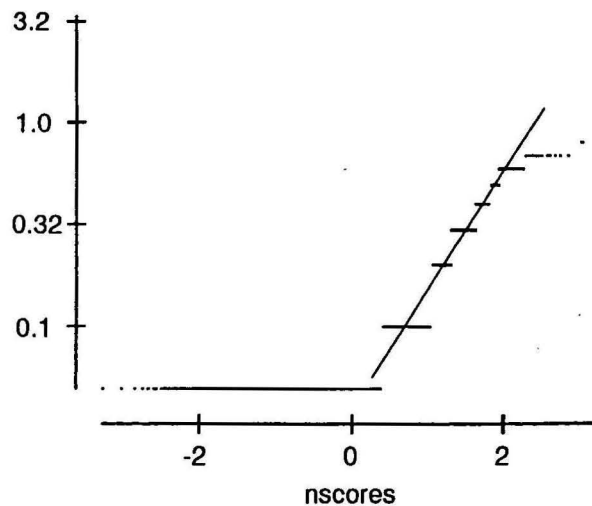
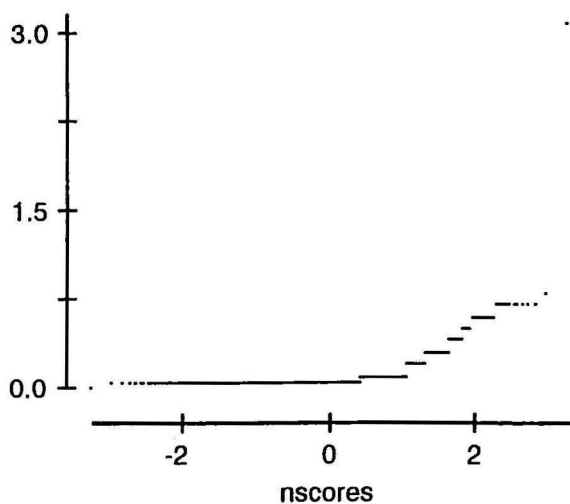
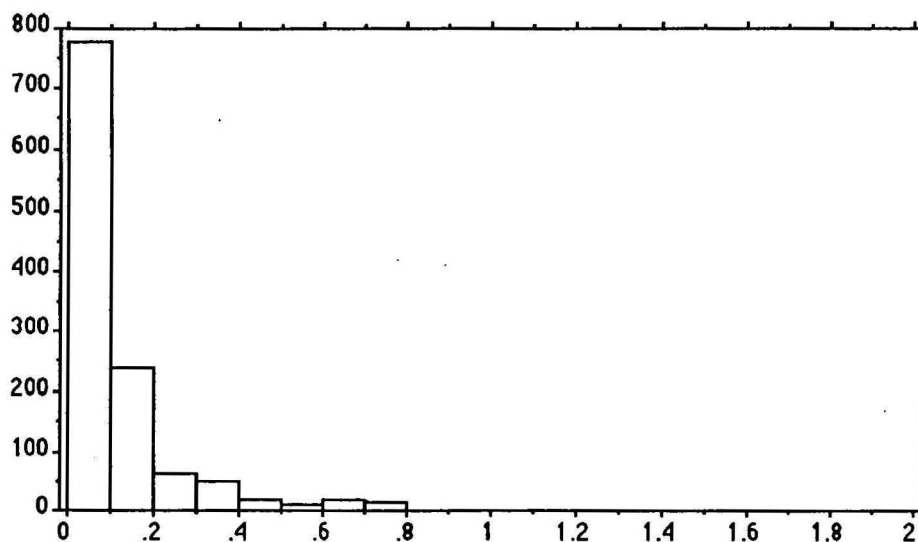


**Bi\***

# **X<sub>1</sub> : Cd\* ppm**

Mean:	Std. Dev.:	Std. Error:	Variance:	Coef. Var.:	Count:
.106	.148	.004	.022	139.898	1190
Minimum:	Maximum:	Range:	Sum:	Sum of Sqr.:	# Missing:
.05	3.1	3.05	126.2	39.555	0
t 95%:	95% Lower:	95% Upper:	# < 10th %:	10th %:	25th %:
.008	.098	.114	0	.05	.05
50th %:	75th %:	90th %:	# > 90th %:	Mode:	Geo. Mean:
.05	.1	.2	113	.05	.075
Har. Mean:	Kurtosis:	Skewness:			
.064	142.217	8.554			

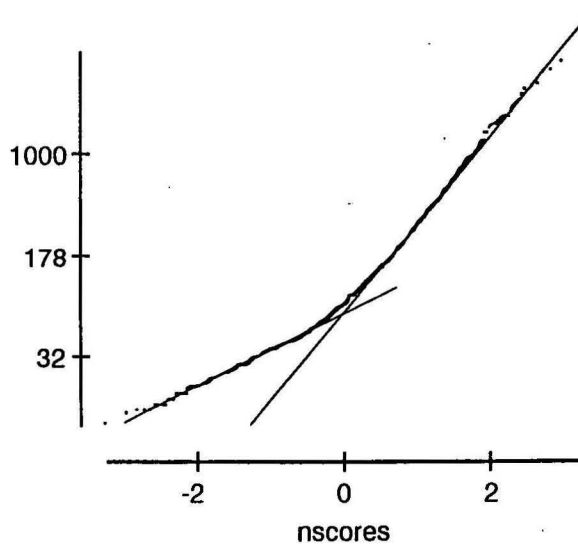
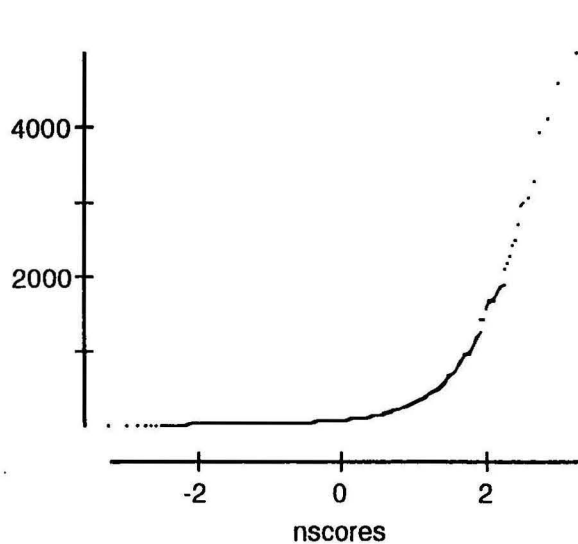
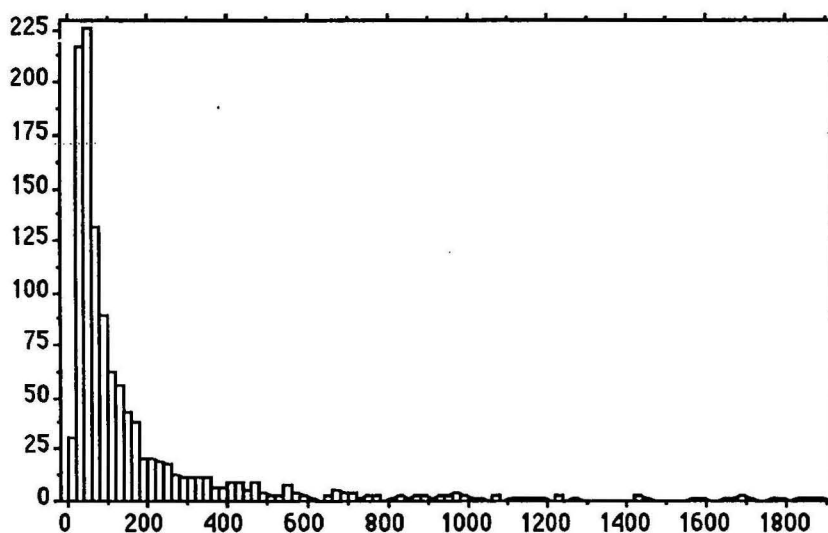
Detection limit is 0.10ppm - a value of 0.05ppm has been used in calculations and table



**Cd\***

# X<sub>1</sub> : Ce ppm

Mean:	Std. Dev.:	Std. Error:	Variance:	Coef. Var.:	Count:
211.448	430.723	12.481	185522.103	203.701	1191
Minimum:	Maximum:	Range:	Sum:	Sum of Sqr.:	# Missing:
10	4951	4941	251835	274021401	0
t 95%:	95% Lower:	95% Upper:	# < 10th %:	10th %:	25th %:
24.489	186.959	235.938	111	29	42
50th %:	75th %:	90th %:	# > 90th %:	Mode:	Geo. Mean:
78	175	460.8	119	40	97.045
Har. Mean:	Kurtosis:	Skewness:			
61.789	41.081	5.597			



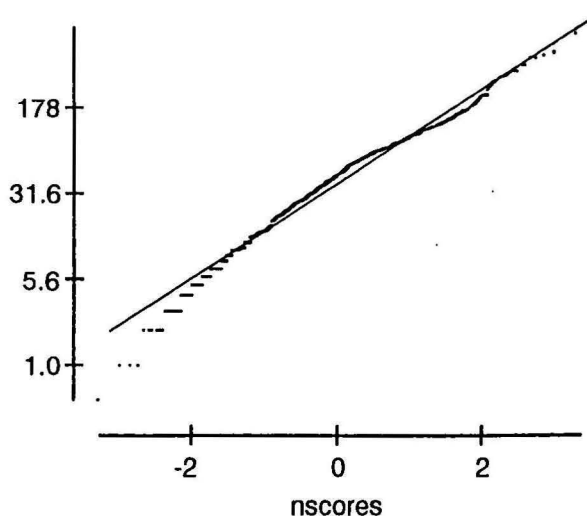
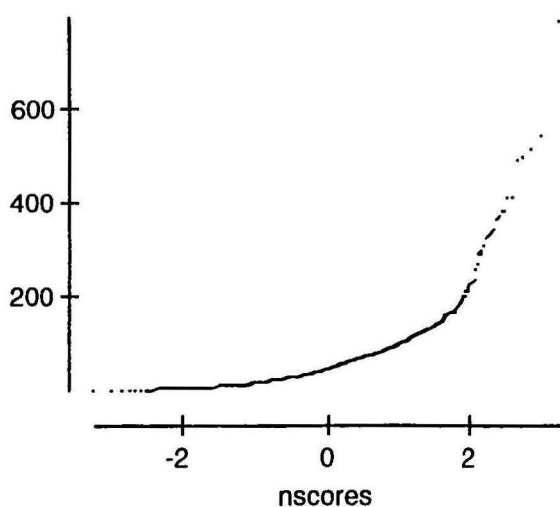
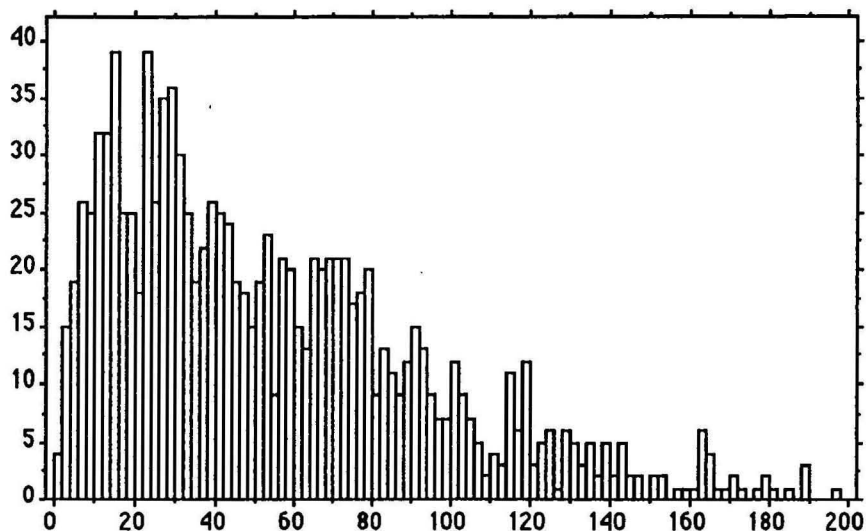
Ce



# **X1 : Cr ppm**

Mean:	Std. Dev.:	Std. Error:	Variance:	Coef. Var.:	Count:
61.905	63.84	1.85	4075.492	103.126	1191
Minimum:	Maximum:	Range:	Sum:	Sum of Sqr.:	# Missing:
.5	787	786.5	73728.5	9413976.25	0
t 95%:	95% Lower:	95% Upper:	# < 10th %:	10th %:	25th %:
3.63	58.275	65.534	104	11	23
50th %:	75th %:	90th %:	# > 90th %:	Mode:	Geo. Mean:
47	79	119	117	15	41.208
Har. Mean:	Kurtosis:	Skewness:			
22.767	26.142	3.927			

Detection limit is 1.0ppm - a value of 0.5ppm has been used in calculations and table

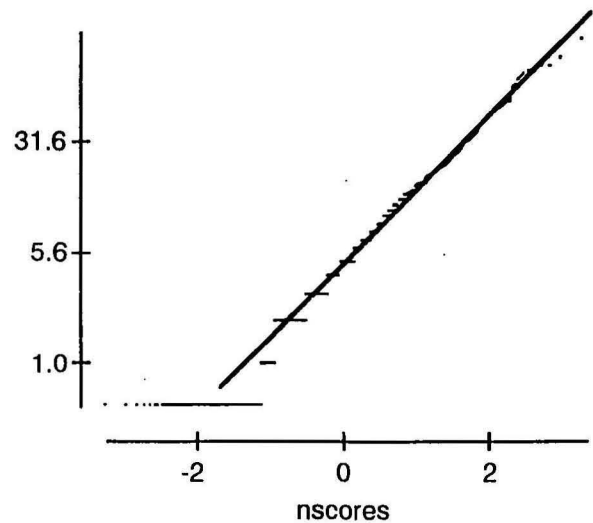
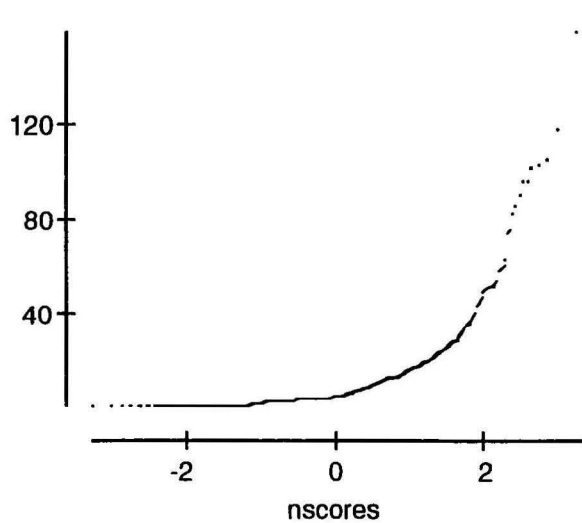
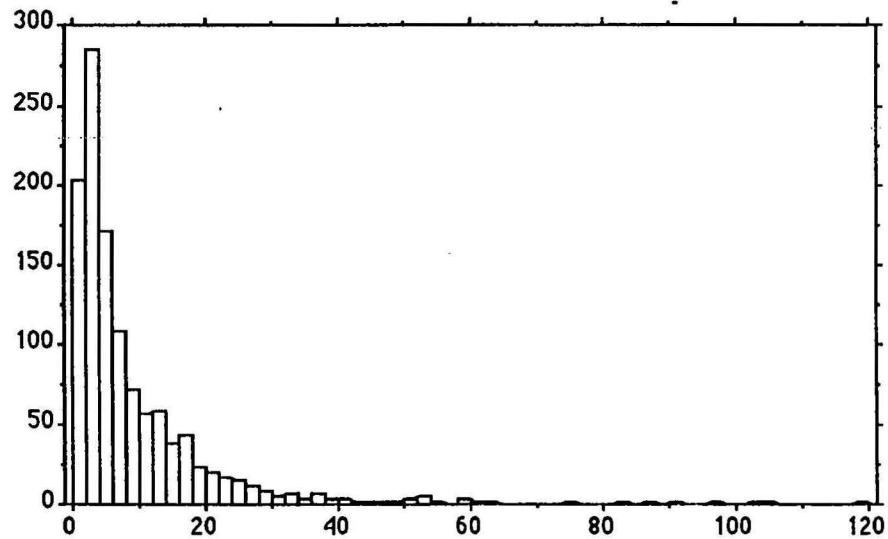


Cr

# **X<sub>1</sub> : Cu ppm**

Mean:	Std. Dev.:	Std. Error:	Variance:	Coef. Var.:	Count:
9.102	13.371	.387	178.774	146.904	1191
Minimum:	Maximum:	Range:	Sum:	Sum of Sqr.:	# Missing:
.5	159	158.5	10840	311402	0
† 95%:	95% Lower:	95% Upper:	# < 10th %:	10th %:	25th %:
.76	8.341	9.862	0	.5	2
50th %:	75th %:	90th %:	# > 90th %:	Mode:	Geo. Mean:
5	11	21	111	2	4.492
Har. Mean:	Kurtosis:	Skewness:			
2.125	29.441	4.445			

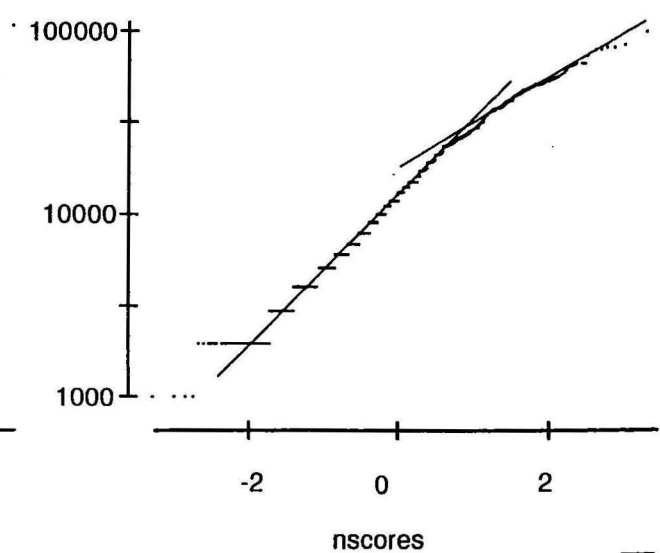
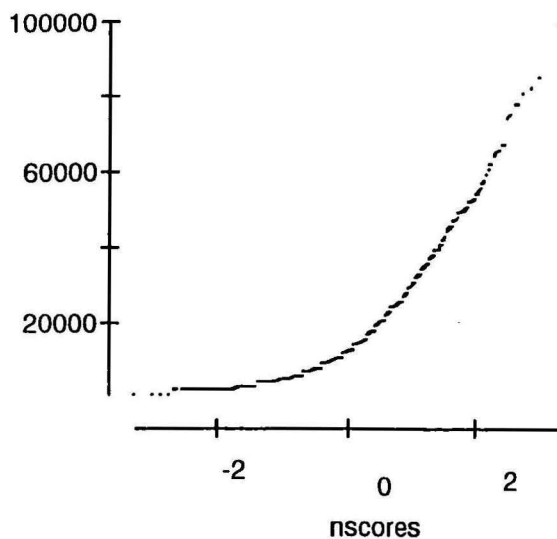
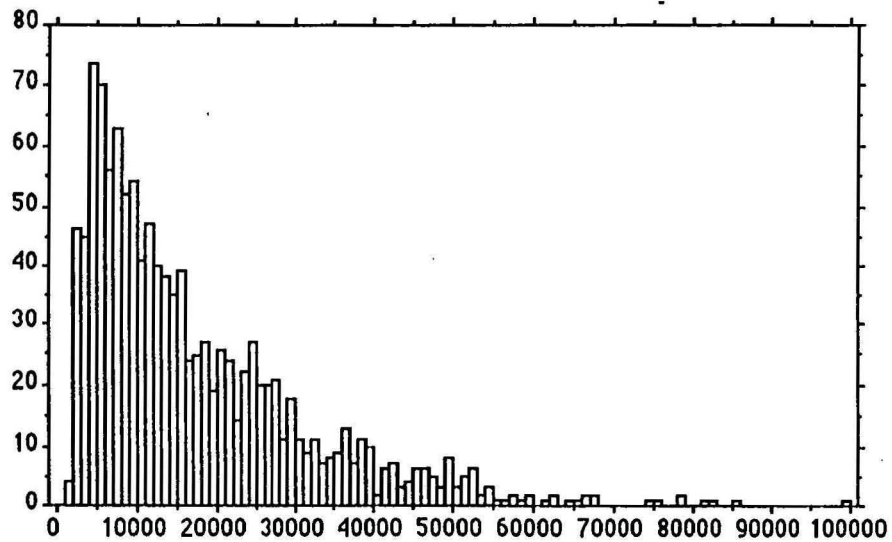
Detection limit is 1.0ppm - a value of 0.5ppm has been used in calculations and table



**Cu**

# X1 : Fe ppm

Mean:	Std. Dev.:	Std. Error:	Variance:	Coef. Var.:	Count:
17015.113	14183.424	410.984	2.012E8	83.358	1191
Minimum:	Maximum:	Range:	Sum:	Sum of Sqr.:	# Missing:
1000	99000	98000	20265000	5.842E11	0
† 95%:	95% Lower:	95% Upper:	# < 10th %:	10th %:	25th %:
806.413	16208.7	17821.527	95	4000	7000
50th %:	75th %:	90th %:	# > 90th %:	Mode:	Geo. Mean:
13000	24000	37000	114	4000	12109.328
Har. Mean:	Kurtosis:	Skewness:			
8287.92	3.174	1.599			

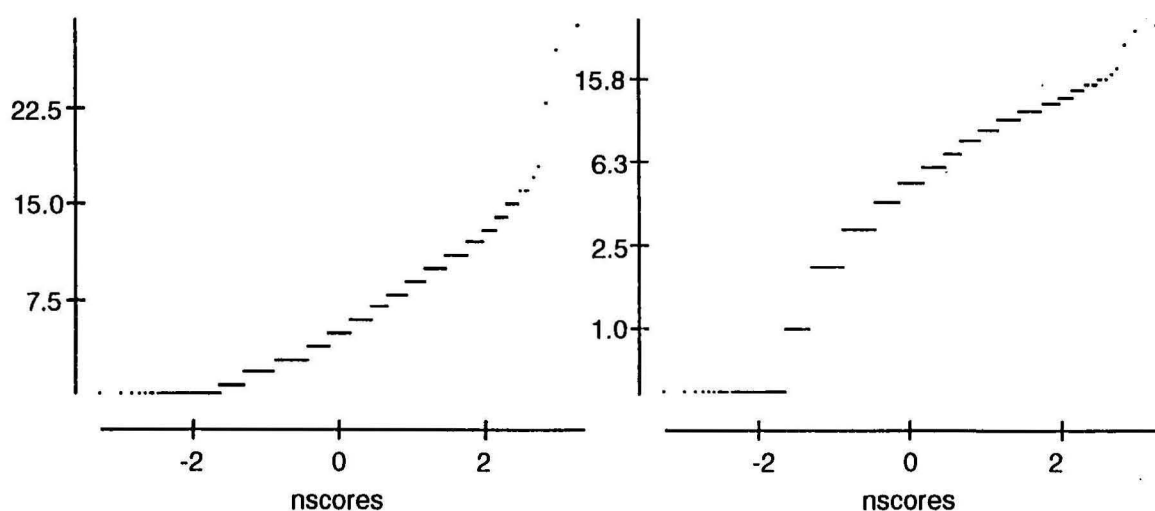
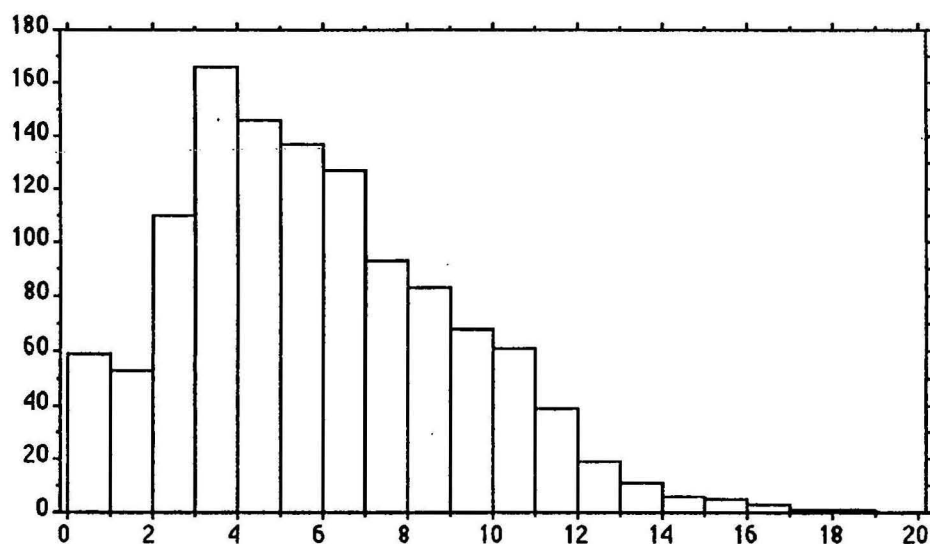


Fe

# X1 : Ga ppm

Mean:	Std. Dev.:	Std. Error:	Variance:	Coef. Var.:	Count:
5.449	3.374	.098	11.384	61.922	1191
Minimum:	Maximum:	Range:	Sum:	Sum of Sqr.:	# Missing:
.5	29	28.5	6489.5	48906.75	0
t 95%:	95% Lower:	95% Upper:	# < 10th %:	10th %:	25th %:
.192	5.257	5.641	112	2	3
50th %:	75th %:	90th %:	# > 90th %:	Mode:	Geo. Mean:
5	8	10	88	3	4.288
Har. Mean:	Kurtosis:	Skewness:			
2.899	3.483	1.132			

Detection limit is 1.0ppm - a value of 0.5ppm has been used in calculations and table

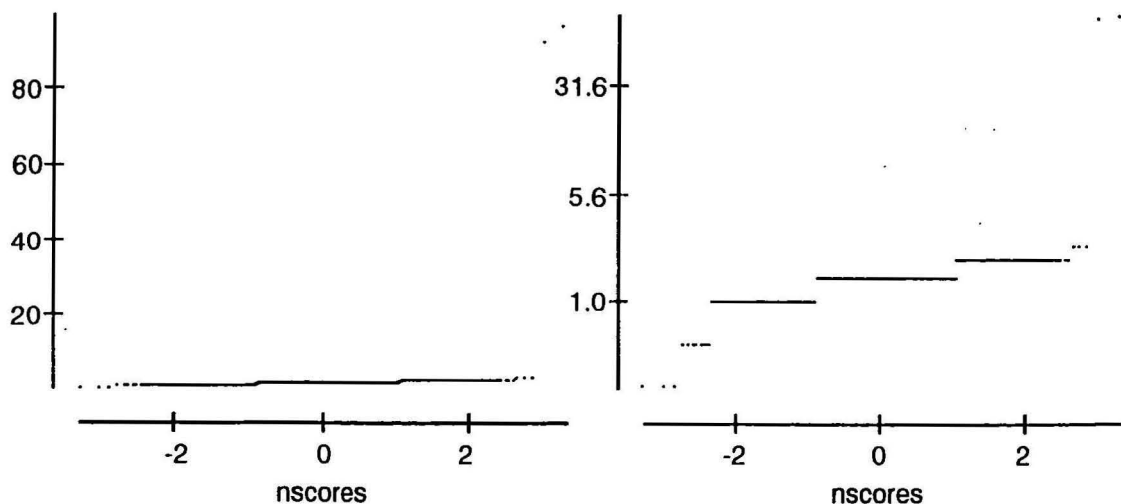
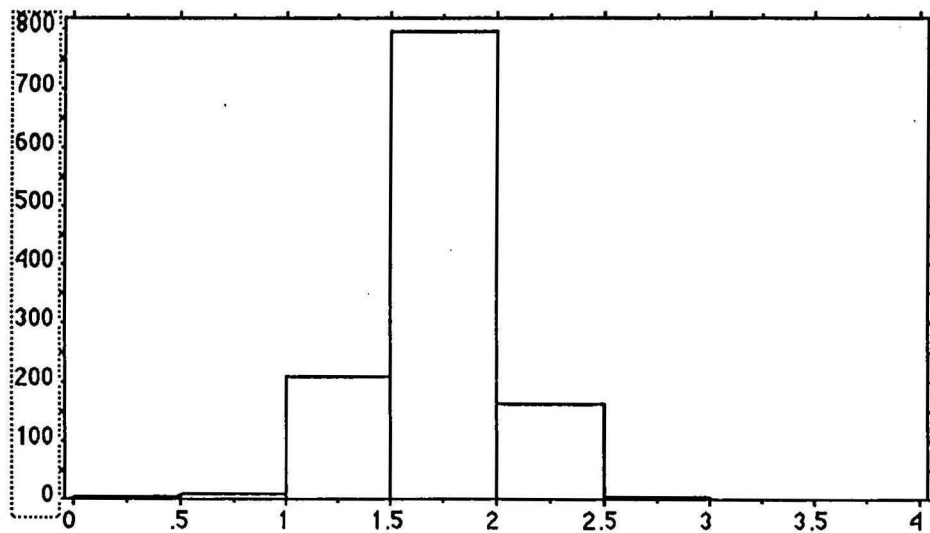


Ga

# X1 : Ge ppm

Mean:	Std. Dev.:	Std. Error:	Variance:	Coef. Var.:	Count:
1.63	3.823	.111	14.618	234.633	1191
Minimum:	Maximum:	Range:	Sum:	Sum of Sqr.:	# Missing:
.25	96.5	96.25	1940.75	20558.188	0
† 95%:	95% Lower:	95% Upper:	# < 10th %:	10th %:	25th %:
.217	1.412	1.847	11	1	1.5
50th %:	75th %:	90th %:	# > 90th %:	Mode:	Geo. Mean:
1.5	1.5	2	5	1.5	1.448
Har. Mean:	Kurtosis:	Skewness:			
1.392	584.186	24.129			

Detection limit is 0.50ppm - a value of 0.25ppm has been used in calculations and table



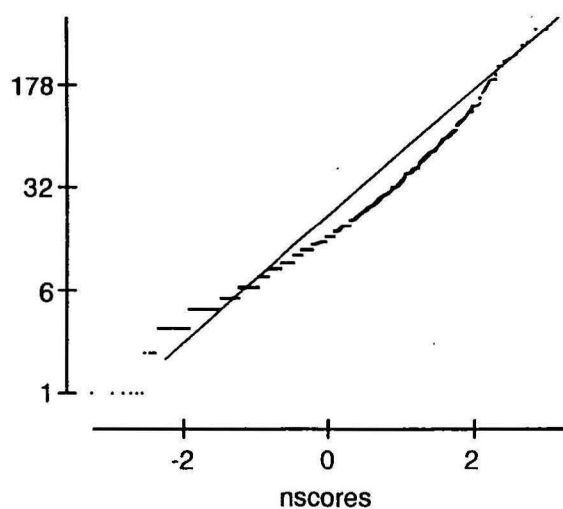
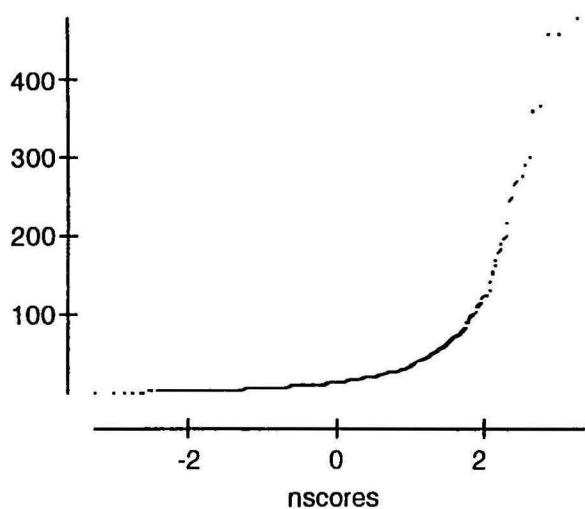
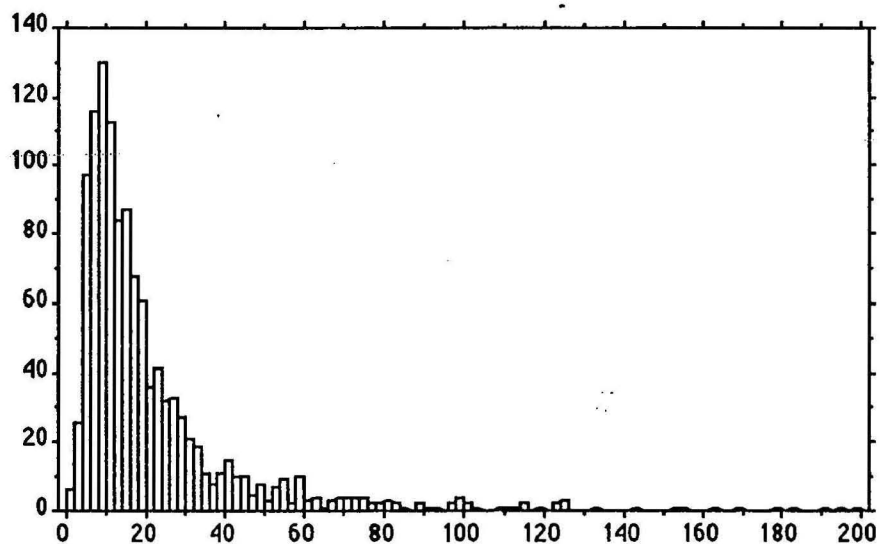
Ge



# **X<sub>1</sub> : Hf ppm**

Mean:	Std. Dev.:	Std. Error:	Variance:	Coef. Var.:	Count:
24.898	40.833	1.183	1667.311	164.003	1191
Minimum:	Maximum:	Range:	Sum:	Sum of Sqr.:	# Missing:
1	480	479	29653	2722387	0
† 95%:	95% Lower:	95% Upper:	# < 10th %:	10th %:	25th %:
2.322	22.576	27.219	78	5	8
50th %:	75th %:	90th %:	# > 90th %:	Mode:	Geo. Mean:
14	25	49	116	9	15.132
Har. Mean:	Kurtosis:	Skewness:			
10.54	49.396	6.126			

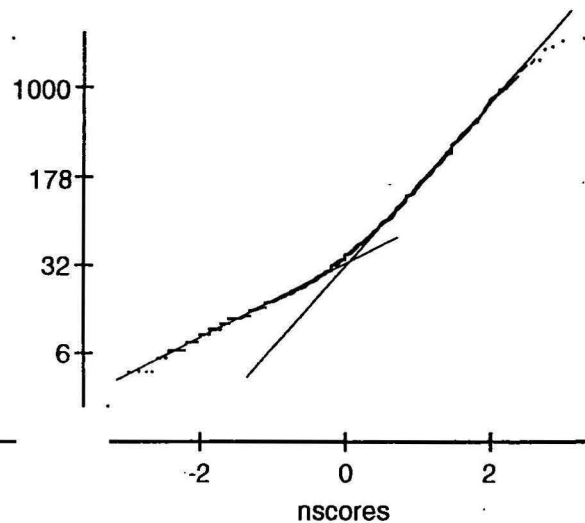
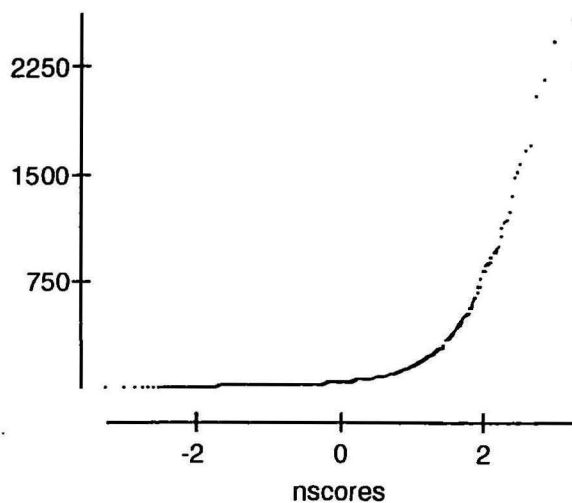
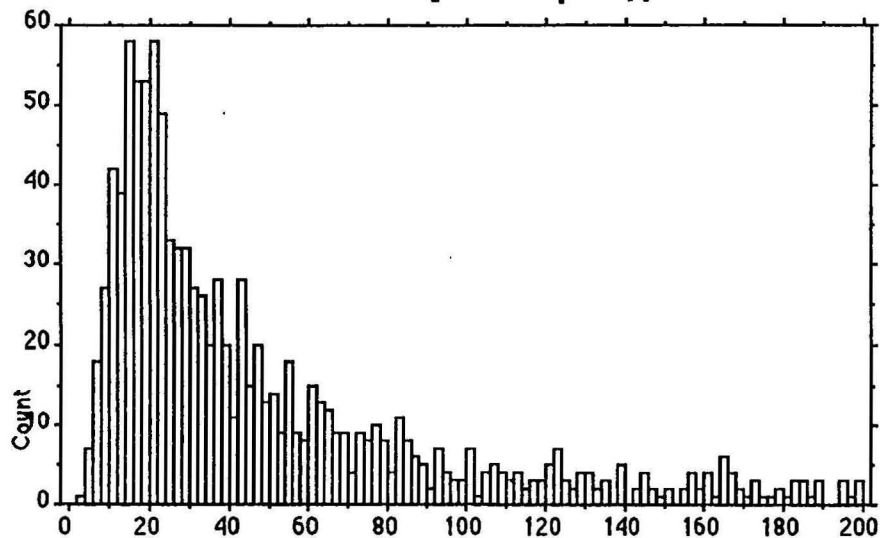
Detection limit is 2.0ppm - a value of 1.0ppm has been used in calculations and table



Hf

# X<sub>1</sub> : La ppm

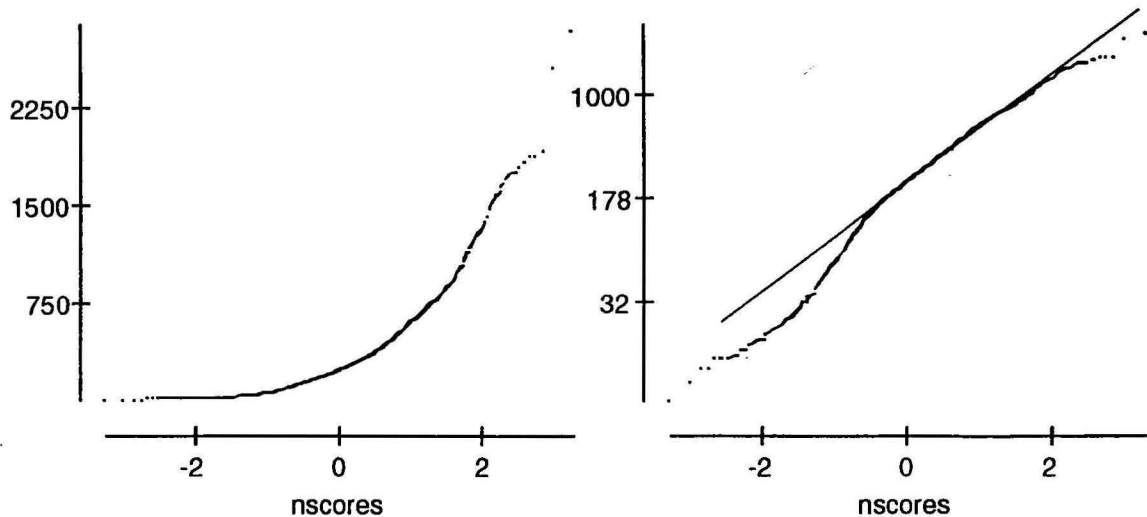
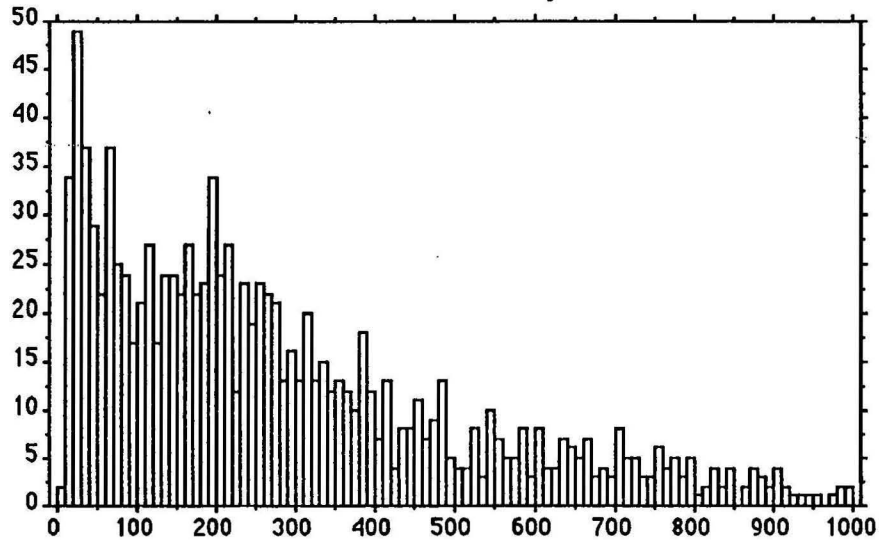
Mean:	Std. Dev.:	Std. Error:	Variance:	Coef. Var.:	Count:
106.202	225.677	6.539	50930.316	212.499	1191
Minimum:	Maximum:	Range:	Sum:	Sum of Sqr.:	# Missing:
2	2560	2558	126486	74040080	0
t 95%:	95% Lower:	95% Upper:	# < 10th %:	10th %:	25th %:
12.831	93.37	119.033	113	13	19.25
50th %:	75th %:	90th %:	# > 90th %:	Mode:	Geo. Mean:
37	87	231.4	119	15	45.446
Har. Mean:	Kurtosis:	Skewness:			
27.16	41.342	5.646			



La

# **X1 : Mn ppm**

Mean:	Std. Dev.:	Std. Error:	Variance:	Coef. Var.:	Count:
335.902	337.995	9.794	114240.406	100.623	1191
Minimum:	Maximum:	Range:	Sum:	Sum of Sqr.:	# Missing:
6	2863	2857	400059	270326607	0
t 95%:	95% Lower:	95% Upper:	# < 10th %:	10th %:	25th %:
19.217	316.685	355.119	118	39	110
50th %:	75th %:	90th %:	# > 90th %:	Mode:	Geo. Mean:
237	445.75	748.2	119	●	203.905
Har. Mean:	Kurtosis:	Skewness:			
102.436	7.571	2.272			

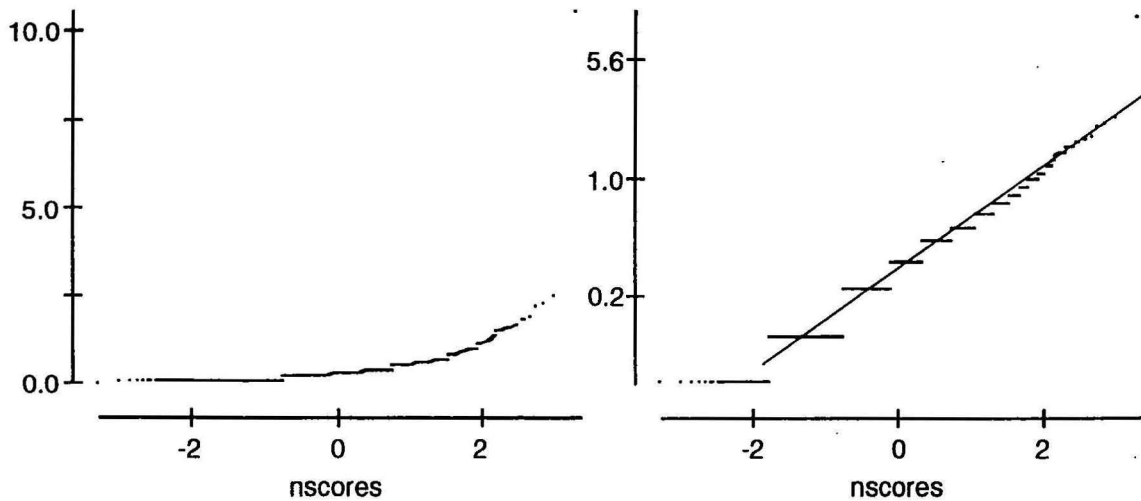
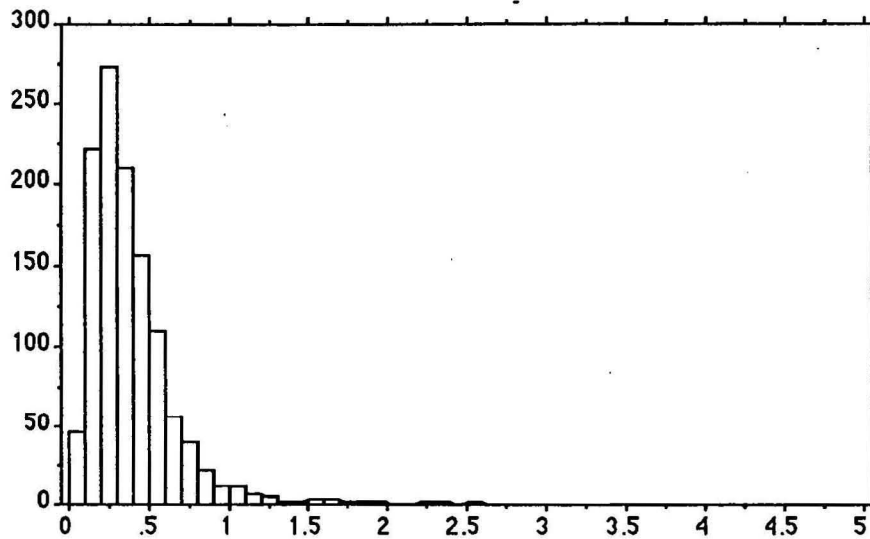


Mn

# $X_1: Mo \pm ppm$

Mean:	Std. Dev.:	Std. Error:	Variance:	Coef. Var.:	Count:
.351	.406	.012	.165	115.74	1190
Minimum:	Maximum:	Range:	Sum:	Sum of Sqr.:	# Missing:
.05	10.5	10.45	417.65	342.773	0
t 95%:	95% Lower:	95% Upper:	# < 10th %:	10th %:	25th %:
.023	.328	.374	45	.1	.2
50th %:	75th %:	90th %:	# > 90th %:	Mode:	Geo. Mean:
.3	.4	.6	116	.2	.262
Har. Mean:	Kurtosis:	Skewness:			
.198	328.105	13.953			

Detection limit is 0.10ppm - a value of 0.05ppm has been used in calculations and table

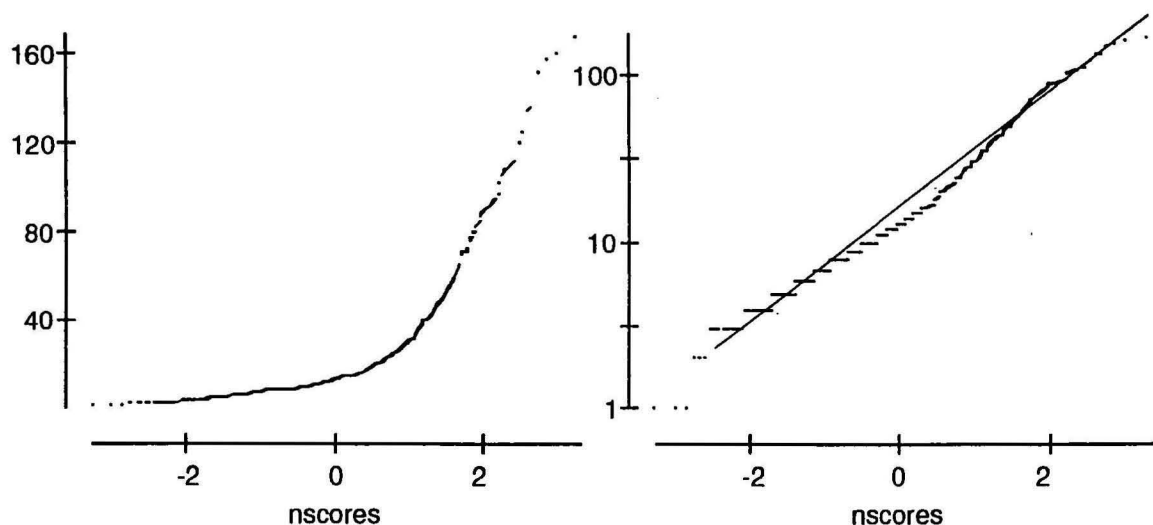
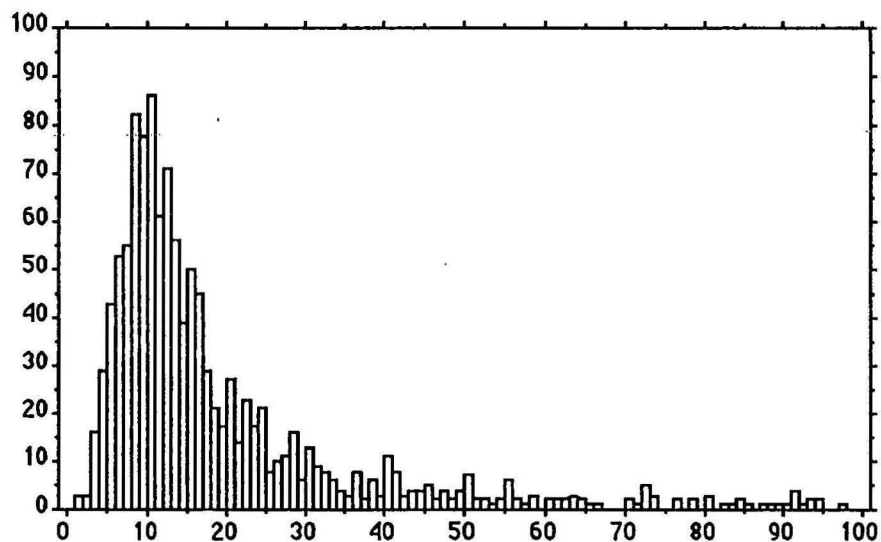


Mo\*

# X<sub>1</sub> : Nb ppm

Mean:	Std. Dev.:	Std. Error:	Variance:	Coef. Var.:	Count:
19.94	20.805	.603	432.828	104.338	1191
Minimum:	Maximum:	Range:	Sum:	Sum of Sqr.:	# Missing:
1	167	166	23748	988590	0
† 95%:	95% Lower:	95% Upper:	# < 10th %:	10th %:	25th %:
1.183	18.757	21.122	94	6	9
50th %:	75th %:	90th %:	# > 90th %:	Mode:	Geo. Mean:
13	22	42	117	10	14.292
Har. Mean:	Kurtosis:	Skewness:			
10.91	11.762	3.044			

Detection limit is 2.0ppm - a value of 1.0ppm has been used in calculations and table

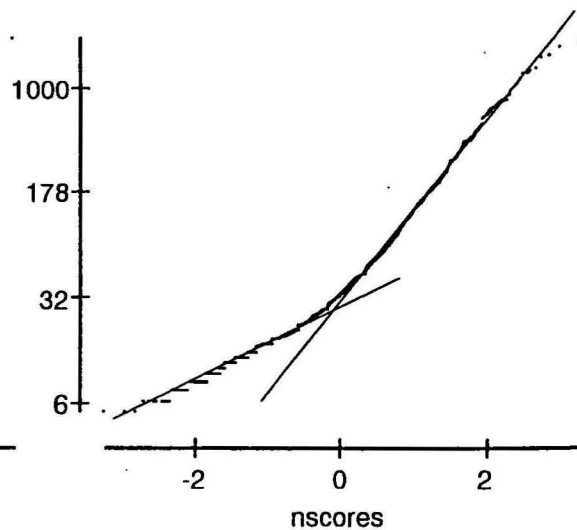
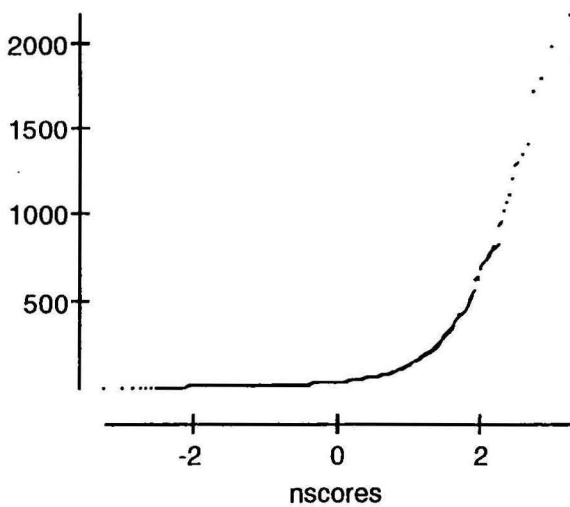
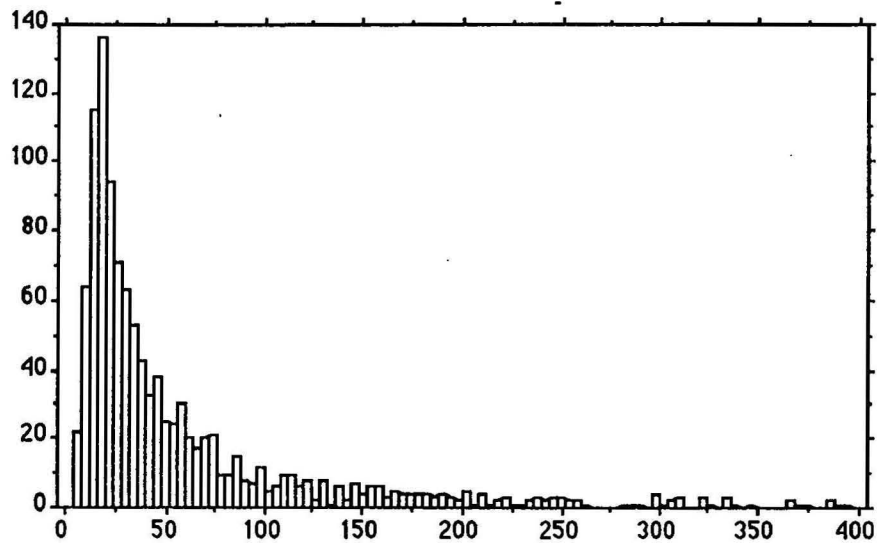


Nb



# **X<sub>1</sub> : Nd ppm**

Mean:	Std. Dev.:	Std. Error:	Variance:	Coef. Var.:	Count:
92.369	188.671	5.467	35596.899	204.257	1191
Minimum:	Maximum:	Range:	Sum:	Sum of Sqr.:	# Missing:
5	2173	2168	110012	52522056	0
† 95%:	95% Lower:	95% Upper:	# < 10th %:	10th %:	25th %:
10.727	81.642	103.097	86	12	18
50th %:	75th %:	90th %:	# > 90th %:	Mode:	Geo. Mean:
33	76.75	203	116	16	41.907
Har. Mean:	Kurtosis:	Skewness:			
26.427	40.648	5.565			

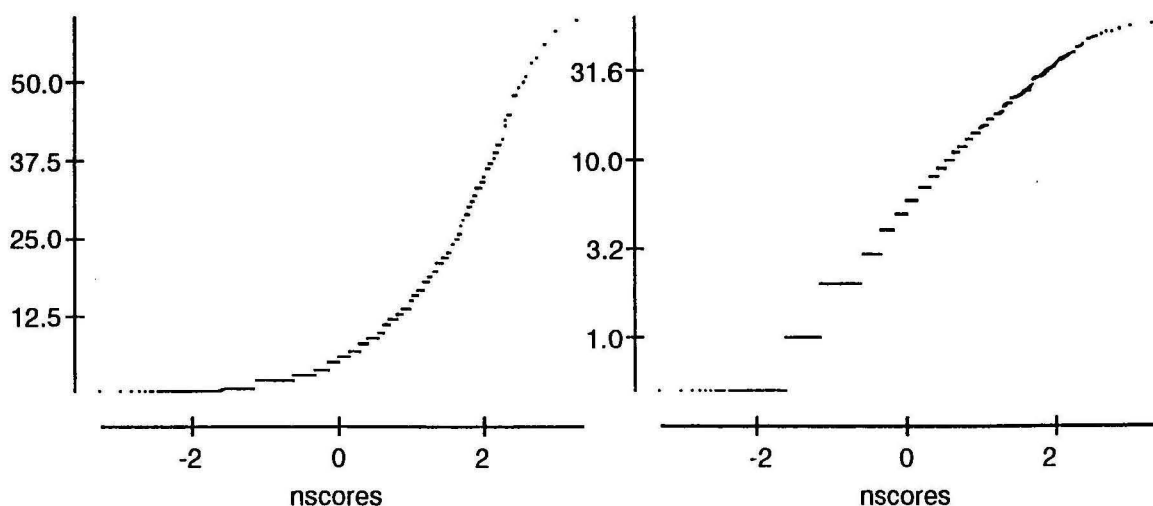
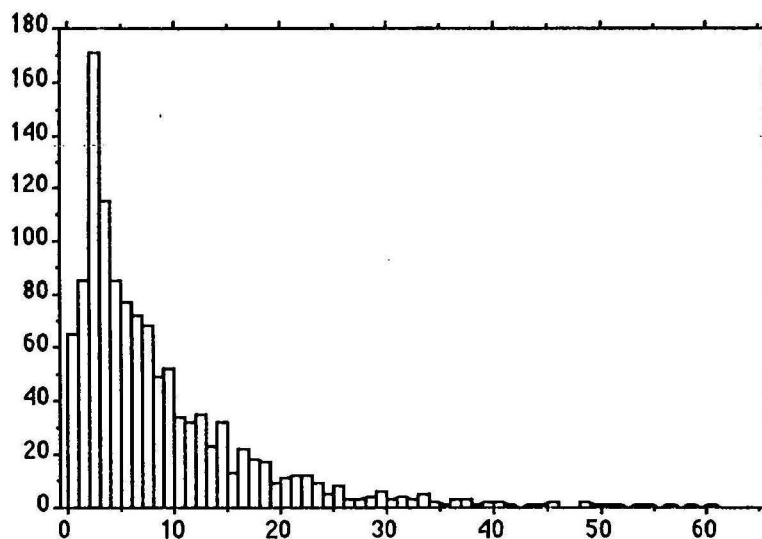


Nd

# X1 : Ni ppm

Mean:	Std. Dev.:	Std. Error:	Variance:	Coef. Var.:	Count:
8.34	8.831	.256	77.982	105.889	1191
Minimum:	Maximum:	Range:	Sum:	Sum of Sqr.:	# Missing:
.5	60	59.5	9932.5	175632.25	0
t 95%:	95% Lower:	95% Upper:	# < 10th %:	10th %:	25th %:
.502	7.838	8.842	65	1	2
50th %:	75th %:	90th %:	# > 90th %:	Mode:	Geo. Mean:
5	11	19	117	2	5.004
Har. Mean:	Kurtosis:	Skewness:			
2.761	6.508	2.249			

Detection limit is 1.0ppm - a value of 0.5ppm has been used in calculations and table

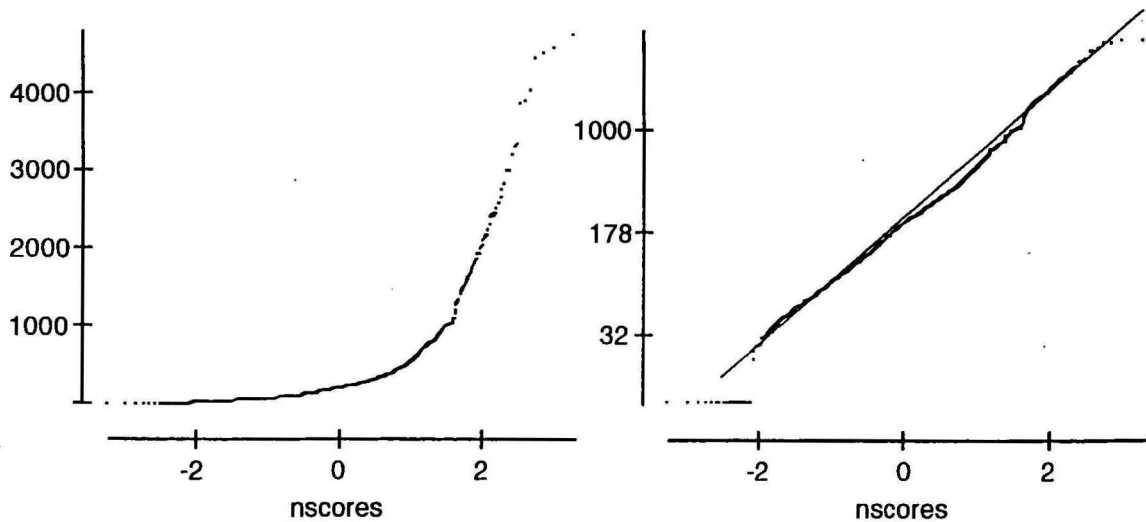
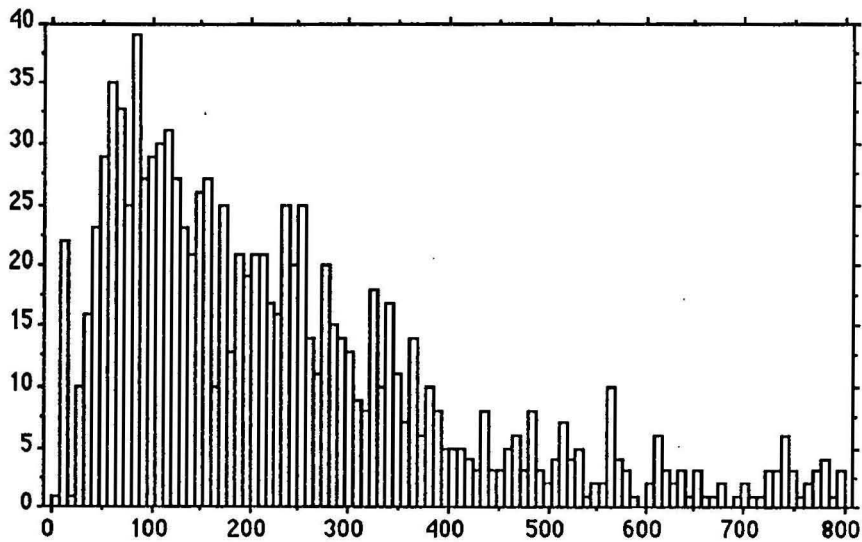


Ni

# **X1 : P\* ppm**

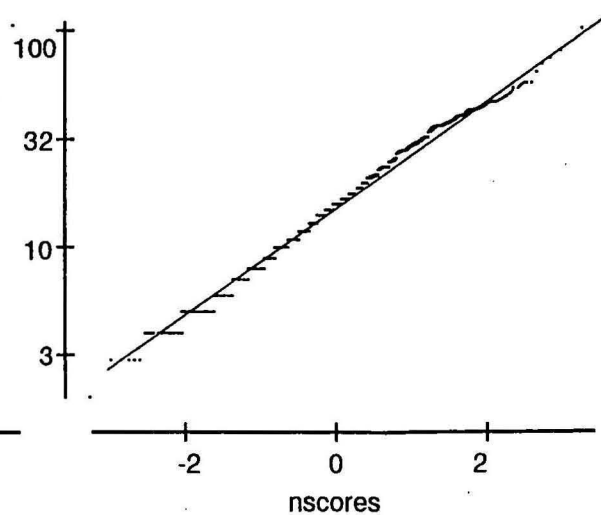
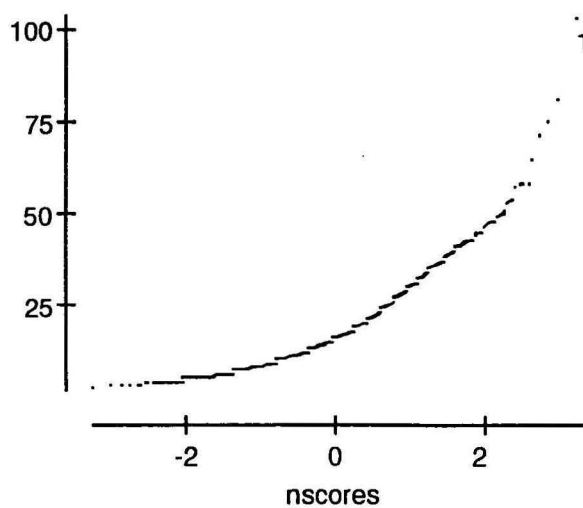
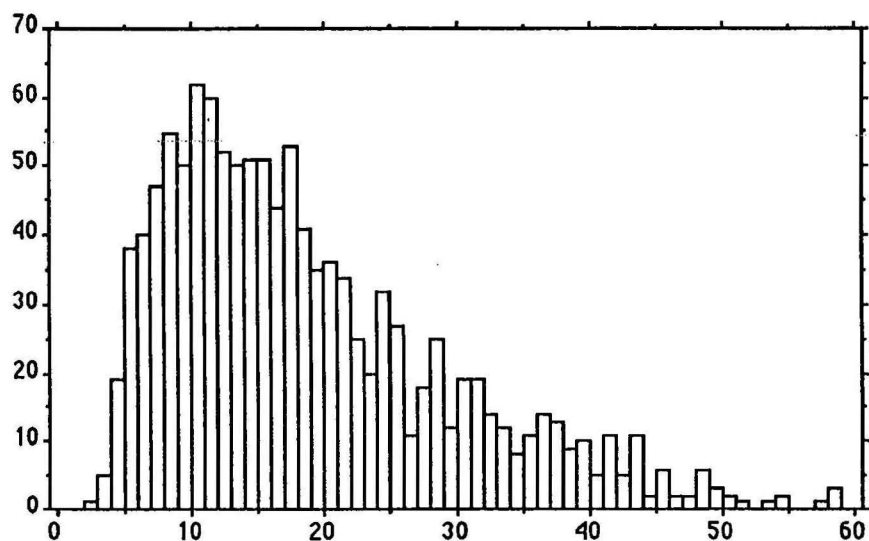
Mean:	Std. Dev.:	Std. Error:	Variance:	Coef. Var.:	Count:
366.532	532.89	15.448	283971.751	145.387	1190
Minimum:	Maximum:	Range:	Sum:	Sum of Sqr.:	# Missing:
10	4770	4760	436173	497513745	0
t 95%:	95% Lower:	95% Upper:	# < 10th %:	10th %:	25th %:
30.311	336.221	396.843	111	59	106
50th %:	75th %:	90th %:	# > 90th %:	Mode:	Geo. Mean:
212	373	781	118	10	207.84
Har. Mean:	Kurtosis:	Skewness:			
116.263	22.662	4.198			

Detection limit is 20ppm - a value of 10ppm has been used in calculations and table



# **X<sub>1</sub> : Pb ppm**

Mean:	Std. Dev.:	Std. Error:	Variance:	Coef. Var.:	Count:
18.571	11.431	.331	130.664	61.552	1191
Minimum:	Maximum:	Range:	Sum:	Sum of Sqr.:	# Missing:
2	103	101	22118	566242	0
† 95%:	95% Lower:	95% Upper:	* < 10th %:	10th %:	25th %:
.65	17.921	19.221	103	7	10
50th %:	75th %:	90th %:	* > 90th %:	Mode:	Geo. Mean:
16	24	35	114	10	15.525
Har. Mean:	Kurtosis:	Skewness:			
12.844	4.068	1.493			

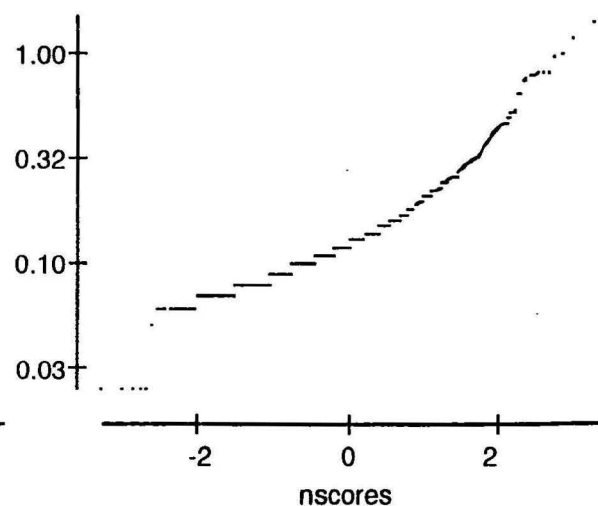
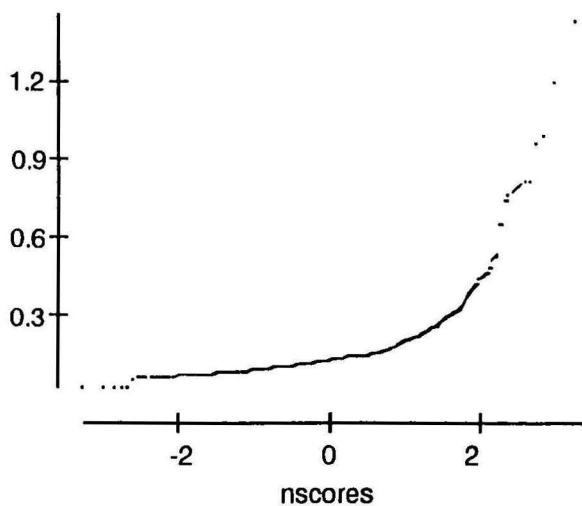
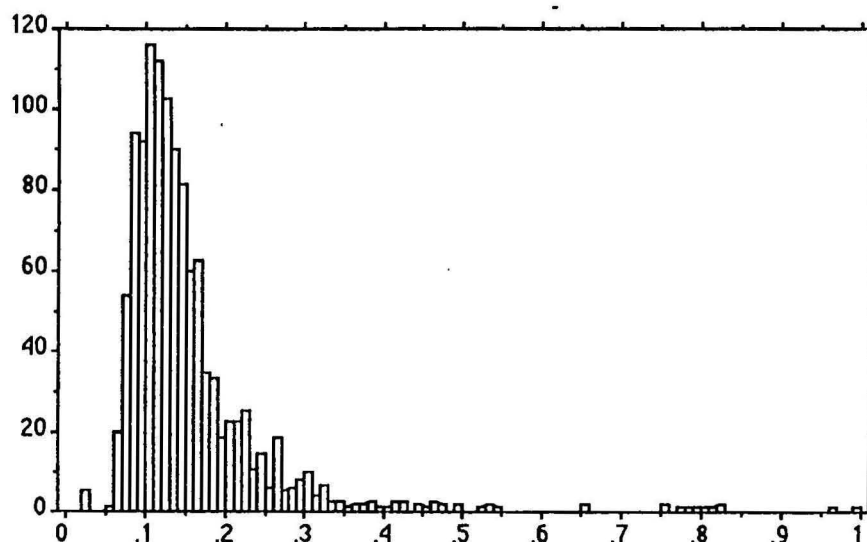


Pb

# **X<sub>1</sub> : Pd\* ppb**

Mean:	Std. Dev.:	Std. Error:	Variance:	Coef. Var.:	Count:
.153	.111	.003	.012	72.557	1191
Minimum:	Maximum:	Range:	Sum:	Sum of Sqr.:	# Missing:
.025	1.44	1.415	182.155	42.514	0
† 95%:	95% Lower:	95% Upper:	# < 10th %:	10th %:	25th %:
.006	.147	.159	80	.08	.1
50th %:	75th %:	90th %:	# > 90th %:	Mode:	Geo. Mean:
.12	.17	.24	120	.1	.133
Har. Mean:	Kurtosis:	Skewness:			
.12	34.314	4.769			

Detection limit is 0.05ppb - a value of 0.025ppb has been used in calculations and table



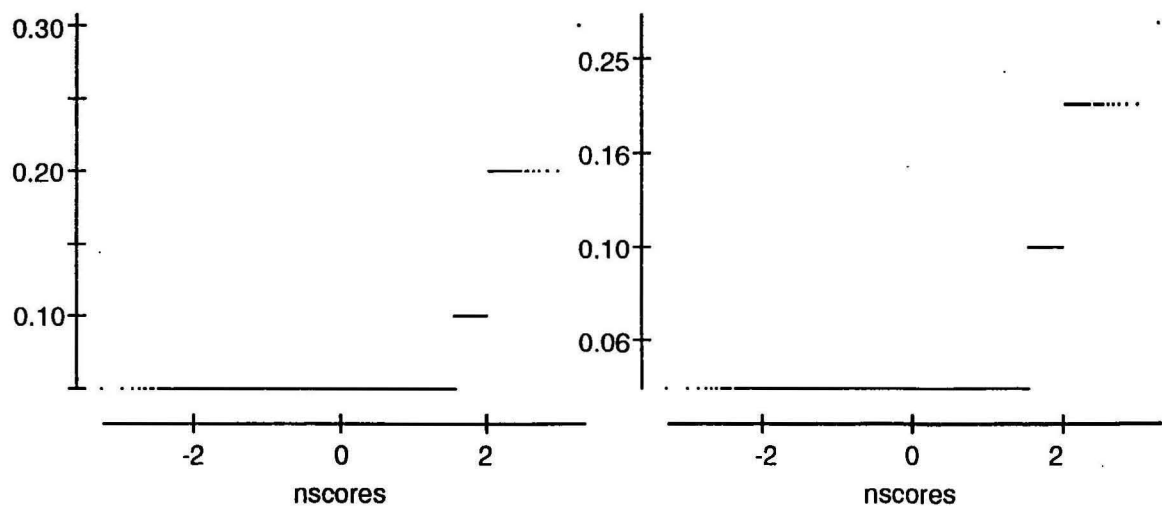
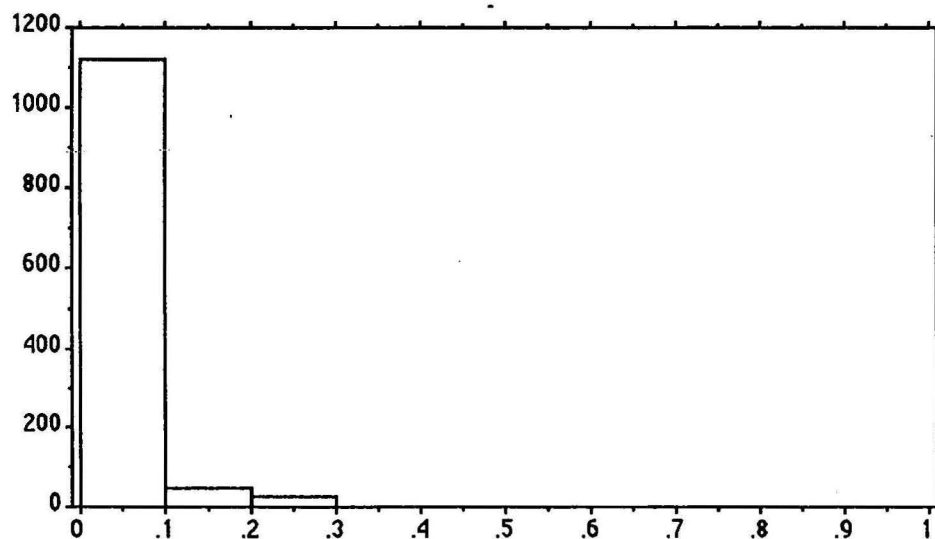
Pd#



# **X1 : Pt# ppb**

Mean:	Std. Dev.:	Std. Error:	Variance:	Coef. Var.:	Count:
.055	.024	.001	.001	44.075	1191
Minimum:	Maximum:	Range:	Sum:	Sum of Sqr.:	# Missing:
.05	.3	.25	65.85	4.348	0
t 95%:	95% Lower:	95% Upper:	# < 10th %:	10th %:	25th %:
.001	.054	.057	0	.05	.05
50th %:	75th %:	90th %:	# > 90th %:	Mode:	Geo. Mean:
.05	.05	.05	72	.05	.053
Har. Mean:	Kurtosis:	Skewness:			
.052	32.139	5.482			

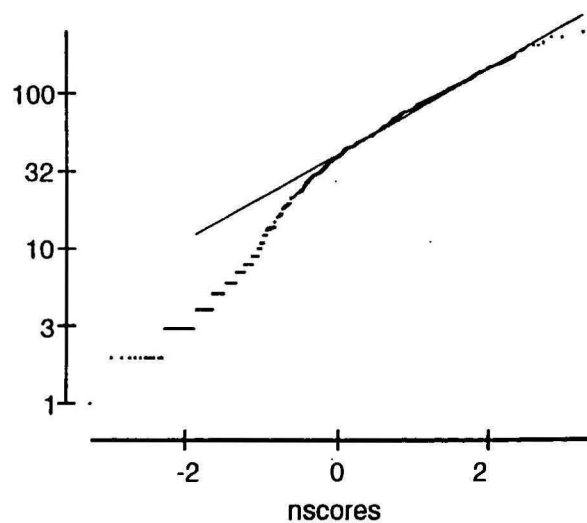
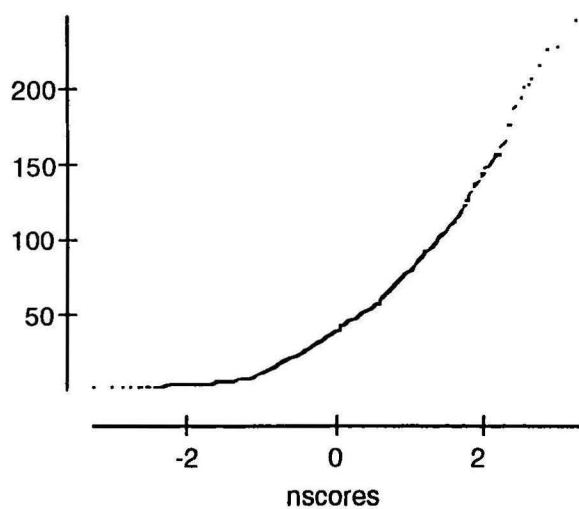
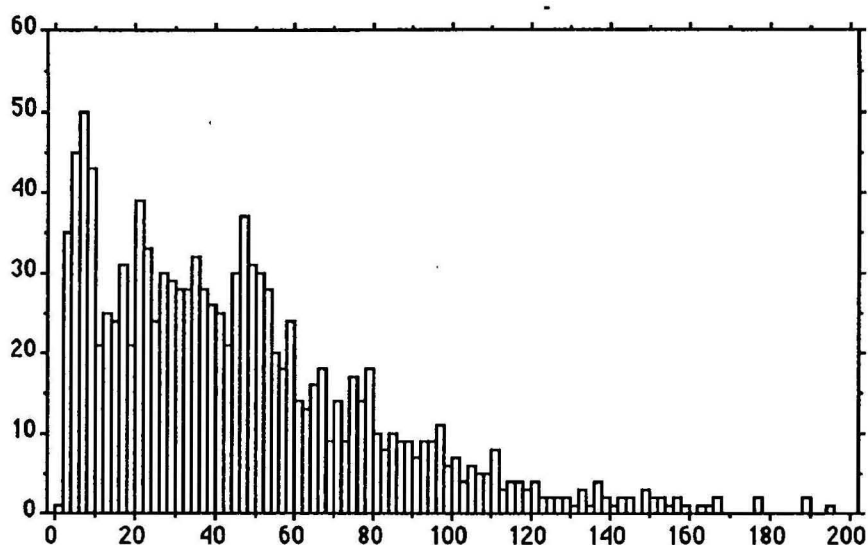
Detection limit is 0.10ppb - a value of 0.05ppb has been used in calculations and table



Pt#

# X1 : Rb ppm

Mean:	Std. Dev.:	Std. Error:	Variance:	Coef. Var.:	Count:
46.941	37.247	1.079	1387.341	79.348	1191
Minimum:	Maximum:	Range:	Sum:	Sum of Sqr.:	# Missing:
1	246	245	55907	4275279	0
t 95%:	95% Lower:	95% Upper:	# < 10th %:	10th %:	25th %:
2.118	44.824	49.059	107	7	20
50th %:	75th %:	90th %:	# > 90th %:	Mode:	Geo. Mean:
40	65	96	116	•	32.172
Har. Mean:	Kurtosis:	Skewness:			
17.933	2.982	1.44			

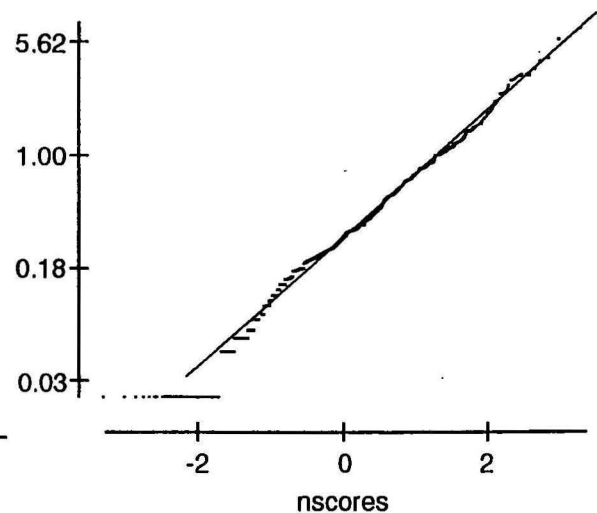
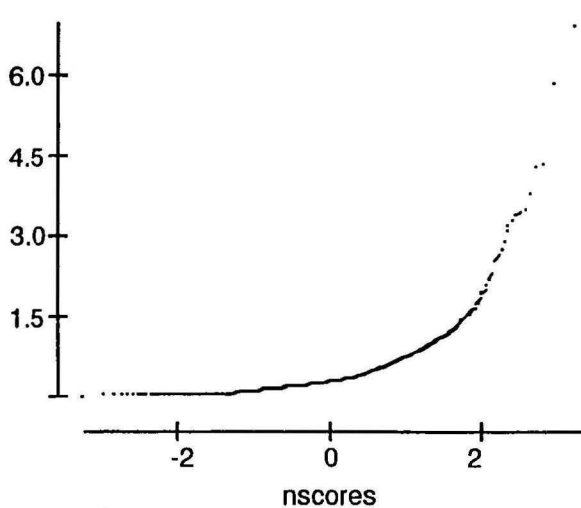
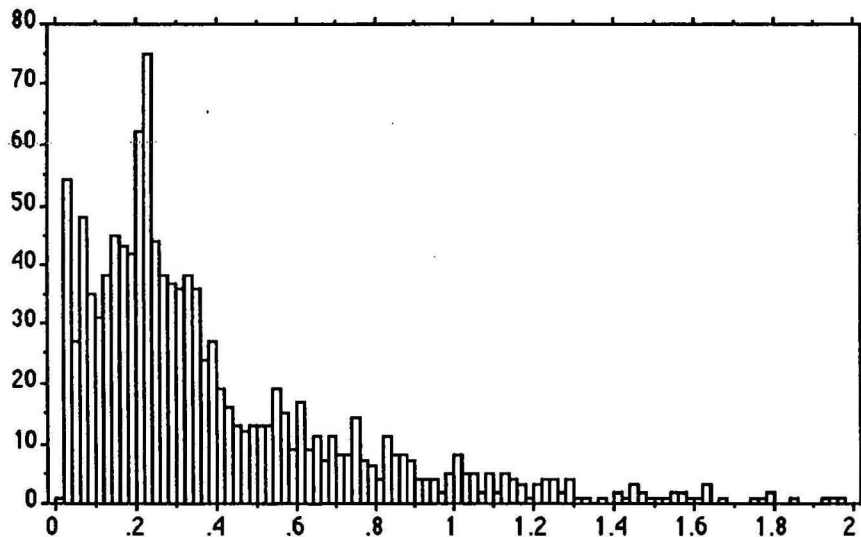


Rb

# **X<sub>1</sub> : Sb\* ppm**

Mean:	Std. Dev.:	Std. Error:	Variance:	Coef. Var.:	Count:
.448	.552	.016	.305	123.135	1190
Minimum:	Maximum:	Range:	Sum:	Sum of Sqr.:	# Missing:
.025	6.89	6.865	533.58	601.7	0
t 95%:	95% Lower:	95% Upper:	# < 10th %:	10th %:	25th %:
.031	.417	.48	113	.07	.17
50th %:	75th %:	90th %:	# > 90th %:	Mode:	Geo. Mean:
.28	.55	.96	118	.025	.278
Har. Mean:	Kurtosis:	Skewness:			
.16	32.703	4.529			

Detection limit is 0.050ppm - a value of 0.025ppm has been used in calculations and table

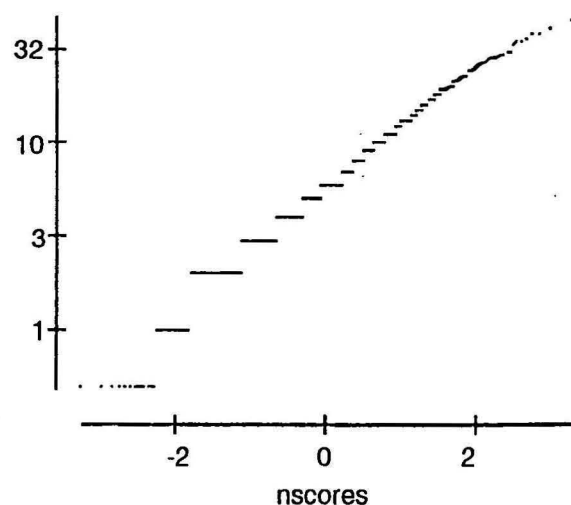
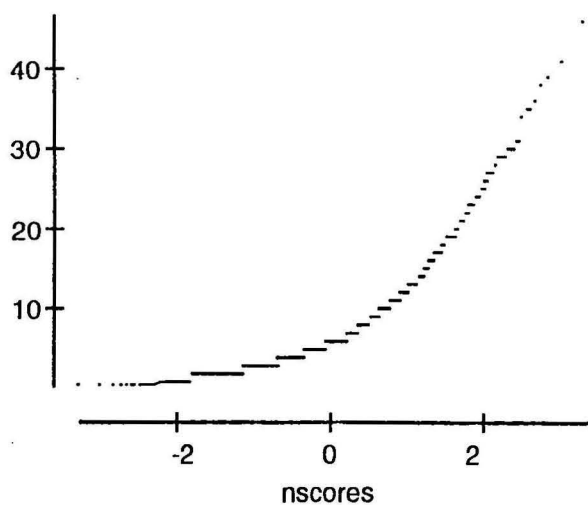
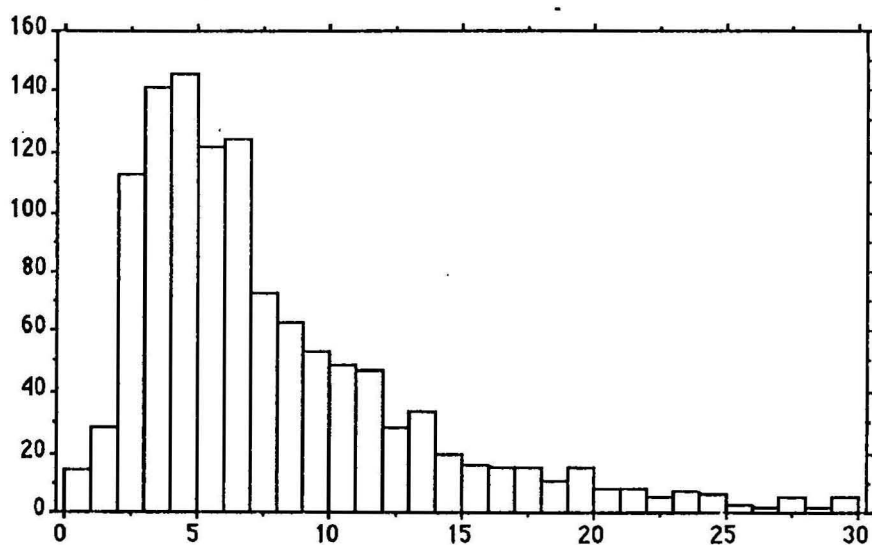


**Sb\***

# X1 : Sc ppm

Mean:	Std. Dev.:	Std. Error:	Variance:	Coef. Var.:	Count:
7.606	6.141	.178	37.712	80.736	1191
Minimum:	Maximum:	Range:	Sum:	Sum of Sqr.:	# Missing:
.5	46	45.5	9059	113781.5	0
t 95%:	95% Lower:	95% Upper:	# < 10th %:	10th %:	25th %:
.349	7.257	7.955	42	2	4
50th %:	75th %:	90th %:	# > 90th %:	Mode:	Geo. Mean:
6	10	16	105	4	5.732
Har. Mean:	Kurtosis:	Skewness:			
4.14	5.246	1.99			

Detection limit is 1.0ppm - a value of 0.5ppm has been used in calculations and table

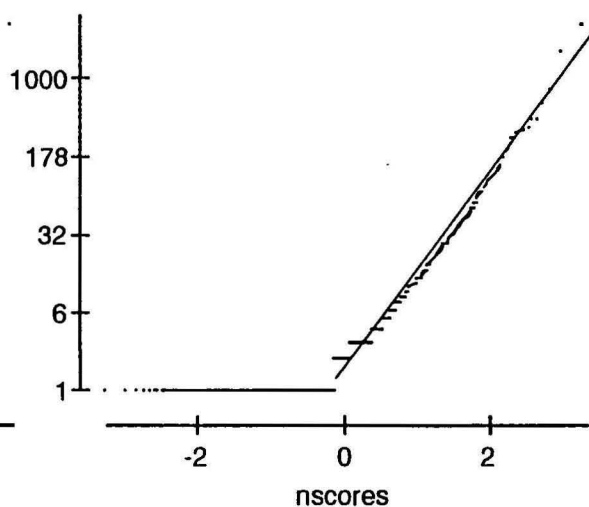
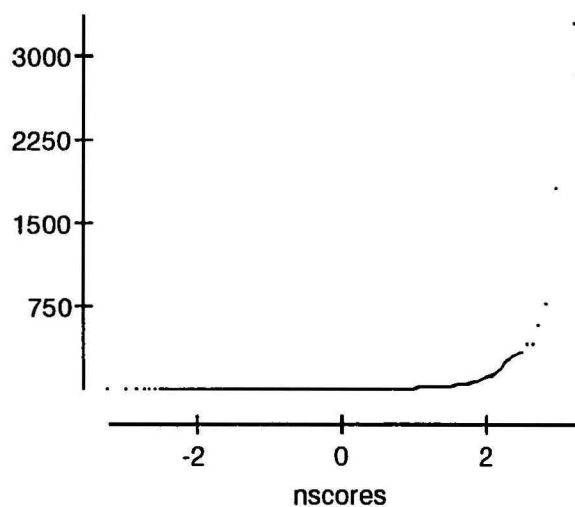
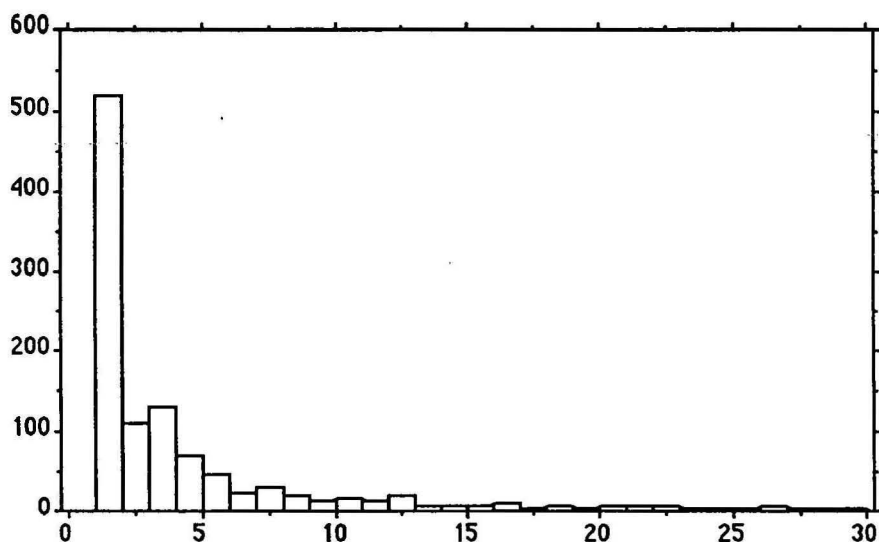


Sc

# X1 : Sn ppm

Mean:	Std. Dev.:	Std. Error:	Variance:	Coef. Var.:	Count:
16.369	117.521	3.405	13811.157	717.965	1191
Minimum:	Maximum:	Range:	Sum:	Sum of Sqr.:	# Missing:
1	3299	3298	19495	16754383	0
† 95%:	95% Lower:	95% Upper:	* < 10th %:	10th %:	25th %:
6.682	9.687	23.05	0	1	1
50th %:	75th %:	90th %:	* > 90th %:	Mode:	Geo. Mean:
2	6	22	114	1	3.085
Har. Mean:	Kurtosis:	Skewness:			
1.787	558.555	21.885			

Detection limit is 2.0ppm - a value of 1.0ppm has been used in calculations and table

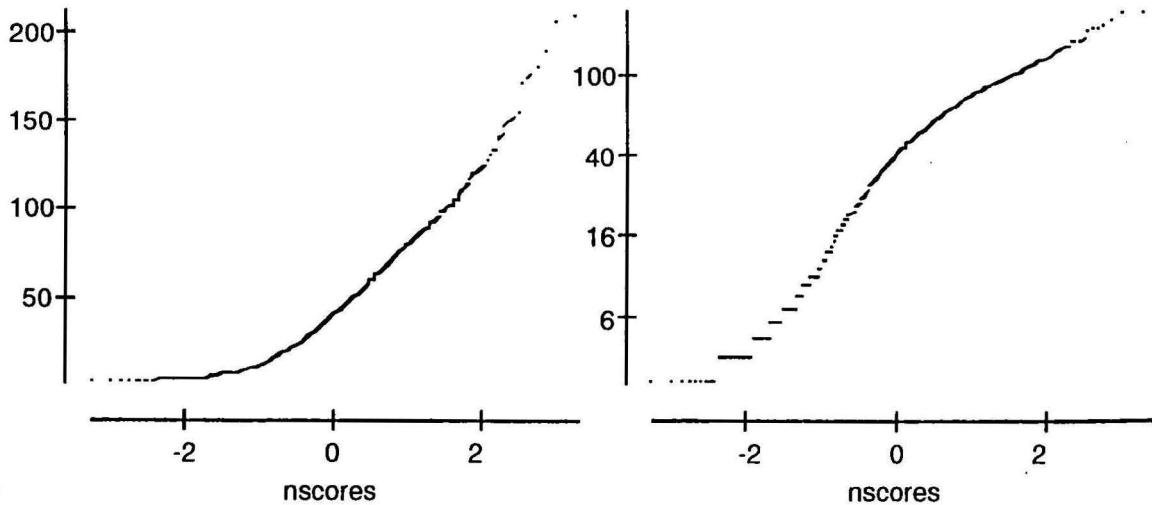
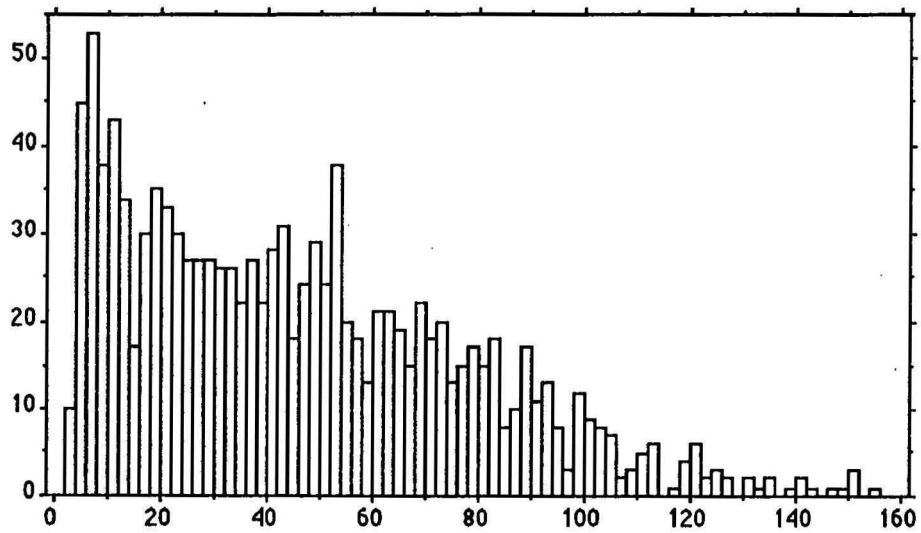


Sn



# X1 : Sr ppm

Mean:	Std. Dev.:	Std. Error:	Variance:	Coef. Var.:	Count:
46.374	33.348	.966	1112.112	71.912	1191
Minimum:	Maximum:	Range:	Sum:	Sum of Sqr.:	# Missing:
3	209	206	55231	3884675	0
† 95%:	95% Lower:	95% Upper:	# < 10th %:	10th %:	25th %:
1.896	44.478	48.27	108	8	19
50th %:	75th %:	90th %:	# > 90th %:	Mode:	Geo. Mean:
41	68	91	116	7	33.397
Har. Mean:	Kurtosis:	Skewness:			
20.887	1.307	.997			

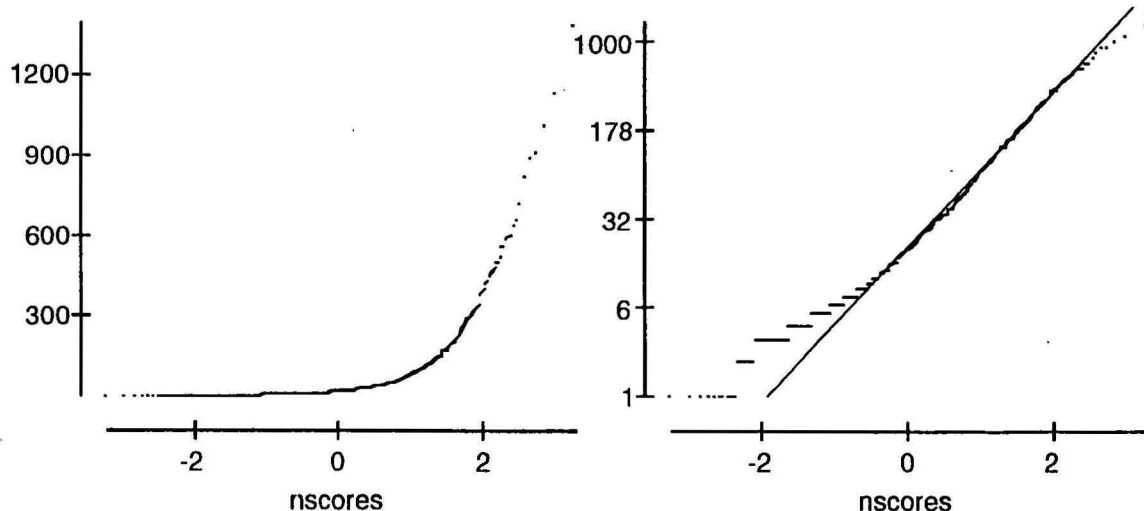
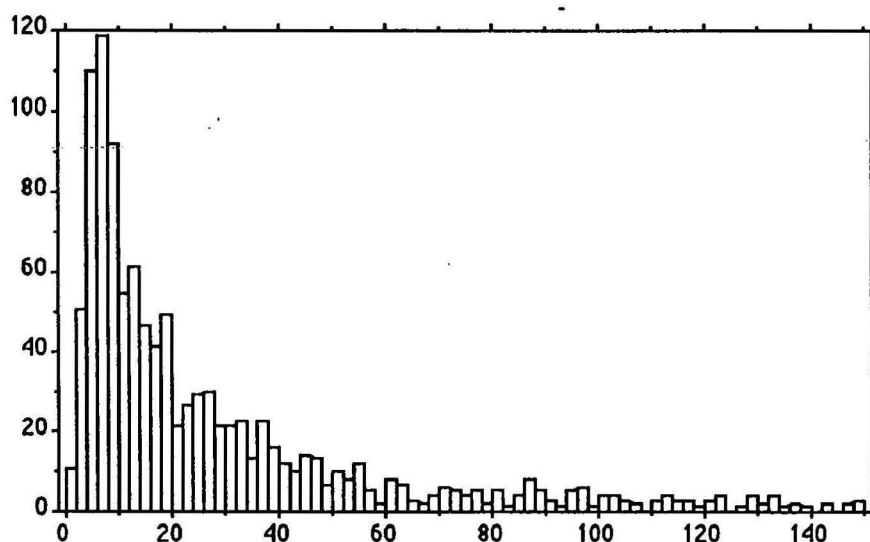


Sr

# **X<sub>1</sub> : Th ppm**

Mean:	Std. Dev.:	Std. Error:	Variance:	Coef. Var.:	Count:
52.887	111.021	3.217	12325.695	209.919	1191
Minimum:	Maximum:	Range:	Sum:	Sum of Sqr.:	# Missing:
1	1381	1380	62989	17998907	0
t 95%:	95% Lower:	95% Upper:	# < 10th %:	10th %:	25th %:
6.312	46.575	59.2	111	5	8
50th %:	75th %:	90th %:	# > 90th %:	Mode:	Geo. Mean:
18	45	124.2	119	7	20.487
Har. Mean:	Kurtosis:	Skewness:			
10.426	41.379	5.509			

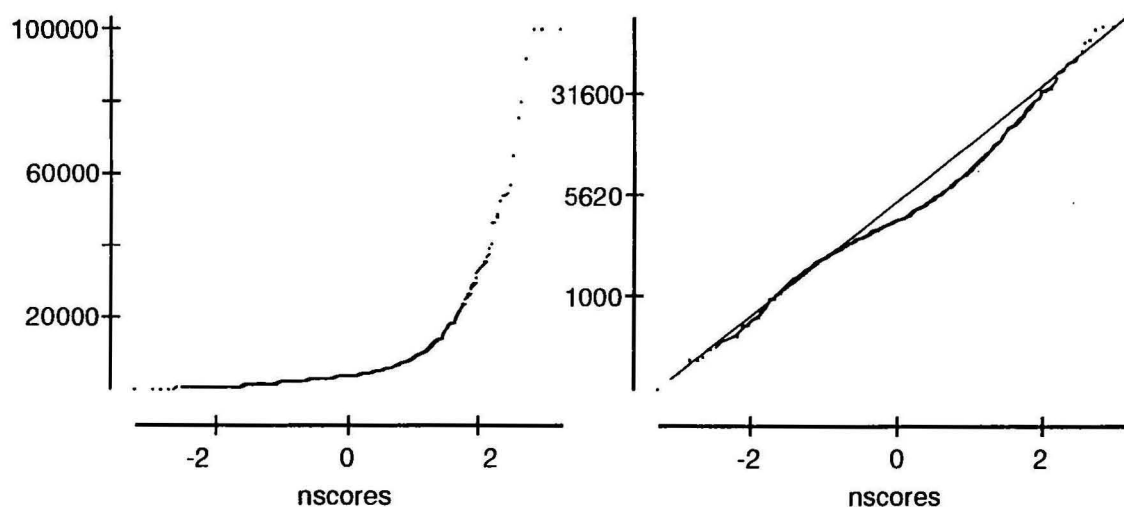
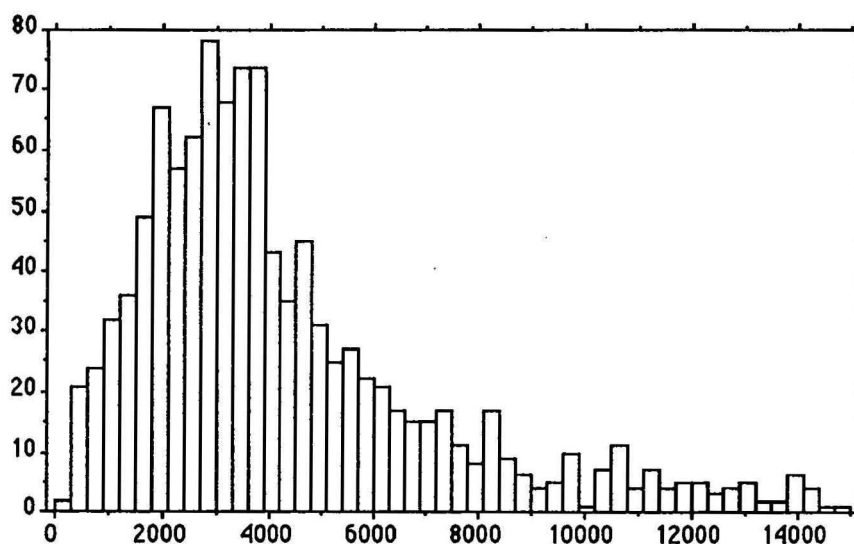
Detection limit is 2.0ppm - a value of 1.0ppm has been used in calculations and table



Th

# X1: Ti ppm

Mean:	Std. Dev.:	Std. Error:	Variance:	Coef. Var.:	Count:
6353.672	9399.411	272.361	88348935.92	147.937	1191
Minimum:	Maximum:	Range:	Sum:	Sum of Sqr.:	# Missing:
208	99999	99791	7567223	1.532E11	0
† 95%:	95% Lower:	95% Upper:	# < 10th %:	10th %:	25th %:
534.413	5819.258	6888.085	119	1527.4	2455
50th %:	75th %:	90th %:	# > 90th %:	Mode:	Geo. Mean:
3704	6314	12354	119	2733	4029.432
Har. Mean:	Kurtosis:	Skewness:			
2793.109	40.259	5.473			

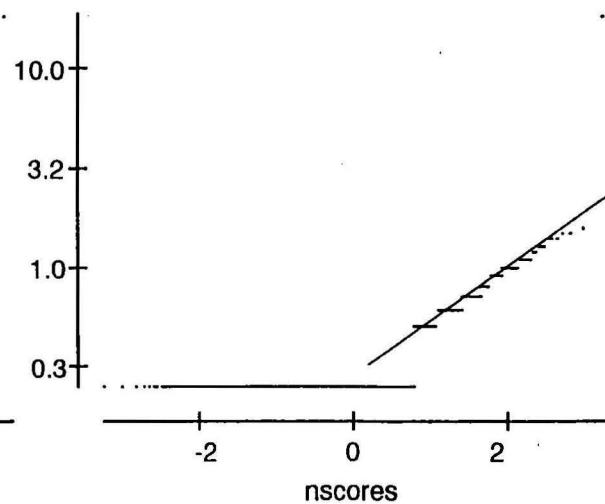
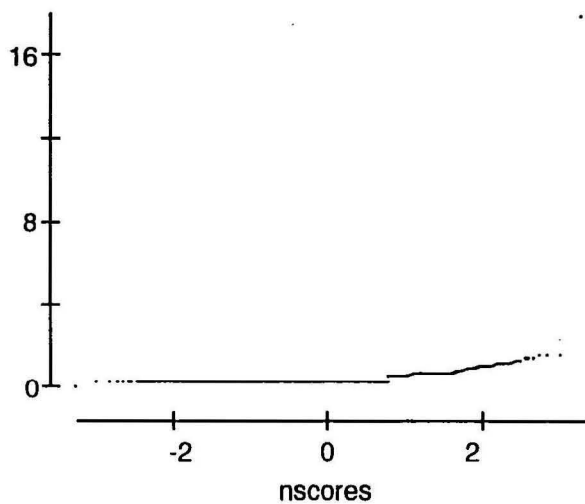
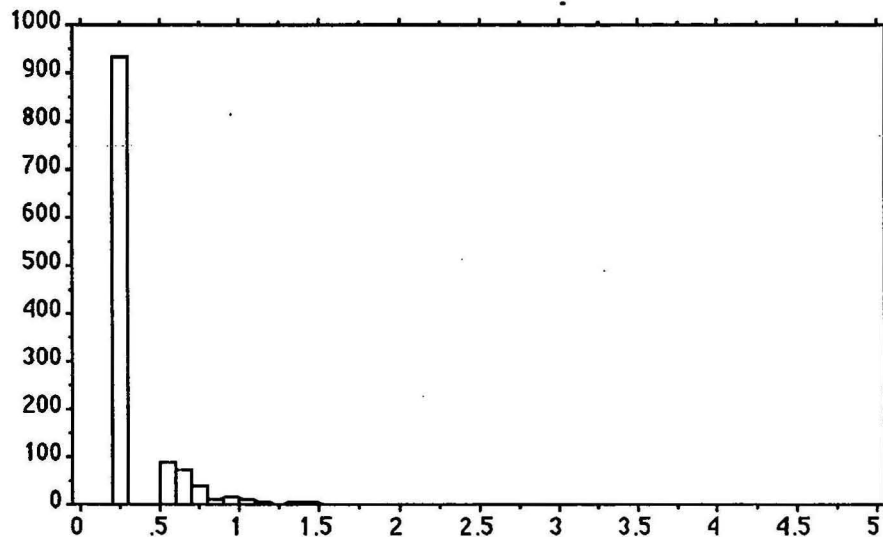


Ti

# **X1 : TI\* ppm**

Mean:	Std. Dev.:	Std. Error:	Variance:	Coef. Var.:	Count:
.354	.544	.016	.296	153.543	1190
Minimum:	Maximum:	Range:	Sum:	Sum of Sqr.:	# Missing:
.25	17.8	17.55	421.7	501.45	0
† 95%:	95% Lower:	95% Upper:	# < 10th %:	10th %:	25th %:
.031	.323	.385	0	.25	.25
50th %:	75th %:	90th %:	# > 90th %:	Mode:	Geo. Mean:
.25	.25	.6	94	.25	.307
Har. Mean:	Kurtosis:	Skewness:			
.287	886.754	27.854			

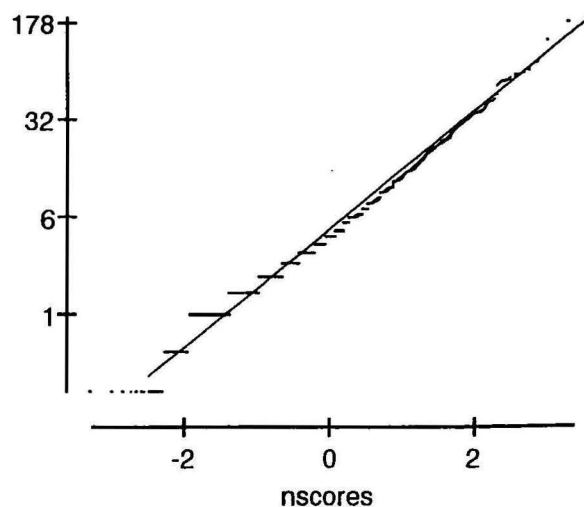
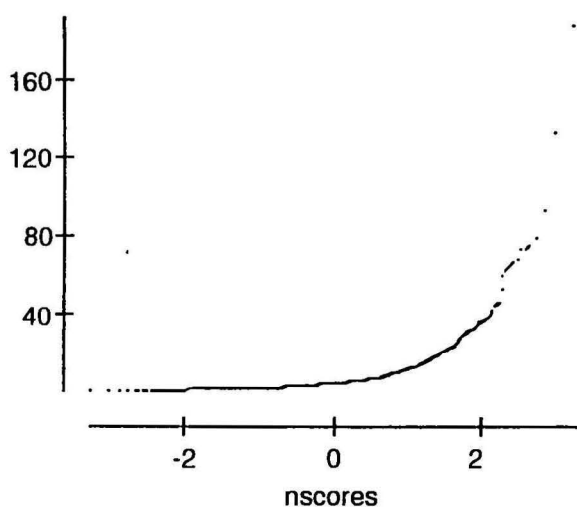
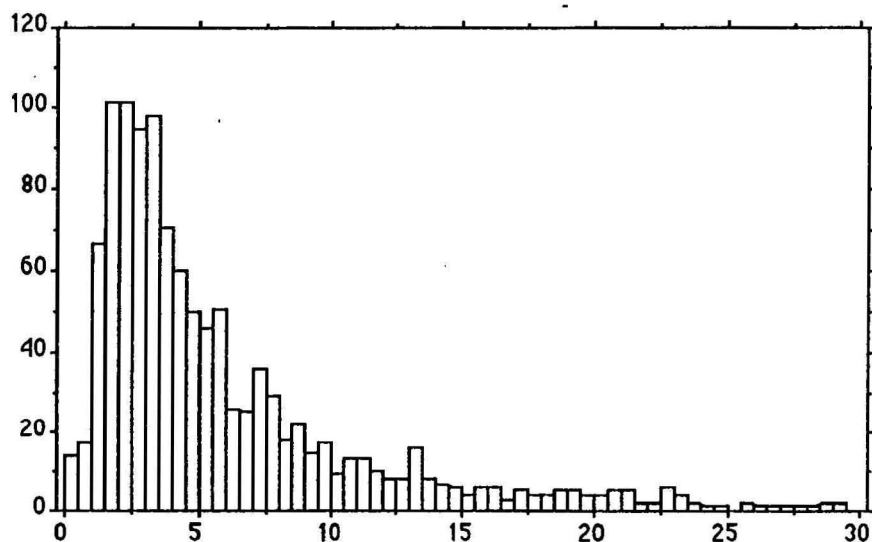
Detection limit is 0.50ppm - a value of 0.25ppm has been used in calculations and table



# **X<sub>1</sub> : U ppm**

Mean:	Std. Dev.:	Std. Error:	Variance:	Coef. Var.:	Count:
7.407	11.426	.331	130.564	154.27	1191
Minimum:	Maximum:	Range:	Sum:	Sum of Sqr.:	# Missing:
.25	187.5	187.25	8821.5	220710.375	0
† 95%:	95% Lower:	95% Upper:	# < 10th %:	10th %:	25th %:
.65	6.757	8.056	98	1.5	2
50th %:	75th %:	90th %:	# > 90th %:	Mode:	Geo. Mean:
4	8	16	118	•	4.312
Har. Mean:	Kurtosis:	Skewness:			
2.648	72.045	6.588			

Detection limit is 0.50ppm - a value of 0.25ppm has been used in calculations and table

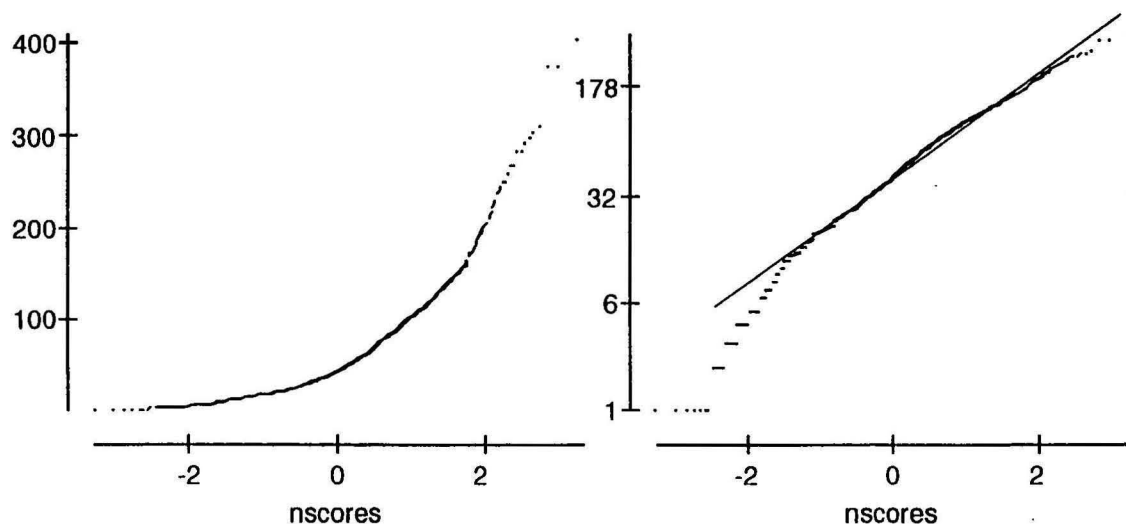
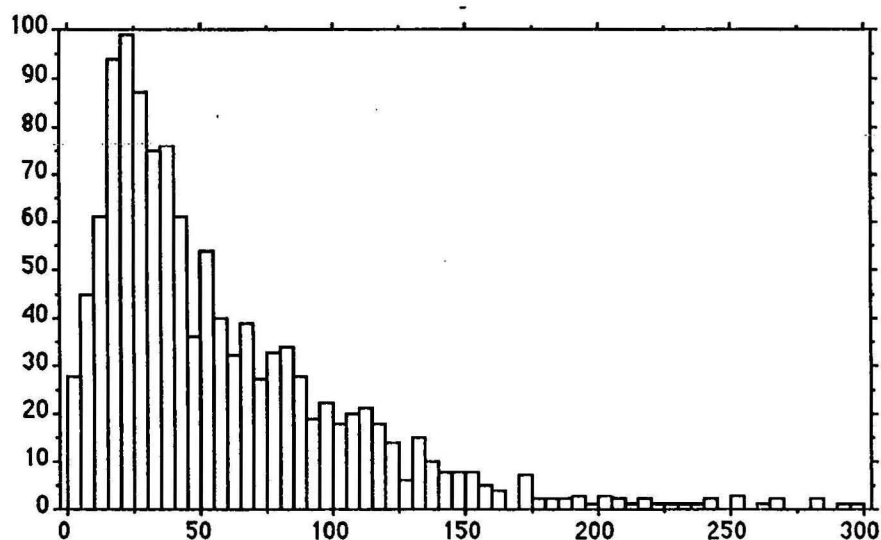




# X<sub>1</sub> : V ppm

Mean:	Std. Dev.:	Std. Error:	Variance:	Coef. Var.:	Count:
58.622	51.582	1.495	2660.696	87.99	1191
Minimum:	Maximum:	Range:	Sum:	Sum of Sqr.:	# Missing:
1	403	402	69819	7259169	0
† 95%:	95% Lower:	95% Upper:	# < 10th %:	10th %:	25th %:
2.933	55.689	61.555	107	13	23
50th %:	75th %:	90th %:	# > 90th %:	Mode:	Geo. Mean:
42	81	121	116	22	40.452
Har. Mean:	Kurtosis:	Skewness:			
22.79	6.676	2.097			

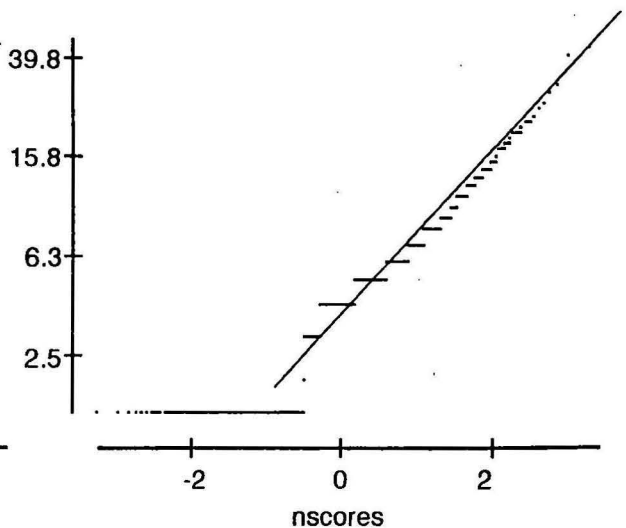
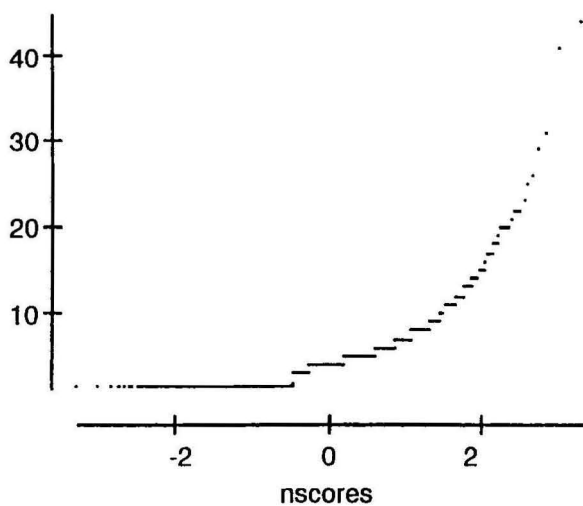
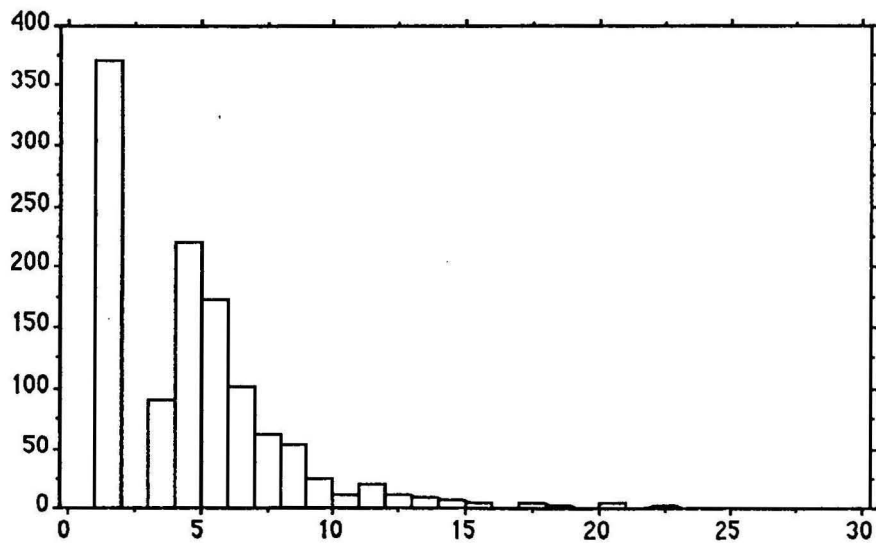
Detection limit is 2.0ppm - a value of 1.0ppm has been used in calculations and table



# **X<sub>1</sub> : V ppm**

Mean:	Std. Dev.:	Std. Error:	Variance:	Coef. Var.:	Count:
4.72	3.927	.114	15.421	83.207	1191
Minimum:	Maximum:	Range:	Sum:	Sum of Sqr.:	# Missing:
1.5	44	42.5	5621	44880	0
t 95%:	95% Lower:	95% Upper:	# < 10th %:	10th %:	25th %:
.223	4.496	4.943	0	1.5	1.5
50th %:	75th %:	90th %:	# > 90th %:	Mode:	Geo. Mean:
4	6	8	115	1.5	3.658
Har. Mean:	Kurtosis:	Skewness:			
2.9	20.082	3.318			

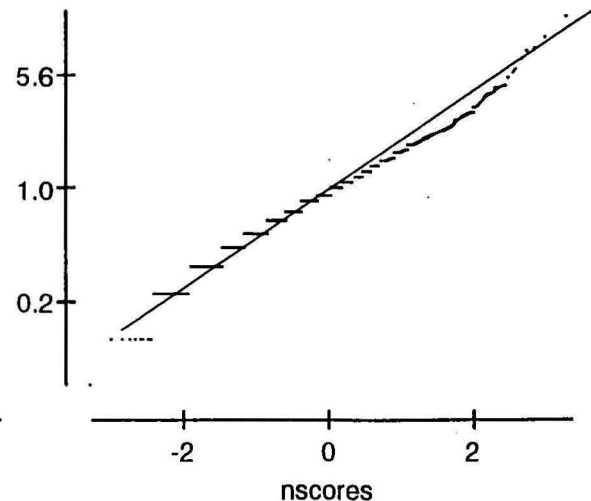
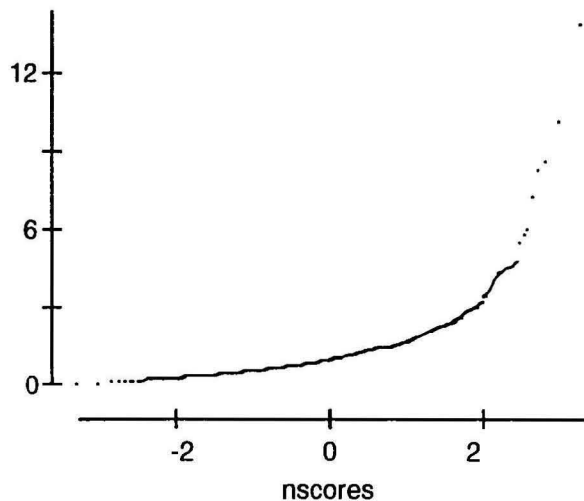
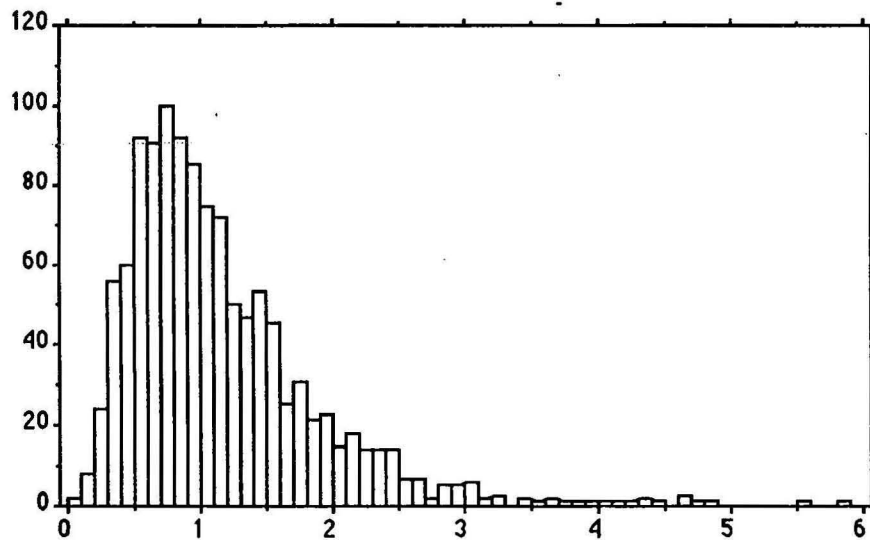
Detection limit is 3.0ppm - a value of 1.5ppm has been used in calculations and table



# **X1: V<sup>±</sup> ppm**

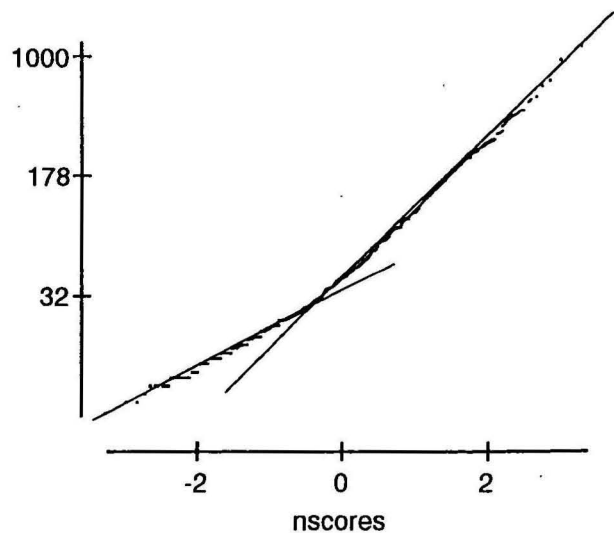
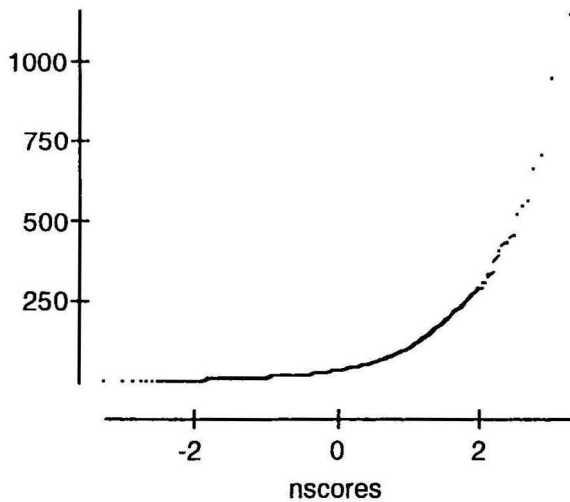
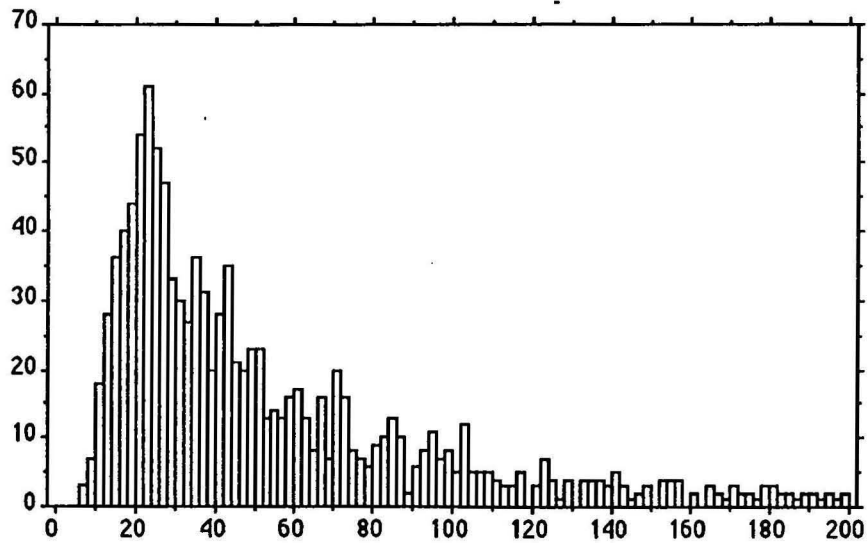
Mean:	Std. Dev.:	Std. Error:	Variance:	Coef. Var.:	Count:
1.15	.944	.027	.891	82.032	1190
Minimum:	Maximum:	Range:	Sum:	Sum of Sqr.:	# Missing:
.05	13.9	13.85	1369.05	2634.022	0
t 95%:	95% Lower:	95% Upper:	# < 10th %:	10th %:	25th %:
.054	1.097	1.204	89	.4	.6
50th %:	75th %:	90th %:	# > 90th %:	Mode:	Geo. Mean:
.9	1.4	2.1	106	.7	.921
Har. Mean:	Kurtosis:	Skewness:			
.725	43.024	4.745			

Detection limit is 0.10ppm - a value of 0.05ppm has been used in calculations and table



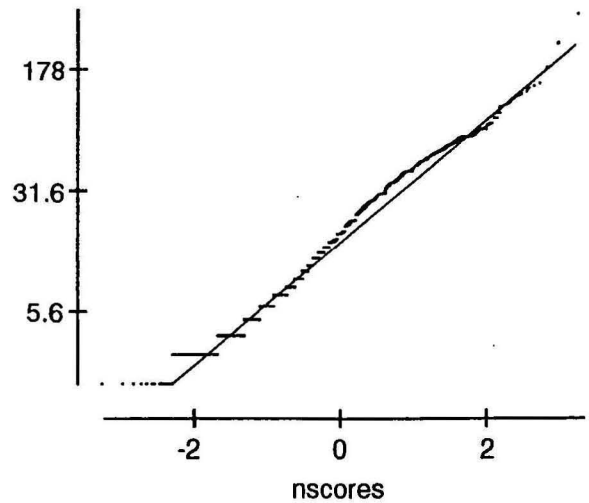
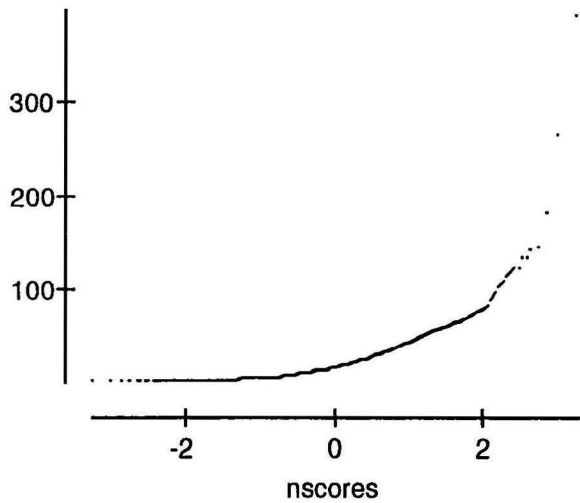
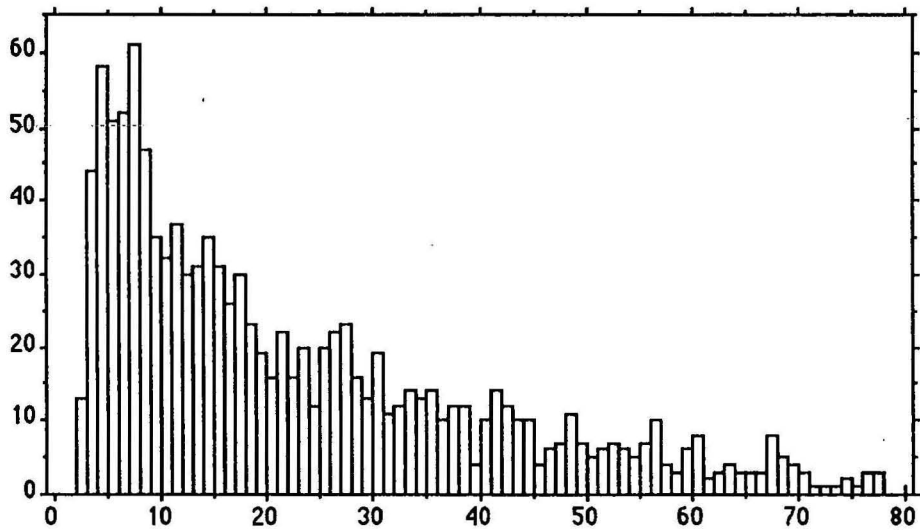
# X1 : Y ppm

Mean:	Std. Dev.:	Std. Error:	Variance:	Coef. Var.:	Count:
69.008	85.805	2.486	7362.513	124.342	1191
Minimum:	Maximum:	Range:	Sum:	Sum of Sqr.:	# Missing:
6	1148	1142	82188	14432984	0
† 95%:	95% Lower:	95% Upper:	# < 10th %:	10th %:	25th %:
4.879	64.129	73.886	114	17	24
50th %:	75th %:	90th %:	# > 90th %:	Mode:	Geo. Mean:
42	80.75	152.4	119	22	45.656
Har. Mean:	Kurtosis:	Skewness:			
33.52	38.108	4.781			



# X1 : Zn ppm

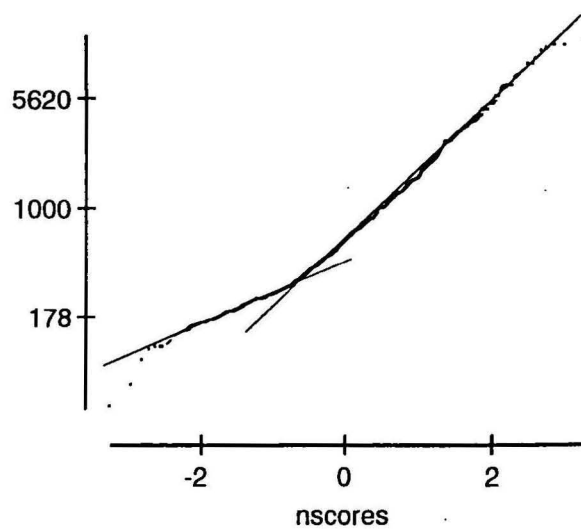
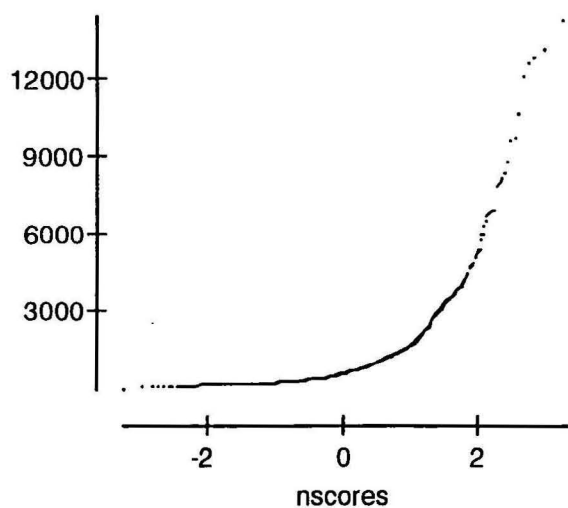
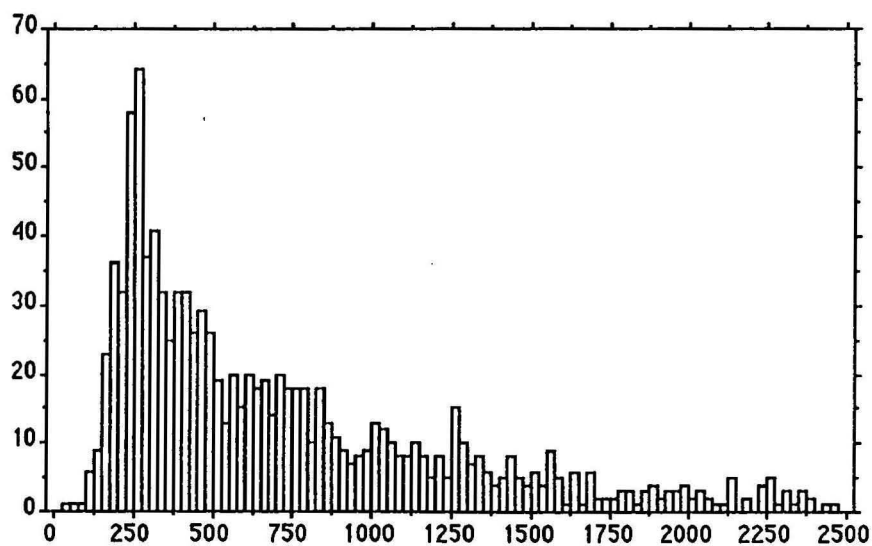
Mean:	Std. Dev.:	Std. Error:	Variance:	Coef. Var.:	Count:
24.527	25.233	.731	636.72	102.879	1191
Minimum:	Maximum:	Range:	Sum:	Sum of Sqr.:	# Missing:
2	392	390	29212	1474188	0
† 95%:	95% Lower:	95% Upper:	# < 10th %:	10th %:	25th %:
1.435	23.093	25.962	115	5	8
50th %:	75th %:	90th %:	# > 90th %:	Mode:	Geo. Mean:
17	34	54	115	7	16.388
Har. Mean:	Kurtosis:	Skewness:			
10.825	46.797	4.56			



Zn

# **X1 : Zr ppm**

Mean:	Std. Dev.:	Std. Error:	Variance:	Coef. Var.:	Count:
1098.062	1488.067	43.119	2214344.361	135.518	1191
Minimum:	Maximum:	Range:	Sum:	Sum of Sqr.:	# Missing:
44	14277	14233	1307792	4071106662	0
t 95%:	95% Lower:	95% Upper:	# < 10th %:	10th %:	25th %:
84.606	1013.457	1182.668	119	229.6	317.25
50th %:	75th %:	90th %:	# > 90th %:	Mode:	Geo. Mean:
622	1240.75	2408.4	119	192	672.08
Har. Mean:	Kurtosis:	Skewness:			
467.779	23.185	4.118			



**Zr**



# Appendix C

**Table C1.** Pearson product moment correlation coefficients for RAW DATA and LOG-TRANSFORMED DATA (N=1191).

	Ag*	As	Au#	Ba	Be*	Bi	Bi*	Cd*	Ce	Cr	Cu	Fe	Ga	Ge	Hf	La	Mn	Mo	Mo*	Nb	Nd	Ni
Ag*		0.20	0.02	0.03	0.03	0.18	0.06	0.04	0.14	0.05	0.08	0.12	0.08	-0.01	0.23	0.13	0.12	0.01	0.08	0.06	0.13	0.09
As	0.17		0.25	-0.02	0.26	0.15	0.40	0.10	-0.05	0.21	0.32	0.39	0.27	0.02	0.09	-0.06	0.22	0.07	0.23	-0.01	-0.06	0.33
Au#	0.08	0.40		0.04	0.09	0.10	0.06	0.13	0.04	0.07	0.45	0.35	0.23	-0.02	0.02	0.04	0.24	0.12	0.03	0.04	0.04	0.38
Ba	0.05	-0.02	0.15		0.40	0.06	-0.07	-0.01	0.13	-0.20	0.03	0.07	<b>0.52</b>	0.03	0.02	0.13	0.21	-0.05	0.12	0.05	0.13	0.07
Be*	0.07	0.26	0.30	<b>0.65</b>		0.04	0.30	0.01	0.05	-0.05	0.08	0.16	0.43	0.05	-0.01	0.04	0.18	-0.01	0.12	0.03	0.05	0.13
Bi	0.18	0.16	0.15	0.07	0.07		0.04	0.13	<b>0.58</b>	0.14	0.20	0.35	0.13	-0.02	<b>0.66</b>	<b>0.58</b>	0.45	0.08	0.12	0.42	<b>0.58</b>	0.22
Bi*	0.04	0.25	0.14	-0.07	0.35	-0.08		0.05	0.01	-0.04	0.05	0.04	0.05	0.00	-0.08	0.02	0.12	-0.02	0.06	0.26	0.01	-0.06
Cd*	0.10	0.28	0.32	0.04	0.11	0.21	0.04		0.09	0.06	0.29	0.29	0.29	-0.02	0.09	0.09	0.22	0.01	0.15	0.19	0.09	0.26
Ce	0.09	-0.11	0.15	0.44	0.34	0.42	-0.03	0.18		0.10	0.10	0.36	0.22	-0.02	<b>0.72</b>	<b>1.00</b>	<b>0.56</b>	-0.02	0.08	<b>0.64</b>	<b>1.00</b>	0.17
Cr	0.08	0.49	0.27	-0.17	0.08	0.19	0.04	0.19	0.16		0.28	0.38	0.08	0.01	0.23	0.09	0.21	0.18	0.10	0.19	0.10	0.41
Cu	0.14	<b>0.58</b>	<b>0.52</b>	0.04	0.28	0.23	0.16	0.39	0.21	<b>0.68</b>		<b>0.82</b>	<b>0.51</b>	0.00	0.06	0.10	<b>0.57</b>	0.15	0.10	0.17	0.10	<b>0.87</b>
Fe	0.14	<b>0.62</b>	0.48	0.16	0.41	0.29	0.12	0.35	0.34	<b>0.71</b>	<b>0.88</b>		<b>0.64</b>	0.02	0.32	0.35	<b>0.79</b>	0.09	0.18	0.45	0.36	<b>0.86</b>
Ga	0.09	0.25	0.36	<b>0.71</b>	<b>0.70</b>	0.09	0.05	0.23	0.39	0.16	0.46	<b>0.57</b>		0.03	0.11	0.22	<b>0.53</b>	-0.02	0.20	0.23	0.22	<b>0.60</b>
Ge	-0.02	0.14	-0.02	0.03	0.16	-0.09	0.14	-0.03	-0.15	0.01	-0.02	0.00	0.05		-0.01	-0.02	0.01	-0.01	0.01	0.00	-0.02	0.01
Hf	0.15	0.18	0.05	-0.07	-0.07	0.46	-0.13	0.15	<b>0.55</b>	0.40	0.25	0.35	0.00	-0.10		<b>0.71</b>	0.46	0.08	0.13	<b>0.51</b>	<b>0.72</b>	0.13
La	0.08	-0.11	0.15	0.45	0.35	0.41	-0.02	0.17	<b>1.00</b>	0.15	0.21	0.34	0.41	-0.15	<b>0.52</b>		<b>0.56</b>	-0.02	0.07	<b>0.64</b>	<b>1.00</b>	0.17
Mn	0.10	0.37	0.43	<b>0.52</b>	<b>0.62</b>	0.28	0.17	0.28	<b>0.52</b>	0.40	<b>0.63</b>	<b>0.74</b>	<b>0.67</b>	-0.02	0.15	<b>0.53</b>		0.04	0.13	<b>0.63</b>	<b>0.57</b>	<b>0.63</b>
Mo	0.03	0.09	0.09	-0.04	0.00	0.10	-0.01	0.02	-0.03	0.11	0.08	0.09	-0.03	-0.06	0.02	-0.04	0.04		-0.01	-0.01	-0.02	0.10
Mo*	0.12	0.31	0.15	0.20	0.27	0.15	-0.03	0.22	0.09	0.27	0.28	0.35	0.34	0.09	0.10	0.09	0.27	0.01		0.03	0.08	0.17
Nb	0.09	0.15	0.16	0.05	0.13	0.38	0.19	0.28	<b>0.69</b>	0.41	0.43	0.48	0.17	-0.11	<b>0.67</b>	<b>0.67</b>	0.40	-0.01	0.06		<b>0.64</b>	0.20
Nd	0.08	-0.11	0.15	0.44	0.34	0.42	-0.04	0.18	<b>1.00</b>	0.17	0.22	0.35	0.40	-0.15	<b>0.55</b>	<b>0.99</b>	<b>0.53</b>	-0.03	0.09	<b>0.68</b>		0.17
Ni	0.10	<b>0.54</b>	0.47	0.17	0.41	0.20	0.05	0.32	0.22	<b>0.73</b>	<b>0.87</b>	<b>0.88</b>	<b>0.57</b>	0.02	0.16	0.22	<b>0.72</b>	0.07	0.38	0.33	0.23	
P*	0.08	-0.08	0.20	<b>0.55</b>	0.42	0.35	-0.14	0.16	<b>0.83</b>	0.15	0.24	0.38	<b>0.54</b>	-0.12	0.33	<b>0.83</b>	<b>0.55</b>	0.02	0.21	0.44	<b>0.83</b>	0.31
Pb	0.06	-0.13	0.10	<b>0.75</b>	<b>0.57</b>	0.20	0.21	0.06	<b>0.64</b>	-0.25	-0.05	0.06	<b>0.54</b>	0.01	0.07	<b>0.64</b>	0.43	-0.05	0.06	0.28	<b>0.63</b>	-0.02
Pd#	0.13	0.24	0.39	0.14	0.17	0.13	-0.01	0.17	0.08	0.25	0.43	0.39	0.27	-0.03	-0.06	0.08	0.38	0.10	0.16	0.05	0.08	0.45
Pt#	0.05	0.16	0.37	-0.02	0.04	0.00	-0.02	0.07	-0.11	0.15	0.23	0.20	0.11	-0.07	-0.14	-0.11	0.14	0.16	0.05	-0.08	-0.11	0.23
Rb	0.07	0.13	0.21	<b>0.84</b>	<b>0.77</b>	0.00	0.16	0.01	0.29	-0.19	0.03	0.15	<b>0.68</b>	-0.12	-0.25	0.32	<b>0.53</b>	-0.02	0.24	-0.07	0.29	0.20
Sb*	0.14	0.45	0.10	0.02	0.01	-0.08	0.08	0.08	-0.34	0.00	0.05	0.01	0.03	0.11	-0.15	-0.34	-0.10	0.06	0.25	-0.27	-0.35	0.03
Sc	0.15	<b>0.54</b>	0.47	0.15	0.33	0.33	0.05	0.40	0.35	<b>0.68</b>	<b>0.86</b>	<b>0.91</b>	<b>0.54</b>	-0.04	0.39	0.35	<b>0.68</b>	0.09	0.32	<b>0.51</b>	0.36	<b>0.83</b>
Se	-0.01	-0.09	0.00	0.03	0.03	0.02	0.02	-0.04	0.07	-0.02	0.00	0.00	0.01	-0.01	0.05	0.06	0.02	-0.01	-0.01	0.05	0.07	-0.01
Sn	0.08	0.14	-0.13	-0.29	-0.26	-0.02	0.16	-0.04	-0.23	0.07	-0.08	-0.08	-0.29	0.02	0.24	-0.25	-0.32	0.09	0.00	0.10	-0.23	-0.19
Sr	0.05	0.09	0.26	<b>0.89</b>	<b>0.64</b>	0.10	-0.17	0.07	0.37	-0.02	0.16	0.30	<b>0.73</b>	0.02	-0.14	0.39	<b>0.60</b>	0.02	0.26	-0.05	0.37	0.34
Ta	0.06	0.00	0.03	0.03	0.11	0.04	0.15	0.08	0.11	0.04	0.07	0.07	0.04	-0.02	0.04	0.11	0.10	-0.02	-0.05	0.23	0.11	0.05
Th	0.09	-0.12	0.13	0.46	0.35	0.39	-0.01	0.18	<b>0.98</b>	0.10	0.17	0.28	0.40	-0.13	<b>0.54</b>	<b>0.98</b>	0.49	-0.06	0.08	<b>0.67</b>	<b>0.97</b>	0.18
Ti	0.09	0.30	0.33	-0.07	0.14	0.35	0.26	0.35	<b>0.57</b>	<b>0.59</b>	<b>0.68</b>	<b>0.70</b>	0.22	-0.09	<b>0.59</b>	<b>0.56</b>	<b>0.53</b>	0.04	0.04	<b>0.86</b>	<b>0.57</b>	<b>0.54</b>
Ti*	0.08	-0.05	-0.06	0.48	0.35	-0.05	0.18	-0.10	-0.01	-0.42	-0.30	-0.26	0.23	0.12	-0.25	0.00	0.04	-0.04	0.12	-0.20	-0.01	-0.26
U	0.08	-0.24	-0.02	0.37	0.26	0.34	0.02	0.03	<b>0.88</b>	-0.01	-0.06	0.06	0.22	-0.13	<b>0.52</b>	<b>0.87</b>	<b>0.28</b>	-0.07	0.04	<b>0.59</b>	<b>0.87</b>	-0.04
V	0.12	<b>0.57</b>	0.43	-0.08	0.17	0.29	0.10	0.34	0.26	<b>0.79</b>	<b>0.87</b>	<b>0.92</b>	0.35	-0.04	0.46	0.25	<b>0.56</b>	0.09	0.26	<b>0.54</b>	0.27	<b>0.80</b>
W	0.10	-0.11	-0.01	0.19	0.15	0.26	0.13	-0.03	<b>0.58</b>	0.01	-0.05	0.02	0.08	-0.08	0.34	<b>0.58</b>	0.15	0.00	-0.01	0.46	<b>0.58</b>	-0.07
W*	0.10	0.28	0.11	0.13	0.26	0.07	0.19	0.06	0.07	0.05	0.08	0.13	0.22	0.07	0.03	0.07	0.11	0.01	0.38	0.04	0.06	0.12
Y	0.07	-0.24	0.04	0.43	0.27	0.34	0.00	0.07	<b>0.89</b>	-0.01	-0.02	0.10	0.26	0.17	0.43	<b>0.89</b>	0.33	-0.02	0.02	<b>0.58</b>	<b>0.89</b>	0.00
Zn	0.13	0.47	0.48	0.37	<b>0.60</b>	0.26	0.28	0.31	0.47	<b>0.55</b>	<b>0.77</b>	<b>0.85</b>	<b>0.65</b>	0.01	0.22	0.48	<b>0.84</b>	0.06	0.26	<b>0.52</b>	0.48	<b>0.78</b>
Zr	0.13	0.09	0.00	-0.09	-0.12	0.43	-0.16	0.12	<b>0.57</b>	0.37	0.17	0.28	-0.06	-0.12	<b>0.96</b>	<b>0.54</b>	0.09	0.01	0.07	<b>0.67</b>	<b>0.56</b>	0.08

Ag\* As Au# Ba Be\* Bi Bi\* Cd\* Ce Cr Cu Fe Ga Ge Hf La Mn Mo Mo\* Nb Nd Ni

LOG-TRANSFORMED DATA

# RAW DATA

P*	Pb	Pd#	Pt#	Rb	Sb*	Sc	Se	Sn	Sr	Ta	Th	Ti	Ti*	U	V	W	W*	Y	Zn	Zr	
0.12	0.05	0.10	0.02	0.06	0.19	0.14	-0.01	0.02	0.03	0.04	0.14	0.03	0.03	0.09	0.09	0.09	0.07	0.06	0.07	0.22	Ag*
-0.05	-0.01	0.16	0.12	0.22	<b>0.58</b>	0.31	-0.06	-0.02	0.03	0.03	-0.05	0.00	0.07	-0.10	0.32	-0.04	0.31	-0.14	0.24	0.06	As
0.10	-0.01	0.34	0.39	0.05	0.20	0.37	0.04	-0.03	0.21	0.00	0.05	0.07	-0.03	0.00	0.34	0.00	0.08	0.02	0.22	0.00	Au#
0.24	<b>0.68</b>	0.06	-0.05	<b>0.73</b>	0.08	0.09	0.03	-0.04	<b>0.79</b>	-0.01	0.16	-0.02	0.20	0.15	-0.03	0.17	0.10	0.26	0.12	-0.01	Ba
0.09	0.38	0.03	0.00	<b>0.52</b>	0.15	0.11	0.03	0.00	0.34	0.04	0.06	0.02	0.13	0.10	0.06	0.11	0.21	0.09	0.22	-0.04	Be*
<b>0.58</b>	0.22	0.09	-0.01	-0.04	0.05	0.43	0.01	0.04	0.12	0.00	<b>0.61</b>	0.28	-0.02	0.43	0.34	0.28	0.04	0.35	0.22	<b>0.64</b>	Bi
-0.09	0.27	-0.05	-0.03	0.18	0.19	0.01	0.04	0.02	-0.19	0.08	-0.02	0.33	0.09	0.09	0.06	0.18	0.20	0.08	0.33	-0.09	Bi*
0.11	-0.01	0.15	0.07	-0.07	0.08	0.32	-0.03	-0.02	0.08	0.00	0.11	0.15	-0.04	0.02	0.29	-0.04	0.05	0.01	0.19	0.09	Cd*
<b>0.92</b>	<b>0.51</b>	0.04	-0.05	-0.04	-0.14	0.41	0.04	-0.03	0.14	0.00	<b>0.99</b>	0.49	-0.05	<b>0.86</b>	0.34	<b>0.61</b>	0.02	<b>0.77</b>	0.34	<b>0.69</b>	Ce
0.11	-0.19	0.13	0.14	-0.25	0.02	0.36	-0.02	0.03	-0.04	0.03	0.09	0.18	-0.10	0.03	0.42	0.04	0.01	0.01	0.24	0.29	Cr
0.19	-0.08	<b>0.61</b>	0.42	-0.05	0.29	<b>0.83</b>	0.00	-0.04	0.36	0.02	0.11	0.24	-0.07	-0.01	<b>0.83</b>	-0.08	0.02	-0.02	<b>0.56</b>	0.04	Cu
0.40	0.03	0.46	0.27	-0.07	0.18	<b>0.94</b>	0.00	-0.01	0.34	0.03	0.37	0.49	-0.09	0.16	<b>0.96</b>	0.02	0.05	0.11	<b>0.72</b>	0.29	Fe
0.34	0.35	0.28	0.11	0.42	0.17	<b>0.62</b>	0.03	-0.05	<b>0.61</b>	0.03	0.25	0.20	0.06	0.13	<b>0.54</b>	0.05	0.19	0.12	0.49	0.08	Ga
-0.02	0.01	-0.01	-0.01	0.02	-0.01	0.01	0.00	-0.01	0.02	0.00	-0.01	0.00	0.00	-0.03	0.01	-0.01	-0.01	-0.03	0.02	-0.02	Ge
<b>0.68</b>	0.19	0.00	-0.06	-0.12	0.01	0.41	0.04	0.07	0.04	0.00	<b>0.74</b>	0.33	-0.04	<b>0.50</b>	0.31	0.36	0.05	0.41	0.17	<b>0.97</b>	Hf
<b>0.91</b>	<b>0.51</b>	0.04	-0.05	-0.05	-0.14	0.41	0.04	-0.03	0.14	0.01	<b>0.99</b>	<b>0.50</b>	-0.05	<b>0.86</b>	0.34	<b>0.61</b>	0.02	<b>0.77</b>	0.35	<b>0.68</b>	La
<b>0.55</b>	0.28	0.33	0.15	0.05	0.04	<b>0.80</b>	0.01	-0.07	0.36	0.04	<b>0.58</b>	<b>0.64</b>	-0.04	0.34	<b>0.75</b>	0.20	0.00	0.30	<b>0.69</b>	0.41	Mn
-0.01	-0.04	0.11	0.14	-0.04	0.03	0.11	-0.01	0.05	0.03	-0.01	-0.03	0.00	-0.01	-0.02	0.11	0.01	0.00	-0.02	0.04	0.09	Mo
0.13	0.06	0.08	0.00	0.15	0.19	0.17	-0.01	0.03	0.12	0.00	0.09	-0.03	0.03	0.05	0.13	0.02	0.19	0.03	0.08	0.12	Mo*
<b>0.56</b>	0.35	0.01	-0.06	-0.14	-0.16	0.48	0.06	0.03	-0.03	0.05	<b>0.64</b>	<b>0.85</b>	-0.05	0.49	0.49	0.42	-0.01	0.47	<b>0.63</b>	<b>0.53</b>	Nb
<b>0.92</b>	<b>0.51</b>	0.04	-0.05	-0.04	-0.14	0.41	0.04	-0.03	0.14	0.01	<b>0.99</b>	<b>0.50</b>	-0.05	<b>0.86</b>	0.34	<b>0.61</b>	0.02	<b>0.77</b>	0.35	<b>0.69</b>	Nd
0.28	-0.10	<b>0.55</b>	0.36	-0.03	0.21	<b>0.85</b>	-0.01	-0.02	0.41	0.02	0.19	0.20	-0.09	0.03	<b>0.82</b>	-0.08	0.05	0.01	<b>0.55</b>	0.10	Ni
	0.46	0.10	-0.02	0.04	-0.09	0.48	0.07	-0.03	0.30	-0.01	<b>0.93</b>	0.34	-0.04	<b>0.77</b>	0.36	<b>0.54</b>	0.06	<b>0.73</b>	0.29	<b>0.68</b>	P*
<b>0.60</b>		-0.06	-0.11	<b>0.61</b>	0.00	0.03	0.07	0.09	0.46	0.02	<b>0.50</b>	0.31	0.19	<b>0.60</b>	-0.01	<b>0.52</b>	0.12	<b>0.61</b>	0.27	0.17	Pb
0.17	-0.01		0.42	0.03	0.18	0.48	-0.02	-0.04	0.31	-0.02	0.05	0.04	-0.01	0.00	0.46	-0.03	0.03	0.02	0.29	-0.01	Pd#
-0.01	-0.12	0.33		-0.03	0.09	0.29	-0.02	-0.02	0.15	-0.01	-0.06	0.00	-0.03	-0.06	0.29	-0.07	-0.03	-0.06	0.14	-0.07	Pt#
0.44	<b>0.70</b>	0.17	0.02		0.28	-0.08	0.01	-0.03	<b>0.55</b>	0.00	-0.02	-0.19	0.32	0.05	-0.19	0.10	0.29	0.09	0.01	-0.17	Rb
-0.19	-0.10	0.10	0.09	0.18		0.18	-0.03	0.02	0.09	0.00	-0.12	-0.14	0.09	-0.09	0.14	-0.01	0.35	-0.11	0.05	-0.01	Sb*
0.38	0.06	0.39	0.21	0.09	0.03		0.01	-0.03	0.37	0.02	0.43	0.46	-0.08	0.19	<b>0.92</b>	0.07	0.06	0.16	<b>0.66</b>	0.38	Sc
0.07	0.08	-0.03	-0.01	0.01	-0.05	0.01		0.16	0.02	-0.01	0.04	0.03	0.00	0.05	0.00	0.09	-0.02	0.05	0.00	0.06	Se
-0.29	-0.15	-0.17	-0.02	-0.29	0.30	-0.05	0.01		-0.06	0.01	-0.03	-0.01	0.00	-0.01	0.01	0.05	0.01	0.00	0.01	0.11	Sn
<b>0.58</b>	<b>0.58</b>	0.29	0.10	<b>0.80</b>	0.05	0.26	0.02	-0.36		-0.02	0.17	-0.07	0.10	0.11	0.25	0.08	0.05	0.20	0.20	0.00	Sr
0.03	0.07	-0.02	-0.02	0.02	-0.13	0.07	-0.02	0.06	0.00		0.00	0.05	-0.01	0.00	0.02	0.01	0.04	0.00	0.05	-0.01	Ta
<b>0.81</b>	<b>0.67</b>	0.04	-0.17	0.34	-0.31	0.30	0.06	-0.22	0.37	0.10		0.46	-0.04	<b>0.85</b>	0.34	<b>0.58</b>	0.02	<b>0.76</b>	0.32	<b>0.71</b>	Th
0.36	0.13	0.20	0.05	-0.16	-0.29	<b>0.69</b>	0.04	0.01	-0.07	0.17	<b>0.52</b>		-0.07	0.35	<b>0.57</b>	0.29	-0.07	0.32	<b>0.72</b>	0.32	Ti
0.07	0.49	-0.05	-0.07	<b>0.58</b>	0.24	-0.26	0.00	0.00	0.34	-0.04	0.05	-0.37		-0.01	-0.11	0.02	0.09	-0.01	-0.04	-0.05	Ti*
<b>0.70</b>	<b>0.65</b>	-0.06	-0.21	0.29	-0.26	0.10	0.08	-0.08	0.25	0.08	<b>0.90</b>	0.36	0.15		0.15	<b>0.76</b>	0.05	<b>0.92</b>	0.21	<b>0.52</b>	U
0.25	-0.13	0.36	0.20	-0.15	-0.02	<b>0.87</b>	0.01	0.05	0.06	0.06	0.19	<b>0.78</b>	-0.43	0.01		0.02	-0.01	0.10	<b>0.72</b>	0.30	V
0.43	0.44	-0.03	-0.11	0.17	-0.09	0.06	0.08	0.07	0.10	0.07	<b>0.58</b>	0.27	0.13	<b>0.67</b>	0.00		0.17	<b>0.86</b>	0.15	0.39	W
0.15	0.16	0.06	-0.01	0.27	0.41	0.14	-0.02	0.10	0.14	-0.03	0.08	-0.05	0.22	0.11	0.04	0.21		0.04	0.01	0.04	W*
<b>0.76</b>	<b>0.67</b>	0.02	-0.12	0.32	-0.24	0.14	0.08	-0.10	0.34	0.07	<b>0.89</b>	0.38	0.13	<b>0.93</b>	0.03	<b>0.71</b>	0.11		0.20	0.43	Y
0.48	0.32	0.38	0.16	0.39	-0.11	<b>0.77</b>	0.01	-0.20	0.45	0.14	0.43	<b>0.68</b>	-0.07	0.21	<b>0.72</b>	0.12	0.12	0.26		0.15	Zn
0.35	0.07	-0.09	-0.16	-0.28	-0.16	0.33	0.06	0.28	-0.16	0.05	<b>0.55</b>	<b>0.55</b>	-0.25	<b>0.56</b>	0.40	0.38	0.01	0.48	0.15		Zr

P\* Pb Pd# Pt# Rb Sb\* Sc Se Sn Sr Ta Th Ti Ti\* U V W W\* Y Zn Zr

Table C2. Spearmans rank correlation coefficients (N=1191).

Ag*	As	Au#	Ba	Be*	Bi	Bi*	Cd*	Ce	Cr	Cu	Fe	Ga	Ge	Hf	La	Mn	Mo	Mo*	Nb	Nd	Ni
Ag*	0.18	0.10	0.08	0.09	0.15	0.03	0.10	0.06	0.12	0.16	0.16	0.13	-.02	0.09	0.06	0.13	0.06	0.13	0.10	0.06	0.13
As		0.42	-.06	0.26	0.15	0.25	0.27	-.13	<b>0.50</b>	<b>0.57</b>	<b>0.63</b>	0.29	0.19	0.14	-.14	0.39	0.10	0.33	0.14	-.13	<b>0.54</b>
Au#			0.13	0.32	0.15	0.16	0.33	0.15	0.29	<b>0.53</b>	0.48	0.40	0.02	0.06	0.16	0.44	0.07	0.18	0.18	0.16	0.47
Ba				<b>0.58</b>	0.06	-.09	0.07	<b>0.50</b>	-.14	0.06	0.14	<b>0.66</b>	0.02	-.07	<b>0.51</b>	0.42	-.05	0.21	0.05	<b>0.50</b>	0.15
Be*					0.06	0.40	0.10	0.35	0.08	0.31	0.38	<b>0.63</b>	0.23	-.07	0.36	<b>0.51</b>	-.01	0.29	0.15	0.35	0.38
Bi						-.06	0.18	0.30	0.22	0.24	0.29	0.12	-.11	0.32	0.29	0.28	0.12	0.15	0.32	0.30	0.20
Bi*							0.06	0.05	-.01	0.18	0.13	0.04	0.20	-.08	0.05	0.17	-.02	-.01	0.23	0.04	0.05
Cd*								0.17	0.22	0.40	0.36	0.24	-.02	0.13	0.17	0.32	0.02	0.23	0.28	0.17	0.32
Ce									0.14	0.23	0.29	0.41	-.14	0.46	<b>0.99</b>	0.46	-.05	0.11	<b>0.63</b>	<b>1.00</b>	0.21
Cr										<b>0.66</b>	<b>0.73</b>	0.26	-.02	0.36	0.13	0.48	0.10	0.32	0.35	0.15	<b>0.73</b>
Cu											<b>0.90</b>	<b>0.58</b>	-.03	0.24	0.23	<b>0.73</b>	0.07	0.34	0.43	0.24	<b>0.89</b>
Fe												<b>0.65</b>	0.00	0.32	0.29	<b>0.78</b>	0.09	0.41	0.43	0.30	<b>0.89</b>
Ga													0.06	0.05	0.42	<b>0.67</b>	0.02	0.40	0.21	0.41	<b>0.63</b>
Ge														-.11	-.14	-.04	-.07	0.11	-.11	-.14	0.01
Hf															0.42	0.15	-.04	0.08	<b>0.67</b>	0.45	0.12
La																0.46	-.05	0.11	<b>0.61</b>	<b>0.99</b>	0.21
Mn																	0.07	0.30	0.38	0.46	<b>0.76</b>
Mo																		0.00	-.03	-.05	0.08
Mo*																			0.15	0.11	0.42
Nb																				<b>0.62</b>	0.30
Nd																					0.21
Ni																					
P*																					
Pb																					
Pd#																					
Pt#																					
Rb																					
Sb*																					
Sc																					
Se																					
Sn																					
Sr																					
Ta																					
Th																					
Ti																					
Tl*																					
U																					
V																					
W																					
W*																					
Y																					
Zn																					
Zr																					
As	Au#	Ba	Be*	Bi	Bi*	Cd*	Ce	Cr	Cu	Fe	Ga	Ge	Hf	La	Mn	Mo	Mo*	Nb	Nd	Ni	

P*	Pb	Pd#	Pt#	Rb	Sb*	Sc	Se	Sn	Sr	Ta	Th	Ti	Ti*	U	V	W	W*	Y	Zn	Zr	
0.07	0.05	0.11	0.08	0.08	0.15	0.17	-0.02	0.08	0.07	0.05	0.06	0.12	0.07	0.07	0.14	0.10	0.10	0.07	0.16	0.08	Ag*
-0.11	-0.16	0.25	0.18	0.10	0.47	<b>0.55</b>	-0.09	0.20	0.05	0.01	-0.15	0.35	-0.08	-0.25	<b>0.58</b>	-0.10	0.30	-0.25	<b>0.50</b>	0.06	As
0.20	0.10	0.35	0.33	0.16	0.10	0.48	-0.01	-0.11	0.24	0.05	0.15	0.39	-0.05	0.00	0.44	-0.02	0.13	0.04	<b>0.50</b>	0.01	Au#
<b>0.59</b>	<b>0.77</b>	0.11	-0.05	<b>0.83</b>	0.02	0.15	0.03	-0.29	<b>0.85</b>	0.02	<b>0.51</b>	-0.06	<b>0.55</b>	0.43	-0.04	0.21	0.14	0.47	0.31	-0.09	Ba
0.38	<b>0.52</b>	0.18	0.02	<b>0.69</b>	0.02	0.32	0.03	-0.22	<b>0.51</b>	0.11	0.34	0.19	0.38	0.25	0.20	0.14	0.27	0.25	<b>0.56</b>	-0.13	Be*
0.28	0.19	0.12	0.02	-0.03	-0.07	0.30	0.02	-0.06	0.09	0.06	0.29	0.34	-0.05	0.29	0.31	0.25	0.08	0.29	0.27	0.32	Bi
-0.11	0.20	0.01	-0.03	0.15	0.10	0.09	0.01	0.17	-0.23	0.15	0.06	0.28	0.15	0.04	0.08	0.14	0.21	0.03	0.27	-0.12	Bi*
0.16	0.06	0.13	0.04	-0.02	0.11	0.40	-0.05	-0.02	0.11	0.11	0.18	0.40	-0.10	0.03	0.37	-0.03	0.07	0.09	0.33	0.09	Cd*
<b>0.81</b>	<b>0.67</b>	0.08	-0.13	0.31	-0.26	0.32	0.06	-0.26	0.38	0.12	<b>0.98</b>	0.49	0.10	<b>0.89</b>	0.22	<b>0.57</b>	0.10	<b>0.91</b>	0.43	0.48	Ce
0.18	-0.21	0.28	0.16	-0.22	-0.01	<b>0.69</b>	-0.02	0.04	0.02	0.06	0.08	<b>0.58</b>	-0.39	-0.02	<b>0.78</b>	0.00	0.07	0.00	<b>0.60</b>	0.33	Cr
0.28	0.00	0.42	0.19	-0.01	0.05	<b>0.88</b>	0.01	-0.08	0.17	0.10	0.20	<b>0.73</b>	-0.29	-0.02	<b>0.88</b>	-0.03	0.11	0.02	<b>0.82</b>	0.17	Cu
0.36	0.05	0.39	0.18	0.05	0.03	<b>0.93</b>	0.01	-0.08	0.26	0.10	0.24	<b>0.72</b>	-0.26	0.05	<b>0.95</b>	0.00	0.15	0.08	<b>0.87</b>	0.25	Fe
<b>0.57</b>	0.49	0.30	0.11	<b>0.58</b>	0.07	<b>0.65</b>	0.03	-0.27	<b>0.69</b>	0.05	0.40	0.34	0.24	0.23	<b>0.50</b>	0.08	0.25	0.27	<b>0.68</b>	-0.02	Ga
-0.14	0.03	0.00	-0.05	0.18	0.14	-0.02	-0.01	0.05	0.00	-0.03	-0.13	-0.10	0.18	-0.13	-0.04	-0.07	0.12	-0.16	0.01	-0.15	Ge
0.22	0.05	-0.03	-0.14	-0.29	-0.12	0.36	0.05	0.20	-0.18	0.07	0.45	<b>0.57</b>	-0.26	0.46	0.42	0.30	-0.01	0.39	0.21	<b>0.97</b>	Hf
<b>0.82</b>	<b>0.68</b>	0.08	-0.13	0.33	-0.26	0.31	0.06	-0.29	0.39	0.11	<b>0.98</b>	0.48	0.10	<b>0.88</b>	0.21	<b>0.56</b>	0.10	<b>0.90</b>	0.43	0.44	La
<b>0.52</b>	0.35	0.41	0.15	0.33	-0.07	<b>0.74</b>	0.02	-0.26	<b>0.50</b>	0.13	0.43	<b>0.60</b>	-0.01	0.24	<b>0.67</b>	0.12	0.10	0.28	<b>0.85</b>	0.09	Mn
0.03	-0.07	0.06	0.15	-0.04	0.07	0.09	-0.01	0.05	0.05	-0.03	-0.07	0.06	-0.05	-0.06	0.09	-0.02	0.01	-0.03	0.07	-0.04	Mo
0.22	0.07	0.16	0.04	0.22	0.19	0.38	-0.01	-0.01	0.26	-0.03	0.09	0.18	0.10	0.06	0.34	0.01	0.38	0.04	0.33	0.06	Mo*
0.38	0.27	0.07	-0.10	-0.08	-0.14	0.47	0.04	0.12	-0.08	0.21	<b>0.62</b>	<b>0.80</b>	-0.16	<b>0.57</b>	0.47	0.46	0.08	<b>0.57</b>	0.48	<b>0.66</b>	Nb
<b>0.82</b>	<b>0.66</b>	0.08	-0.13	0.31	-0.27	0.32	0.07	-0.27	0.38	0.11	<b>0.97</b>	0.49	0.09	<b>0.88</b>	0.23	<b>0.56</b>	0.09	<b>0.91</b>	0.44	0.47	Nd
0.32	-0.02	0.45	0.21	0.10	0.04	<b>0.85</b>	-0.01	-0.17	0.32	0.07	0.16	<b>0.57</b>	-0.26	-0.03	<b>0.82</b>	-0.06	0.14	0.01	<b>0.81</b>	0.06	Ni
	<b>0.61</b>	0.14	-0.01	0.42	-0.15	0.37	0.06	-0.33	<b>0.61</b>	0.04	<b>0.80</b>	0.36	0.15	<b>0.71</b>	0.27	0.41	0.16	<b>0.75</b>	0.47	0.26	P*
	-0.01	-0.13	<b>0.70</b>	-0.09	0.07	0.09	-0.22	<b>0.56</b>	0.06	<b>0.69</b>	0.11	<b>0.54</b>	<b>0.65</b>	-0.08	0.44	0.15	<b>0.68</b>	0.27	0.05		Pb
		0.21	0.11	0.04	0.37	-0.03	-0.15	0.25	-0.01	0.06	0.24	-0.07	-0.02	0.36	-0.02	0.04	0.02	0.40	-0.06		Pd#
			-0.01	0.08	0.17	-0.02	0.00	0.08	0.00	-0.17	0.06	-0.08	-0.18	0.18	-0.09	-0.00	-0.13	0.15	-0.15		Pt#
				0.24	0.02	0.02	-0.22	<b>0.74</b>	-0.01	0.34	-0.19	<b>0.70</b>	0.31	-0.17	0.18	0.29	0.33	0.26	-0.32		Rb
					0.05	-0.06	0.36	0.06	-0.12	-0.25	-0.15	0.23	-0.21	0.01	-0.05	0.39	-0.21	-0.07	-0.14		Sb*
						0.02	-0.04	0.25	0.09	0.27	<b>0.72</b>	-0.26	0.09	<b>0.91</b>	0.05	0.17	0.13	<b>0.81</b>	0.30		Sc
							-0.02	0.02	-0.02	0.06	0.04	0.01	0.09	0.01	0.08	-0.02	0.08	0.01	0.05		Se
								-0.34	0.03	-0.27	0.01	-0.02	-0.15	0.02	0.04	0.11	-0.16	-0.16	0.22		Sn
									-0.03	0.38	-0.04	0.39	0.27	0.10	0.08	0.14	0.34	0.38	-0.20		Sr
										0.11	0.16	-0.05	0.09	0.09	0.06	-0.02	0.08	0.14	0.07		Ta
											0.47	0.13	<b>0.90</b>	0.17	<b>0.57</b>	0.10	<b>0.91</b>	0.40	0.47		Th
												-0.35	0.32	<b>0.77</b>	0.23	0.01	0.35	<b>0.70</b>	<b>0.53</b>		Ti
													0.22	-0.38	0.16	0.21	0.20	-0.09	-0.27		Ti*
														-0.01	<b>0.66</b>	0.12	<b>0.94</b>	0.19	<b>0.51</b>		U
															-0.03	0.07	0.02	<b>0.78</b>	0.36		V
																0.21	<b>0.68</b>	0.10	0.35		W
																	0.11	0.15	-0.02		W*
																		0.24	0.44		Y
																			0.14		Zn
																					Zr

P\* Pb Pd# Pt# Rb Sb\* Sc Se Sn Sr Ta Th Ti Ti\* U V W W\* Y Zn Zr